UNIVERSITY OF CALIFORNIA

Santa Barbara

Assessing the Risk of Engineered Nanomaterials in the Environment: Modeling Fate,

Exposure, and Bioaccumulation

A dissertation submitted in partial satisfaction of the

requirements for the degree Doctor of Philosophy

in Environmental Science and Management

by

Kendra L. Garner

Committee in charge:

Professor Arturo Keller, Chair

Professor Roger Nisbet

Professor Sangwon Suh

June 2016

The dissertation of Kendra L. Garner is approved.

_____

Sangwon Suh

_____

Roger Nisbet

_____

Arturo A. Keller, Committee Chair

June 2016

[This page is optional]

Assessing the Risk of Engineered Nanomaterials in the Environment: Modeling Fate,

Exposure, and Bioaccumulation

ACKNOWLEDGEMENTS

While my name is alone on the front cover of this dissertation, I am not its sole contributor. Rather, there are a number of people without whom this research would never have been completed who deserve my endless thanks. I want to acknowledge the guidance, support and encouragement of my doctoral advisor, Dr. Keller, and the members of my committee Dr. Nisbet and Dr. Suh during my time at UC Santa Barbara. Dr. Keller's rapid responses and tendency to be two steps ahead of me always kept me on my toes; Dr. Suh's seemingly random question in my written exam that became a link between my chapters; and several discussions with Dr. Nisbet really helped me look at certain issues differently. I would also like to extend my appreciation to the projects that funded much of my PhD including CLiCC and UC-CEIN and every member of each project that ever provided help, support, guidance and most importantly -- data (especially my assistants in this last year – Dillon and Rucha to whom I am endlessly grateful).

I want to thank those that guided me to this point including Mr. Hoover, my phenomenal IB environmental science teacher when I was studying in India who first got me interested in environmental science as well as the faculty and staff at Colorado College and Bren who helped prepare me to take on the challenge of a PhD. I am grateful to all of my friends who reminded me that I was not alone in this endeavor, particularly the other Bren PhD students who worked with me on nights, weekends, and holidays when I needed a study buddy to stay motivated.

To Charlie for providing cuddles and to Sadie for always trying to sit on my computer at the least (most) opportune time. To my godmother, Jeanne, who always had positive words and encouragement for me. To my partner, Marc, who always had faith in me and my

abilities, even when I didn't. To my parents; there are not enough ways to thank them for their unconditional love, support, guidance and raising me to believe I could do anything I set my mind to.

And finally, to anyone who ever reminded me that I would be fine – thank you.

Kendra L. Garner

June 2016

kegarner@bren.ucsb.edu | 2002 Bath St. Santa Barbara, CA | 202-577-4522

Personal Summary

Kendra Garner has a PhD in environmental science and a Master's in water resource management. She has a background in environmental modeling having developed various predictive models during her time in school. She can code in multiple scientific and programming languages including MATLAB, R, and Python and is familiar with a range of scientific software including GIS, and specialized watershed management tools such as WARMF. She has strong data management, processing, analysis, and visualization skills from working on projects that involved the compilation of large datasets; this work included development of an innovative Life Cycle Assessment (LCA) tool. She has experience working on large multipart research grants that required managing corporate and government client expectations and deliverables. She has experience managing undergraduate and masters' level researchers. She has taught masters level students as both a guest lecturer and teaching assistant in a range of subjects including biogeochemistry, fate and transport of chemical pollutants, and watershed quality management. She has applied experience as a consultant and intern, in the US, Sri Lanka and India and has lived in both India and Pakistan.

Education

Doctor of Environmental Science & Management, UC Santa Barbara, June 2016
- Dissertation: Assessing the Risk of Engineered Nanomaterials in the Environment: Modeling Fate, Exposure, and Bioaccumulation

Master of Environmental Science & Management, UC Santa Barbara, June 2012
- Dissertation: Impact of Sea Level Rise on Plant Species: A Threat Assessment for the Central California Coast

Bachelor of Arts in Environment Science, Colorado College, June 2010 (cum laude)
- Honors thesis: Population Dynamics of the Flammulated Owl: Modeling with GIS

Experience

Consultant at Keller Research (Consulting) Team, Santa Barbara
Oct 2015-Present
- Developed Watershed Model for EPRI Ohio River Basin Water Quality Trading Scheme
- Manage one other consultant on same project

Guest Lecturer at Bren School, UCSB, Santa Barbara
2014 – Present

- Gave lectures on watershed modeling, fate and transport of pollutants, and risk assessment of emerging pollutants

Teaching Assistant (TA) at Bren School, UCSB, Santa Barbara
2012 – Present
- TA for sustainable watershed management and biogeochemistry
- Guided students through process of developing watershed model and use of Best Management Practices

Research Specialist at Bren School, UCSB, Santa Barbara
2010 – Present
- Worked on Chemical Life Cycle Collaborative (CLiCC) Project to develop novel LCA tool with several major corporate sponsors and the EPA
- Work with the Center for the Environmental Implications of Nanotechnology (UC-CEIN)

Intern at International Water Management Institute, Sri Lanka
Summer 2011
- Collected data on wastewater use in agriculture to understand global implications
- Developed Access database on wastewater use by country

Intern for Sustainability Team, City of Colorado Springs, Colorado
Jan 2010 – June 2010
- Helped develop the first ever sustainability plan for the city
- Collected and analyzed data to determine utility use efficiency throughout city

Research Assistant at Colorado College, Colorado
Jan 2009 – Dec 2009
- Assisted in field research and developed mathematical biology model of owl populations

Intern at Management System International, Washington DC
Summer 2007, Winter 2007, and Summer 2008
- Worked for Business Development Unit, Contracts, and on a $100 million Iraq project

Intern at the US Agency for International Development, New Delhi
Summer 2004 and Summer 2005
- Worked for the Office of Social Development and Office of Energy and the Environment

Publications

- Garner, K. L.; Suh, S.; Lenihan, H. S.; Keller, A. A. Species Sensitivity Distributions for Engineered Nanomaterials. *Environ. Sci. Technol.* **2015**, *49* (9), 5753–5759.

- Garner, K. L.; Chang, M. F.; Fulda, M. T.; Berlin, J. A.; et al. Impacts of sea level rise and climate change on coastal plant species in the central California coast. *PeerJ* **2015**.
- Adeleye, A. S.; Conway, J. R.; Garner, K. L.; Huang, Y.; Su, Y.; Keller, A. A. Engineered nanomaterials for water treatment and remediation: Costs, benefits, and applicability. *Chem. Eng. J.* **2015**.
- Aceves-Bueno, E.; Adeleye, A. S.; Bradley, D.; Brandt, W. T.; Callery, P.; Garner, K. L.; et al. Citizen Science as an Approach for Overcoming Insufficient Monitoring and Inadequate Stakeholder Buy-in in Adaptive Management: Criteria and Evidence. *Ecosystems* **2015**, 1–14.
- Garner, K.; Keller, A. Emerging Patterns for Engineered Nanomaterials in the Environment: A Review of Fate and Toxicity Studies. *J. Nanoparticle Res.* **2014**, *2503* (16), 1–28.
- Keller, A. A.; Garner, K.; Miller, R. J.; Lenihan, H. S. Toxicity of Nano-Zero Valent Iron to Freshwater and Marine Organisms. *PLoS ONE* **2012**, *7* (8), e43983.

Awards

- Sustainable Nanotechnology Student Award 2012 and 2013
- American Chemical Society, Top Six Student Poster Presenters' Award, 2012
- Schuyler Fellowship, University of California, Santa Barbara, 2010-11
- Undergraduate Biology and Mathematics Grant from the National Science Foundation

Conferences

- Poster, Society of Environmental Toxicology and Chemistry, Salt Lake City, 2015
- Oral, Sustainable Nanotechnology Organization, Boston, 2014
- Poster, Sustainable Nanotechnology Organization, Santa Barbara, 2013
- Poster, Sustainable Nanotechnology Organization, Vienna, 2012
- Poster, American Chemical Society, Philadelphia, 2012

Skills

- Computer Skills: Microsoft Office, ArcGIS, MATLAB, R, Python, SPSS, JMP, BASINs, WARMF, Illustrator
- Languages: some Hindi, nominal Spanish, nominal French

ABSTRACT

Assessing the Risk of Engineered Nanomaterials in the Environment: Modeling Fate,

Exposure, and Bioaccumulation

by

Kendra L. Garner

Engineered nanomaterials (ENMs) are a relatively new class of material for which the risks of negative environmental impacts are still being determined. A comprehensive assessment of the environmental risks of ENMs entering the environment is essential, in part due to the continued increase in ENM production and release to the environment. The technical difficulty in measuring ENM fate and toxicity in complex and dynamic environmental media necessitates the use of mathematical models. In this research, the environmental risks of ENMs are assessed through: (i) the collection and analysis of emerging information on significant fate and transport processes; (ii) development of an ENM-specific fate and transport model to predict the accumulation of ENMs and their exposure to organisms in the environment; (iii) development of a statistical model to predict the distribution of species toxicity from specific ENMs in freshwater; and (iv) development of a bioaccumulation model to predict the long-term accumulation of ENMs through a food chain.

The NanoFate model, which was developed as part of the research described in this paper, is used to predict the temporal variability in fate across a broad range of complex environmental media at various spatial scales using both traditional fate and transport processes such as advection, deposition, and erosion, but also using ENM-specific processes and transformations such as heteroaggregation, sedimentation, and dissolution. A case study on San Francisco is then used to explore how fate and accumulation may vary among 4 different metallic ENMs, n-CeO$_2$, n-CuO, n-TiO$_2$, and n-ZnO, because the rates of fate processes and the toxicity are known to vary among these four ENMs.

Chapter 1 specifically explores how these processes and toxicities vary among different types of ENMs. Chapter 2 explores how species sensitivities vary between different ENMs within a freshwater ecosystem. A species sensitivity distribution (SSD) is a cumulative probability distribution of a chemical's toxicity measurements obtained from single-species bioassays that can be used to estimate the ecotoxicological impacts of that ENM. The SSD results indicate that size, formulation, and the presence of a coating can alter toxicity, and therefore the corresponding range of toxic concentrations. Chapter 3 describes the development of the NanoFate model and explores the implications of the San Francisco case study. By investigating both the range in rate processes and release scenarios, ENM fate was found to vary by multiple orders of magnitude among different environmental media and that even with an improved understanding of ENM fate, predictions of environmental concentrations are still very uncertain. We compare the predicted environmental concentrations for San Francisco Bay across many different release scenarios with the results of the SSDs and found that while CuO, TiO$_2$, and ZnO are likely to exceed No Observed Effect Concentrations (NOEC) in freshwater, this is not the case for soils. The

worst-case scenario, where the predicted concentrations would exceed lethal concentrations (LC_{50}), was not found in any scenario explored within the case study. Chapter 4 explores the range in bioaccumulation that could result from the NanoFate predictions for a freshwater ecosystem. A toxicokinetics model, using as much species-specific and ENM-specific uptake, biotransformation, and elimination rates as were available for CuO, TiO_2, and ZnO is used to predict the likelihood of bioconcentration and biomagnification through a simple food chain. Though bioconcentration was found for most species, biomagnification was not predicted to be significant with increasing trophic levels. Uncertainty analysis indicates that these results may vary by as much as two orders of magnitude. A parameter sensitivity analysis highlights key biological and environmental parameters that can be used to focus future research. While further developments will improve these predictions as our understanding of ENM fate and toxicity progresses, current understanding indicates that risk is likely low for most ENMs at predicted environmental concentrations though there is some concern that under high and localized release scenarios, toxic impacts will occur.

TABLE OF CONTENTS

LIST OF FIGURES

LIST OF TABLES

Introduction

Engineered nanomaterials (ENMs) are a relatively new and wide ranging class of emerging materials with unique properties and largely unknown impacts. Although the risks of ENMs to human and the environment are poorly understood, over 1800 consumer products currently on the market contain at least one ENM and the list continues to grow exponentially. The use of most of these products will lead to release of ENMs into many different ecosystems and several studies have demonstrated that ENMs can have adverse ecological impacts. As they enter ecosystems, their unique properties make identifying how they will interact with the environment and the organisms present difficult to predict. We do not yet understand the scale at which they will accumulate in ecosystems; the exposure concentrations they will represent within ecosystems; or the extent to which they will accumulate in and impact biota. Understanding all of these variables is necessary in order to fully appreciate the risks of ENMs.

In this doctoral research, the following questions are addressed: (i) What is the range of probable environmental concentrations under different production and release scenarios for different ENMs? (ii) How does the fate of ENMs vary across ecosystems and different ENMs? (iii) Which processes cause these variations? (iv) What concentrations of ENMs are toxic? (v) Are ENMs likely to bioaccumulate and biomagnify? Based on answers to these questions, we can identify when and where we are likely to see impacts from ENMs, particularly as production, use, and release quantities increase with time. We can also compare across nanomaterials to identify those which may pose a relatively greater risk from both a fate and a toxicity perspective. In addition, this research helps to identify some of our biggest limitations in understanding and improving the quality of ENM fate and

toxicity predictions.

To answer these five main questions, we focus on a subset of high-use ENMs, specifically engineered metallic nanomaterials, for which release into the environment is expected to be high and interactions with the environment and biota may be substantial since metallic ENMs tend to be highly reactive. We start by identifying and quantifying key parameters effecting fate and toxicity. We then develop a series of three predictive models. The first is a statistical model that predicts ecosystem toxicity across a range of exposure concentrations for each ENM through species sensitivity distributions (SSDs). The second model, is a dynamic multimedia fate and transport model using mass balance equations to predict the variability in long term fate of specific ENMs in different geographic regions. Finally, the third model is a simple bioaccumulation model to predict how much and in what form bioaccumulation and biomagnification of ENMs will occur in a freshwater food chain, based on the limited information we have on biological interactions with ENMs. Then by integrating the results of these models, we are able to investigate the broader implications of releasing ENMs into specific ecosystems over different time periods.

Predicting potential environmental exposure of ENMs using models is currently necessary because technology for environmental detection and measurements of ENMs *in situ* is still in development. Fate and transport models are used by risk assessors to estimate the movement and chemical alteration of contaminants as they move through environmental media (e.g., air, soil, water, and groundwater). There are two basic goals of these fate and transport models: to predict where a contaminant will go and to predict how fast it will get there. To predict where it will go, we use a series of equations describing the chemical and physical processes that occur in the environmental compartments. Common methods for this

include (i) materials flow analysis (MFA) which predicts environmental concentrations based on production, use, and release; and (ii) fugacity modeling, where mass balance calculations are completed using chemical-specific partition coefficients. For nanoparticles, however, traditional MFA and multimedia fugacity models cannot be applied with sufficient accuracy to predict the environmental concentrations of ENMs, because they are unable to account for the unique properties of ENMs.

To address such deficiencies, our nanomaterials fate and transport model (NanoFate) is designed to predict dynamic environmental concentrations in a complex environment using nanomaterial specific transport and transformation processes. The fate and transport model can be run under various release scenarios and at various spatial and temporal scales. Because this model is designed to have just a single box per medium (air, water, soil, etc.), it may prove more useful for predicting local scale scenarios rather than continental or global scale scenarios, although the design of the model does allow for any scenario. Because it is a dynamic model, both short-term and long-term exposure concentrations are predicted, which allows for better insight into both the possibility of short-term acute toxicity under an accidental release scenario as well as long-term chronic toxicity.

While other researchers have developed a few other models to predict ENM fate in the environment, those models greatly simplify the environment and do not effectively predict interactions with biota. To address this, we pair our NanoFate model with our nanomaterials bioaccumulation model. This provides predictions of bioaccumulation within a freshwater food chain at somewhat more realistic exposure scenarios than have previously been explored in bioaccumulation studies for ENMs. The bioaccumulation model also accounts for multiple sources of exposure to ENM, including the water column and free or

agglomerated particles, dietary, and sedimentary exposure. Given the limited understanding of ENM uptake and transformation processes within organisms, a full Monte Carlo analysis also is also conducted on the bioaccumulation model in order to determine the uncertainty in predictions and sensitivity in biological and environmental parameters.

We use a case study to explore the immediate risk of releasing different ENMs into the environment, looking specifically at the San Francisco Bay. This is done by exploring the long term environmental concentrations resulting from releasing ENMs at different rates into the Bay Area using the NanoFate model. These results are then compared with freshwater and soil SSDs for the corresponding ENMs, which tell us at what concentrations a fraction of species in a specific ecosystem (e.g. freshwater, marine, benthic, etc.) will experience acute or chronic toxicity or alternatively will show 'no observed effect'. This comparison provides an indication of risk across ENMs with various release scenarios that can be ranked by the relative risk within that specific ecosystem. These exposure concentrations are then incorporated into the bioaccumulation model to predict the range in likely bioaccumulation and biomagnification occurring in a simplified freshwater ecosystem in the Bay Area.

While we explore only one case study, we hypothesize that there are likely to be localized and regional toxic impacts from nanomaterials that will vary across ENMs, environmental locations, and media, which makes predicting bioaccumulation rather complicated. Because of this complexity, our goal was to develop simple-to-use models that do not require substantial data inputs that can also provide early exposure and accumulation predictions for environments and ecosystems so we can begin to determine risk in real time.

Outline of chapters

Chapter 1 is a literature review to identify key environmental fate processes and synthesize observed patterns in the rates of these processes as well as how they may impact fate and toxicity across a range of environmental media.

Chapter 2 develops a statistical model (species sensitivity distribution) using literature-based laboratory toxicity data to predict the ENM exposure concentrations that will cause toxicity to x% of the species in a given ecosystem. We focus specifically on the HC_5, the concentration at which 5% of species will be harmed.

Chapter 3 involves developing a nanomaterial fate model (NanoFate) and exploring the possible range of multimedia concentrations for four metallic nanomaterials under realistic release scenarios using a case study based on releases into the San Francisco Bay.

Chapter 4 includes the development of a metallic nanomaterial bioaccumulation model to estimate the range in bioaccumulation and biomagnification that is possible with different ENMs in a freshwater ecosystem.

Chapter 1. Emerging Patterns for Engineered Nanomaterials in the Environment: A Review of Fate and Toxicity Studies

A comprehensive assessment of the environmental risks of engineered nanomaterials (ENMs) entering the environment is necessary, in part due to the recent predictions of ENM release to the environment and because ENMs have been identified in waste leachate. Emerging information on the environmental fate and toxicity of many ENMs also provides a better understanding of their implications. The technical complexity of measuring ENM fate and transport processes in all environments necessitates identifying trends in ENM processes across environments. We collected data on the most significant fate and transport processes and toxicity of ENMs. Little research has been conducted on the fate of ENMs in the atmosphere; however, most studies indicate that ENMs will in general have limited transport in the atmosphere due to rapid settling. Studies of ENM fate in aquatic media indicate that in general, ENMs are more stable in freshwater and stormwater than in seawater or groundwater, which indicates that both transport and exposure risk might be higher in freshwater than in seawater. ENMs in saline waters will sediment out rapidly (hours to days), with a potential for increasing ENM concentrations in sediments over time. Dissolution is significant for specific ENMs (e.g. Ag, ZnO, copper ENMs, nano zero valent iron), which can result in their disappearance over time, but releases metal ions which may be more toxic than the ENM. In soil, the fate of ENMs is strongly dependent on the size of the ENM aggregates, groundwater chemistry, as well as the pore size and soil particle size. Most groundwater studies have focused on unfavorable deposition conditions, but that is unlikely to be the case in many natural groundwaters with significant ionic strength due to hardness or salinity. While much still needs to be better understood, emerging patterns with

regards to ENM fate, transport, and exposure combined with emerging information on toxicity indicate that risk of hazard is low for most ENMs at predicted environmental concentrations.

1.1 Introduction

Until a few years ago, little was known about the fate of nanomaterials in the environment, but recent studies suggest important emerging patterns. There are still major strategic knowledge gaps for even the most widely used nanoparticles (NPs) involving their post-production life cycles, including entry into the environment, environmental pathways, eventual environmental fate, and potential ecotoxicological effects. Actual environmental concentrations of engineered nanomaterials (ENMs) are almost unknown[1], although estimates of release to various environmental compartments have recently been conducted[2–5] and there is emerging evidence that manufactured NPs of less than 100 nm, including TiO_2, are present in waste leachate[6].

By most definitions, ENMs encompass NPs synthesized and modified to enhance their performance for technical or industrial purposes that have at least one dimension less than 100 nm. They are increasingly used in a variety of consumer products including electronics, textiles, cosmetics, medicine, and food.[1,4] ENMs are released into the environment; either during their use, by accidental spill, by intentional release for environmental remediation applications, or as end-of-life waste.[4] Studies estimate that more than 1,300 products on the market today contain NPs[7] and production estimates of major ENMs range from 270,000 to 320,000 metric tons per year, of which as much as 17% may be release to soils, 21% to water, and 2.5% to air, with the balance ending in landfills.[8] Thus understanding the environmental and health risks associated with ENMs is of great importance. The fact that

7

some ENMs are known to be toxic emphasizes the need for a comprehensive assessment of the environmental risks of large quantities of ENMs entering our environment.[9,10]

Once released, ENMs will interact with the environment in several ways. These interactions are controlled by the inherent properties of the ENMs (solubility in water, colloidal stability, reactivity, etc.) and the properties of the environment into which they are released (temperature, flows of air, water, and solids, and the physicochemical characteristics of each phase).[11] Properties such as ionic strength, pH, the presence of organic matter, and compartment composition are all important parameters that will modify ENM behavior[9,12–14] It is important to understand both how ENMs interact with their environment and how their environment alters the expected interactions.

The objective of this review is to identify the emerging trends in fate and toxicity to understand the behavior of ENMs under a variety of environmental conditions as a preliminary step in understanding the general trends in the environmental impacts of ENMs. Since it will be virtually impossible to conduct a full battery of tests on each ENM that adequately describes interactions among environmental compartments and biological systems,[15] the focus must be on identifying patterns in data that allow us to simplify our understanding of the complex interactions among ENMs and abiotic and biotic compartments across a range of conditions.[15] A review of the literature on fate and toxicity of ENMs in water, soil, and air showed that patterns are emerging that begin to characterize rates of aggregation, sedimentation, dissolution, and toxicity in various aquatic media including stormwater, freshwater, groundwater, and seawater; as well as more general patterns in air and soil. By comparing fate and transport patterns with potential

environmental release concentrations and toxicity data, one may assess which ENMs are of greatest concern.

1.2 ENM Fate and Transport

There are many fate and transport processes that need to be considered to understand ENM mobility, bioavailability and ultimate fate (Figure 1.1). These include emissions to air, water, and soil; advection out of the system; diffusive transport; volatilization to air; transformation into other ENMs or compounds; aggregation; sedimentation; dissolution; filtration; and sorption to suspended particles and the subsequent deposition to sediment.[16]
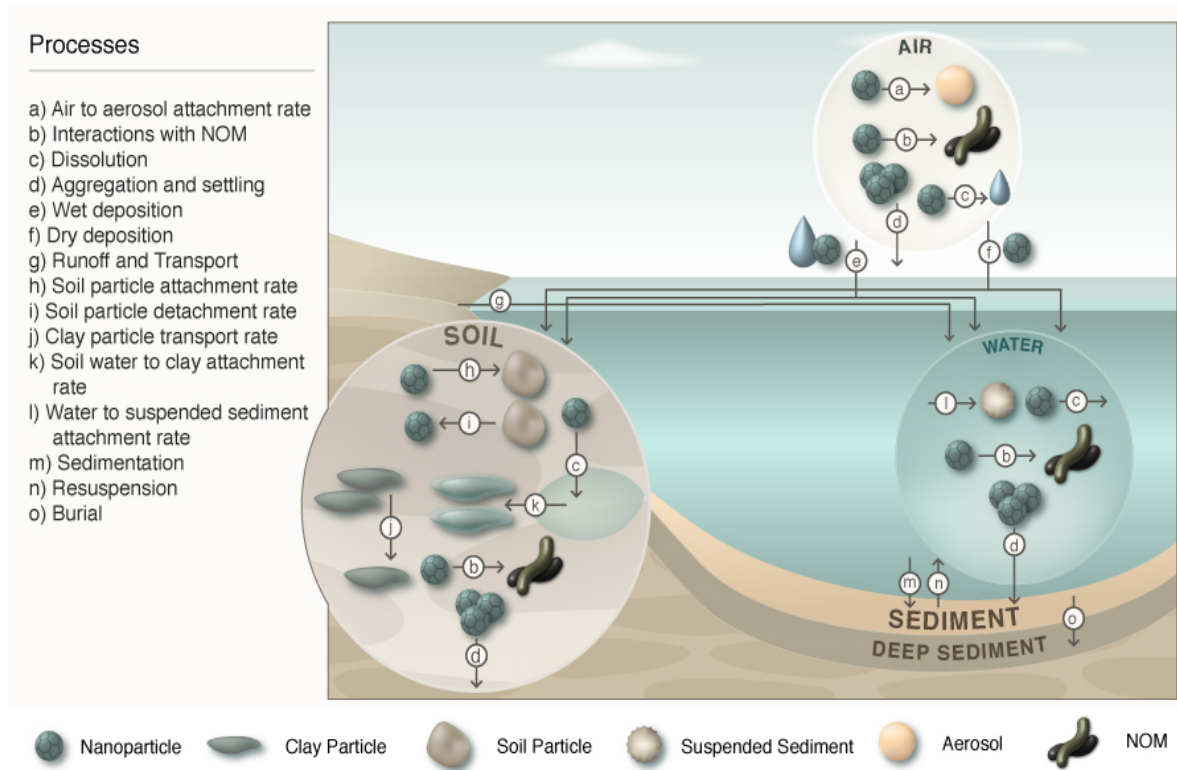
Figure 1.1 Conceptual Model of Key ENM Fate Processes

At the nanometer scale, materials exhibit unique properties due to effects resulting from high surface area to volume ratios. Many processes are important to ENMs that may not be

relevant to the environmental behavior of traditional contaminants,[16] such as aggregation, dissolution, deposition and sorption. These are all functions of their size, surface properties, and ambient environmental characteristics. Further, because some ENMs dissolve, they may be present in aquatic environments as both suspended particles and their dissolution products.[17] In addition, some transformation processes, such as aggregation, will create an altered state where the NP may behave in unexpected ways.[18] For example, NP agglomerates with complex fractal dimensions are likely to interact in different ways and at different rates in the environment compared with individual NPs and their dissolution products.[19,20] Most ENMs will undergo transformation processes (e.g. oxidation, sulfidation) that alter their original properties.[18] These transformations include acquiring coatings that will alter their chemical properties and environmental behavior.[18] Some important challenges to understanding the role of these processes on the fate of ENMs in the environment include managing uncertainties regarding NP emissions into the environment, ENM coatings, interactions with natural colloids and natural organic matter (NOM), and the effect of ambient environmental properties.[21]

1.2.1 Fate and Transport in Air

Atmospheric ultrafine particles (UFP) are those with diameters less than 100 nm.[22] UFPs are typically formed via nucleation in one of three ways: (i) at high temperature sources that are then emitted directly to the atmosphere; (ii) processes that emit hot supersaturated vapors which undergo nucleation and condensation while cooling; and (iii) chemical reactions in the atmosphere that can create NPs through a variety of nucleation processes.[22] These processes can be broken down into coagulation, condensation, and evaporation.

10

Coagulation is the process in which particles collide due to random Brownian motion and coalesce to form larger aggregates and agglomerates.[23] Brownian motion is enhanced by van der Waals forces, viscous forces, and fractal geometry of aggregates.[23] Coagulation is especially efficient between particles of different sizes, with smaller particles having high mobility and larger particles providing a larger cross-section with which to attach.[23] As with aggregation, coagulation reduces the number of smaller particles while it preserves the total mass.

Condensation is a diffusion-limited mass transfer process between the gas phase and the particle phase governed by the high vapor pressure of condensable species in the air around the particles.[23] Condensation causes an increase in the volume of particles, but does not change number concentrations.[23] Whereas evaporation is the reverse process of condensation because it reduces the volume concentration of particles.[23] It occurs when molecules on a particle surface change to the gas phase and diffuse away from the surface because of the lower vapor pressure of the air.[24] NPs will evaporate faster than coarse particles due to the Kelvin effect,[25] and lose more volume because of their reactive nature.[26] However, most ENMs have negligible evaporation rates.

ENMs in the atmosphere will be removed via wet or dry deposition. Dry deposition removes particles through transfer to air-surface interfaces. This process is mainly driven by Brownian diffusion and inertial impaction.[22] Under dry deposition, the size of the ENMs and their aggregates contribute to the rate of removal.[19] This is because gravitational sedimentation velocities are proportional to the particle's diameter and density.[19] Thus sedimentation rates should correlate with aggregation rates, much as in aquatic systems, and will be lower for smaller particles than for larger particles. Wet deposition is the removal of

11

particles through precipitation.[27] This can occur by nucleation scavenging (rain out meaning the inertial capture of dust particles by falling rain drops) and aerosol-hydrometeor coagulation (i.e. washout through formation of raindrops around particles as condensation nuclei).[19,28] Particle size also determines the efficiency of washout of airborne particles by rain.[19] Typically, the rainfall washout coefficient is likely to be larger for 100 nm size particles than for 5 μm size particles.[19] Dry and wet deposition from air to water and to soil occurs approximately according to the ratio of land areas covered by water and soil.[29]

The size of NPs will increase in the atmosphere due to the condensation of organic and inorganic vapors on the particle nuclei as a result of condensation/evaporation and dilution, with some contribution from coagulation and deposition.[30] Environmental factors, such as temperature, relative humidity, and atmospheric turbulence, will affect the size and concentration of ENMs in the atmosphere.[31] One study found that higher particle number concentrations persisted at high temperatures.[32] Others found that higher particle concentrations were observed in winter because of the combination of lower temperatures and less dilution.[33,34]

Little is known about the rates of aggregation and deposition of specific ENMs in the atmosphere, due largely to the complex nature of the system and the lack of instrumentation for measuring ENMs at such small sizes and concentrations. However, one study suggests that if we assume a 10 day retention time for UFPs in the lower atmosphere, approximately 1/36th of the ENM input to the air compartment constantly remains in the lower atmosphere.[29] This indicates that a majority of ENMs will likely settle very quickly, even given their small size. Transport within the atmosphere will likely be limited as concentrations in the atmosphere are predicted to be low because most nanomaterials do not

volatile and aggregation and sedimentation will be relatively rapid.[16] Recent release estimates suggest that as much as 8,300 metric tons of ENMs per year may be released to the air around the world,[8] mostly in urban areas. Yet, while some studies indicate that ENM release to the atmosphere is small,[8,35] we essentially do not know to what extent ENMs may contribute to the presence of NPs in the atmosphere or how long they will reside in the atmosphere.[31] In addition, not enough data were available to determine the rates of aggregation and sedimentation in the atmosphere for specific ENMs.

1.2.2 Fate and Transport in Water

Current predictions indicate that as much as 66,400 metric tons of ENMs are released directly to global surface waters every year.[8] The fate and transport of ENMs in water largely depends on the chemical properties of the water. In this review, we consider the effects of freshwater, stormwater, groundwater, and seawater on rates of aggregation, sedimentation, and dissolution. Some studies did not specifically use any of the above four water types; where necessary we categorized the water using the ionic strength (IS) or concentration of NOM according to the ranges in.[12,36] Differences in aquatic characteristic can significantly impact the rate of many fate and transport processes. For example, the ionic strength and concentration of NOM present in seawater versus freshwater will impact rates of aggregation, sedimentation, and dissolution for some ENMs. Dissolved or particulate organic matter can sorb to ENM surfaces and thus influence particle properties in various ways. For example, NOM is generally found to have a stabilizing effect on many ENMs in aqueous suspension, thus potentially slowing aggregation and sedimentation as a result of its negative charge.[16]

1.2.2.1 Aggregation in Water

Particle aggregation refers to the formation of clusters in colloidal suspension. This is most likely to occur during the use phase of the ENMs while the ENM concentration is high. During this process, particles dispersed in a liquid adhere to one another, and form irregular particle clusters - aggregates or agglomerates. Following release to water most NPs will aggregate to some degree and the behavior of the resulting aggregates is expected to be very different from that of primary NPs.[19,20] The degree of aggregation and the size range of the aggregates depend on the characteristics of the particle, the concentration of the particles, and the characteristics of the environmental system.[19] NP aggregation and deposition behavior will dictate particle transport potential and thus the environmental fate, bioavailability, and potential ecotoxicological impacts of these materials.[19,37,38]

Aggregation of spherical NPs can generally be described using extended Derjaguin-Landau-Verwey-Overbeek (DLVO) theory.[17,39–41] The basic DLVO theory predicts that the stability of NPs suspended in aqueous environments can be evaluated as the balance between attractive van der Waals (VDW) forces and repulsive electrical double layer (EDL) forces.[39,40] A stable suspension requires a dominant repulsive force to maintain dispersion of particles. However, if attractive forces dominate, or particles collide with sufficient energy to overcome repulsion, they will form aggregates that then sediment out of suspension.[42] Extended DLVO theory takes into account non-electrostatic ion-specific forces such as acid-base, steric, magnetic, and hydrodynamic forces,[17,38,43,44] all of which can play important roles in the aggregation of ENMs. Additional considerations need to be made for non-spherical NP morphologies.[45–47]

In theory, aggregation rate can be calculated using the ENM collision rate and attachment efficiency.[16,18] The attachment efficiency represents the fraction of collisions

between particles that result in attachment,[48] since simply making contact with another particle does not ensure that aggregation will occur as various forces (such as the EDL) may prevent aggregation.[48] Attachment efficiency depends on environmental conditions such as pH, IS, ion valence, temperature, and ENM and other particle concentrations.[21]

The stability of NPs in aquatic environments depends on the properties of the ENM itself (size, charge, zeta potential, coatings, ENM point of zero charge (PzC), particle density, and magnetization), the ambient environmental characteristics (pH, ionic strength, NOM), and the initial ENM concentration. In general for uncoated ENMs, the further the environmental pH is from the ENM's PzC, the higher the charge (and corresponding zeta potential) on the particle. This increases their stability, since like charges will repel.[49–52] However, high IS can minimize the forces keeping NPs separate and cause aggregation and sedimentation[9,53] even for a pH that is far from the PzC. Divalent ions, such as calcium and magnesium, are prevalent in many aquatic systems, and affect aggregation of ENMs by compressing the electric double layer surrounding the NPs.[9,53] This allows attractive forces to dominate, so that the primary particles floc and form aggregates that eventually sediment out of solution.[42] Thus, the zeta potential is a key parameter for predicting whether an ENM will be stable or will tend to aggregate in a given aqueous matrix. Zeta potentials for Ag, CeO_2, and NiO, and nZVI, and TiO_2 are generally fairly negative, particularly in freshwater.[54–58] Surprisingly, the zeta potential for nZVI remains relatively negative even at high IS and pH ranging from 7 to 10.[49,59] Similarly, the zeta potential for Al_2O_3 is generally fairly negative even in the presence of some IS at pH ranging from 4 to 9.[55,60] Conversely, the zeta potential for TiO_2 at 10 mM $CaCl_2$ is close to zero at pH 7.[61] The zeta potential for ZnO seems to vary significantly from very positive to very negative at pH values ranging from 4 to 10.[51,61–63]

The zeta potentials for Au and Cu/CuO tend to be close to zero for a pH between 5.5 and 8.5, except in groundwater for Au and in algal growth media for Cu/CuO.[50,52,55,64]

Aggregation is generally regarded as irreversible.[21] Zhang et al. (2008) found that it is very difficult to disaggregate metal oxide NPs and neither sonication nor dispersants were effective in fully disaggregating these ENMs. However, Zhou et al. (2012) found that fractal agglomeration of TiO_2 and other metal oxide ENMs was partially reversible during exposure to sunlight and diurnal temperature variations. Silver agglomerates were also found to break apart with agitation and the primary particles were easily resuspended.[42] Thus partial disaggregation can occur under natural conditions.

Stabilization of ENMs by surface coatings may cause them to remain in the water column and increase their transport distances.[65] Stabilizers may be used in the manufacturing process to reduce aggregation and enhance the dispersion of engineered NPs, which decreases the collision efficiency.[19] Stabilizers work either by electrostatic repulsion (where a charged stabilizer is adsorbed to the particle increasing repulsion between particles) or steric hindrance (where a bulky stabilizer is used to impede particle attraction).[19] A wide range of stabilizers have been found to be effective including thiols, carboxylic acids, surfactants, and polymers. The stabilizers not only affect the behavior of the NP within a product but can also enhance the mobility of ENMs in the environment.[19]

The effect of NOM on aggregation is complex since it can both enhance and reduce aggregation, and is usually interconnected with other ambient environmental properties.[21] The presence of NOM generally results in a more negatively charged particle because NOM can form a surface coating that enhances particle stability via electrosteric stabilization mechanisms.[66–68] ENM interaction with NOM is best described as a heteroaggregation

16

process, where ENMs collide with NOM on the basis of their respective diffusion velocities and will adhere to the NOM depending on the surface properties of both.[18] NOM can also affect the structure of aggregates. For example, iron oxide in the absence of NOM forms porous aggregates, whereas in the presence of NOM, it forms compact aggregates.[69] High concentrations of NOM have been shown to induce full disaggregation of iron oxide (50 – 100 mg NOM L^{-1}) and partial disaggregation of Ag (10 mg NOM L^{-1}). However, these concentrations of NOM are not frequently observed in the environment and thus full disaggregation by NOM alone is unlikely.

Studies conducted on the aggregation rates of ENMs in various types of waters with a range of IS and NOM concentrations can be categorized by rate (hours, days, weeks, months or greater) and water type (Figure 1.2). The ENMs are listed alphabetically within each rate category. Deviations and exceptions to these categorizations are identified in Appendix Table A1.2. Faster aggregation indicates that NPs will not remain in the water column for long (hours to days) and thus exposure to many pelagic aquatic species will be limited. In addition, aggregation will lower the transformation and reactivity of NPs since less effective surface area is exposed.

Residence Time	Stormwater	Freshwater	Groundwater	Seawater
Months	Ag* Au* CeO_2 C_{60} FeO/Fe_2O_3 MWCNTs SiO_2 TiO_2 ZnO	Ag* Au* CeO_2 C_{60} FeO/Fe_2O_3 MWCNTs SiO_2 TiO_2 ZnO	C_{60} MWCNTs SiO_2	SiO_2
Weeks	nZVI* SWCNTs	NiO nZVI* SWCNTs	Au* FeOOH Latex SWCNTs	CuO FeO/Fe_2O_3*
Days		Al_2O_3	Ag* CeO_2 CuO NiO TiO_2	Ag* C_{60} FeOOH SWCNTs
Hours			FeO/Fe_2O_3 nZVI* ZnO	Au* CeO_2 MWCNTs nZVI* TiO_2 ZnO

Figure 1.2 Rate of Aggregation of ENMS in Different Water Types

Most NPs are largely stable in freshwater and stormwater with some aggregation observed for Al_2O_3,[70] NiO,[71] nZVI,[10,72] and SWCNTs.[73,74] Sorption and change in electrophoretic mobility have been shown to occur on exposure of NOM to metal and metal oxide NPs.[67] Keller et al. (2010) found that NOM adsorbed onto TiO_2, ZnO, and CeO_2 and significantly reduced their aggregation, stabilizing them under many conditions. This is consistent with our findings that many metal oxides are less likely to aggregate in stormwater and freshwater given their high NOM content. However, with the exception of SiO_2,[75] most NPs will aggregate fairly rapidly in seawater. This is due to the high ionic strength, which compresses the EDL, and low presence of NOM, which does not provide sufficient electrosteric stabilization in seawater. Groundwater had the most variable results with some ENMs aggregating rapidly, such as FeO/Fe_2O_3,[20] nZVI,[10,59] and ZnO,[20,46,62] while

others remained fairly stable over the long term, such as Au,[76,77] C$_{60}$,[78,79] FeOOH,[68] MWCNTs,[80] SiO$_2$,[20,75] and SWCNTs.[73] This likely is due as much to an individual ENM's characteristics as it is to the high variability in the ionic strength of groundwater and difficulty categorizing water samples as groundwater equivalent. Many groundwater studies are conducted in the laboratory with artificial groundwater under unfavorable aggregation conditions that may not be representative of natural systems. For ZnO and nZVI, the fast aggregation in groundwater is similar to the fast aggregation in seawater, and thus may be explained by the IS of groundwater. However, aggregation of FeO/Fe$_2$O$_3$ was much slower in seawater[81] than in groundwater,[20] so there may be other factors at work.

1.2.2.2 Sedimentation in Water

ENMs can be deposited to the sediment compartment via discrete settling of primary NPs, gravitational settling of aggregates, or settling of ENMs sorbed to NOM or other suspended particles. There is a strong correlation between aggregation and sedimentation since particle size is such a strong determining factor in the rate of sedimentation. However, particle buoyancy is also a factor. Generally there is a delay between aggregation and sedimentation, which results in rates of sedimentation that are slightly slower than those for aggregation. In many instances, initial aggregation is so fast that it results in almost simultaneous sedimentation. Aggregate particle size is a major factor affecting the rate of sedimentation along with ambient environmental characteristics, such as the presence of NOM or other stabilizing agents and the ionic strength or presence of different electrolytes as well as the viscosity of the fluid and the initial ENM concentration.[16,82] The rate of sedimentation depends on the density and size of the particles, regardless of whether they are primary particles or complex aggregates, as well as the density of the fluid.[18] Discrete

settling can be estimated using Stoke's law.[16] For sedimentation to occur, the settling velocity must be equal to or greater than the critical settling velocity for the system.[18,83] This is valid for aggregates as well as primary particles. Phenrat et al (2007) found that the rate of sedimentation tends to follow three phases: an initial slow phase as aggregation is still occurring; a fast phase; and then another slow phase where the overall concentrations of particles is low as a result of sedimentation.

In addition to ENM aggregation, collisions of ENMs with suspended particles, such as clays, can lead to accelerated sedimentation.[84] This is dependent on the nature of the suspended particle and whether attachment of the ENM to the suspended particle is highly favorable, unfavorable, or somewhere in between. For example, at low pH values and intermediate IS, clay particles with positive surface charges reduce the stability of negatively charged Ag and positively charge TiO_2 ENMs.[84]

As with aggregation, a review of the literature was conducted on the sedimentation rates of ENMs in various types of waters based on their IS and NOM concentration. These were categorized by rate and water type (Figure 1.3) with details on specific sources provided in Appendix Table A1.3. Faster sedimentation (i.e. within hours to days) generally may result in lower exposure doses to species living in the water column, with corresponding accumulation in sediment.[85] Slower sedimentation (i.e. multiple weeks or longer) indicates greater transport distances, but with increasing dilution over time as the ENMs move away from the source via advection and dispersion.

Residence Time	Stormwater	Freshwater	Groundwater	Marine
Months	Au* CeO$_2$ C$_{60}$ MWCNTs SiO$_2$ SWCNTs TiO$_2$	Au * C$_{60}$ MWCNTs SiO$_2$ SWCNTs TiO$_2$	C$_{60}$ FeOOH SiO$_2$	SiO$_2$
Weeks	Ag* ZnO	Ag* CeO$_2$ CuO NiO ZnO	Au* CeO$_2$ NiO ZnO	Au
Days	nZVI*	FeO/Fe$_2$O$_3$ nZVI*	nZVI* TiO$_2$	Ag* C$_{60}$ FeOOH nZVI* ZnO
Hours			FeO/Fe$_2$O$_3$	CeO$_2$ MWCNTs TiO$_2$

Figure 1.3 Rate of Sedimentation of ENMs in Different Water Types

In general, sedimentation is faster in seawater than in the other water types, much as with aggregation. Also, there are fewer notable differences in rates of sedimentation for stormwater, freshwater, and groundwater than there are for aggregation. This is because of ENMs such as NiO,[20,55] nZVI,[72,86,87] and ZnO[12,14,20,46,88] have similar sedimentation rates for groundwater, stormwater, and freshwater. Further, Ag,[55,89,90] nZVI,[87] and ZnO[12,14,46,88] appear to have sedimentation rates that are marginally faster than the rate of aggregation in both freshwater and stormwater (weeks instead of months, or days instead of weeks). CeO$_2$[12,14,57] and FeO/Fe$_2$O$_3$[91] have sedimentation rates that are faster than the rate of aggregation in freshwater (days or weeks instead of months). This may be a result of different ENM primary particle sizes or coatings in the various studies.

Much as with aggregation, these results indicate that sedimentation will occur more quickly in seawater than other natural waters, whereas in freshwater and stormwater,

21

particles are likely to remain suspended for extended lengths of time. This will lead to higher exposures of freshwater aquatic species to ENMs and higher exposures of benthic marine species to ENMs.

1.2.2.3 Dissolution in Water

Dissolution is important for some ENMs, though it is very specific both to the ENM and environmental medium. It involves the release of dissolved ions from the NP, even within an aggregate.[16] Dissolution is a surface controlled process that is dependent on the surface area of the ENM and the concentration of the dissolved ions near the particle's surface.[16] Greater surface to volume ratios of NPs generally result in increased dissolution.[16] Additionally, most metal NPs show increased dissolution at extreme pH values, particularly low pH.[16]

NOM can act as a complexing agent that decreases the dissolution of some ENMs. For example, ENMs can bind to NOM (or sediments) while dissolution is still occurring.[92] One study found that small size of fulvic acid results in little impact on Ag particle dissolution; however, larger molecular weight humic acids appear to decrease stability and increase dissolution.[93] As with NOM, ENM surface oxidation or sulfidation can decrease dissolution rates for ENMs such as Ag, which can also decrease toxicity.[94] This is because oxidation and sulfidation can produce coatings on the ENMs which hinder the release of the metal ions from the inner core of the ENM.

Many studies have been conducted on the dissolution rates of ENMs in various types of waters based on their IS and NOM concentration. These were categorized by rate (hours, days, weeks, months or greater) and water type (Figure 1.4). Carbonaceous NPs such as C_{60}, MWCNTs, and SWCNTs do not dissolve and thus were not included in this study. However, in many cases carbonaceous NPs include metal catalyst residuals, which can leach ions to a significant extent.[73] The carbonaceous NPs are not included in Figure 1.4, since the type of

metal ions depends on the method of synthesis. The ENMs are listed alphabetically within each rate category. The categories are based on many different studies and there are deviations and exceptions to some of these categorizations, identified in Appendix Table A1.4. Faster dissolution means decreased NP concentrations and increased dissolved ions.

Residence Time	Stormwater	Freshwater	Groundwater	Marine
Months	Au* FeO/Fe$_2$O$_3$ NiO TiO$_2$	Au* CeO$_2$ FeO/Fe$_2$O$_3$ TiO$_2$	Au* CeO$_2$* CuO NiO TiO$_2$	Au* CeO$_2$ CuO TiO$_2$
Weeks	CuO ZnO	Ag* Al$_2$O$_3$ CuO NiO PbS	Ag* ZnO nZVI*	Ag* Al$_2$O$_3$ NiO
Days		ZnO		
Hours				ZnO

Figure 1.4 Rate of Dissolution of ENMs in Different Water Types

With the exception of ZnO in seawater[95–99] and freshwater[51,62,88,96,100], dissolution is generally very slow, occurring over the course of weeks or months, if at all. Dissolution of ZnO is highly pH dependent and the presence of phosphate can significantly alter the rate of dissolution so that it can be either very high or very low.[101,102] ENMs such as Au,[55,64] CeO$_2$,[102–104] and TiO$_2$[12,55,97] are not expected to dissolve to any significant extent, even over long periods of time regardless of water type. There is a slight increase in rate of dissolution from weeks to months as IS increases and NOM decreases, but this could also be driven by the presence of Cl$^-$ and other ions that enhance precipitation of the dissolved ions, as in saline media. These studies also indicate that most NPs are unlikely to dissolve in stormwater, particularly due to the short residence times in this medium. Additionally, ENM

with coatings, such as PVP-coated Au, are less likely to dissolve, regardless of the water type.[64]

It is also worth noting that the toxic effect observed with some of these ENMS, such as CuO and ZnO, strongly correlate with the fraction of ENMs dissolved in the aquatic media.[96,98,101,105] While faster dissolution may mean that the NPs are not remaining in particle form, the ionic form of a metal is often toxic and this may have as much or more significant effects if dissolved than in particle form. At the same time, dissolution of ENMs can decrease the hydrodynamic diameter of the NPs, which may increase their toxicity.[93]

These results indicate that dissolution may occur marginally faster in seawater and groundwater than in stormwater or freshwater, with some exceptions (e.g. Ag). This means that many ENMs will remain in NP form, within aggregates, for significant periods of time. If they remain suspended, as they do in some water for Au, CeO_2, Cr_2O_3, CuO, NiO, SiO_2, and TiO_2 (Figure 1.3), this will lead to high exposure of aquatic species to particulate ENMs rather than dissolved ENMs. However, if they tend to sediment quickly in some waters, as with Ag, FeO, and nZVI (Figure 1.3), this will lead to high exposure of benthic marine species to particulate ENMs rather than dissolved ENMs. The exception is ZnO, which is the only ENM predicted to dissolve rapidly, specifically in seawater and freshwater. Given the slower sedimentation rates relative to the dissolution rates of ZnO, one can expect that water column species will have a higher probability of exposure to dissolved Zn^{2+} ions. However, Zn^{2+} can form precipitates with phosphate,[106] which can moderate the dissolve Zn^{2+} concentrations.

1.2.3 Fate and Transport in Soil

Soils are characterized by the presence of a heterogeneous mixture of gas, liquid and soil phases, the interfaces between them, and the presence of organic matter and microbial communities. The complex nature of soil systems mean that our understanding of processes affecting the fate of ENMs in soil is limited, especially in unsaturated soils. This is due in part to the complexity of measuring how ENMs interact with unsaturated soil as opposed to groundwater.[107,108] As in water, most ENMs in soil are likely to aggregate, sorb to surfaces, sediment and dissolve,[19,88,108,109] which can be determined by the estimated rates of aggregation, sedimentation, and dissolution in groundwater (Figures 1.2-1.4), with some possible exceptions. In unsaturated soil, work with colloids suggests that ENMs will likely be trapped in the air/water interface.[110]

Transport in porous media can be described by three mechanisms: i) direct interaction of ENMs with soil; ii) sedimentation due to gravity; and iii) diffusion due to Brownian motion. [109,111] Gravitational sedimentation will be negligible without significant aggregation.[111] For transport to occur, forces that cause ENMs to attach to soil particles, such as electrostatic forces, London van der Waals forces, hydrodynamic forces, hydration/structural forces, hydrophobic forces, and steric interactions must be minimized.[87,112] A number of studies have determined that the fate of ENMs in soil is strongly dependent on primary particle size,[113,114] aggregate particle size,[113] and surface charge, as well as environmental conditions such as pH, ionic strength, the presence of organic matter, clay content, and flow velocity.[108] These characteristics will affect physical and chemical processes that affect ENMs such as aggregation and dissolution.[108]

25

Transport is strongly dependent on the size of the ENMs; it is the aggregate size, not the primary particle size, which tends to correlate with mobility.[113] One study with Al_2O_3 found that at larger primary particle size and larger aggregate size, ENMs are less mobile.[113] Another study confirmed that attachment efficiency increased with increasing particle size for latex NPs.[114] Conversely, a study with SiO_2 found that smaller NPs resulted in higher relative retention in column experiments, which could be caused by the relative charge on the NPs.[115] There are likely two mechanisms responsible for this observed size effect: (i) size directly affects the interaction energy between ENMs and soil surfaces, and (ii) size may influence the physical and chemical properties of ENMs, so that smaller particles are more reactive.[115] Surface charge can affect particle-particle interactions as well as particle-soil interactions.[72] As with water, when an ENM is in a system where the pH causes the zeta potential to be close to zero, the ENM is likely to aggregate because the surface charges causing repulsion between particles is minimized.

Transport also explicitly depends on the size of the soil particles and the pore size. If the aggregate size is of similar dimensions or larger than the soil pore throats and is trapped, transport will likely be reduced by straining,[110,116] and by filtration if the particle is removed by interception, diffusion, and/or sedimentation.[109,111,112,117] As a result, it is possible that larger aggregates will be retained in the upper soil layers.[111] The presence of clay particles and humic acid in soil can also cause adsorption of the ENMs if there are opposing surface charges between the ENMs and the surface mineral or organic deposits.[108] Sorption can be caused by electrostatic attraction, surface bridging, hydrogen bonding, or hydrophobic interactions,[19] which in turn are influenced by soil properties such as pH, metal oxide content, ionic strength, organic fraction, and cation exchange capacity.[19] However, if the

ENM is similarly charged to the clay or NOM, such as nZVI doped with carbon or poly-acrylic acid (PAA), both of which have anionic surface charges, transport through soil will be facilitated because the similar charge causes repulsion between the ENM and soil constituents.[87] Similarly, positively charged Al_2O_3 has little mobility and deposits rapidly in soils because the NPs sorb to the negatively charged soil particles. A phosphate coating on the Al_2O_3, however, creates a negative charge and thus greater mobility.[113]

Much as in water, soil pH affects the aggregation of ENMs by altering surface charge, which strongly modulates ENM mobility in soils.[109] For example, when the pH is near the point–of-zero-charge for both ZnO and TiO_2, transport is low.[118,119] In one set of column experiments, a neutral pH prevented transport of TiO_2, whereas at most other pH values (such as 1, 10, and 12), 90 to 100% of the TiO_2 NPs were transported the entire length of the soil column.[109] This was also the case for Cu^0 NPs, which are positively charged at a neutral pH and thus essentially immobile, whereas at high pH, surface charge becomes more negative, allowing transport by decreasing attachment efficiency.[120]

The ionic strength can also affect the surface charge of ENMs; when the IS is high it compresses the EDL, which decreases repulsive forces and mobility by increasing aggregation and sorption.[108,111] For example, the presence of sodium chlorate reduced the electrostatic repulsion between particles and soil for CuO, Fe_2O_3, latex, TiO_2, nZVI, and ZnO, due to aggregation and reduced mobility.[72,111,114,121] Another study found that the compression of the EDL caused by increasing IS created a net attractive force for CeO_2, C_{60}, and MWCNTs NPs, which caused both increased aggregation and deposition.[122–125] Similarly, studies with TiO_2 and ferrihydrite NPs indicated that mobility was high in low ionic strength soils and low in high ionic strength soils.[111,126]

Several studies have indicated that the species of electrolyte matters significantly, much as it does in water.[125,127–129] For C_{60}, little aggregation occurred in the presence of NaCl, but significant aggregation occurred in the presence of $CaCl_2$, and mobility was equally affected by both.[125] Similarly deposition and filtration of C_{60} and MWCNTs increase with both increasing ionic strength and also from monovalent to divalent cations.[125,127–129] However, at high IS (>30 mM), this effect can disappear and mobility will be minimal regardless of the electrolyte species, such as for CNTs.[125] Thus, in groundwater that has traveled through calcareous deposits or with increased salinity, ENM transport is likely to be significantly decreased. Similarly, in marine or estuarine sediments one would expect very limited mobility due to high attachment efficiencies to the sediments.

Much as in water, in soils dissolved or particulate organic matter can sorb to ENM surfaces, which can influence the fate of ENMs in soil. Soil organic matter may enhance the stability of ENMs and thus increase their mobility in soil.[111,121,125,127,130] This is in part because humic substances tend to be negatively charged at typical environmental pH values, which can create an overall negative charge on an ENM-NOM agglomerate.[131] For example, NOM in soil suspensions was found to have a stabilizing effect on TiO_2, nZVI, and SWCNTs, thus increasing their mobility.[21,111,129,130,132] The presence of 2 to 20 mg L^{-1} NOM greatly increased the mobility of nZVI over the absence of NOM.[130] It also decreased the attachment efficiency of both latex and Cu^0 ENMs.[114,120,130] Similarly, deposition of TiO_2 was highest in the absence of NOM or bacteria and lowest in the presence of both NOM and bacteria, with NOM having a greater impact.[133] Under some conditions, however, the presence of NOM may destabilize particle dispersions.[108] For example, the presence of polysaccharide-based natural organic matter, which is produced by algae or bacteria, may

have the opposing effect to humic-based organic matter and thus may cause deposition and limit mobility.[127]

The liquid flow rate in soil has also been shown to affect the mobility of ENMs.[108] A low flow rate reduces ENM transport due to increase probability of collision, whereas a higher flow rate increases mobility in part due to the reduced likelihood of attachment.[121,134] For example, at the low flow velocity typical of groundwater (0.38 m/day), C_{60} NPs showed limited mobility.[135] Conversely, another study determined that while doubling the flow velocity did increase the transport of TiO_2, this increase was not significant.[118]

Transport estimates vary by NP and also by characteristics of the soil and flow. Thus, comparing transport rates across very different experiments has limited use. Most studies show some transport for all ENMs. The highest transport is predicted for ferrihydrite (30 m) and functionalized fullerenes (10 m).[126,136] Silica is also expected to have a high mobility, in part because of the limited aggregation that occurs in soil.[137] TiO_2 transport is expected to range from 41 to 370 cm, which may allow TiO_2 ENMs to reach deeper soil layers.[111] SWCNTs are expected to experience some mobility in low IS soils (1.7 m), but transport could also be as low as 5 – 20 cm.[128,129] CNTs, MWCNTs, and Ag are expected to be relatively mobile, approximately to the same extent as natural clay colloids.[138,139] Al_2O_3 and uncoated nZVI, on the other hand, are expected to experience very little transport.[87,113,128]

These studies suggest that under some conditions, such as a neutral pH, high ionic strength, low NOM, and low flow, many ENMs may have limited mobility and will be unlikely to enter deeply into groundwater aquifers or transport laterally to other water bodies.[122] Conversely, in areas with high NOM, ENM transport may be significant during periods of saturation due to heavy rain. This is especially the case for ENMs that have

29

coatings to make them less reactive, less likely to aggregate, and more mobile, such as functionalized fullerenes or iron doped NPs, as well as certain other ENMs including TiO_2, Silica, MWCNTs, and Ag.

1.3 Toxicity

Many studies have been conducted on the toxicity of ENMs in many different systems. Most tests have been conducted on freshwater or marine species, with only a few on soil organisms. Toxic effects have been observed for many NPs at a range of concentrations to many different species. Studies use various measures of toxicity including: no observed effect concentration (NOEC), minimum inhibitory concentration (MIC), least observed effect concentration (LOEC), median lethal dose (LD_{50}), median lethal concentration (LC_{50}), half maximal effective concentration (EC_{50}). For the purposes of this screening analysis, no distinction was made between chronic and acute toxicity.

The results of 61 ENM toxicity studies were put into context by comparing them against the high end of the predicted environmental concentrations[2,8] in freshwater and seawater media (Figure 1.5), in order to estimate the level of risk an ENM poses in each media. Release concentration estimates for ENMs considered in this review range from the low ng L^{-1} to ug L^{-1}.[2,8] There will likely be some hotspots and other exceptions for instances where nZVI is directly injected into soil for groundwater remediation, or for accidental spills or improper disposal of ENMs outside of landfills. We grouped the risk of hazard, based on maximum predicted environmental concentrations and toxicity to the most sensitive species, into five categories: (1) toxic at maximum predicted environmental concentrations; (2) toxic at 100 times the maximum predicted environmental concentrations; (3) toxic at any concentration up to 10 mg L^{-1}; (4) toxic at concentrations $> 10^{1}$; and (5) non-toxic at all

30

tested concentrations. Details for the studies considered in Figure 1.5 are provided in Appendix Table A1.5.

Freshwater	Seawater
SiO_2	FeO/Fe_2O_3 SWCNTs
Au FeO/Fe_2O_3	Al_2O_3 Cr_2O_3 MWCNTs NiO TiO_2
Al_2O_3 CeO_2 Cu CuO C_{60} Fe_3O_4 Latex MWCNTs NiO SWCNTs TiO_2	Au CeO_2 CuO C_{60} SiO_2
Ag nZVI ZnO	Ag nZVI ZnO

No toxicity observed

Toxic at >10 mg/L

Toxic at <10 mg/L

Toxic at 100x environmentally relevant concentrations

Figure 1.5 Toxicity of ENMs in Freshwater and Marine Systems

None of the ENMs considered are expected to cause toxicity at environmentally relevant release concentrations (Figure 1.5). Even if current production and subsequent release quantities were to increase 100-fold, only three ENMs would raise concern. These include Ag, nZVI, and ZnO. Of these, ZnO is the greatest concern since all studies indicate ZnO is

toxic at some concentration to all species tested.[88,96–98,101] If production of ZnO were to increase significantly, it is clear that its release and effects on the environment would need to be monitored closely. Also, special care should be given to the use of nZVI in soil and groundwater remediation as toxicity is observed at concentrations > 0.5 to 1 mg L^{-1},[10] and typical remediation concentrations can range as high as g L^{-1}.[82,140] Additionally, while the production of Ag is currently quite low,[4] most studies indicate some level of toxicity to a variety of species and thus consideration should be given should production increase.

Carbon-based NPs, including C$_{60}$, SWCNTs, and MWCNTs show some toxicity at concentration below 10 mg L^{-1},[141–143] and all other studies indicate some toxicity though not at concentrations likely to occur in the environment. Similarly, Cu/CuO, Fe$_2$O$_3$/Fe$_3$O$_4$, and NiO also caused some toxicity at all tested concentrations. Some studies indicated toxicity at concentrations less than 10 mg L^{-1},[55,105,144–146] while others indicated toxicity at far greater concentrations.[71,91,101,147,148]

Al$_2$O$_3$, CeO$_2$, and TiO$_2$ ENMs cause some toxicity at concentrations below 10 mg L^{-1}, and are clearly toxic at greater concentrations, although some studies indicated no toxicity at any tested concentration ranging from 25 mg L^{-1} to 20 g L^{-1}.[63,97,99,141,146] Interestingly for CeO$_2$, studies done on the same species and at similar concentrations occasionally resulted in toxic effects occurring at fairly different concentrations, which resulted in them being placed in different categories in this study.[104,144,149,150] A similar variety of concentrations of TiO$_2$ caused differing toxic effects.[142,144,146,151,152]

Au, Cr$_2$O$_3$, Sb$_2$O$_3$, SiO$_2$, and ZrO$_2$ exhibit very low toxicity. Au caused toxicity only at 70 mg L^{-1}.[153] Cr$_2$O$_3$ and ZrO$_2$ did not cause any toxicity at concentrations up to 100 mg L^{-1}.[141,154,155] Sb$_2$O$_3$ caused toxicity only at concentrations greater than 140 mg L^{-1}.[147] SiO$_2$

caused toxicity at very different concentrations for the same species; the lowest being 20 mg L^{-1}.[63,151]

Most of these studies focused on toxicity of ENMs to aquatic organisms. A few, however, considered toxicity to terrestrial organisms in soil. A number of studies have indicated toxicity of ENMs to soil organisms as well as the ability for ENMs such as Au and Ag to enter terrestrial food webs and biomagnify.[50,90,156] At high exposure concentrations, reproduction of *E. fetida* decreased for both Au and Al_2O_3.[77,157] Along with harming reproduction in *E. fetida*, Ag was found to cause acute toxicity at 7.41 mg kg^{-1} in soil.[158] Both CuO and Fe_3O_4 were found to cause changes in soil microbial communities, caused by toxicity, at 1 and 5% w/w dry soil.[159] Conversely C_{60} caused no change in the functioning of microbial soil communities, even at very high concentrations, suggesting that toxicity may be strongly connected with bioavailability and thus solubility.[160] While these are clearly toxic effects at both the acute and chronic level, specifically for bioavailable ENMs, there is virtually no information on actual exposure to ENMs in soils.

1.4 Conclusions

While there is still a need to better understand the implications of ENMs, emerging patterns with regards to ENM fate, transport, and exposure combined with emerging information on toxicity indicate that risk is low for most ENMs at predicted environmental concentrations.

In the atmosphere, removal of ENMs will likely be via either wet or dry deposition, both of which correlate strongly with both the size of the particles as well as environmental factors such as temperature, relative humidity, and atmospheric turbulence. A majority of

ENMs are expected to settle very quickly, in spite of their small size. This will limit transport in the atmosphere.

The fate and transport of ENMs in natural waters is dependent on the characteristics of the ENM and the chemical properties of the water, specifically the ionic strength and the presence of NOM. We found that there are clear differences in the fate of ENMs and the rate of ENM specific processes in different types of water, such as stormwater, freshwater, groundwater, and seawater.

Aggregation and sedimentation generally have similar time scales for most ENMs across the different water types. Faster aggregation indicates that NPs will not remain in the water column for long (residence times of hours to days) and thus exposure to many aquatic species will be limited, whereas slower aggregation, such as in stormwater or freshwater, may result in greater likelihood of exposure. Faster sedimentation (hours to days) generally indicates lowered exposure to species living in the water column, but increased and prolonged exposure to benthic species. Slower sedimentation (> weeks) indicates that ENMs will be transported over greater distances, but it may also mean greater dilution over time. ENMs will most likely exhibit low mobility in marine systems because of the higher rates of aggregation and sedimentation observed for many ENMs relative to freshwater. Areas near points of release (e.g. wastewater effluent discharge) may develop higher ENM concentrations in sediments over time, and may need to be monitored carefully for environmental impacts.

In most cases, dissolution does not vary significantly by water type, but is highly dependent on ENM composition. Over relevant time scales (days to weeks), ENMs such as Ag, Al_2O_3, CuO, and NiO will dissolve, while ZnO dissolves even faster (hours to days).

This results in the release of the metal ions and disappearance of the NP, although under some conditions the ENM may acquire a coating that slows down dissolution. Currently available data suggests that NPs that dissolve require close monitoring and merit more intensive follow-up research compared to those that do not dissolve. This is because, in many instances, the ionic form of a metal is very toxic and may have more significant effects if dissolved than in particle form. Frequently there is a strong correlation between toxicity and dissolution. The ENM may also be ingested by an organism and then dissolve, resulting in a high toxic dose. NPs that do not dissolve (e.g. SiO_2, TiO_2) tend to be much less toxic than those that do.

The fate of ENMs in soil is expected to be similar to those of traditional chemicals and colloids. For transport to occur, forces that cause ENMs to attach to soil particles must be minimized. In saturated soils rates of aggregation, sedimentation, and dissolution are predictable based on their behavior in groundwater. In unsaturated soils, work with colloids suggests that ENMs will be trapped at the air/water interface.[110] The fate is strongly dependent on both primary particle size and aggregate particle size, as well as soil pore size, soil particle size, and soil characteristics. Under neutral pH, high ionic strength (e.g. high salinity or hardness), low NOM, and low flow conditions, ENMs are unlikely to be transported great distances and are thus unlikely to enter groundwater aquifers to a significant depth. This information can be used to design ENM removal mechanisms in soil applications.

Toxicity is not expected at current predicted environmental concentrations for the ENMs considered in this study. However, direct use of ENMs in the environment (e.g. nZVI) or spills and other direct releases may have significant local effects. Even if current production

and release were to increase 100-fold, only Ag, nZVI, and ZnO are of significant concern. Generally, toxicity was highest for Ag, CuO, NiO, nZVI, and ZnO, as expected based on their dissolution behavior. Additionally, while fewer studies have been conducted on the toxicity of ENMs to soil organisms, in part because of the complexity with which organisms are exposed to ENMs in the different soil phases, studies do indicate that ENMs such as Ag, Au, Al_2O_3, CuO, and Fe_3O_4 will cause toxicity if ENM concentrations in soil become high enough.

The results from these 61 toxicity studies, combined with emerging exposure predictions, indicate that there are some areas of concern. ENMs such as Ag, nZVI, and ZnO are all relatively well studied and may pose risks under some release scenarios. After these, research should be directed towards the possible effects of C-based NPs, Cu ENMs, Fe ENMs, and NiO since all will cause toxicity but only if production and release quantities increase by several orders of magnitude. In additional, because Al_2O_3 and TiO_2 both have high production levels that are likely to increase, their risk should be carefully evaluated as well.

1.5 Appendix

Many studies were considered for determining the merging patterns for fate and toxicity represented in Figures 1.2-1.5. These sources are summarized in Table A1.1. Some of these sources provided direct process rate information, while others provided additional conditions or exceptions to the generalized results, as discussed in the main manuscript.

Table A1.1 References for Rate of Aggregation, Sedimentation, Dissolution, and Interactions

NP Specific Process	References
Aggregation Rates	9,10,12,17,20,36,42,45,46,48,49,52,54–56,59–62,66,67,69–82,87–89,91,93,95,97,98,103,105,109,111,120,132,141,149,152,153,161–182
Sedimentation Rates	12,14,17,20,36,43,44,46,49,55–57,59,62,68,72–76,79,86–91,95,97,102,105,111,120,132,143,163,164,168,174,175,179–181,183–186
Dissolution Rates	12,17,37,42,49–52,55,59,61,62,64,67,69,70,88,93–104,111,152,156,165,170,172–174,176,182,187–197
Interactions with NOM	43,46,48,52,54,56,57,59,60,62,64,67,69,73–76,83,86,88–90,101,120,132,158,162,167,170,171,177,179–181,185,191,198
Zeta Potential	9,42,49–64,74,183,186,199
Fate and Transport in Porous Media	19,48,61,72,87,107,108,111–115,118–131,134–139,158,164,173,181,200–208
Toxicity	4,10,50,55,63,67,70,71,73,86,88,91,96–101,104,105,141–155,157–160,176,182,183,185,189,190,199,203,209–223

Figure 1.2 was created using Table A1.2, which considers aggregation rates observed in many different waters. For ENMs with multiple studies on the rates of aggregation in a water type, we used the most common rate provided, meaning that if two sources estimated the rate of aggregation as days and one sources as weeks, we put days, and noted in the

footnotes that the third source estimated weeks. Red indicates aggregation within hours, orange indicates aggregation within days, yellow indicates aggregation within weeks, and green indicates minimal aggregation over months or longer. These categorizations are solely with respect to the rate of aggregation without evaluating exposure or risk. Key details, deviations and exceptions are noted in the footnotes. Asterisks indicate the presence of a coating on the ENMs.

Table A1.2 Aggregation Rates by Water Type

NP	Stormwater (low IS, high NOM)	Freshwater (low IS, mid NOM)	Groundwater (mid IS, low NOM)	Seawater (high IS, low NOM)
Ag	67, 170*, 89*	67, 170*, 89*	170*, 89*	172a, 89*b
Al_2O_3		70		
Au	76*	76*, 153	77, 161*c, 76*	161*
CeO_2	12	12, 103*	12	12, 149
CuO			120d	
C_{60}	224, 78	224, 78	224e, 79, 78	224f, 163, 79, 78
FeOOH			68g	68h
FeO/Fe_2O_3	162	162	20	81*
Latex			48	
MWCNTs	177	177	80i	80j
NiO		71	20	
nZVI	72*	10*k	10*, 59	10*, 59*
SiO_2	75	75	75, 20	75

[a] Aggregation of coated Ag is on the order of weeks at IS below 400 mMol NaCl
[b] Aggregation of Ag in seawater occured within hours
[c] Coated Au aggregates within hours in the presence of common groundwater cations
[d] Aggregation of CuO in groundwater ranges from days to weeks
[e] Significant C_{60} aggregation occurs within hours in groundwater
[f] Significant C_{60} aggregation occurs within hours in seawater
[g] Tests completed at g L^{-1} concentrations
[h] Tests completed at g L^{-1} concentrations
[i] Tests completed at 200 mg L^{-1}
[j] Tests completed at 200 mg L^{-1}
[k] Uncoated nZVI will aggregate within minutes in freshwater

SWCNTs	73, 74	73, 74	73	73
TiO$_2$	166, 180, 178	141a, 12, 179, 166, 180, 178	179, 20, 9b, 132, 180, 178	12, 164, 166, 9, 132, 180, 152, 178
ZnO	46	46, 12, 88c	46, 20d, 62	46, 12, 97, 95, 62, 98

Figure 1.3 was created using the Table A1.3, which considers sedimentation rates observed in different studies. Colors follow Table A1.2. Categorizations do not evaluate exposure or risk. Key details, deviations and exceptions are noted in the footnotes.

Table A1.3 Sedimentation Rates by Water Type

NP	Stormwater (low IS, high NOM)	Freshwater (low IS, mid NOM)	Groundwater (mid IS, low NOM)	Seawater (high IS, low NOM)
Ag	89*	90, 89*, 55, 36*		17*, 89*, 36*e
Au	76*	76*	76*	184
CeO$_2$	12, 57, 56	12f, 14, 57, 36	12	12, 95, 102, 57, 56, 36g
CuO		55		
C$_{60}$	224, 79, 44	224, 79, 44, 36h	224i, 79, 44	224j, 163, 79, 44, 36
FeOOH			68	68
FeO/Fe$_2$O$_3$		91k	20	
MWCNTs	74, 43, 171, 80	74, 43, 171, 80		44, 43, 80
NiO		55	20	

[a] No significant aggregation of TiO2 occurred in pond water over the course of weeks
[b] TiO2 aggregates in hours in the presence of any IS
[c] ZnO aggregates within 6 hours for in freshwater
[d] ZnO aggregates within days in tap water
[e] Ag will sediment over the course of weeks to months
[f] CeO$_2$ sedimentation takes more than weeks in freshwater
[g] CeO$_2$ sediments in seawater over the course of days to weeks
[h] C$_{60}$ sediments within days in freshwater
[i] Significant sedimentation of C$_{60}$ occurred within 8 days
[j] Some C$_{60}$ was still found in seawater after 8 days, indicating sedimentation over the course of weeks
[k] Uncoated Fe$_2$O$_3$ settles within days in zebrafish culture medium

NP				
nZVI	87*	87*	86*, 72*	86, 59*a
SiO$_2$	75	75	75, 20b	75
SWCNTs	74	74		
TiO$_2$	12, 181, 180	12, 14c, 181, 180, 183d	12, 20, 132, 111e, 180	12, 95, 132
ZnO	12,	46, 12f, 14, 88g	12, 20h	46, 12, 97i, 95

Figure 1.4 on dissolution rates was created using the studies in Table A1.4. Red indicates dissolution within hours, orange indicates dissolution within days, yellow indicates dissolution within weeks, and green indicates minimal dissolution over months or longer. These categorizations do not evaluate exposure or risk. Key details, deviations and exceptions are noted in the footnotes. Asterisks indicate the presence of a coating on the ENM.

Table A1.4 Dissolution Rates by Water Type

NP	Stormwater (low IS, high NOM)	Freshwater (low IS, mid NOM)	Groundwater (mid IS, low NOM)	Seawater (high IS, low NOM)
Ag		188*j, 67, 170*, 55, 104, 36*k	158*, 191*, 156	191*l, 93*, 36*m
Al$_2$O$_3$		55, 70		152, 195
Au	64*n	64*	77, 64*, 50*	64*

---

[a] Coated nZVI sedimented in the presence of IS over the course of hours
[b] SiO$_2$ sediments over the course of weeks in tap water
[c] TiO$_2$ sediments over weeks in low IS freshwater
[d] TiO$_2$ sediments within hours in natural lake water
[e] TiO$_2$ sediments in days to weeks in soil water
[f] ZnO did no aggregate in 8 hours in freshwater
[g] ZnO sedimentation occurred with 6 hours in freshwater
[h] ZnO sedimented in tapwater within days
[i] ZnO sediments in seawater within hours at ZnO concentrations above 10 mg L^{-1}, but may take a week at lower concentrations
[j] In river water, only half of the coated Ag dissolved over four months
[k] Coated Ag dissolution may take months in freshwater
[l] Ag dissolved in seawater between 6 and 125 days
[m] Coated Ag dissolution in seawater will take from weeks to months
[n] PVP-stabilized Au is essentially insoluble in all media

CeO$_2$		103*, 104, 36	103*	102, 36
CuO	52	101, 105, 55, 52, 100	52	52
FeO/ Fe$_2$O$_3$	69	69		
NiO	193a	55, 193	193	193
nZVI			49*	
PbS		173		
TiO$_2$	12, 97	97, 55	12, 97	12, 97
ZnO	96	96, 62, 101b, 88, 51, 100	51, 203,	97, 95, 96, 98, 99, 102c, 187

Table A1.5 includes a summary of toxicity tests for various ENMs on various species in different media. Toxicity observed at environmentally relevant concentrations are highlighted in red. Toxicity observed at environmentally relevant concentrations if they were to increase 100-fold are highlighted in orange. Toxicity observed at < 10 mg L^{-1} are highlighted in yellow. Minimal toxicity observed at concentrations > 10 mg L^{-1} are highlighted in light green. When no toxicity was observed at all tested concentrations, the cells are highlighted in dark green. White indicates that not enough data were given to place the study into one of the above categories. Asterisks indicate the presence of a coating on the ENM.

Table A1.5 Toxicity of ENMs to Various Species

NP	Species	Toxic Concentration	Ref.
Ag	*E. coli*	Minimum inhibitory concentration 100 μM	189*
Ag	Hemolytic toxicity	All AgNPs caused at least 75% hemolysis at the highest concentration of 100 ug ml^{-1}, and caused no additional hemolysis compared to the	182*

---

[a] NiO dissolution is negligible between pH7-11, even in presence of salts for all media
[b] ZnO at 10 mg L^{-1} dissolved over hours to days
[c] ZnO at concentrations below 10 mg L^{-1} dissolves over the course of days

NP	Species	Toxic Concentration	Ref.
		DMEM at the lowest concentration of 10 ug ml^{-1}.	
Ag	P. fluorescens	Ag reduced bacterial growth entirely at 2000 ppb (19 μM) under all conditions and adversely affected growth at 200 ppb (1.9 μM) under some conditions, indicating some toxicity	67
Ag	E. fetida	Toxicity observed at 7.41 mg kg^{-1} in sandy loam soil	158*
Ag	E. coli	Dissolved Ag concentrations measured in the E. coli growth inhibition media with AgNP concentrations equal to 50 mg L^{-1} were 8−10 μg L^{-1} for the unsulfidized and lowest sulfidized AgNP (agg) samples	176*
Ag	D. magna	LC$_{50}$ ~ 3 ug L^{-1}	153
Ag	D. pulex, D. rerio, P. kirchneriella	LC$_{50}$ 0.04-7.2 mg L^{-1}	55
Ag	D. magna	Acute toxicity 56% death at 0.1 mg L^{-1}, 100% death at 1 mg L^{-1}, chronic toxicity at 0.001 mg L^{-1}	104
Ag	Thalassiosira weissflogii	Photosynthesis and chlorophyll were severely suppressed beyond around 1*10^-11 M.	220
Al$_2$O$_3$	Microtox (bacteria), pulse-amplitude modulation (algae), Chydotox (crustaceans), and Biolog (soil enzymes)	No effects were observed up to 100 mg L^{-1}	141
Al$_2$O$_3$	C. metallidurans CH34 and E. coli MG1655	Toxic at all concentrations (10 – 500 mg L^{-1})	152
Al$_2$O$_3$	B. subtilis, E. coli and P. fluorescens	36-70% of bacteria died at 20 mg L^{-1}	63
Al$_2$O$_3$	D. magna	EC$_{50}$ ~114.357 mg L^{-1}, LC$_{50}$ LC$_{50}$ LC$_{50}$ ~162.392	142
Al$_2$O$_3$	D. pulex, D. rerio, P. kirchneriella	LC$_{50}$ 3.99 - >10 mg L^{-1}	55
Al$_2$O$_3$	E. fetida	No mortality occurred in subchronic exposures, although reproduction decreased at ≥3,000 mg kg^{-1} nano-sized Al$_2$O$_3$	157
Au	E fetida	Bioavalable and reproduction was negatively affected at 8 and 3.4% of bulk soil concentrations	77

NP	Species	Toxic Concentration	Ref.
Au	*D. magna*	$LC_{50} \sim 70$ mg L^{-1}	153
Au	*M. sexta*	biomagnification factor 6.2 - 11.6	50*
Au	*Mytilus edulis*	Oxidative stress occurred within 24 hours at 750 ppb	223
CeO$_2$	Microtox (bacteria), pulse-amplitude modulation (algae), Chydotox (crustaceans), and Biolog (soil enzymes)	No effects were observed up to 100 mg L^{-1}	141
CeO$_2$	*P. subcapitata, D. magna,* and *T. platyurus,* and embryos of *D. rerio*	No acute toxicity was observed for the two crustaceans and *D. rerio* embryos, up to test concentrations of 1000, 5000, and 200 mg L^{-1}, respectively. In contrast, significant chronic toxicity to *P. subcapitata* with EC_{10}s between 2.6-5.4 mg L^{-1} was observed.	149
CeO$_2$	RAW 264.7 and BEAS-2B cell lines	CeO$_2$ (25 ug mL^{-1}) NPs were taken up intact the cells without inflammation or cytotoxicity	99
CeO$_2$	*D. magna*	$LC_{50} \sim 0.012$ mg ml^{-1}	144
CeO$_2$	*P. subcapitata*	LC_{50} 10.3 mg L^{-1}	150
CeO$_2$	*D. magna*	No acute toxicity. Chronic toxicity at 10 mg L^{-1}	104
Cr$_2$O$_3$	*E. coli*	As the concentration of Cr$_2$O$_3$ (100 nm) in the culture media increased from 0 – 100 ug mL^{-1}, the percentage of live cells decreased linearly	155
Cr$_2$O$_3$	Human lung carcinoma A549 cells and human keratinocyte HaCaT cells	HaCaT cells showed a greater reduction in cell viability by Cr$_2$O$_3$ exposure than A549 cells. In particular, the cytotoxicity of NPs was higher than that for fine particles at a high concentration of Cr$_2$O$_3$ (0.5 mg mL^{-1})	154
Cu	*D. rerio*	LC_{50} 1.56 mg L^{-1}	145
CuO	*D. magna, T. platyurus,* and *T. thermophila*	The L(E)C$_{50}$ values of nanoCuO for both crustaceans in natural water ranged from 90 to 224 mg Cu L^{-1}	101
CuO	*P. subcapitata*	$EC_{50} = 0.71$ mg Cu L^{-1}	105
CuO	Soil microbe community	soil microbe community changed, indicating toxicity at 1 and 5% w/w dry soil	81
CuO	*E. coli, B.*	EC_{50} ranged from 28.6 – 65.9 mg L^{-1}	147

NP	Species	Toxic Concentration	Ref.
	subtilis, and *S. aureus*		
CuO	*V. fischeri, D. magna,* and *T. platyurus*	L (E)$C_{50} \sim 2.1 - 79$ mg L^{-1}	146
CuO	*D. pulex, D. rerio, P. kirchneriella*	LC_{50} 0.06 - 0.94 mg L^{-1}	55
CuO	*S. cerevisiae*	8-h EC_{50} were 20.7 mg L^{-1} and 24-h EC_{50} were 13.4 mg L^{-1}	190
CuO	*T. thermophila*	EC_{50} 128 mg L^{-1}	100
CuO	*Mytilus galloprovincialis*	CuO NPs induced oxidative stress in mussels by overwhelming gills antioxidant defense system at 10 ug L^{-1}	213
C_{60}	Microtox (bacteria), pulse-amplitude modulation (algae), Chydotox (crustaceans), and Biolog (soil enzymes)	Toxic effects were observed at greater than 1 mg L^{-1}	141
C_{60}	*P. subcapitata* and *D. magna*	The mobility of daphnids was not affected in the tested concentrations ($\leq$50 mg C_{60} L^{-1}). The algal growth rate was inhibited up to 30% at 90 mg C_{60} L^{-1}, but no reproducible concentration–response relationships could be established	209
C_{60}	*D. rerio*	C_{60} at 1.5 mg L^{-1} delayed zebrafish embryo and larval development	143
C_{60}	*D. magna*	$EC_{50} \sim$9.344 mg L^{-1} and $LC_{50} \sim$ 10.515 mg L^{-1}	142
C_{60}	Soil microbe community	No effect on structure, function, or processes	160
C_{60}	*Crassostrea virginica*	Significant toxicity at 10 ppb	222
C_{60}	*Mytilus galloprovincialis*	Some effects observed at 5 mg L^{-1}	210
Fe_2O_3	*D. rerio*	$EC_{50} \sim 36.06$ mg L^{-1}, $LC_{50} \sim 53.35$mg L^{-1}	91
Fe_2O_3	*Mytilus galloprovincialis*	no significant effect was detected following exposure of embryos to Fe up to 8 mg L^{-1}	215
Fe3O4	Soil microbe community	minimal changes to microbial community, indicating limited toxicity at 1 and 5% w/w dry soil	81

NP	Species	Toxic Concentration	Ref.
Fe3O4	*D. magna*	LC_{50} ~23·10-4 mg mL^{-1}	144
Latex	*O. latipes*	Survival decreased under some conditions at 1 mg L^{-1}	218
MWCNTs	C. metallidurans CH34 and E. coli MG1655	50 – 60% viability loss at 100 mg L^{-1}	152
MWCNTs	*C. dubia, L. plumulosus* and *H. azteca*	Aqueous exposures to raw MWNTs *decreased C. dubia* viability, but such effects were not observed during exposure to functionalized MWNTs (>80 mg L^{-1}). Sediment exposures of the amphipods indicated mortality increased as particle size decreased, although raw MWNTs induced lower mortality (LC_{50} 50 to >264 g kg^{-1}) than carbon black (LC_{50} 18–40 g kg^{-1}) and activated carbon (LC_{50} 12–29 g kg^{-1}).	185
MWCNTs	*D. magna*	EC_{50} ~8.723 mg L^{-1} and LC_{50} ~22.751 mg L^{-1}	142
NiO	*C. vulgaris*	NiO NPs had severe impacts on the algae, with 72 h EC_{50} values of 32.28 mg NiO L^{-1}	71
NiO	*E. coli, B. subtilis,* and *S. aureus*	EC_{50} ranged from 121.1 – 160.2 mg L^{-1}	147
NiO	Human keratinocyte HaCaT cells, Human lung carcinoma A549 cells	The cell proliferation was completely inhibited by 50 μg mL^{-1} $Ni2+$	148
NiO	*D. pulex, D. rerio, P. kirchneriella*	LC_{50} 0.35 - >10 mg L^{-1}	55
nZVI	*I. galbana, D. tertiolecta, T. pseudonana, P. subcapitata,* and *D. magna*	Growth was suppressed between 0.4 and 12 mg L^{-1}	10*
nZVI	*E. coli*	Minimum inhibitory concentration (MIC) after 24 h was 5 mg L^{-1} for uncoated nZVI. MIC for coated nZVI ranged from 100-500 mg L^{-1}	86*
nZVI	*O. latipes*	Toxicity observed at 0.5 mg L^{-1}	216*
Sb2O3	*E. coli, B. subtilis,* and *S. aureus*	EC_{50} ranged from 144.7 – 324 mg L^{-1}	147
SiO_2	*B. subtilis* and *E. coli*	SiO_2 at 5000 mg L^{-1} resulted in 99% growth reduction of *B. subtilis*, but only 48% growth	151

NP	Species	Toxic Concentration	Ref.
		reduction of *E. coli* at 5000 mg L^{-1}	
SiO$_2$	*B. subtilis, E. coli* and *P. fluorescens*	40-70% of bacteria died at 20 mg L^{-1}	63
SiO$_2$	*Mytilus galloprovincialis*	Some negative effects at 10 mg L^{-1}	211
SiO$_2$	*Mytilus galloprovincialis*	No effect observed up to 5 mg L^{-1}	210
SiO$_2$	*Chlorella sp.*	No toxic effect observed up to 1000 mg L^{-1}	214
SWCNTs	*P. subcapitata*	Exposure to 10 mg L^{-1} CNT does negatively influence the growth of algae across most treatments. However, decreased growth was observed compared with the control.	73
SWCNTs	*D. magna*	EC$_{50}$ ~1.306 mg L^{-1} and LC$_{50}$ ~2.425 mg L^{-1}	142
SWCNTs	*A. abdita, A. bahia, L. plumulosus*	No significant mortality to any species via sediment or food matrices was observed at concentrations up to 100 ppm.	221
TiO$_2$	Microtox (bacteria), pulse-amplitude modulation (algae), Chydotox (crustaceans), and Biolog (soil enzymes)	No effects were observed up to 100 mg L^{-1}	141
TiO$_2$	*T. pseudonana,* and *S. marinoi, D. tertiolecta* and *I. galbana*	No toxic effects up to g L^{-1} concentrations	97
TiO$_2$	*B. subtilis* and *E. coli*	72% growth reduction in *E. coli* exposed to 5000 mg L^{-1} and 75% growth reduction in *B. subtilis* exposed to 1000 mg L^{-1}	151
TiO$_2$	*C. metallidurans* CH34 and E. coli MG1655	Significant loss of viability was observed after exposure to the smallest TiO$_2$ NP (10 to 25 nm) and viability decreased from 15-52% at 100 mg L^{-1}	152
TiO$_2$	RAW 264.7 and BEAS-2B cell lines	TiO$_2$ (25 ug mL^{-1}) did not elicit any adverse or protective effects	99
TiO$_2$	*P. subcapitata*	EC$_{50}$ =5.83 mg Ti L^{-1}	105
TiO$_2$	Phytoplankton and Biofilms	24 h of exposure nano-TiO$_2$ (initial concentration, 5.3mg L^{-1}) had significantly damaged cell membranes. Similar, but less damaging effects	183

NP	Species	Toxic Concentration	Ref.
		were observed in biofilms	
TiO$_2$	*B. subtilis, E. coli* and *P. fluorescens*	TiO$_2$ NPs did not affect bacterial populations	63
TiO$_2$	*V. fischeri, D. magna,* and *T. platyurus*	Not toxic even at 20 g L^{-1}	146
TiO$_2$	*D. rerio*	Not toxic up to 100 mg L^{-1}	199
TiO$_2$	*D. magna*	EC$_{50}$ ~ 35.306 mg L^{-1} and LC$_{50}$ ~ 143.387 mg L^{-1}	142
TiO$_2$	*D. magna*	LC$_{50}$ ~0.016 mg mL^{-1}	144
TiO$_2$	*D. pulex, D. rerio, P. kirchneriella*	LC$_{50}$ >10 mg mL^{-1}	55
TiO$_2$	*S. cerevisiae*	Not toxic even at 20000 mg L^{-1}	190
ZnO	*T. pseudonana,* and *S. marinoi, D. tertiolecta* and *I. galbana*	NEC 428 μg L^{-1} for S. marinoi, 233 μg L^{-1} for *T. pseudonana*. NEC for other two species around 500 - 1000 μg L^{-1}	97
ZnO	*E. coli*	Toxic in soft water at 1.2 mg L^{-1}, no toxicity observed at 100 mg L^{-1} in hard water	96
ZnO	*S. costatum, T. pseudonana, T. japonicas, E. Rapax,* and *O. melastigma*	96 hour LC$_{50}$ values ranged from 0.85 – 4.56 mg L^{-1}	98
ZnO	*B. subtilis* and *E. coli*	At 10 mg L^{-1}, ZnO resulted in 90% growth reduction of *B. subtilis* but only 48% growth reduction in *E. coli* resulted at 1000 mg L^{-1} ZnO	151
ZnO	*D. magna, T. platyurus,* and *T. thermophila*	L (E)C$_{50}$ values for nanoZnO were 1.1–16 mg Zn L^{-1}	101
ZnO	*P. subcapitata*	72-h LC$_{50}$ value near 60 μg Zn L^{-1}, attributable solely to dissolved zinc	88
ZnO	RAW 264.7 and BEAS-2B cell lines	ZnO (25 ug mL^{-1}) induced toxicity in both cells, leading to the generation of reactive oxygen species (ROS), oxidant injury, excitation of inflammation, and cell death.	99
ZnO	*P. subcapitata*	72 h EC$_{50}$ ~0.04 mg Zn L^{-1}	105
ZnO	*E. coli, B. subtilis,* and *S. aureus*	EC$_{50}$ ranged from 85.5 - >125 mg L^{-1}	147
ZnO	*E. coli*	All media exhibited strong toxicity with 3 h LC$_{50}$ at lower than 0.1 mg Zn L^{-1}.The bacterial	217

NP	Species	Toxic Concentration	Ref.
		mortality all exceeded 90% at concentrations of zinc higher than 1.0 mg L^{-1}	
ZnO	*B. subtilis, E. coli* and *P. fluorescens*	All bacteria died at 20 mg L^{-1}	63
ZnO	*V. fischeri, D. magna,* and *T. platyurus*	L(E)C$_{50}$ ~ 0.18 – 3.2 mg L-1	146
ZnO	*D. magna*	EC$_{50}$ ~ 0.622 mg L^{-1} and LC$_{50}$ ~1.511 mg L^{-1}	142
ZnO	*S. cerevisiae*	8-h EC$_{50}$ 121–134 mg ZnO L^{-1} and 24-h EC$_{50}$ 131–158 mg L^{-1}	190
ZnO	*T. thermophila*	EC$_{50}$ 5 mg L^{-1}	100
ZnO	*F. candida*	No effect up to 6400 mg kg^{-1}. Reproduction was affected at just under 2000 mg kg^{-1}	203
ZrO2	Microtox, algae, Chydotox, and Biolog	No effects were observed up to 100 mg L^{-1}	141

Chapter 2. Species Sensitivity Distributions for Engineered Nanomaterials

Engineered nanomaterials (ENMs) are a relatively new strain of materials for which little is understood about their impacts. A species sensitivity distribution (SSDs) is a cumulative probability distribution of a chemical's toxicity measurements obtained from single-species bioassays of various species that can be used to estimate the ecotoxicological impacts of a chemical. The recent increase in the availability of acute toxicity data for ENMs enabled the construction of 10 ENM-specific SSDs, with which we analyzed (1) the range of toxic concentrations, (2) whether ENMs cause greater hazard to an ecosystem than the ionic or bulk form, and (3) the key parameters that affect variability in toxicity. The resulting estimates for hazardous concentrations at which 5% of species will be harmed ranged from < 1 ug L^{-1} for PVP-coated n-Ag to >3.5 mg L^{-1} for CNTs. The results indicated that size, formulation, and the presence of a coating can alter toxicity, and thereby corresponding SSDs. Few statistical differences were observed between SSDs of an ENM and its ionic counterpart. However, we did find a significant correlation between the solubility of ENMs and corresponding SSD. Uncertainty in SSD values can be reduced through greater consideration of ENM characteristics and physiochemical transformations in the environment.

2.1 Introduction

Engineered nanomaterials (ENMs) represent a new and emerging class of pollutants but we understand relatively little about their effects in the environment. ENMs are used in a variety of consumer products including electronics, textiles, cosmetics, medicine, and food [1].

They are also used in energy, aeronautics, and military applications. The International Organization for Standardization (ISO) classifies ENMs into three main groups: (i) nanoparticles, for which all three dimensions are between 1 and 100 nm; (ii) nanoplates, for which only one dimension is between 1 and 100 nm; and (iii) nanofibers, for which two dimensions are between 1 and 100 nm.[225] Seven major classes of ENMs are carbonaceous nanomaterials (e.g. CNTs), semiconductors (ex. Quantum dots), metals (ex. n-Ag), metal oxides (ex. TiO_2), nanopolymers (ex. dendrimers), emulsions (ex. acrylic latex), and nanoclays. Various ENMs exist as single, aggregated, or agglomerated particles and can be manufactured with different shapes, coatings, and surface functionalities. Additionally, some ENMs dissolve in the environment, which can result in toxic effects similar to those of the dissolved ion, while other ENMs may not dissolve. In the latter case, toxic effects are usually related to ENM size, reactivity, and coating,[226] resulting in toxicity from the ENM that can exceed that of the ionic or bulk form signifying a nanotoxic effect.[227]

ENMs are released into the environment either during their use, through spillages, by intentional release for environmental remediation applications, or as end-of-life waste.[4] Increasing production and use of ENMs enhances the potential for release into the environment, thus increasing environmental exposures and incentives to better understand and quantify the ecosystem impacts of ENMs.[228] Substantial effort is now being made to quantify releases, exposures, and toxicity of ENMs throughout their industrial lifecycle.[3,229,230]

A few studies have developed preliminary estimates of the range of ENM exposure concentrations[8,29,228] and the few environmental concentrations that have been measured empirically fall within the same order of magnitude as those predicted by models.[90,229,231,232]

50

What we do not yet adequately understand is the impacts of exposure to biological receptors under natural environmental conditions. To provide predictions of the potential biological impacts in nature the relatively large volume of information from laboratory toxicity tests with ENMs can be used to generate Species Sensitivity Distributions (SSDs), which model the range in sensitivities of different species to a wide range of ENMs.[233] SSDs provide an estimate of the potentially affected fraction (PAF) of species that will be harmed from exposure to ENMs, and are used to establish threshold concentrations, which, when exceeded, indicate that management actions should be taken. For example, the lower 5th percentile of the SSD indicates that 95% of species are not impacted by a pollutant and thus, hypothetically, provides environmental concentrations that are expected to safeguard most species, and thus an ecosystem's structure and function.[233] While our understanding of ENM toxic effects is still relatively limited, progress is being made in determining toxic concentrations for a wide-variety of both terrestrial and aquatic species.

Single species toxicity data from multiple species can be combined to predict the exposure concentrations at which a percent of species in an ecosystem will be affected.[13] Specifically, SSDs are models of the variation in sensitivity of species to a particular stressor,[233] and are generated by fitting a statistical or empirical distribution function to the proportion of species affected as a function of stressor concentration or dose. Traditionally, SSDs were created using data from single-stressor laboratory toxicity tests, such as median lethal concentrations (LC_{50}). The key assumption in applying SSDs is that the species toxicity data represent a random sample from a statistical distribution that is representative of a community or ecosystem, with the idea that limited toxicity testing of only a handful of species can allow us to extrapolate to a community level of risk associated with a specific

toxicant. As more data become available for various species, the accuracy of SSDs in predicting ecosystem toxicity effects will increase.

Many SSDs have been developed for a variety of organic and inorganic pollutants[234,235] with many focused on pesticides[236–239] and herbicides.[240,241] There are a few examples of SSDs constructed specifically for metals. SSD and the corresponding predicted hazardous concentration at which no species are harmed (HC_0) and at which 5% of species are harmed (HC_5) were created for zinc for aquatic species with the goal of finding the best cumulative distribution function.[242] SSDs have also been developed for specific taxonomic groups for copper to estimate acute-chronic ratios for different taxa.[243] An acute toxicity SSD was developed for mercury to estimate HC_5 and the predicted no effect concentration (PNEC) for freshwater species.[244] SSDs can also be used in life cycle assessments (LCAs) to determine characterization factors (CFs) for ecotoxicity.[245,246] CFs for toxic pollutants are substance-specific, quantitative factors that convert life-cycle emissions of toxic substances to the common unit of the toxic impact indicator.[247] As LCAs are being developed for nanoparticles, SSDs can provide the information on PAF needed to calculate the CF.[247–249]

SSDs are used in ecological risk assessment to derive maximum acceptable concentrations of pollutants in the environment from a limited set of laboratory based ecotoxicity data.[238,244,245] The utility of an SSD depends on the quality and relevance of the data used, which usually are secondary data taken from literature or a database. The objective of this study is to develop SSDs for as many nanoparticles as possible and to determine if, according to the SSDs, the ENMs cause greater toxicity than the ionic or bulk form. The results of this work can be used to begin to make judgments regarding the risk of using and releasing different ENMs into the environment.

2.2 Methods

Data were collected from >300 published articles that explicitly provided single species toxicity data including median lethal concentration (LC_{50}), half maximal effect concentration (EC_{50}), median lethal dose (LD_{50}), lowest observed effect concentration (LOEC), no observed effect concentration (NOEC), and the half maximal inhibitory concentration (IC_{50}). If a published article did not specifically state one of these values, even if they provided dose-response curves, the information was not used in our analysis. Our initial search did not limit the types of nanoparticles that could be included, as we needed to determine the extent of available data across both environmental media and ENMs. Not all ENMs or environments had enough data points to create an SSD. However, as research progresses and more data become available, they can be combined with the data provided in Appendix Table A2.1 to create improved SSDs.

While there was sufficient data to build SSDs from EC_{50} values, there were more data available across all types of ENMs to build SSDs using LC_{50} values. These studies varied in length from 15-minute to 28-day exposures depending on the species and end-points. We elected not to account for the time range by using dose as our SSD metric because concentration is the standard metric used in SSDs. In addition, because the data cover a range of species with very different life histories and life spans, dose is not always a comparable metric.

SSDs are frequently based on chronic, sub-lethal toxic effects because exposure to toxins in the environment is typically at low concentrations over the long term. However, we only had sufficient data to develop SSDs for acute freshwater toxicity because of the limited data available in both marine and terrestrial toxicity and the limited number of studies conducted

to date on chronic ENM toxicity.[248–251] In some cases, short term toxicity data can make use of an extrapolation factor to accurately describe the chronic SSD.[149,252] One approach for converting data from acute to chronic is to simply use a factor of 10 [i.e., a left shift of SSD based on LC_{50} to obtain an SSD for the no observed effect concentration (NOEC)].[252] Another study found that using an acute to chronic ratio ranging from 1.6 to 4.4 was more accurate.[149] We determined that there is not yet sufficient evidence to implement a conversion factor based on data available for ENMs.

We also collected toxicity data on freshwater species for both the ions of the associated metals and nominal data on bulk particles to compare to the ENM data. We did this by reviewing data collected for the ENMs where comparative tests were often done on ionic or bulk equivalents, through a general literature review, and querying the EPA's ECOTOX database by compound. We limited the search to studies completed in a lab as opposed to field research so as to match the ENM dataset, in freshwater systems that reported LC_{50} values.

To build SSDs, we implemented the Species Sensitivity Distribution Generator, provided by the Environmental Protection Agency (EPA), which has been used for many other chemicals.[203,240,253–255] The process requires a list of exposure intensities at which different species exhibit a standard response to a stressor. The reported LC_{50} values are then ranked and plotted along the x-axis. The cumulative probability, calculated as the fraction of species affected at a certain concentration, is plotted along the y-axis, along with the 95% confidence interval, using a probability density function (PDF). We then calculated the hazardous concentration at which 5% of species will likely be harmed (HC_5),[247] indicating that 95% of species in an ecosystem will be protected provided that the environmental

54

concentration remains below that associated with the HC_5. A minimum of four data points are needed to generate an SSD, though the predictive power of SSD models greatly increased with 10 or more data points from published studies.[90,245,247] Our ENM SSD data varied from 8 – 64 data points from published studies covering a range of species, though they did not always include a wide range of taxa, which is also preferred when creating a SSD.[233]

2.3 Results

A comprehensive review of the literature on Web of Knowledge and Google Scholar using a range of search terms to cover all types of ENMs, environments, toxicity tests, and species resulted in over 300 studies, although only 101 studies reported data adequate in quality for our analysis (Appendix Table A2.1). Sufficient data were collected to build SSDs for uncoated n-Ag, PVP-coated n-Ag, n-Al_2O_3, n-C_{60}, CNTs, n-Cu, n-CuO, n-TiO_2, and n-ZnO using acute LC_{50} values. For n-CeO_2, we collected sufficient data to build an SSD using only acute EC_{50} values.

The SSD for uncoated n-Ag (Figure 2.1) indicates that the ENM was toxic to some species at ug L^{-1} concentrations, while other species tolerate concentrations three or more orders of magnitude higher, at g L^{-1} concentrations with a range of one order of magnitude for the 95% confidence interval (shown in grey around the curve in Figure 2.1).
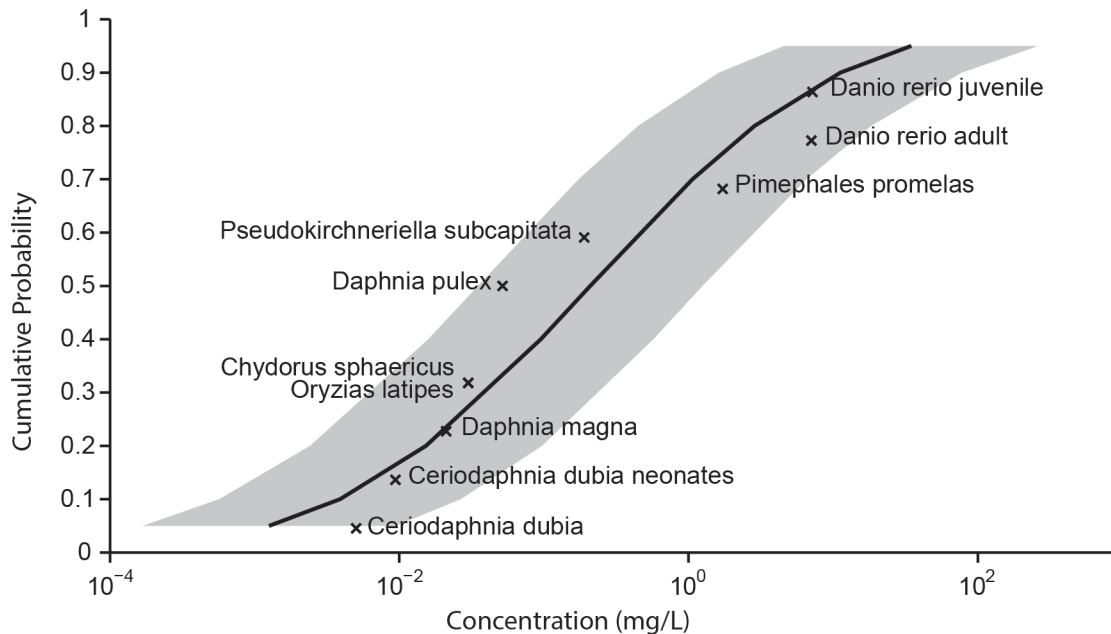
Figure 2.1 Species Sensitivity Distribution for uncoated n-Ag, Based on 10 Species

We constructed separate SSDs for PVP-coated n-Ag (Appendix Figure A2.1) and ionic silver from either AgCl or AgNO$_3$ (Appendix Figure A2.2). Ag$^+$ derived from dissolving AgNO$_3$ was considerably more toxic than when AgCl was used, but given that the toxicity is probably due to metal ion exposure rather than the salt, we chose to combine the datasets to develop a more robust SSD. The ENM SSDs were then compared to the Ag$^+$ ion SSD to determine whether the toxicities varied (Figure 2.2). While Ag$^+$ is generally more toxic than coated or uncoated n-Ag, at low exposure concentrations, there are only minor differences between Ag-PVP and Ag$^+$. For most species, uncoated n-Ag was considerably less toxic than PVP-coated Ag, most likely due to increased aggregation and reduced bioavailability.[246] Uncoated n-Ag has a higher toxicity threshold than Ag$^+$, particularly at higher exposure concentrations.
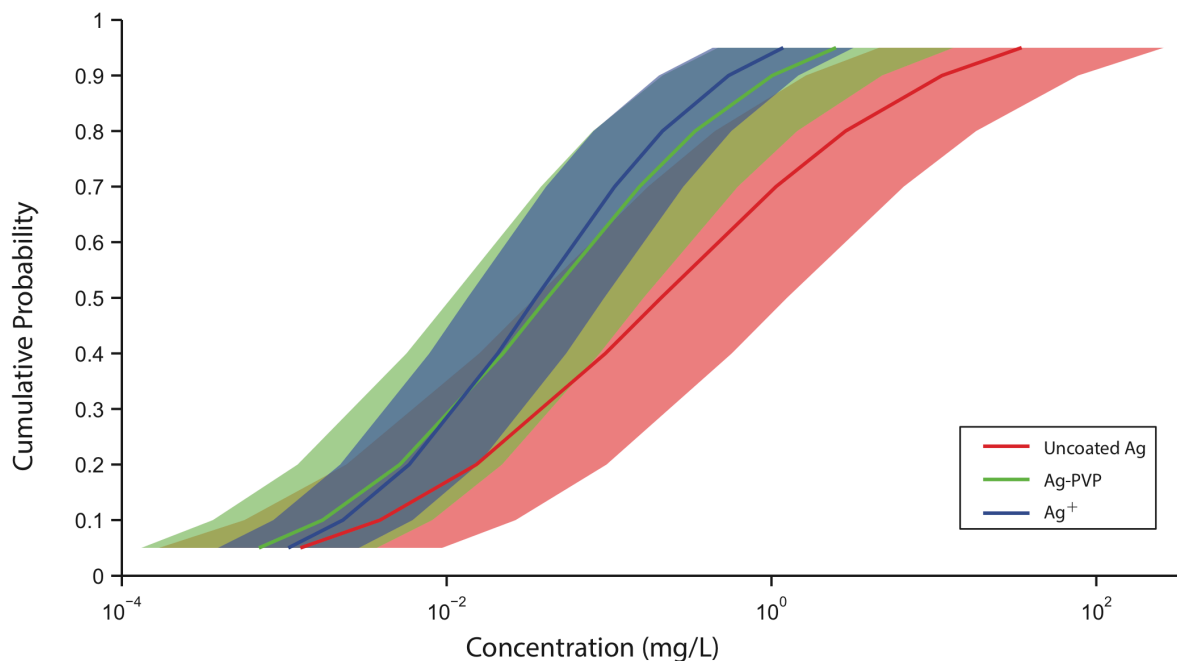
Figure 2.2 Comparison of Silver SSDs, including uncoated n-Ag, PVP-coated n-Ag, and Ag$^+$ Derived from Dissolving AgCl and AgNO$_3$

We then constructed SSDs for two copper nanoparticles, n-Cu (Appendix Figure A2.3) and n-CuO (Appendix Figure A2.4), and Cu^{2+} derived from combining toxicity endpoints for CuCl$_2$, Cu(NO$_3$)$_2$ and CuSO$_4$ (Appendix Figure A2.5). The difference in Cu^{2+} toxicity between the various copper salts was smaller than observed for the silver salts (Appendix Figure A2.5), possibly due to the larger number of data points for each Cu^{2+} SSD. However, the toxicity threshold was significantly lower for Cu^{2+} from CuCl$_2$ than from Cu(NO$_3$)$_2$ and CuSO$_4$. A comparison of the nano and ionic copper SSDs indicated that the toxicity thresholds for n-CuO were much higher than for n-Cu or Cu^{2+} (Figure 2.3). Additionally, the difference between the SSDs for n-Cu and Cu^{2+} was smaller than between n-CuO and Cu^{2+}, with n-CuO consistently less toxic than either n-Cu or Cu^{2+}. As expected, given the much smaller number of data points for the two nanoparticles, the confidence intervals were much

wider than for Cu^{2+}. The lower toxicity of n-CuO in freshwater may reflect its slower dissolution at low ionic strength and in the presence of organic matter (present in any aquatic system with biota).[256]
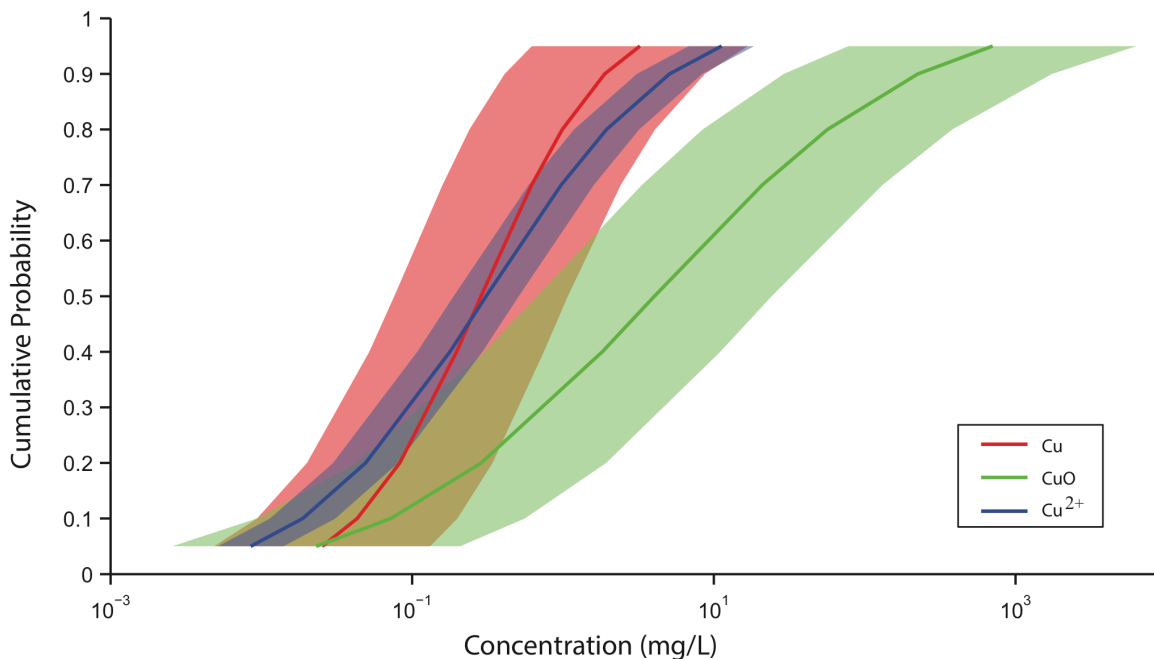
Figure 2.3 Comparison of Copper SSDs, including n-Cu, n-CuO, and Cu^{2+} Derived from Dissolving CuCl$_2$, Cu(NO$_3$)$_2$ or CuSO$_4$

For zinc, we compared n-ZnO (Appendix Figure A2.6), bulk ZnO (Appendix Figure A2.7), and Zn^{2+} derived from ZnCl$_2$ and ZnSO$_4$ (Appendix Figure A2.8). There were minimal differences in the SSDs for Zn^{2+} derived from ZnCl$_2$ and ZnSO$_4$. A comparison shows that the SSDs for n-ZnO and Zn^{2+} are nearly identical, and that of bulk ZnO is also similar (Figure 2.4), indicating that for this ENM most of the toxicity is due to dissolved Zn^{2+}. There was little statistical difference between the three lines because the small sample size results in low statistical power.
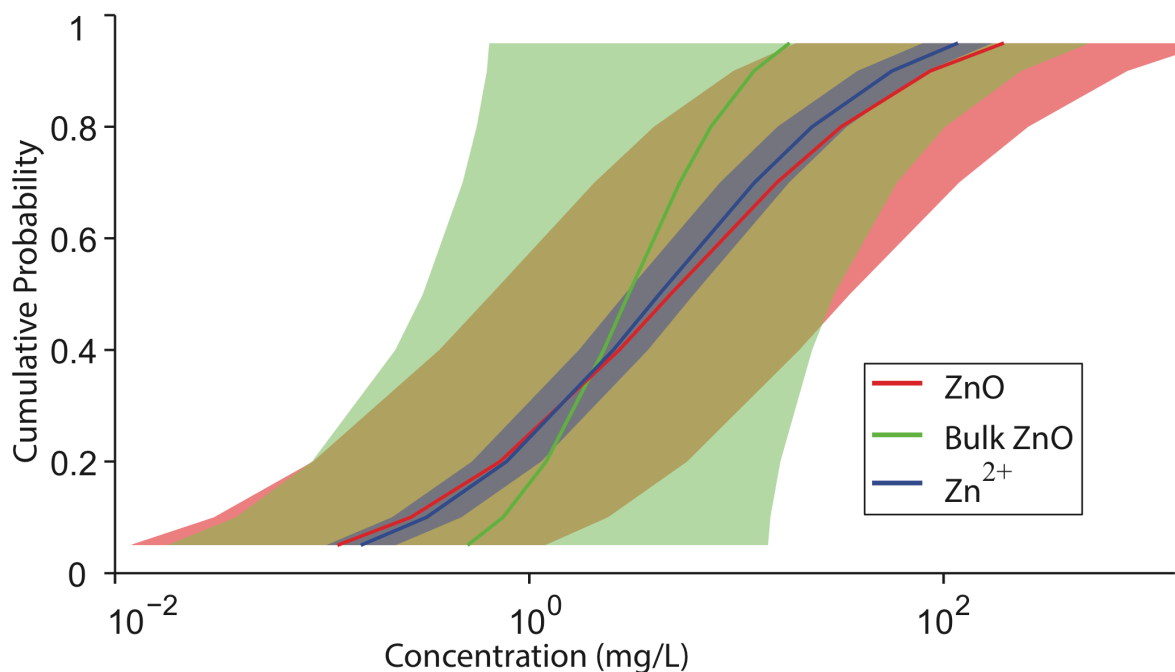
Figure 2.4 Comparison of Zinc SSDs, including ZnO, bulk-ZnO, and Zn^{2+} Derived from Dissolving ZnCl$_2$ and ZnSO$_4$

The SSDs of n-Al$_2$O$_3$ (Appendix Figure A2.9) and Al^{3+} (Appendix Figure A2.10) indicate that except at high concentrations, n-Al$_2$O$_3$ is less toxic that Al^{3+} (Appendix Figure A2.11). There are some difference in toxicity between Al^{3+} derived from AlCl$_3$ and Al$_2$(SO$_4$)$_3$ (Appendix Figure A2.10), with AlCl$_3$ slightly more toxic than Al$_2$(SO$_4$)$_3$, although there is overlap in their confidence intervals which are broad due to the lower number of data points. For n-CeO$_2$ (Appendix Figure A2.12) and n-TiO$_2$ (Appendix Figure A2.13) n-CeO$_2$ appears to be more toxic than n-TiO$_2$ (Appendix Figure A2.14), even though n-TiO$_2$ has shown phototoxicity while n-CeO$_2$ generally quenches photoactivity. A recent review of n-CeO$_2$ provides a more detailed analysis of the behavior and toxicity of this nanomaterial.[257]

We collected sufficient data to develop SSDs for two carbonaceous nanomaterials, n-C$_{60}$ (Appendix Figure A2.15) and CNTs (Appendix Figure A2.16), though not enough to create

distinct SSDs for single-walled carbon nanotubes (SWCNTS) or multi-walled carbon nanotubes (MWCNTs). Overall n-C_{60} is more toxic than CNTs, with overlap in the confidence intervals only in the higher concentrations (Figure 2.5). C_{60} has a notably lower toxicity threshold than CNTs. It is important to note that CNTs have a very wide range of properties (e.g. tube diameter, tube length, surface functionalization, residual metals, chirality) that complicate the analysis. As more toxicity information becomes available, separate SSD may be needed for different classifications of CNTs.
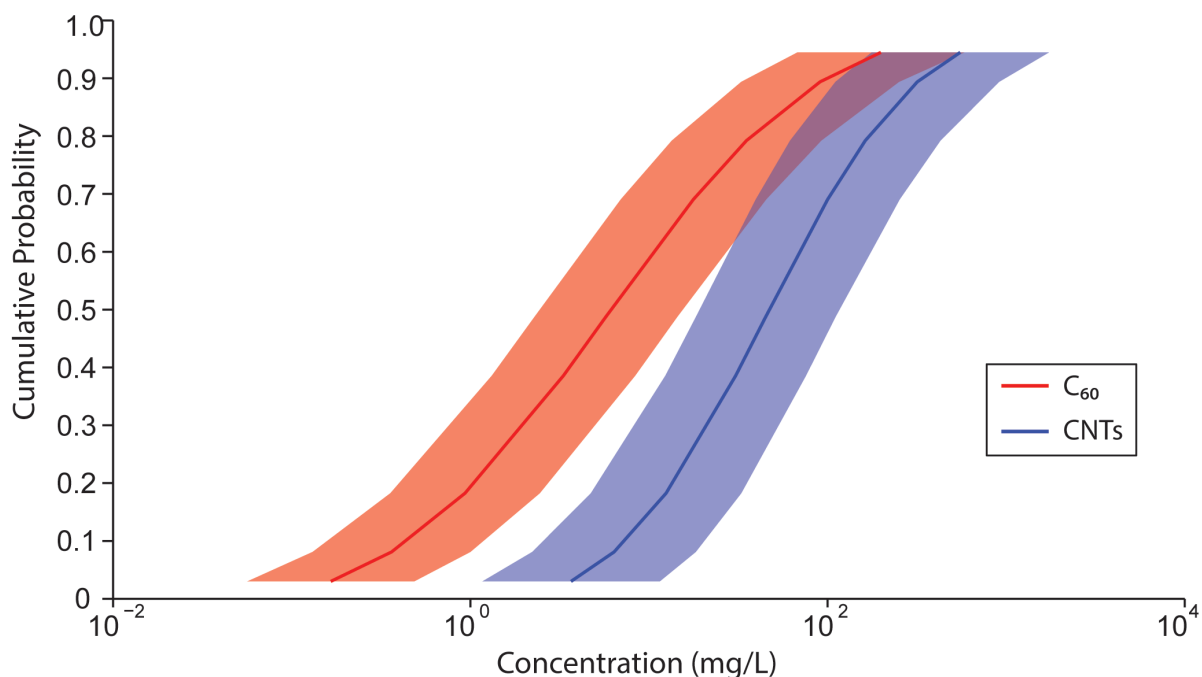
Figure 2.5 Comparison of Carbonaceous Nanoparticle SSDs, including n-C_{60} and CNTs

One approach for considering the relative toxicity of the ENMs is to compare their HC_5. For the ENMs considered in this study, HC_5 values range over four orders of magnitude (from <1 ug L^{-1} for silver nanoparticles to >3.5 mg L^{-1} for CNTs) (Figure 2.6). The results confirm the hypothesis that nanoparticle solubility, with the corresponding release of metal ions, is a strong predictor of toxicity, as seen for n-Ag, n-ZnO, n-Al_2O_3 and nano-copper

compounds. For Ag and Zn there was little to no difference between the mean of the HC_5 for a nanoparticle and the HC_5 for the corresponding metal ion. For Cu and Al, the differences are more significant, reflecting the slower dissolution rates of these nanomaterials, particularly Al_2O_3. For the ENMs that are less likely to dissolve (C_{60}, CNTs, CeO_2, and TiO_2) the HC_5 values range from $0.1 - 10$ mg L^{-1}, which are concentrations that are less likely to be encountered, on average, in aquatic systems based on recent estimates.[8,228,232] The breadth of the range is largely a result of availability of data; compounds with more data generally had a much smaller range than those with fewer data available.
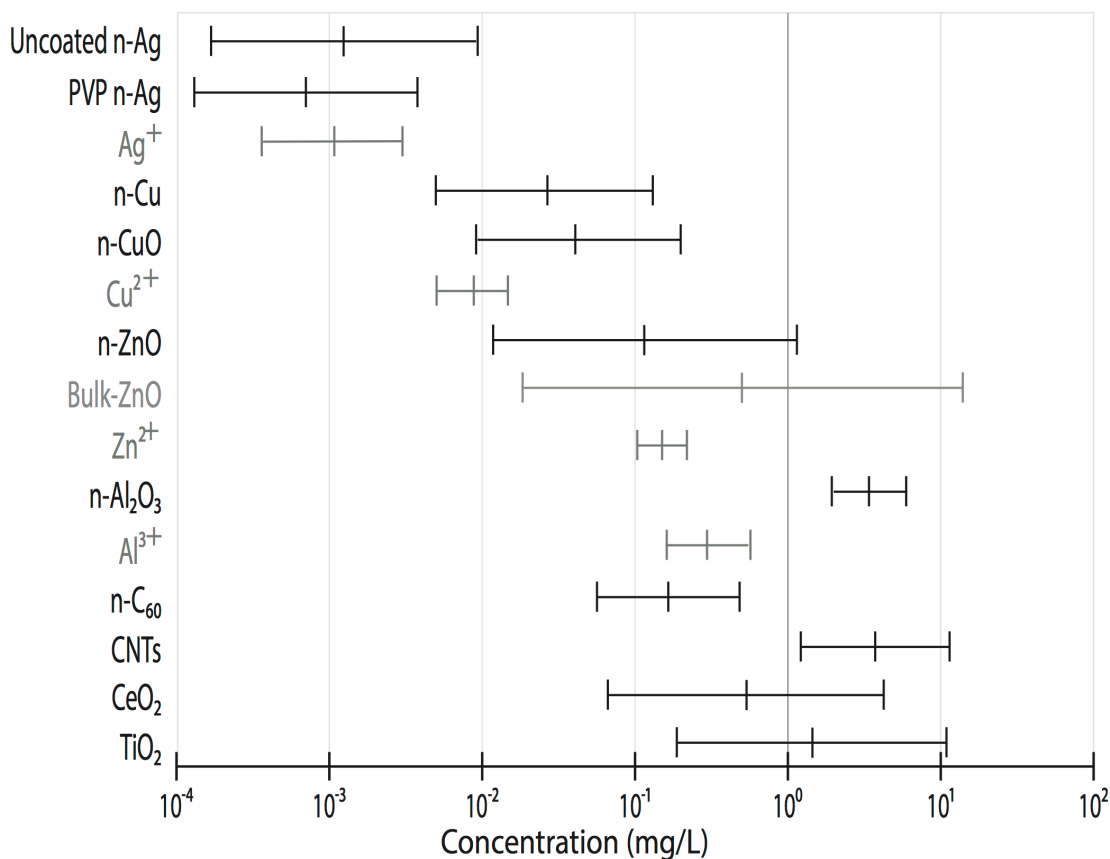
Figure 2.6 Mean and 5th and 95th Percentile HC_5 for Nanomaterials in Black and Corresponding Ions in Grey

2.4 Discussion

ENMs are released into the environment at various stages during their life-cycle, but our understanding of the environmental implications is still quite limited.[226] Our results serve to identify concentrations of concern for various ENMs with regard to freshwater ecological toxicity. While these SSDs are preliminary estimates, they represent the first attempt at predicting the PAF of species at various exposure concentrations in the aquatic environment for multiple ENMs. Exposure models that estimate the exposure of individuals or populations can be compared with the HC_5 values estimated here to predict the ecotoxicological effects of ENMs and give an idea of how significant the risk associated with their use could be.

When working with ENMs, consideration must be made for the various possible configurations (e.g., size, shape, charge, and presence of a coating or functional group) that can all alter chemical behavior in the environment and impact toxicity.[226] For example, if two different Ag nanoparticles have different primary diameters and one is spherical while the other is cubic, the LC_{50} values for each could be as different as if they were entirely different chemicals (See Table A2.1 for examples). In addition, transformations of the ENM during toxicity tests,[10,256] or the presence of species that can alter how ENMs interact with biota, can influence the outcomes of single species laboratory assays.[224,258] Thus, it is important to take into consideration both ENM characteristics and possible environmental transformations that increase the uncertainty and reliability in toxic outcomes that underlie the SSDs. As such, it would be preferable to separate ENMs by type and structure as well as dispersion media before building SSDs from the data. Given data limitations, we were only able to do this for uncoated versus PVP-coated n-Ag (Figure 2.2). We did not have quite

enough data to also build a separate SSD for citrate-coated n-Ag, which would have improved our understanding of how toxicity is affected by the presence of a coating. There was also insufficient data to separate particles by size group (e.g., 1-10 nm, 10-50 nm, and 50-100 nm). The accuracy of the SSDs will likely improve by incorporating some of these distinctions. For example, the SSD for uncoated n-Ag and PVP-coated n-Ag are statistically different at the higher exposure concentrations, but this distinction would not have been clear had we combined all the Ag ENMs into one SSD (Figure 2.2). Because we only have limited examples of each ENM variable, our conclusions are limited in their strength. However, as more data become available to separate ENMs into clearly defined physico-chemically distinct groups (e.g. those based on size, shape, or coating) when developing SSDs, we will better be able to distinguish between the extent of toxic effects as physico-chemical characteristics are altered.

The accuracy and utility of an SSD depends on the quality and relevance of the data used, which in this case are secondary data taken from literature and the ECOTOX database. Ideally, an SSD should be not generated from the synthesis of results from experiments that used a wide variety of protocols, for example, by combining impacts from chronic sub-lethal effects on reproduction with the impacts on survival or with acute lethal test results, all of which are commonly reported toxicity endpoints.[254] This limits the generation of SSDs for ENMs, especially for aquatic species where there is a bias towards acute mortality data, despite the likelihood that chronic sub-lethal effects may have enormous impacts on the individual survival and reproduction, of populations and thus population abundance and persistence.[259] This is in part due to the difficulty in maintaining a constant state and concentration of a nanoparticle in an aquatic experiment over the long term. As such, we

limited our study to short term acute toxic effects due to the scarcity of chronic toxicity information. More useful SSDs would be generated for each ENM using a variety of species, for instance those that vary in their sensitivity across a range of taxa and trophic levels, for a specific ecosystem or region of concern. Distinguishing SSDs between early and late life stages of a species would also be useful as the values can differ in sensitivity with each life stage. While there are a reasonable number of species represented in these SSDs, the diversity in taxa and life stage is not comprehensive. It is important to recognize the uncertainty associated with our results as the range of sensitivities of the species we included is quite variable from ENM to ENM, and no SSD was constructed with enough species to represent a comprehensive ecosystem. Despite these limitations, our results are useful in gauging and comparing the ecotoxicological impact of different ENMs. Useful next steps would include generating SSDs for ENMs based on chronic toxicity data, [254,260,261] and developing a robust framework for predicting long-term effects on populations, communities, or ecosystems.

2.5 Appendices

Table A2.1 Data on all nanoparticles for all toxicity endpoints

Available in Excel Spreadsheet. References include: [55,88,95,96,98,100,101,105,141,142,144–146,149,150,153,185,190,192,203,217,252,253,262–292,292–341]
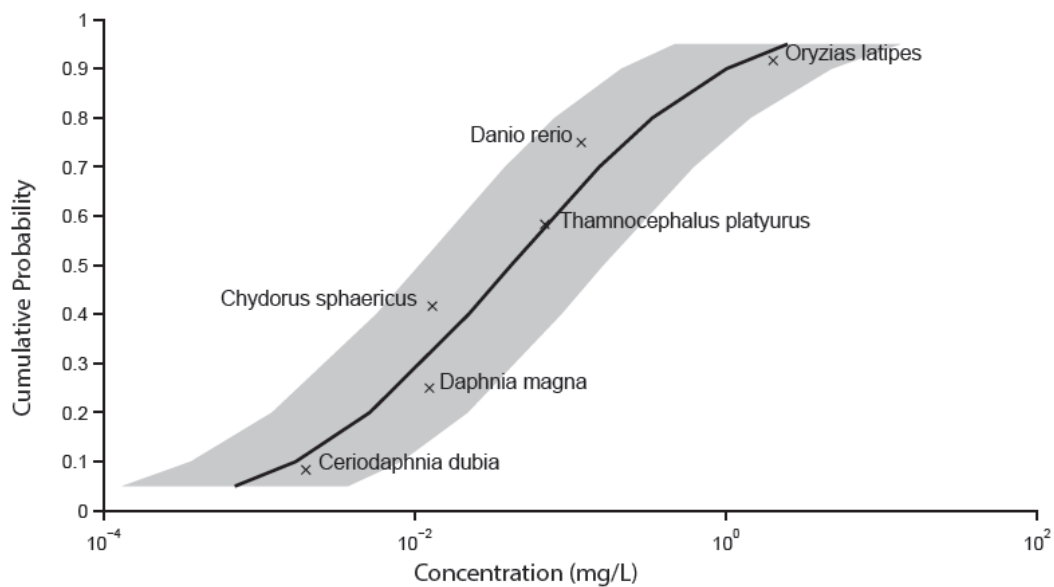


Figure A2.1 SSD for PVP-coated n-Ag
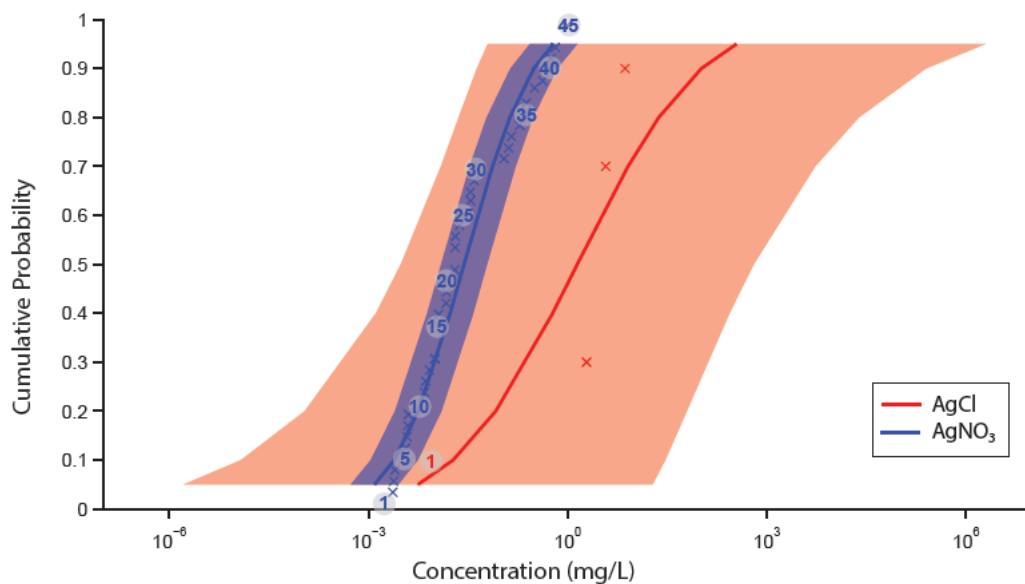
Figure A2.2 Comparison of SSDs for AgCl and AgNO₃

Figure A2.2 is a comparison of SSDs for AgCl and AgNO$_3$ to determine whether it was appropriate to combine compounds when creating an SSD for Ag$^+$. The numbers correspond to Table A2.2 where we have provided a list of the species in rank order that were used to build each SSD. There are cases where multiple species hold the same rank, in which case the x can represent multiple species.

Table A2.2 List of Species in Rank Order used to Build Silver Ion SSD

AgCl	Species	AgNO$_3$	Species
1	*Lepidocephalichthys guntea*	1	*Daphnia pulex*
	Pimephales promelas		*Daphnia magna*
	Daphnia magna		*Hyalella azteca*
	Culicoides furens		*Leuctra sp.*
	Chironomus plumosus	5	*Leptophlebia sp.*
			Ceriodaphnia dubia
			Fundulus heteroclitus
			Stenonema modestum
			Gammarus pulex
		10	*Isonychia bicolor*
			Duttaphrynus melanostictus
			Cambarus diogenes
			Radix luteola
			Daphnia pulex
		15	*Lithobates pipiens*
			Lithobates palustris
			Gastrophryne carolinensis
			Spirostomum ambiguum
			Pimephales promelas
		20	*Ictalurus punctatus*
			Oncorhynchus mykiss
			Puntius sophore
			Rana catesbeiana
			Carassius auratus
		25	*Jordanella floridae*
			Poecilia reticulata
			Gambusia affinis
			Euphlyctis hexadactylus
			Channa punctata
		30	*Anguilla*
			Nephelopsis obscura
			Actinonaias pectorosa
			Micropterus salmoides
			Lepomis macrochirus

| | 35 | *Aplexa hypnorum* |
		Pseudokirchneriella subcapitata
		Bufo woodhousei ssp. fowleri
		Ambystoma opacum
		Psephenus herricki
	40	*Tanytarsus dissimilis*
		Oryzias latipes
		Orconectes immunis
		Danio rerio
		Chironomus tentans
	45	*Caenorhabditis elegans*
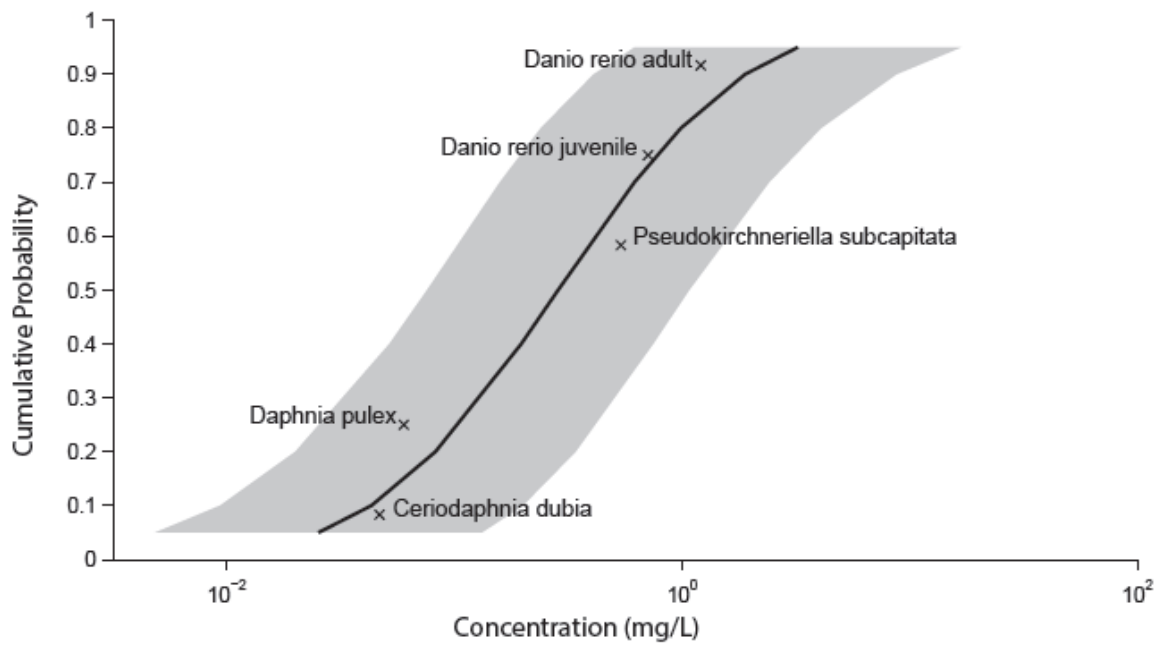
**Figure A2.3 SSD for n-Cu**
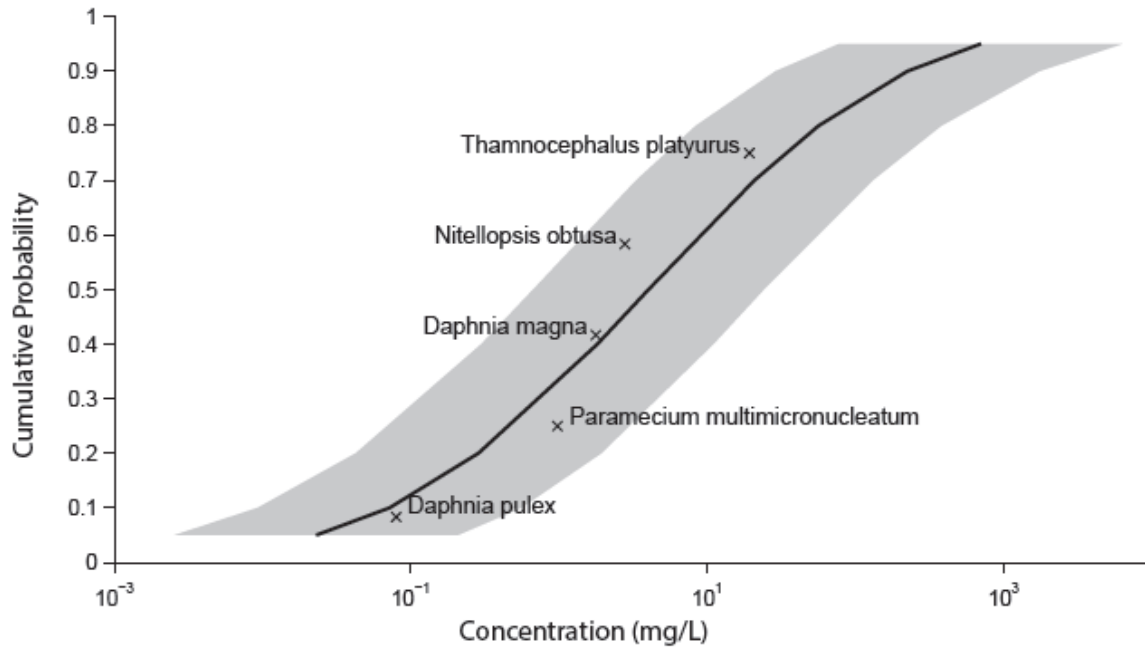
Figure A2.4 SSD for n-CuO
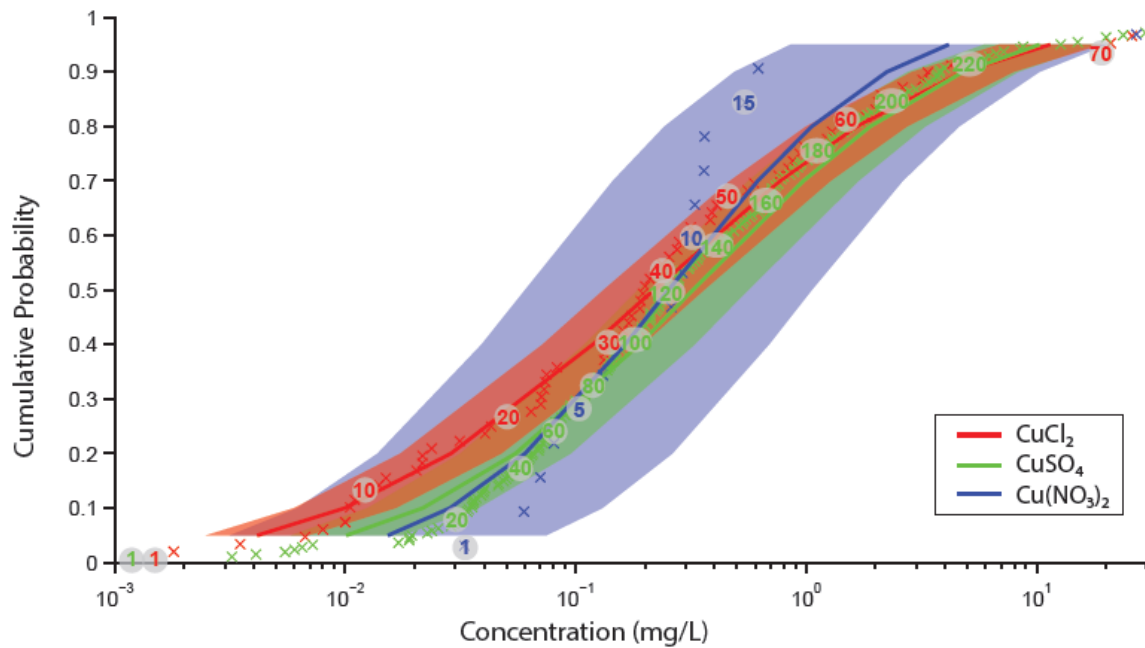
Figure A2.5 Comparison of SSDs for CuCl2, Cu(NO$_3$)$_2$, and CuSO$_4$

Figure A2.5 is a comparison of SSDs for CuCl$_2$, Cu(NO$_3$)$_2$, and CuSO$_4$ to determine whether it was appropriate to combine compounds when creating an SSD for Cu^{2+}. The

numbers correspond to Table A2.3 where we have provided a list of the species in rank order that were used to build each SSD.

**Table A2.1 List of Species in Rank Order used in Copper Ion SSD**

CuC$_2$	Species	Cu(NO$_3$)$_2$	Species	CuSO$_4$	Species
1	Blepharisma americanum	1	Hyalella azteca	1	Cirrhinus mrigala
	Drepanomonas revoluta		Pimephales promelas		Villorita cyprinoides ssp. cochiensis
	Spirostomum teres		Biomphalaria glabrata		Daphnia magna
	Moina irrasa		Utterbackia imbecillis		Daphnia similis
	Fluminicola virens	5	Ceriodaphnia dubia		Prosopium williamsoni
	Halteria grandinella		Gambusia affinis		Spirostomum ambiguum
	Euplotes aediculatus		Pseudambassis ranga		Daphnia ambigua
	Paramecium caudatum		Lumbriculus variegatus		Ceriodaphnia dubia
	Euplotes patella		Cyprinus carpio		Thymallus arcticus
10	Colpidium campylum	10	Etroplus maculatus		Craterocephalus stercusmuscarum
	Uronema nigricans		Gammarus pulex		Brachionus rubens
	Juga plicifera		Oreochromis mossambicus		Hydra viridissima
	Ptychocheilus oregonensis		Danio rerio		Dreissena polymorpha
	Ceriodaphnia dubia		Daphnia magna		Moina macrocopa
	Oncorhynchus mykiss	15	Lepomis macrochirus		Macrobrachium rude
	Oncorhynchus tshawytscha		Chironomus tentans		Posthodiplostomum minimum
	Daphnia magna				Paratya compressa ssp. improvisa
	Daphnia pulex				Oncorhynchus clarkii ssp. stomias
	Chironomus riparius				Cyclops viridis
20	Colpidium colpoda			20	Daphnia carinata
	Euplotes affinis				Acrossocheilus paradoxus
	Oreochromis niloticus				Medionidus conradicus
	Eurytemora affinis				Fusconaia masoni
	Hexagenia sp.				Oncorhynchus kisutch
	Scapholeberis sp.				Physastra gibbosa
	Ephoron virgo				Lampsilis teres
	Corophium sp.				Brachionus calyciflorus
	Gammarus pulex				Spirostomum teres
	Oncorhynchus kisutch				Lampsilis fasciola
30	Gammarus sp.				Stenocypris major
	Acrocheilus alutaceus				Streptocephalus texanus
	Tubifex				Prochilodus scrofa
	Dexiotricha granulosa				Lampetra tridentata

69

	Gammarus italicus				Tubifex
	Nitocra spinipes				Utterbackia imbecillis
	Chydorus sphaericus				Alosa sapidissima
	Aspidisca cicada				Villosa vibex
	Brachionus patulus				Actinonaias pectorosa
	Hyalella azteca				Daphnia pulex
40	Corbicula manilensis			40	Oncorhynchus tshawytscha
	Rhinella arenarum				Etheostoma fonticola
	Cyprinus carpio				Moinodaphnia macleayi
	Pila globosa				Pomacea paludosa
	Dreissena polymorpha				Lampsilis straminea ssp. claibornensis
	Trochilia minuta				Hyalella azteca
	Ambystoma jeffersonianum				Lymnaea acuminata
	Pimephales promelas				Ichthyophthirius multifilis
	Chilodonella uncinata				Oncorhynchus clarkii ssp. henshawi
	Enchytraeus buchholzi				Villosa iris
50	Tilapia zillii				Euphlyctis hexadactylus
	Echinogammarus berilloni				Daphnia longispina
	Anguilla japonica				Cottus bairdi
	Cyrnus trimaculatus				Physella gyrina
	Chironomus tentans				Potamopyrgus jenkinsi
	Panagrellus silusiae				Mesocyclops pehpeiensis
	Hydropsyche angustipennis				Epioblasma capsaeformis
	Oryzias latipes				Candidia barbatus
	Lepomis macrochirus				Streptocephalus rubricaudatus
	Nemata				Branchiura sowerbyi
60	Euplotes sp.			60	Hydra vulgaris
	Aspidisca lynceus				Macrobrachium sp.
	Chlorella vulgaris				Pyganodon grandis
	Vorticella sp.				Erimonax monachus
	Culicoides furens				Galaxias maculatus
	Echinogammarus tibaldii				Danio rerio
	Chironomus plumosus				Morone sp.
	Parreysia cylindrica				Acipenser oxyrhynchus
	Oreochromis mossambicus				Radix luteola
70	Chironomus maddeni				Macrobrachium carcinus
	Pristionchus sp.				Cyprinus carpio ssp. communis
	Caenorhabditis elegans				Acipenser brevirostrum
	Oziotelphusa senex				Notropis mekistocholas

ssp. senex			*Thamnocephalus platyurus*
Notemigonus crysoleucas			*Tetrahymena pyriformis*
Panagrellus redividus			*Barbus gonionotus*
			Bellamya bengalensis
			Bufo boreas ssp. boreas
			Epidalea calamita
		80	*Paratya australiensis*
			Cnesterodon decemmaculatus
			Melanotaenia nigrans
			Rhithrogena hageni
			Etheostoma rubrum
			Lasmigona subviridis
			Gammarus pulex
			Penaeus chinensis
			Anaxyrus boreas
			Radix natalensis
			Bidyanus
			Chironomus plumosus
			Odontesthes bonariensis
			Oncorhynchus gilae ssp. apache
			Macquaria ambigua
			Hediste diversicolor
			Caridina africana
			Biomphalaria glabrata
			Anodonta imbecillis
			Streptocephalus proboscideus
		100	*Catostomus latipinnis*
			Caridina nilotica
			Leporinus obtusidens
			Drunella grandis
			Gambusia affinis
			Morone saxatilis
			Brotia sp.
			Ctenopharyngodon idella
			Lumbriculus variegatus
			Corbicula manilensis
			Ambassis sp.
			Lithobates sphenocephalus ssp. sphenocephalus
			Poeciliopsis occidentalis
			Melanotaenia splendida ssp. inornata
			Onychostoma barbata
			Tilapia guineensis
			Macrobrachium

		rosenbergii
		Scaphirhynchus platorynchus
		Oncorhynchus mykiss
		Hyalella sp.
	120	*Hyalella curvispina*
		Physella acuta
		Hybognathus amarus
		Poecilia vivipara
		Etheostoma lepidum
		Dugesia dorotocephala
		Girardia tigrina
		Duttaphrynus melanostictus
		Planorbella trivolvis
		Gila elegans
		Daphnia lumholtzi
		Ceriodaphnia rigaudi
		Macrobrachium lamarrei
		Etheostoma flabellare
		Melanotaenia splendida ssp. splendida
		Gammarus fasciatus
		Canthocamptus sp.
		Jenynsia multidentata
		Elimia livescens
		Carassius auratus
	140	*Anguilla japonica*
		Planorbis
		Gasterosteus aculeatus
		Danio malabaricus
		Ptychocheilus oregonensis
		Etheostoma nigrum
		Xyrauchen texanus
		Ptychocheilus lucius
		Rasbora daniconius neilgeriensis
		Clarias gariepinus
		Pimephales promelas
		Cyprinodon variegatus
		Perca fluviatilis
		Noemacheilus montanus
		Biomphalaria alexandrina
		Aphelenchus avenae
		Ictalurus furcatus
		Peprilus triacanthus
		Bulinus globosus
		Hoplobatrachus tigerinus
	160	*Viviparus bengalensis*

		Chironomus decorus
		Xenopus laevis
		Macrobrachium dayanum
		Diacypris compacta
		Lymnaea stagnalis
		Morone saxatilis ssp. x chrysops
		Rutilus
		Uronema marinum
		Cephalobus persegnis
		Palaemonetes paludosus
		Diaphanosoma brachyurum
		Bulinus tropicus
		Aspidisca cicada
		Colisa fasciata
		Lepomis macrochirus
		Oreochromis niloticus
		Catostomus commersoni
		Leuciscus
		Chironomus tentans
	180	*Cyprinodon bovinus*
		Oryzias latipes
		Cambarus robustus
		Mystus vittatus
		Mystus bleekeri
		Lepomis gibbosus
		Chironomus crassiforceps
		Channa marulius
		Cichlasoma facetum
		Macrobrachium hendersodayanus
		Labeo rohita
		Cyprinus carpio
		Chironomus riparius
		Esomus danricus
		Cherax destructor
		Cyclops sp.
		Barbus arulius
		Acineria uncinata
		Tilapia aurea
		Oreochromis mossambicus
	200	*Pelophylax perezi*
		Helisoma duryi
		Barbus ticto
		Dugesia tigrina
		Tetrahymena sp.
		Barilius vagra
		Melanoides tuberculata

		Vorticella microstoma
		Caquetaia kraussii
		Lepomis cyanellus
		Clarias lazera
		Lamellidens marginalis
		Polypedilum nubifer
		Poecilia reticulata
		Microhyla ornata
		Channa punctata
		Colpoda steinii
		Clarias anguillaris
		Parreysia favidens
		Schistosoma mansoni
	220	*Heteropneustes fossilis*
		Tympanotonus fuscatus
		Ictalurus punctatus
		Lepidocephalichthys thermalis
		Obliquaria reflexa
		Chironomus luridus
		Corbicula australis
		Asellus intermedius
		Velesunio angasi
		Chironomus sp.
		Procambarus clarkii
		Barytelphusa cunicularis
		Spiralothelphusa hydrodroma
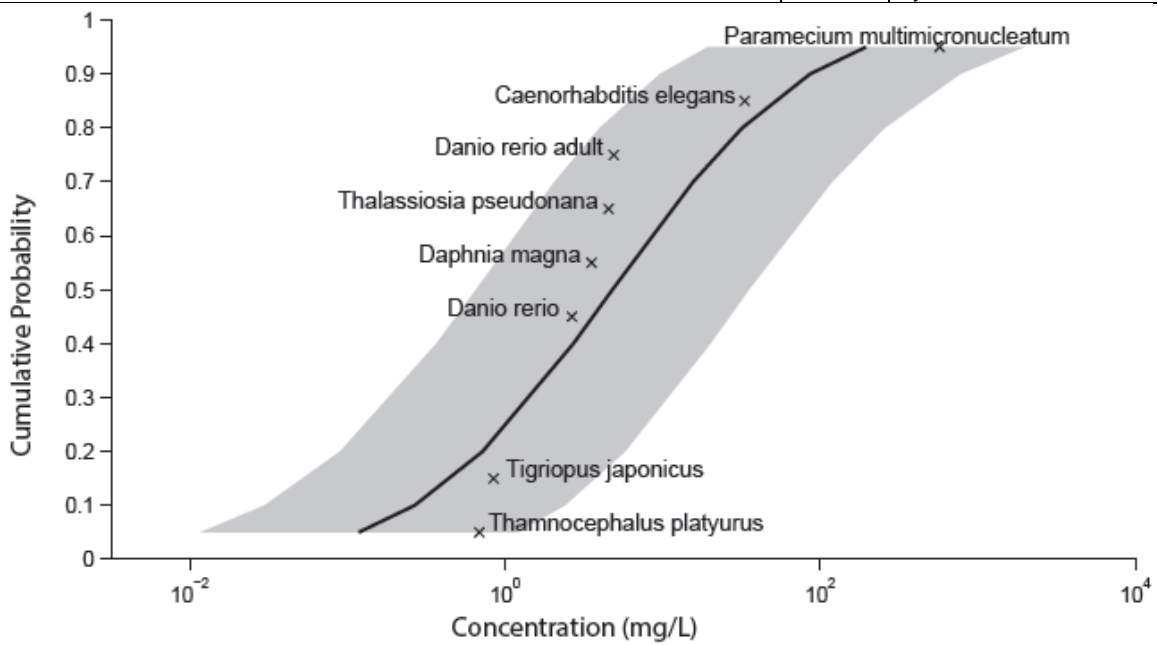
Figure A2.6 SSD for n-ZnO
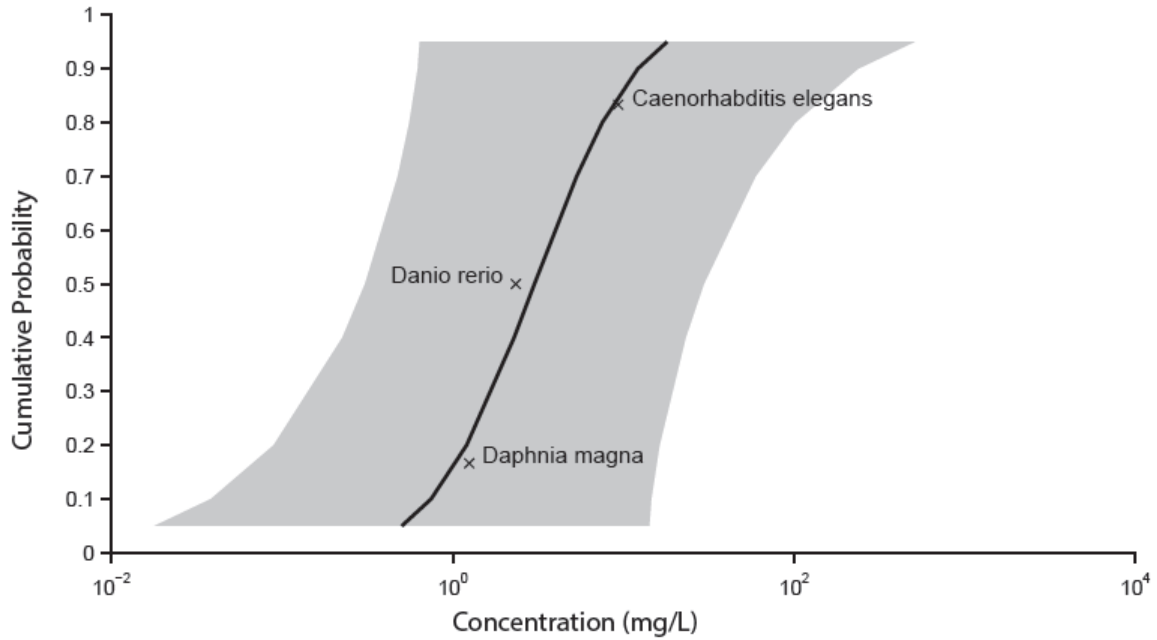
Figure A2.7 SSD for bulk-ZnO
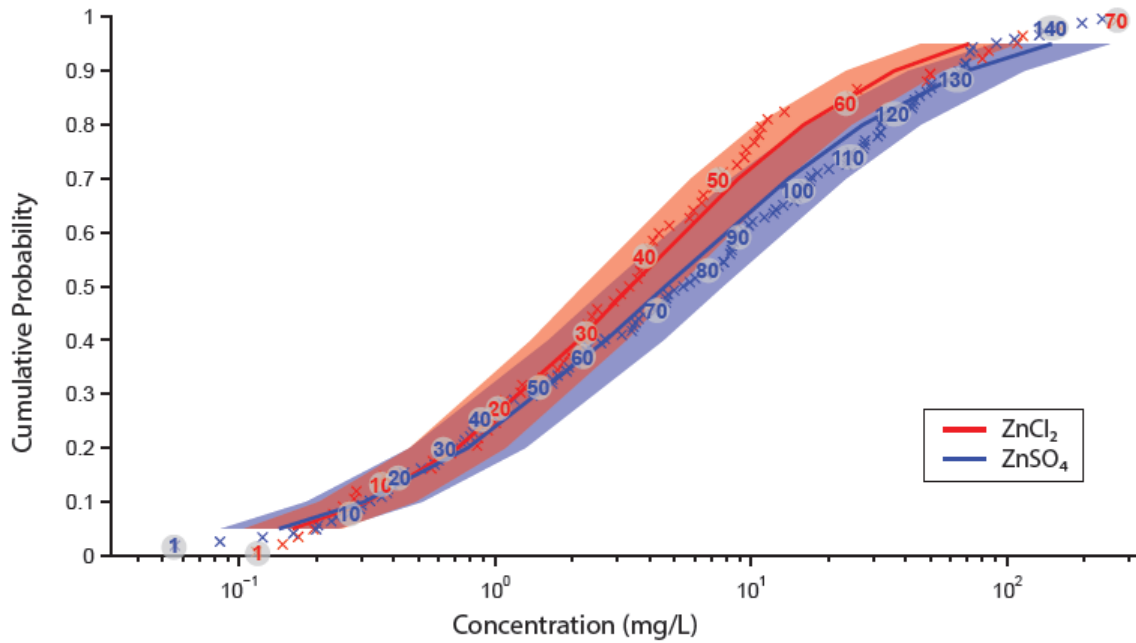
Figure A2.8 Comparison of SSDs for ZnCl₂ and ZnSO₄

Figure A2.8 is a comparison of SSDs for $ZnCl_2$ and $ZnSO_4$ to determine if it was

appropriate to combine compounds when creating an SSD for Zn^{2+}. The numbers

correspond to Table A2.4 where we provide a list of the species in rank order that were used to build each SSD.

Table A2.4 List of Species in Rank Order used to Build the Zinc Ion SSDs

ZnCl$_2$	Species	ZnSO$_4$	Species
1	*Moina irrasa*	1	*Pseudambassis ranga*
	Ceriodaphnia dubia		*Etroplus maculatus*
	Chilodonella uncinata		*Cirrhinus mrigala*
	Villosa vibex		*Oncorhynchus tshawytscha*
	Trochilia minuta		*Mesocyclops hyalinus*
	Daphnia pulex		*Oncorhynchus clarkii*
	Drepanomonas revoluta		*Macrobrachium carcinus*
	Morone saxatilis		*Daphnia similis*
	Lampsilis straminea ssp. claibornensis		*Ceriodaphnia dubia*
	Actinonaias pectorosa		*Mesocyclops pehpeiensis*
10	*Epioblasma capsaeformis*	10	*Daphnia carinata*
	Thymallus arcticus		*Cottus bairdi*
	Vorticella sp.		*Oncorhynchus clarkii ssp. virginalis*
	Spirostomum teres		*Heliodiaptomus viduus*
	Nitocra spinipes		*Streptocephalus texanus*
	Daphnia magna		*Daphnia pulex*
	Hydra viridissima		*Macrobrachium rosenbergii*
	Oncorhynchus mykiss		*Anodonta imbecillis*
	Moina macrocopa		*Moina macrocopa*
	Blepharisma americanum		*Prosopium williamsoni*
20	*Ceriodaphnia rigaudi*	20	*Hyalella azteca*
	Cyprinus carpio		*Oncorhynchus clarkii ssp. pleuriticus*
	Physa gyrina		*Streptocephalus rubricaudatus*
	Brachionus calyciflorus		*Craterocephalus stercusmuscarum*
	Gammarus pulex		*Oreochromis mossambicus*
	Colpidium campylum		*Thamnocephalus platyurus*
	Oreochromis mossambicus		*Oncorhynchus clarkii ssp. stomias*
	Ranatra elongata		*Macrobrachium lanchesteri*
	Oncorhynchus kisutch		*Clarias submarginatus*
	Brachionus havanaensis		*Paratya compressa ssp. improvisa*
30	*Hydra vulgaris*	30	*Daphnia magna*
	Euplotes sp.		*Anaxyrus boreas*
	Paramecium caudatum		*Brachionus calyciflorus*
	Uronema nigricans		*Salmo trutta*
	Euplotes affinis		*Fundulus heteroclitus*
	Cypris sp.		*Tetrahymena pyriformis*
	Ptychocheilus oregonensis		*Spirostomum ambiguum*
	Culicoides furens		*Acrossocheilus paradoxus*
	Vorticella convallaria		*Noemacheilus montanus*
	Daphnia sp.		*Ceriodaphnia reticulata*
40	*Oncorhynchus tshawytscha*	40	*Oncorhynchus mykiss*

	Catostomus commersoni		*Cyclops sp.*
	Clarias gariepinus		*Bryocamptus zschokkei*
	Ptychocheilus lucius		*Stenocypris major*
	Rhinella arenarum		*Penaeus chinensis*
	Xyrauchen texanus		*Rhinichthys cataractae*
	Poecilia reticulata		*Pimephales promelas*
	Danio rerio		*Diacypris compacta*
	Lumbriculus variegatus		*Gammarus pulex*
	Pimephales promelas		*Leptoxis dilatata*
50	*Gila elegans*	50	*Hyalella curvispina*
	Gammarus italicus		*Catostomus latipinnis*
	Chironomus plumosus		*Platygobio gracilis*
	Lymnaea stagnalis		*Girardia tigrina*
	Opercularia coarctata		*Parastenocaris germanica*
	Carassius auratus		*Clarias gariepinus*
	Aspidisca cicada		*Streptocephalus proboscideus*
	Caenorhabditis elegans		*Lepomis macrochirus*
	Echinogammarus berilloni		*Macrobrachium rude*
	Cnesterodon decemmaculatus		*Ancylus fluviatilis*
60	*Oryzias latipes*	60	*Erpobdella octoculata*
	Echinogammarus tibaldii		*Stenocypris malcolmsoni*
	Chironomus riparius		*Gambusia affinis*
	Euplotes patella		*Caridina nilotica*
	Aspidisca lynceus		*Euphlyctis hexadactylus*
	Channa punctata		*Chlorella vulgaris*
	Opercularia minima		*Melanotaenia splendida ssp. inornata*
	Chironomus sp.		*Ambassis sp.*
	Heteropneustes fossilis		*Corbicula manilensis*
	Tubifex		*Echinogammarus meridionalis*
70	*Parreysia cylindrica*	70	*Cyprinus carpio*
			Radix luteola
			Macrobrachium hendersodayanus
			Atyaephyra desmarestii
			Melanotaenia nigrans
			Lirceus alabamae
			Ptychocheilus lucius
			Hydra viridissima
			Spirostomum teres
			Cichlasoma facetum
		80	*Anguilla japonica*
			Xyrauchen texanus
			Baetis tricaudatus
			Gammarus fasciatus
			Lymnaea acuminata
			Galaxias maculatus
			Paratya australiensis
			Channa punctata
			Chanos
			Lumbriculus variegatus

	90	*Chasmagnathus granulata*
		Bellamya bengalensis
		Nephelopsis obscura
		Hydra vulgaris
		Duttaphrynus melanostictus
		Caecidotea sp.
		Leporinus obtusidens
		Microhyla ornata
		Asellus intermedius
		Oreochromis niloticus
	100	*Poecilia reticulata*
		Adenophlebia auriculata
		Tilapia zillii
		Xenopus laevis
		Planorbella trivolvis
		Dugesia tigrina
		Lepidocephalichthys guntea
		Chironomus plumosus
		Channa marulius
		Barbus javanicus
	120	*Puntius sophore*
		Clarias lazera
		Poecilia vivipara
		Aphelenchus avenae
		Lepidostoma sp.
		Rasbora daniconius neilgeriensis
		Rhithrogena hageni
		Cyprinus carpio ssp. communis
		Drunella doddsi
		Panagrellus silusiae
	130	*Danio rerio*
		Ephemerella sp.
		Cinygmula sp.
		Chloroperlidae
		Notopterus
		Colpoda steinii
		Labeo rohita
		Heteropneustes fossilis
		Rasbora heteromorpha
		Cherax tenuimanus
	140	*Chironomus sp.*
		Tetrahymena sp.
		Cephalobus persegnis
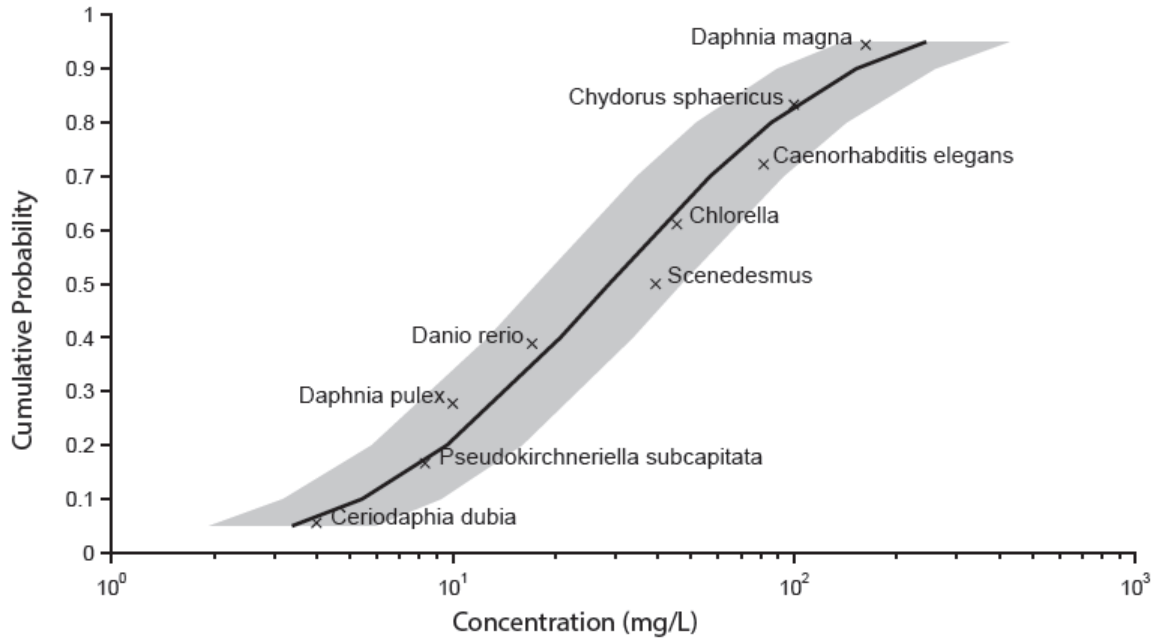
Figure A2.9 SSD for n-Al$_2$O$_3$
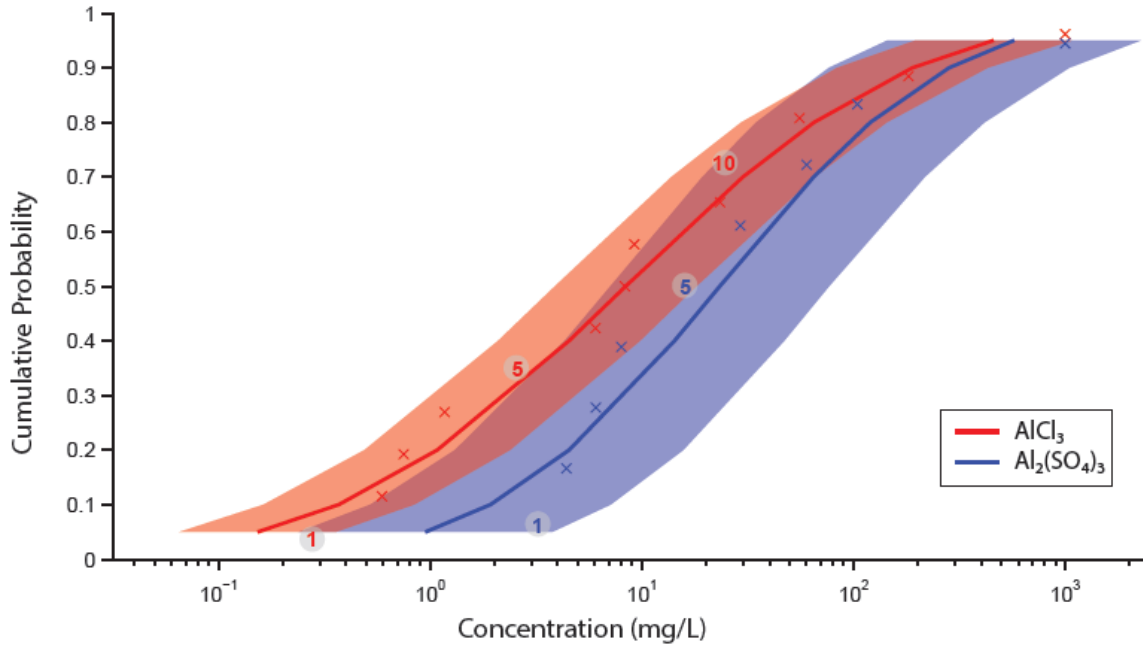
Figure A2.10 Comparison of SSDs for AlCl$_3$ and Al$_2$(SO$_4$)$_3$

Figure A2.10 is a comparison of SSDs for AlCl$_3$ and Al$_2$(SO$_4$)$_3$ to determine if it was appropriate to combine compounds when creating an SSD for Al^{3+}. The numbers correspond to Table A2.5 where we have provided a list of the species in rank order that were used to build each SSD.

Table A2.5 List of Species in Rank Order used to Build Aluminum SSDs

AlCl$_3$	Species	Al$_2$(SO$_4$)$_3$	Species
1	*Hyla cinerea*	1	*Duttaphrynus melanostictus*
	Salmo salar		*Pimephales promelas*
	Lithobates pipiens		*Stenocypris major*
	Bufo americanus		*Oreochromis mossambicus*
5	*Oncorhynchus mykiss*	5	*Dracunculus medinensis*
	Daphnia pulex		*Ceriodaphnia dubia*
	Pseudokirchneriella subcapitata		*Rhabditis sp.*
	Ceriodaphnia sp.		*Dreissena polymorpha*
	Danio rerio		*Plectus parietinus*
10	*Ceriodaphnia dubia*		
	Physa sp.		
	Rhabditis sp.		
	Plectus parietinus		
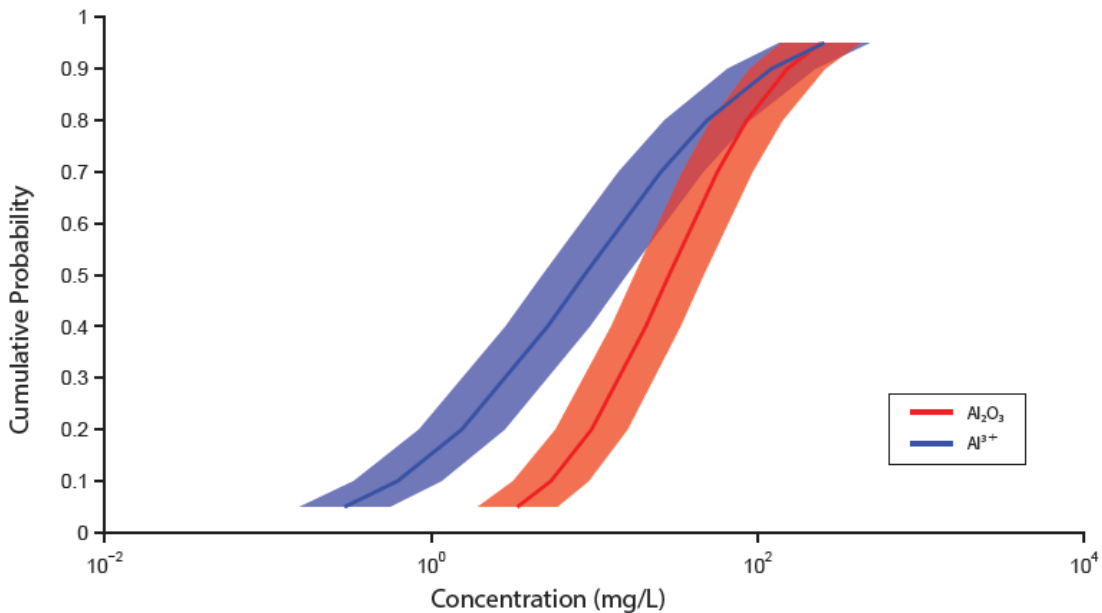
Figure A2.11 Comparison of SSDs for Al$_2$O$_3$ and Al^{3+} Derived from Dissolving AlCl$_3$ and Al$_2$(SO$_4$)$_3$
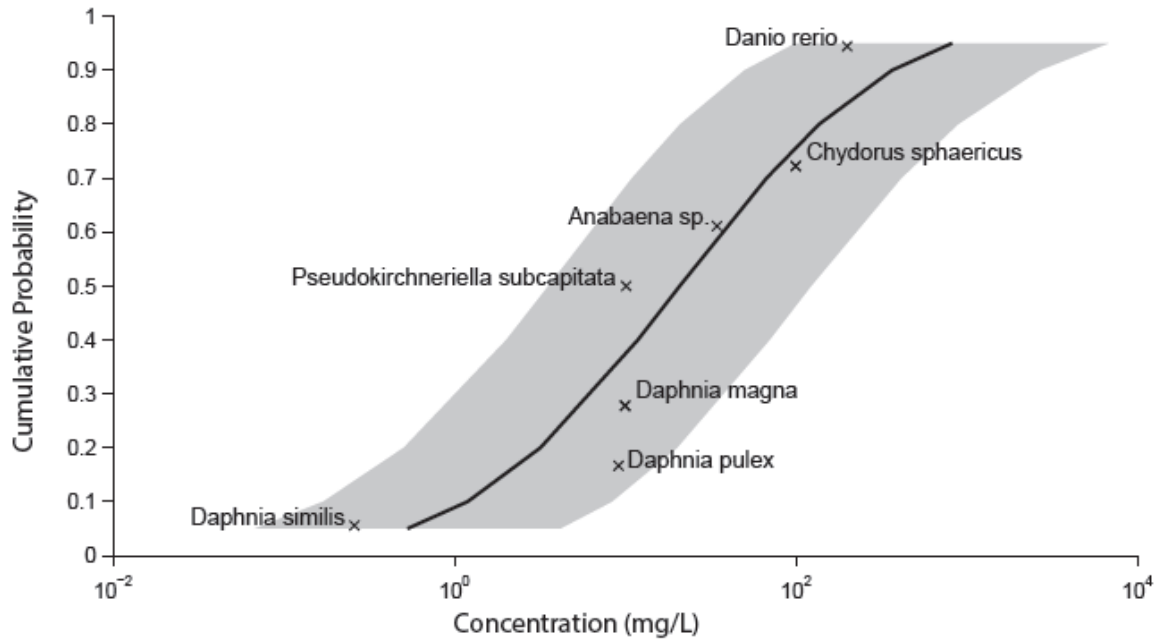
Figure A2.12 SSD for n-CeO$_2$ Derived from EC$_{50}$ Data
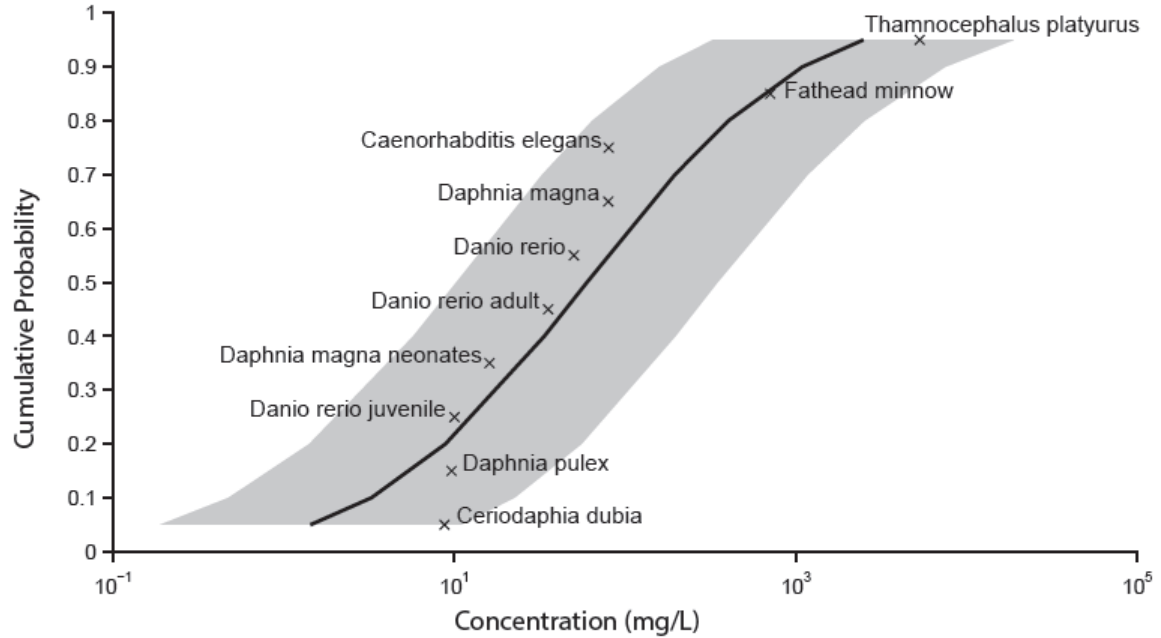
Figure A2.13 SSD for n-TiO$_2$
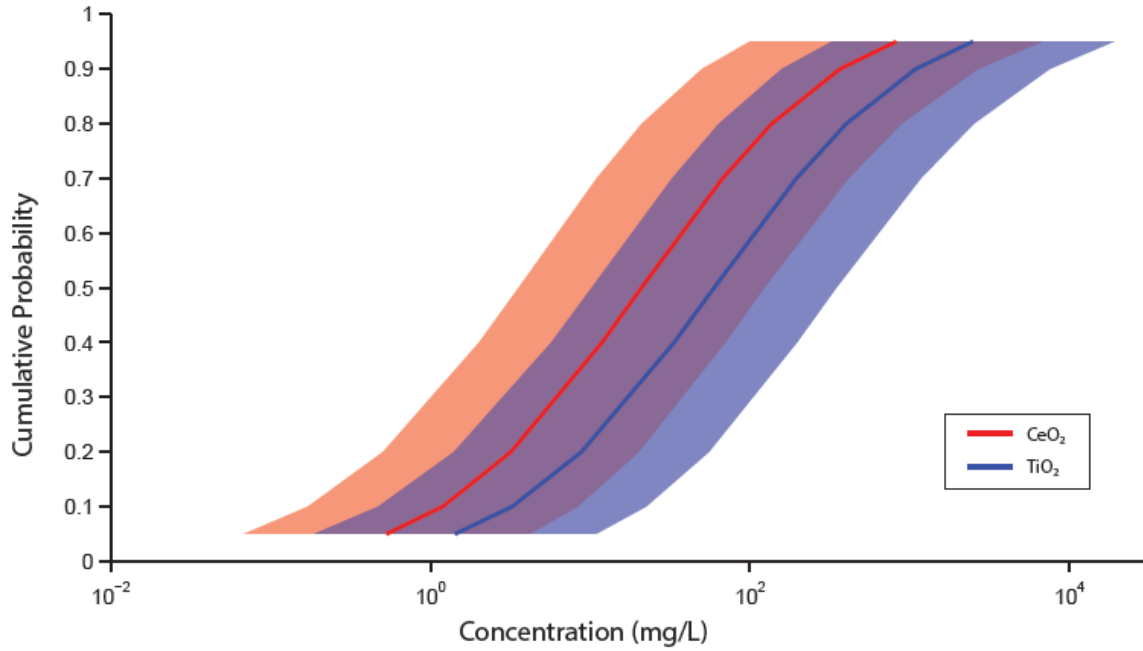
Figure A2.14 Comparison of n-CeO₂ and n-TiO₂ SSDs
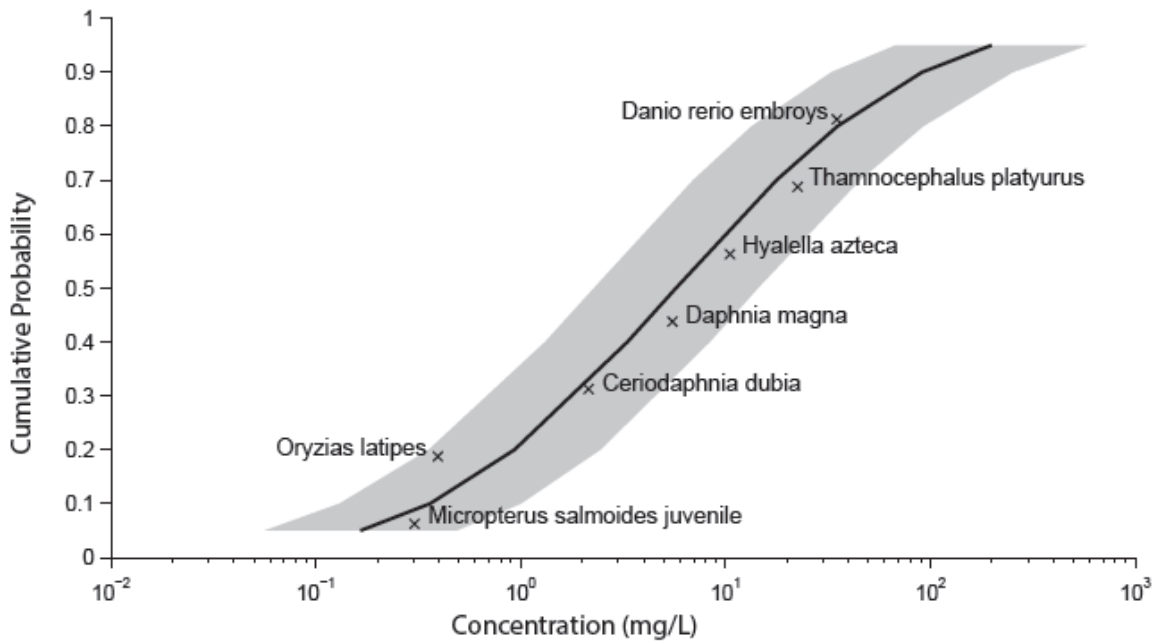
Figure A2.15 SSD for n-C₆₀
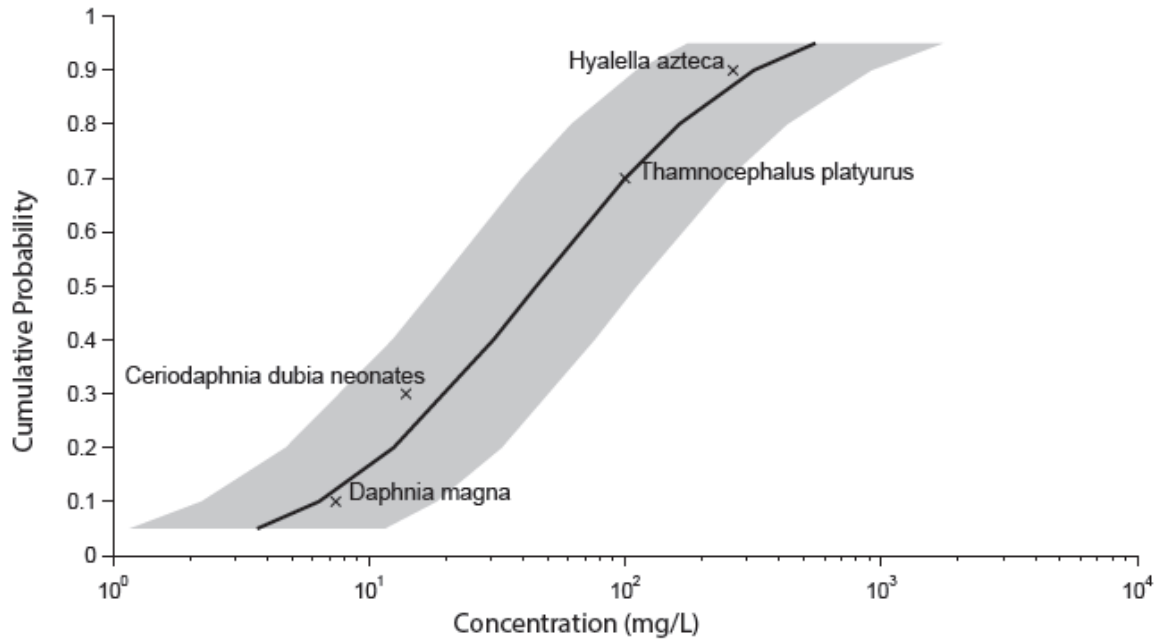
Figure A2.16 SSD for CNTs

Chapter 3. Assessing the Risk of Engineered Nanomaterials in the Environment Using the NanoFate model

We developed a multimedia fate and transport model ("NanoFate" model) to predict the long-term accumulation of engineered nanomaterials (ENMs) across a range of environmental media. Previous studies on the fate of ENMs have focused largely on steady-state conditions of single nanomaterials in simplified environments, and the range of fates across ENMs is not fully understood. The new NanoFate model was designed around key fate and transformation processes that metal and metal oxide ENMs typically experience. While the processes are the same, the rates of transformations can vary significantly among ENMs. Thus the new model was designed to predict the temporal variability in fate across a broad range of environmental media at various spatial scales. We use a case study of the Greater San Francisco Bay Area into which we release n-CeO$_2$, n-CuO, n-TiO$_2$, and n-ZnO at different rates over the course of a decade to demonstrate the applicability and variability resulting from predicting dynamic nanomaterial fate at a regional scale. Within the case study scenarios that were explored, CuO, TiO$_2$, and ZnO are likely to exceed No Observed Effect Concentrations (NOEC) in freshwater but not in soils. None of the freshwater or soil release scenarios result in exposures that exceeds the hazardous concentrations at which 5% of species would be harmed (HC$_5$) at lethal concentrations (LC$_{50}$). However, given that both TiO$_2$ and ZnO exceed the freshwater NOEC, there is some concern that toxic impacts may already be occurring especially under localized release scenarios. More generally, the results show that even when soluble, metal oxide ENMs can accumulate in the environment over the long term in sufficient concentrations to cause potential toxicity. Furthermore, the fluctuations in the climatic variables such as precipitation could cause circumstances where

ENM concentrations reach toxic levels. By investigating both the range in rate processes and release scenarios, we have shown just how wide, and arguably how uncertain environmental concentrations may be. The results call for further identification and calibration of key ENM fate processes to improve the accuracy of these and other nanomaterial fate predictions in order to fully determine the risk of ENMs entering our environment.

3.1 Introduction

Engineered Nanomaterials (ENMs) are a growing class of environmental pollutants, and relatively little is understood about their impacts on our environment. Since the emergence of nanotechnology in the 1980s, ENMs have been used with increasing frequency and volume in industrial applications and in consumer and medical products. The increasing use and associated environmental emissions of ENMs creates a compelling need to understand and predict their distributions and likely concentrations in the environment in order to understand their potential impacts.[4,8,226,228]

ENMs are particles for which at least one dimension falls between 1 and 100 nm in length,[225] though in the environment they will transform and accumulate at different sizes and rates. ENMs can exist as single, aggregated, or agglomerated particles and can be manufactured with various shapes, coatings, and surface functionalities making it a challenge to predict their impact on the environment. Further, nanoparticles can undergo a number of potential transformations that depend on both the properties of the ENM and the local environment, such as aggregation, dissolution, oxidation, sulfidation, and other surface alterations.[85,226,229,342–346] These variables complicate our understanding of what happens to ENMs when they enter the environment and what their long term fate may be.

Field measurements of the concentrations of ENMs ([ENM]) would be valuable for assessing their environmental distribution. However, methods for environmental detection and measurement of ENMs *in situ* are not yet reliable.[18,347] Therefore, determining potential environmental exposure must rely on model-driven and lab-based estimates of fate. Because of their particulate nature, traditional multimedia fate and transport models or material flow analysis models (MFA) can be limited in their ability to predict the long-term environmental distribution of ENMs.[348–351] While some methods have been developed, we expand on them to improve the specificity [ENM] estimates for a range of ecosystems that include sufficient nano-specific rates and processes to reflect likely nanoparticle fate and [ENM] in various media.

Multimedia environmental fate models can provide a powerful framework to help to understand the behavior of pollutants in the environment. The conceptual challenge is to incorporate ENM specific properties into the model. While a few models have already been published,[2,18,19,21,36,342–344,352] they make limited use of material-specific descriptors and are relatively generic or limited regarding the properties, transport, and transformations they include and the spatial scale and environmental compartments they consider. From a methodological standpoint, in most of the existing models the processes affecting the behavior and transport of an ENM in any compartment are parameterized and combined into a system of mass balance equations. The mathematical setup is also similar: (i) various rate constants are multiplied by compartment specific concentrations in order to determine transport between compartments; (ii) rate constants for transformation processes are also dependent on compartment concentrations (which thus vary with time); and (iii) ENMs are released to each compartment.

A model developed by Praetorius et al. (2012) estimates the downstream steady state [TiO$_2$] in moving freshwater, stagnant freshwater, and sediment for the Rhine River through a series of boxes that include transport through them in a single direction. While the model is designed to be used with a variety of ENMs, no specific examples are provided regarding the variability allowed within the model.[18] Another model developed by Liu and Cohen (2014) includes six compartments for air, water, soil, sediment, terrestrial biota, and aquatic biota. The model was designed to work at various spatial scales including large regional, small regional, and local scales. It can be run with Al$_2$O$_3$, CeO$_2$, CuO, Fe$_3$O$_4$, TiO$_2$, ZnO, Ag, SiO$_2$, nanoclays, and CNTs. Both Praetorius et al (2012) and Liu and Cohen (2014) use multiple size classes of nanoparticles, with the same series of mass balance equations applied to each size class using first-order differential equations to express the changes in concentration over time. A screening level model (SimpleBox4Nano) developed by Meesters et al. (2014) considers the transfer of ENMs in air, surface water, soil, and sediment.[232] The processes are modeled mechanistically using first-order rate constants for all processes.[232] Rather than size classes, this model tracks three states of the nanoparticle: (1) freely dispersed; (2) ENMs heteroaggregated with natural colloidal particles (<450 nm); and (3) ENMs attached to larger natural particles (>450 nm).[232]

Many fate and transport processes need to be considered in order to understand ENM mobility, bioavailability, and ultimate fate. These processes include ENM emissions to air, water, and soil from the manufacturing, use and disposal of these materials; advection in and out of the main environmental compartments; diffusive transport; resuspension to air and attachment to aerosols; transformation into other ENMs or compounds; in natural waters aggregation, sedimentation, dissolution, filtration, and sorption to suspended particles and the

subsequent deposition to sediment,[16] many of which are not considered in traditional fate models for organic chemicals.[353–356] Further, some transformation processes, such as homo- or heteroaggregation, create an altered state that change how the particles interact with their environment.[20] Since some ENMs also dissolve over time, the long term accumulation needs to account for both nanoparticles and dissolved metal ions.[17] Most ENMs will also undergo other transformation processes (e.g., oxidation, sulfidation, adsorption of natural organic matter, loss of the original coating) that can alter their chemical properties and environmental behavior.[226,13,18,90]

Our goal is to develop a multimedia box model that can calculate the [ENMs] in specific environmental compartments over time assuming well-mixed compartments. While a few models have already been developed, those that exist are either material flow analysis models (MFA) that lack the ability to include nano-specific considerations or mechanistic fate models that take into account only some key nano fate processes.[348,357,358] The NanoFate model presented here is unique because of: (i) the type and structure of compartments included; (ii) the inclusion of key fate processes that have not previously been considered; (iii) separately tracking the accumulation of multiple states of the ENM; and (iv) the approach taken to calculate fate and transport rates in the face of limited data and mechanistic uncertainty. As observed in a recent study, models developed up to 2015 consider only steady-state, over large regions, ignore surface runoff, and do not track ENM reaction by-products (such as the dissolved ion).[357] We attempted to address all these considerations in this new nanomaterial fate model.

In addition, because of the rapid progress being made in ENM production and applications, we explore the result of a range of release scenarios and how they can alter the long-term estimates of environmental [ENM].

3.2 Methodology

This model predicts the fate of ENMs in the atmosphere (including air and aerosols), soil (including agricultural, urban and natural soils with surface soil solids, surface soil pore water, and deep soil compartments for each soil type), water (including freshwater, coastal water, and suspended sediment in both), and sediment (for both freshwater and marine) (Figure 3.1). The model predicts transfers between compartments as well as transformations to other forms. It tracks three states of the ENM including: (i) free particles and small homoaggregates; (ii) ENM particles heteroaggregated with other particulate matter in the environment; and (iii) the products of dissolution of ENMs in the various waters. The key processes considered are summarized in Figure 3.1. The NanoFate model was coded in *Matlab 2014a* and it incorporates a number of distinct environmental compartments and calculates transfers between compartments using functions that estimate mass transport between each compartment via distinct processes including wet and dry deposition (of air and aerosols), attachment to aerosols from air, advection caused by wind, runoff and erosion during precipitation events, sedimentation in water and of suspended sediment, sorption from water to suspended sediment, dissolution in freshwater and marine water column and sediment, flow from freshwater into coastal areas of water, suspended sediment and sediment bed, advection out of the marine zone, resuspension and burial in sediment, wind erosion from surface soil, splash back from seawater in coastal zones, transfer between soil solids and soil pore water, sorption to soil particles, dissolution in soil pore water, and

sedimentation to deep soil. Details on all processes are provided in the Appendix User Guide, Section 2. Differential equations are used to express the change in concentration over time (mass transfer equations are available in Appendix User Guide, Section 3). Additionally, the model uses a daily time-step and does not assume steady-state, which allows the model to capture the variability of [ENM] due to seasonal trends and flow-dependent patterns.[359]
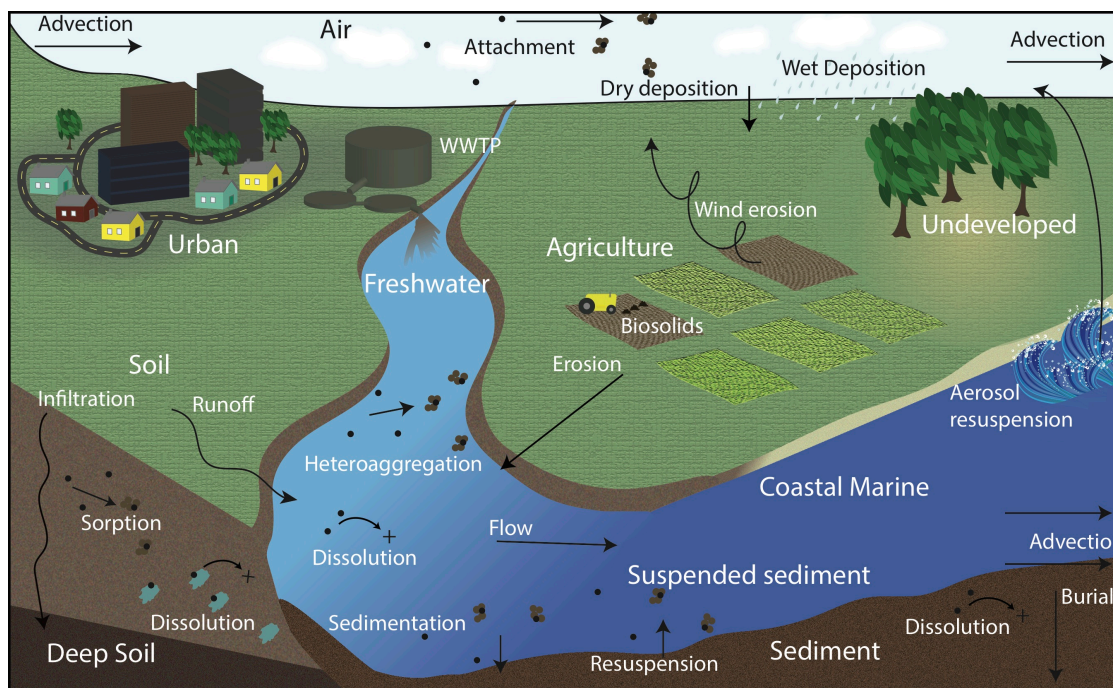
Figure 3.1 Model System with Compartments, Transfers, and Transformations

In addition to requiring dimensions and characteristics of the environment, the model also incorporates observed daily hydro-meteorological data for precipitation, wind speed, and river flow, which improves the regional specificity of the model. A traditional fate and transport model for organic chemicals considers partitioning coefficients (e.g. Henry's constant, octanol-water partitioning),[353] which are not applicable for ENMs. Instead, we assume that ENMs transfer continuously from one compartment to another at a rate controlled by ENM specific processes and [ENM].[346,360] Unlike previous models, we distinguish between the fate

90

of ENMs in freshwater and coastal systems to account for the differences in physicochemical characteristics between the two environments.[2,18,231,232,352,361–365]

The Greater San Francisco Bay Area, defined by its contributing watersheds, was selected for this case study in part because detailed release predictions for various nanomaterials to specific environmental media were developed by Keller and Lazareva (2013).[8] The region consists of 14,419 km^2 of which 11.1% is freshwater, 0.8% is marine, 24.2% is urban, 11.1% is agricultural, and 52.5% is undeveloped natural lands (Figure 3.2). Most of the environmental parameters and physical characteristics of the region were collected from the USEPA, using BASINs (v4.1) software to access the data; NOAA (meteorological data); and the USGS (observed hydrology, SSURGO for soils; and NLCD 2011 for land use). Temporal data extended over ten years from 2005 – 2014. (See Appendix Table A3.1 for environmental input parameters).
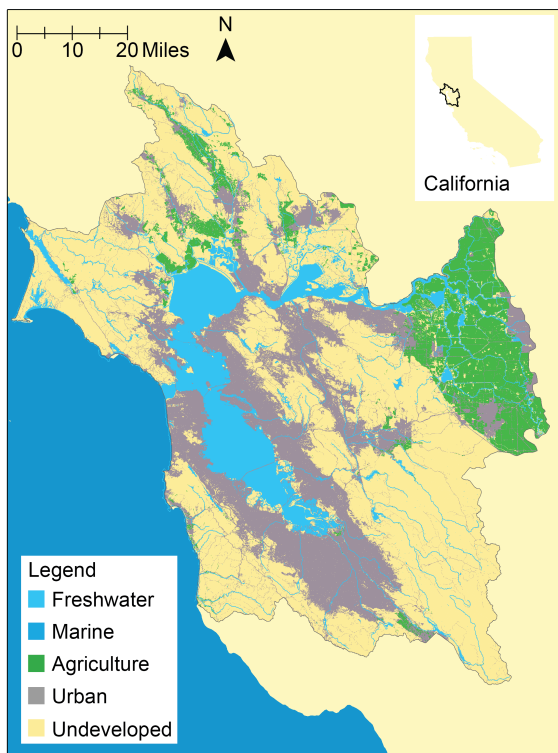
Figure 3.2 Case Study Region of the Greater San Francisco Bay Area

The region is divided into environmental compartments included within the NanoFate model. The agricultural regions include both pasture and cropland, the urban regions include developed high intensity (e.g. apartment complexes, row houses, commercial and industrial regions), developed medium intensity (e.g. single family house units), developed low intensity (e.g. single family houses with large plots of land), and developed open space (e.g. parks, golf courses, etc.), and the undeveloped regions include barren land, deciduous forests, evergreen forests, mixed forests, scrub, shrub, grassland/herbaceous, and wetlands. Land use was computed using the 2011 NLCD (See Appendix User Guide Section 1.1.2.2).

The environmental release estimates were developed using published production, use, disposal and distribution estimates.[8] The regional population and development level was used to narrow the original global estimates to the region of interest. Because these estimates involve annual release to bulk compartments (air, water, and soil), we assumed constant daily release values except in test scenarios for an accidental spill and increasing production and release (Appendix Table A3.3).[8] We also use a ratio of 46% to 54% for ENM release via treated wastewater effluent to freshwater relative to marine, based on the total effluent flows to water bodies in the San Francisco Bay area.[366] ENMs in biosolids (estimated in Lazareva and Keller 2014) are assumed to be directly released to the agricultural soil compartment.[367]

Scenarios considered include both the low and high end ENM release estimates (specified in Appendix Table A3.3); a third scenario where the high end estimate release is increased by an order of magnitude (ten times higher); a fourth scenario with a 10% annual increase in the release quantity every year starting in 2011 based on the high end release estimate to investigate potential future environmental exposure as production and release increase; and two accidental spill scenarios hypothesized to occur on Jan 1, 2013, one considering 1000 kg

to freshwater and another considering 1000 kg to urban soils with the high daily release
scenario in the background.

Methodologically, processes affecting the behavior and transport of a nanoparticle in each
compartment are parameterized and then combined into a system of mass balance equations.
Rate constants that are dependent on the current compartmental concentration determine the
transport and transformation within and between compartments. Data to parameterize the
processes for different ENMs were collected from the available literature and rate constants
were estimated for each ENM (Table 3.1). Key nano-specific rates include heteroaggregation,
sorption, dissolution, and sedimentation for a range of environments and characteristics for
each environment.[226] Many of these parameter values are specific to the ENM and the
environmental medium.[357]

**Table 3.1 ENM-Specific Parameters used for the Greater San Francisco Bay Area
Scenario**

Parameter		CeO_2	CuO	TiO_2	ZnO
Average Primary Diameter (nm)	d_{ENM}	30	30	60	30
Average Aggregate Diameter in FW (nm)	d_{agg}	600	400	1,000	800
Density (kg/m^3)	ρ_{ENM}	7130	6400	3900	5600
Dissolution in FW (d^{-1})	$k_{dis,F}$	0	$3.84*10^{-2}$	0	$3.02*10^{-1}$
Dissolution in FW Sediment (d^{-1})	$k_{dis,Fsed}$	0	$3.84*10^{-3}$	0	$3.02*10^{-2}$
Dissolution in MAR (d^{-1})	$k_{dis,M}$	0	$5.28*10^{-2}$	0	6.89
Dissolution in MAR Sediment (d^{-1})	$k_{dis,Msed}$	0	$5.28*10^{-3}$	0	0.689
Dissolution in Soil GW (d^{-1})	$k_{dis,S}$	0	0.005	0	0.0384
Sedimentation Rate in FW (m/d)	$k_{sed,F}$	0.0348	0.0409	0.1350	0.3327
Sedimentation Rate in MAR (m/d)	$k_{sed,M}$	0.6941	0.0840	0.5884	0.4177
Heteroaggregation in Air (m^3/kg-d)	$k_{het,A}$	0.0073	8.918	1.1489	29.4
Heteroaggregation in FW (m^3/kg-d)	$k_{het,F}$	7.3	8917.5	1148.9	29443.6
Heteroaggregation in MAR (m^3/kg-d)	$k_{het,M}$	8940.3	9339.9	2254	41426.2
Soil-water partitioning UNDEV Soil	$k_{elu,1}$	0.96	0.99	0.99	0.99
Soil-water partitioning AG Soil	$k_{elu,2}$	0.95	0.99	0.99	0.95
Soil-Water partitioning URBN Soil	$k_{elu,3}$	0.97	0.99	0.95	0.99
Enrichment Factor	EF	1	5	1.4	2.5

Note: References are available in Appendix Table A3.4

FW = freshwater, MAR = coastal marine waters, GW = groundwater, UNDEV = undeveloped, AG = agricultural, URBN = urban; enrichment factor and soil-water partitioning defined in text.

Aggregation, dissolution, and other surface transformations of ENMs result in transfer to new forms or chemical species that are represented in parallel to the ENM. We generally assume that, once a nanoparticle has aggregated, dissolved, and/or adsorbed to other particulate matter, the transfers are not reversible and are thus tracked as separate species. We assumed homoaggregation after release is negligible relative to heteroaggregation at realistic environmental [ENM] and suspended particles, and as such only include heteroaggregation in our model (Appendix User Guide Section 2.3.1).[12,36,45,46,179,368,369] We follow the approach provided by Quik et al. (2014) to model heteroaggregation relative to current water and suspended sediment concentrations.[36] We do not assume that complete heteroaggregation occurs as several studies have shown that individual nano-scale particles can be present in surface waters.[370,370,371]

In the air, wet and dry deposition is calculated for both ENMs and ENMs associated with aerosols. ENM attachment to aerosols or suspended sediments is assumed irreversible. Dry deposition is calculated using Stoke's Law for both free nanoparticles and those associated with aerosols (Appendix User Guide Section 2.1.1).[372] For wet deposition of aerosols, we use a scavenging ratio (i.e. the mass mixing ratio or volume concentration of the chemical in precipitation relative to the chemical in air) provided by Mackay (2001), and a conversion factor of 0.01 for raindrop scavenging of nanoparticles (Appendix User Guide Section 2.1.2). This is because studies have found that particles in the 0.01 μm range can have a scavenging ratio of up to 2 orders of magnitude smaller than those in the 1-5 μm

range.[373] Advection both into and out of the system via wind was also included for both the free ENMs in the air and those associated with aerosols (Appendix User Guide Section 2.1.3). Heteroaggregation of ENMs with aerosols has not been studied for specific ENMs. As such, our approach was to take the rate of aggregation used in water systems and assume a lower probability of collision because of different fluid densities and dynamics, specifically three orders of magnitude lower than the rate of heteroaggregation in freshwater because the fluid densities tend to vary by three orders of magnitude (Appendix User Guide Section 2.1.4).[226]

Aerosolization of ENMs from marine splash in the coastal zone and resuspension of ENMs attached to surface soil particles during wind events result in transfer back to the aerosols compartment. Transport from seawater to the aerosol compartment was computed using a flux equation that relies on enrichment factors of trace metals,[374–381] which we assume are comparable to that of their ENM counterparts (Appendix User Guide Section 2.3.5). For wind erosion of surface soil, we use the saltation equation and the vertical flux conversion to estimate total transport of soil particles to aerosols (Appendix User Guide Section 2.2.1).[382–385]

Sedimentation of individual and aggregate nanoparticles was also modeled. Deposition of suspended sediment (and thus the nanoparticles attached to suspended sediment) was estimated using Stoke's Law (Appendix User Guide Section 2.3.2). This accounts for the density of the suspended particles, the density and dynamic viscosity of the fluid (freshwater v. marine), and the concentration of nanoparticles present in the suspended particle compartment.[353] Sedimentation of free nanoparticles and small homoaggregates was

calculated using rate constants estimated from published literature that measured sedimentation over time for corresponding media (Appendix User Guide Section 2.3.3).

The equilibrium dissolution concentration was estimated for soluble ENMs under various water conditions and pH values. Dissolution was modeled using predictions of the maximum dissolution for a given metal or metal oxide and the rate at which dissolution occurs in specific waters for a given ENM (Appendix User Guide Section 2.3.4). *Visual MINTeq* (version 3.1) was used to predict metal speciation in various natural waters (e.g. freshwater, marine, soil water) because the environmental characteristics of a water type will result in different rates of dissolution.[386] This was combined with experimental data on the dissolution rate in specific waters for each ENM (Appendix Table A3.4).[187] Lacking experimental data, dissolution of ENMs in freshwater and marine sediment was assumed to occur at one tenth of the rate of dissolution in the water column.

The transfer of ENMs and suspended sediment from freshwater to coastal waters and the transfer from coastal waters to the marine compartment (out of the modeled system) is considered an advective flux, estimated using regional flow data (Appendix User Guide Section 2.3.6). The advective flux of ENMs associated with suspended sediment is dependent on the flow of water and concentration of suspended sediment in water. The advective flux of ENMs in sediment via bedload transport is assumed to depend on water flow rate. ENM mass in sediment is calculated based on additions by sedimentation and losses from resuspension and burial (Appendix User Guide Section 2.4.1 and 2.4.2). This is because once an ENM is associated with particulate matter, we assume that it will remain associated with that particulate matter; in sediment, all ENMs are associated with sediment, and transfer between compartments is exclusively via sediment processes.[18]

Runoff and erosion during storm events allow for transfer from the landscape to receiving waters. Infiltration transports ENMs to the soil compartments and their corresponding waters. Runoff was calculated using the United States Department of Agriculture's (USDA) Soil Conservation Service (SCS) runoff equation, which uses the USDA's Natural Resources Conservation Service (NRCS) curve number, a value ranging from zero to one hundred used to indicate the amount of runoff or infiltration that will occur during a precipitation event (Appendix User Guide Section 2.2.2).[387] Soil loss resulting from erosion was calculated using the Revised Universal Soil Loss Equation (RUSLE), which accounts for amount of precipitation, soil erodibility, regional slope, cover management, and support practices (Appendix User Guide Section 2.2.3). Dissolution of ENMs in soil water was assumed to occur as the same rate as dissolution in groundwater studies, with the maximum equilibrium dissolved concentration dependent on the soil pH (Appendix User Guide Section 2.2.6). Leaching allows for transfer from the surface soil to the deep soil using the default leaching rate reported in Mackay (2001) (Appendix User Guide Section 2.2.5).[353]

In addition, unlike previous models that consider only soil solids and estimate attachment,[232] we include a factor for partitioning between surface soil solids and surface soil water, using breakthrough curve (BTC) data to estimate the fraction of nanoparticles that attach to the soil solids relative to the soil water (Appendix User Guide Section 2.2.4).[61,72,111,120,121,123,132,135–137,164,181,200,203,207,388–396] In using the BTCs, we assume that the retention rate is equivalent to the fraction of ENMs that sorb to soil solids (regardless of what form those soil solids take) because evidence indicates that once an ENM is in the solid soil phase, it is attached (either adsorbed or agglomerated) to soil solids.[346,397] The

fraction that exits with water at the end of a column experiment is the mass that we consider remains in soil water as it infiltrates. We do not consider a maximum attachment capacity in soils, even with continuous and increasing ENM application via biosolids or from the atmosphere, due to a lack of experimental data. However, post-hoc analysis of several extreme scenarios reveals that under the scope of designed scenario use, attachment is very unlikely to exceed viable attachment quantities.

To estimate the risk to ecosystems, we compared the predicted environmental [ENM] from the various release scenarios to published Species Sensitivity Distributions (SSDs) for freshwater and soil systems where available, and to individual species endpoints (e.g. No Observed Effect Concentration (NOEC) or lethal concentration (LC_{50})) when SSDs were not available.[398–400] SSDs are models of variations in species sensitivity to a particular stressor and can be used to predict the potentially affected fraction (PAF) of species under exposure to a particular concentration of chemical.[233] Specifically, we compare the predicted exposure concentrations (PECs) to the hazardous concentration at which 5% of species will be harmed (HC_5) at both the No Observed *Adverse* Effect Level (NOAEL) and the lethal concentration required to kill 50% of the population (LC_{50}).[270,398,399,401]

3.3 Results

The most conservative release scenario considers continuous daily release to air, freshwater, marine, and agricultural soil compartments under the low release prediction. In a few weeks, even under the low-end release scenario, ENMs transfer to all of the environmental compartments, but accumulation is highest in aerosols, freshwater and marine suspended sediment and sediment beds, dissolved in sediment, and agricultural surface soil solids (Figure 3.3; Appendix Figures A3.1-A3.3). This is primarily because

heteroaggregation (at varying rates for each environment and ENM) is assumed and can be quite substantial for certain ENMs in specific media. The magnitude of these transfers for compartments without direct releases is, however, generally quite low, ranging from less than 1 pg transfer per day up to multiple g per day (with the higher end resulting from heteroaggregation processes). For nano ZnO and CuO, there is also substantial dissolution in the water column and sediment for freshwater and marine systems (with a difference of approximately an order of magnitude in concentration between the two aquatic media), and soil waters (Figure 3.3B and 3.3C; Appendix Figure A3.2B and A3.2C).
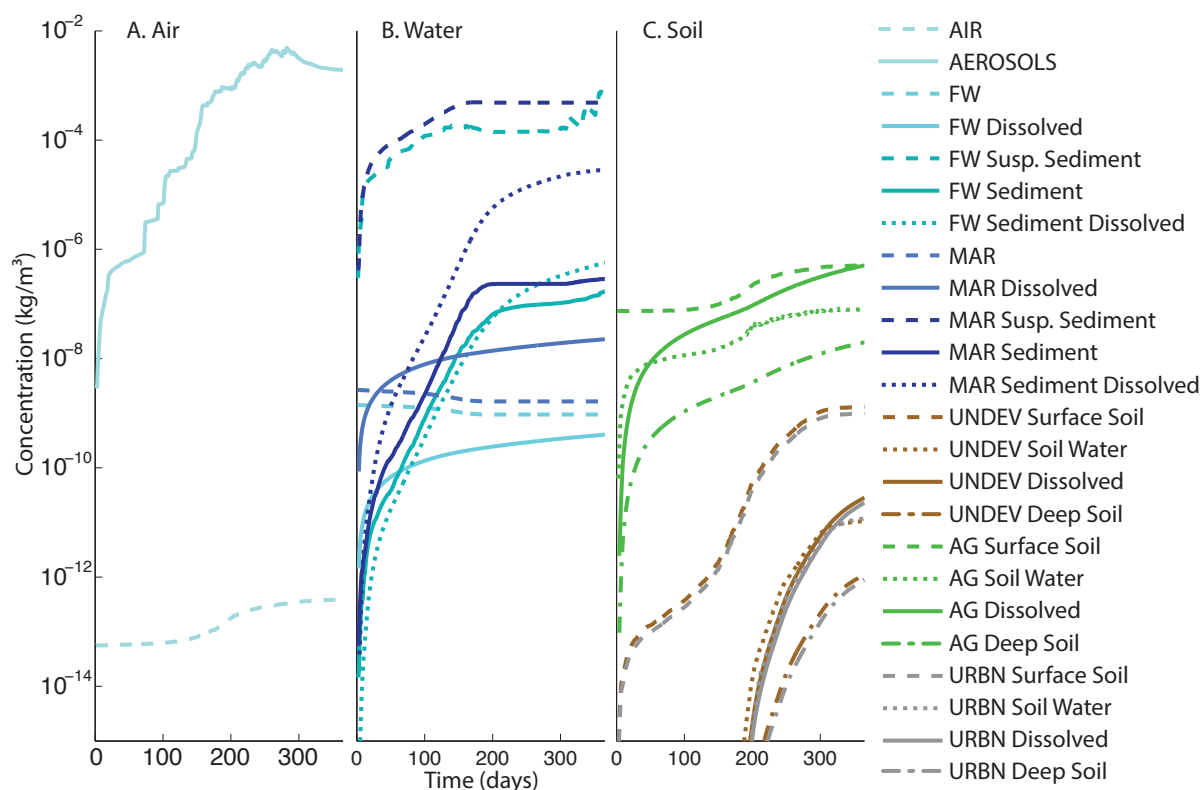
Figure 3.3 ZnO Accumulation across Environmental Media, including (A) Air, (B) Water, and (C) Soil under the Low-End Daily Release Scenario over the First 365 Days of the Model Simulation

In this run, initial concentrations are zero in all media.

Over the long term (e.g. ten years), [ENM] reach a relative steady level, with most concentrations varying less than 15% for all ENMs by the final (10th) year of each scenario. The exception to this is aerosols and freshwater suspended sediment where the natural fluctuation of environmental processes (e.g. precipitation, runoff) and heteroaggregation cause substantial variability. These temporal variations allow for inter-annual concentrations to vary by more than an order of magnitude. These trends are noticeable in the long-term distribution of ZnO under the high release scenario where high variability in the [ZnO] attached to aerosols and freshwater suspended sediment is predicted (Figure 3.4A). Soils exhibit the highest long term relative increase in concentration, though predicted concentrations are not as high as previous studies predicted, likely because the model allows for loss to a deeper soil compartment and in some cases dissolution (Figure 3.4A).[232,349–351]

Although the ENM mass fraction associated with aerosols is small, this compartment has the highest ENM concentrations (Figure 3.4B). Similarly, [ENM] in suspended sediments in freshwater and coastal waters is high, although the overall ENM mass fraction is also small. As expected, the model predicts several orders of magnitude higher ENM concentrations in agricultural soils, due to the continuous application of biosolids with ENMs, while the loading onto urban soils is much smaller, mostly from atmospheric deposition. This may be revised as better models for release of ENMs from paints and coatings used in buildings and transportation are developed, but is unlikely to reach the levels of agricultural solids. Overall, the most common fate of ENMs is to be associated mostly with agricultural soils and freshwater or marine sediments, either aggregated (homo and hetero) or in dissolution products.
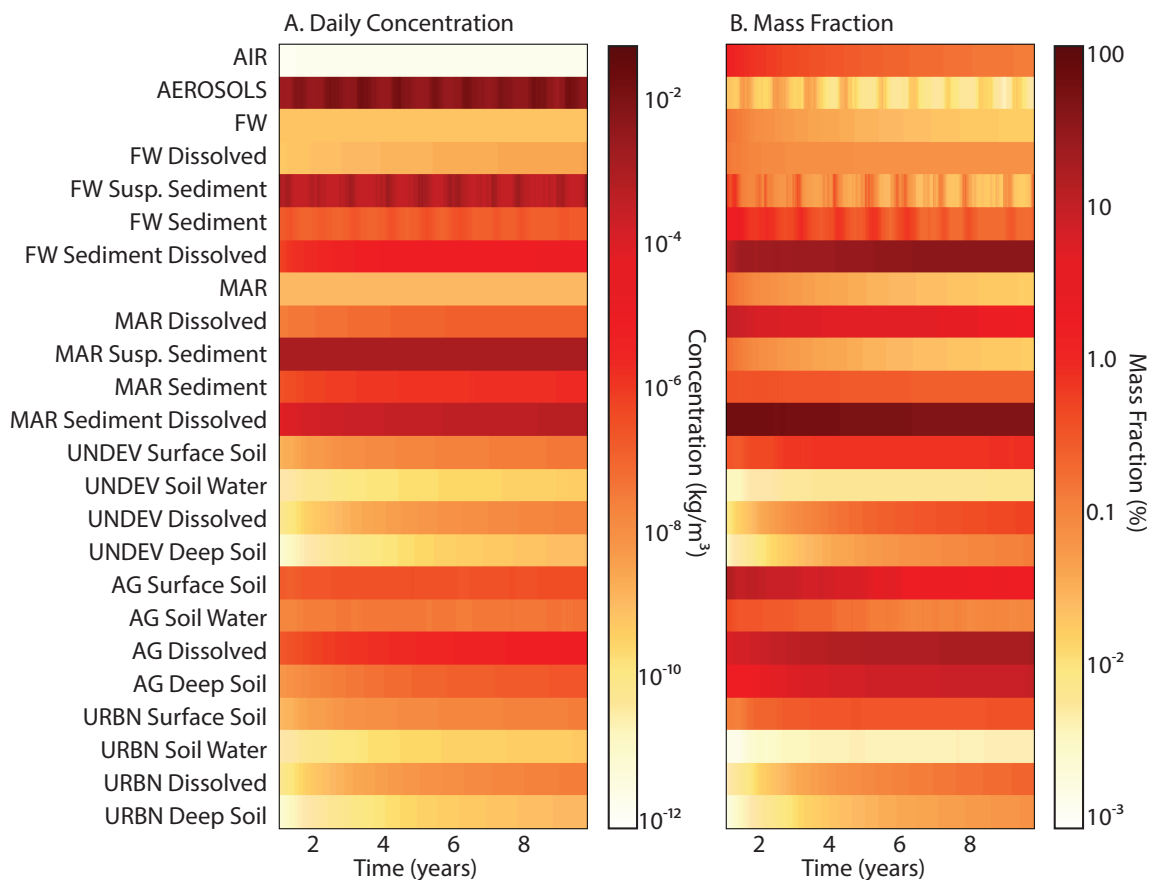
Figure 3.4 (A) Long-Term [ZnO] across all Environmental Compartments and (B) the Mass Fraction Relative to Each Compartment under the High-End Daily Release Scenario.

Each row represents an environmental compartment, daily time progresses on the x-axis, and [ENM] or its transformation products within the compartment is differentiated by color. This figure presents results from a continuous low daily release for ten years. It is worth noting that because of the range in concentrations depicted, a variation of less than half an order of magnitude is not easily visible in compartmental concentrations; variations are more noticeable in the mass fraction (For example, the time lag between increased suspended sediment concentrations and the corresponding sediment concentrations that

follow is much more variable in 3.4B). Daily concentration values for all release scenarios for ZnO, CeO$_2$, CuO, and TiO$_2$ are provided in Appendix Figure A3.4, A3.7-A3.9.

Because of the probability that ZnO is likely to dissolve during wastewater treatment, one additional scenario was explored in the supplemental materials (Figure A3.5-A3.6). We assumed that 90% of the ZnO in the high release scenario would dissolved prior to entering the environment, thus only 10% was release as an ENM. To account for the dissolved component entering the environment, we set the background concentration of the freshwater dissolved, marine dissolved, and agricultural soil water dissolved compartments to the ten-year average from the high release scenario. We found that while the freshwater and freshwater suspended sediment concentrations of nanoparticles both decreased (Appendix Figure A3.5A-B) because releases were lower, the decrease was greater for suspended sediment (Appendix Figure A3.6), indicating less aggregation resulting from lower concentrations and more free/small aggregates. The same was found to be true for marine systems. This also suggests that nano toxic effects depend heavily on the form the ENMs take once in the environment; for example the free ENM and small aggregates concentration is much closer to the concentrations predicted by the low release scenario and thus much closer to the NOAEC concentration than the LC$_{50}$ concentration. Also, since the equilibrium dissolution is being reached in freshwater, marine, and agricultural soils, no further dissolution occurs (Appendix Figure A3.5).

Compartments with substantial fluctuations in concentration are important for two reasons: (1) any single day with a sharp increase in concentration could result in short term toxicity; and (2) seasonal trends can be seen from these daily variations that could have short term impacts if the release of ENMs also corresponds with the seasonal variations. For

example, if the release of an ENM also varies by season (e.g. higher concentrations tend to accumulate in aerosols in summer, and environmental releases are higher in summer, see Figure 4) then this would exacerbate seasonal peaks to the point at which toxicity could occur under a cyclical scenario.

For each release scenario, the average concentration in each compartment is calculated over the final year of a model run. In comparing across the release scenarios, the low-end release scenario tends to result in concentrations that are mostly one order (though occasionally up to three orders) of magnitude lower than the high release scenario (Figure 3.5A; Appendix Figures A3.10-A3.12). For ZnO (Figure 3.5A) as well as for the other ENMs, there is not much difference between the constant-level high release scenario, the increasing high release scenario, and the high release scenarios with accidental spills. The impact of an accidental spill is most visible in the increased mass fractions, although there is no substantial change in the environmental concentration at the end of the simulated period (Figure 3.5B). Increasing the high release scenario by an order of magnitude (x10) (Figure 3.5A, column 4) increases the environmental concentrations by slightly more than a factor of three across most compartments, although this is limited if the equilibrium dissolution concentration is reached. Exceptions to these findings include: (i) dissolved Zn in freshwater; (ii) CuO in freshwater suspended sediment; (iii) Cu dissolved in freshwater sediment; and (iv) copper in all soil compartments (Appendix Figure A3.11), where the increase ranges from a factor of 3.5 to 7. These increases are not proportional because of advective losses from the system and concentration dependent dissolution. TiO_2 tends to increase slightly more under the highest release scenario relative to all other release scenarios, largely because dissolution does not occur for TiO_2 (Appendix Figure A3.12A).
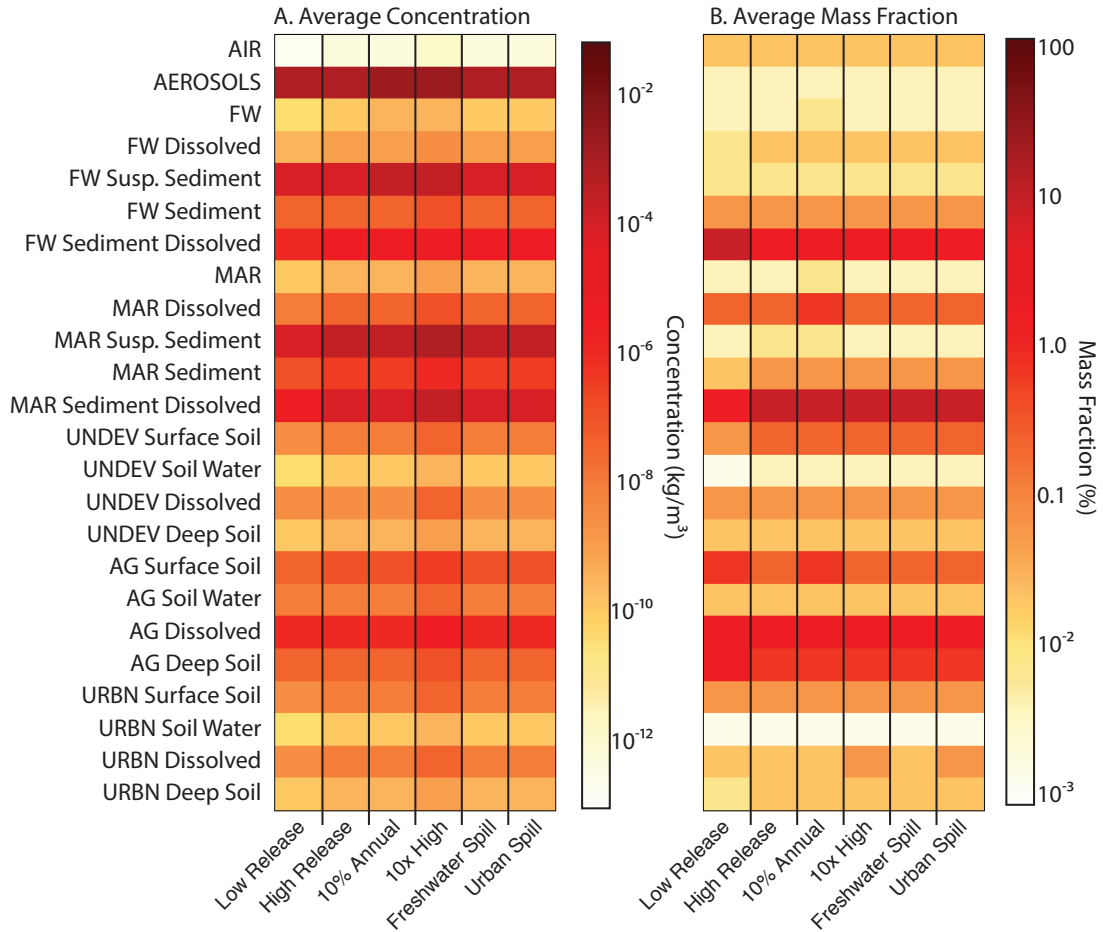
Figure 3.5 Comparison in (A) Average Concentration and (B) Average Mass Fractions of ZnO across All Compartments and Release Scenarios over the Final Year of Each Simulation

Each row represents an environmental compartment, each column represents a different release scenario (column 1 - low release scenario, column 2 - high release scenario, column 3 - annually increasing high release scenario, column 4 - ten times higher than the high release scenario, column 5 - the high release scenario with an accidental spill to freshwater on Jan 1, 2013, and column 6 – the same accidental spill but released to urban soils), and concentration of the ENM within the compartment is differentiated by color.

Comparing across ENMs indicates how important the release estimates are to the resulting long-term concentrations across most compartments. For example, because TiO_2 is produced and released in far higher quantities than any of the other ENMs in this study, the resulting long term concentrations are much higher than CuO, whose estimated release is lower by several orders of magnitude (Figure 3.6). In addition, the release patterns to air, water and agricultural soils vary by ENM due to differences in how ENMs are used in various applications (e.g. paints, personal care products, fuel catalysts, pesticides). For the soluble ENMs (CuO and ZnO) there is also a significant amount of dissolution in freshwater, marine, and agricultural soil water (Figure 3.6), which can result in the formation of Cu and Zn precipitates. Conversely, the white blocks in the CeO_2 and TiO_2 columns indicate that no or minimal dissolution of these ENMs occurs in the water and soil water compartments (Figure 3.6).
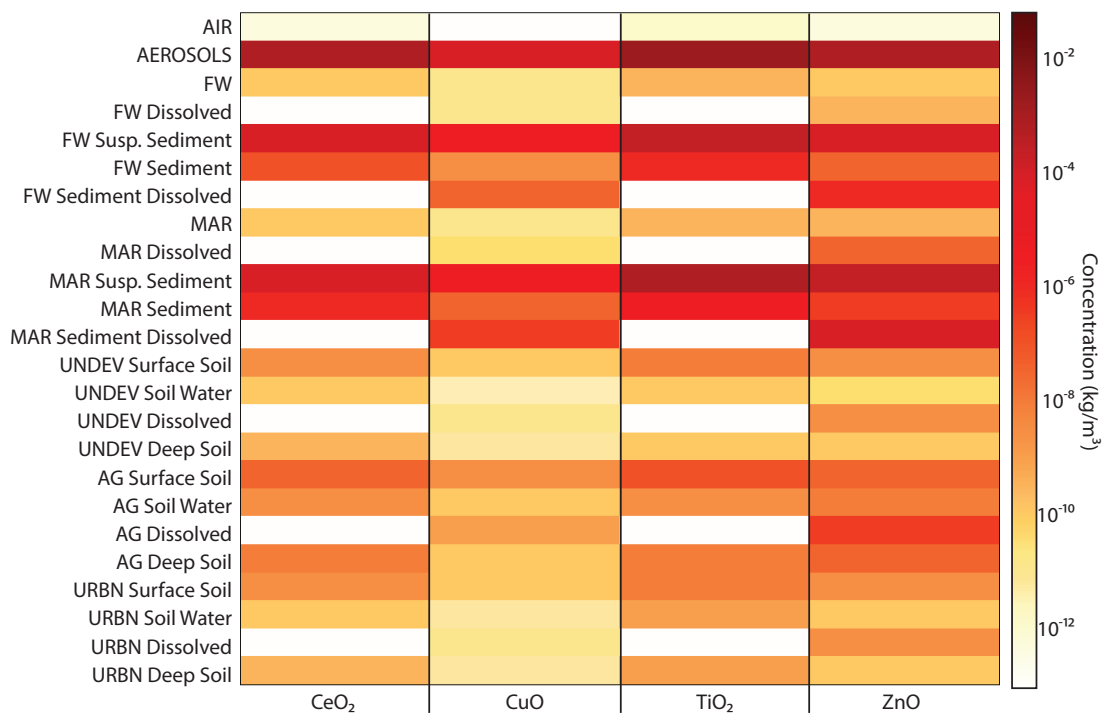
Figure 3.6 Average Long-Term Concentration of ENMs by Compartment under the High Release Scenario

Each row represents an environmental compartment; each column represents a different ENM. The concentration of the ENM within the compartment is differentiated by color and ranges over multiple orders of magnitude.

A comparison of long-term concentrations in freshwater environments with predicted hazardous concentration at which 5% of species in a freshwater ecosystem will be harmed (HC_5) indicates that even under the highest release scenario considered in this study CeO_2 will likely be well below the NOAEC (Figure 3.7A). However, because the NOAEC line is built upon a very limited number of observations (Appendix Figure A3.13A) and has high uncertainty, the lowest observed LOAEC from an SSD (yellow line) was also included.[270] Under all release scenarios, CuO does not exceed the NOAEC HC_5 (Figure 3.7B). However, because the NOAEC line is also built upon a very limited number of observations (Appendix Figure A3.13B), and thus is highly uncertain, the single species NOAEC line (light green line, *D. magna*) indicates that under the considered scenarios it is unlikely that toxic effects would be observed in freshwater (Figure 3.7B).[401] TiO_2 may occasionally exceed the freshwater NOAEC HC_5 in all scenarios except the low release scenario, and every day for the 10x high release scenario (Figure 3.7C).[400] While the predicted freshwater [ZnO] are likely to be several orders of magnitude less than the HC_5 LC_{50}, ZnO still poses the highest concern because under all release scenarios (including the lowest predicted releases), the daily freshwater concentrations are expected to exceed the HC_5 NOAEC, indicating that some effect from ZnO may already be noticeable in the Greater San Francisco Bay Area, particularly because these release scenarios are based on 2013-2014 estimates, which have likely continued to increase over time (Figure 3.7D).[400]
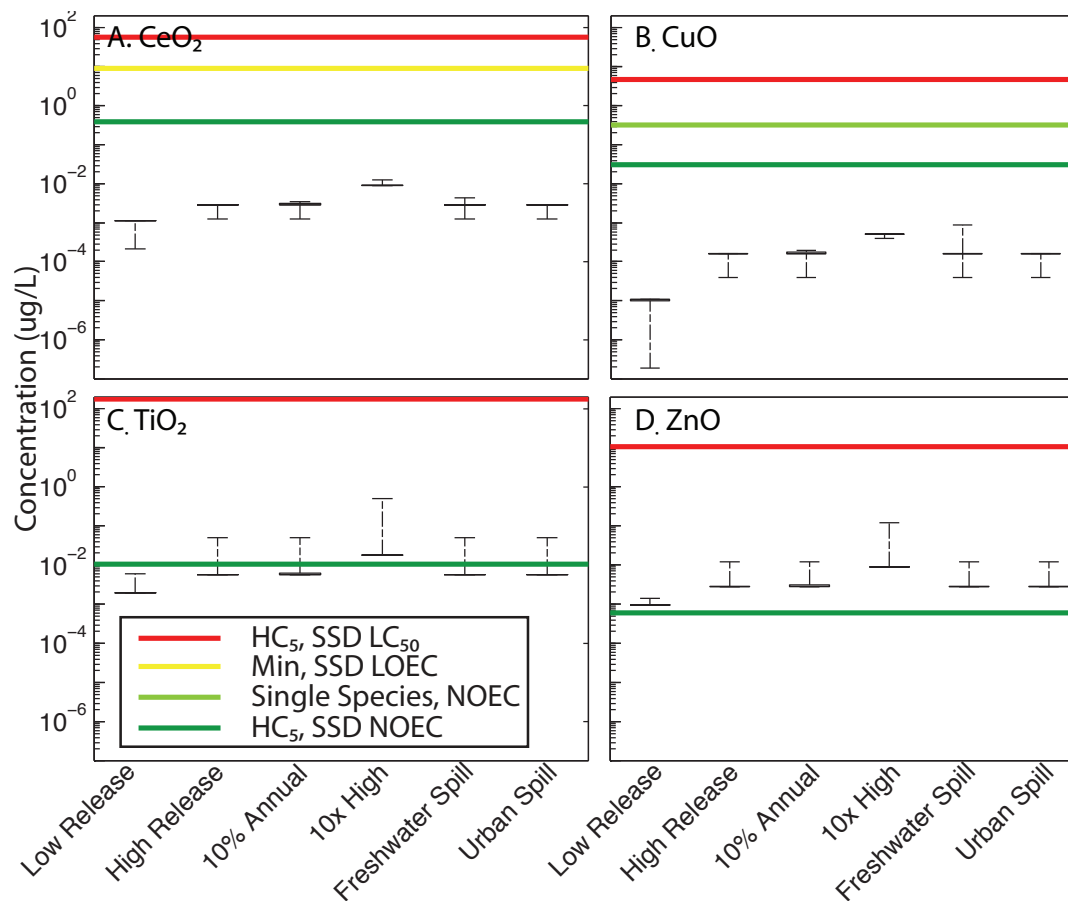
Figure 3.7 Comparison among the Range of Predicted Daily Freshwater Concentrations and Several Toxicity Endpoints above which a Toxic Effect would be Observed for 5% of Species in a Freshwater Ecosystem, either the NOEC, LOEC or LC$_{50}$, for (A) CeO$_2$, (B) CuO, (C) TiO$_2$, and (D) ZnO

Each box and whiskers plot shows the range in daily concentrations for each release scenario (i.e. low release, high release, increasing high release, four times higher than the high release, and the accidental spill scenario) with the mean depicted as a thicker black horizontal line. Because this graphic shows such a wide range in environmental concentrations, the full boxes are difficult to visualize although the boxplot includes the full set of quartiles (2.5%, 25%, 50%, 75%, 97.5%).

In agricultural and urban soils, neither TiO_2 nor ZnO exceed the NOEC for soil

ecosystems under even the most extreme release scenarios (Figure 3.8A and 3.8B).[400] CeO_2

and CuO were not included in this graph because no specific toxic endpoints for soil

organisms could be identified in the literature for comparison. The most significant

difference is that ZnO is only about two orders of magnitude lower that the NOEC whereas

TiO_2 is many orders lower than the NOEC. However, typical background concentrations of

Zn range from 10-300 mg Zn kg^{-1} soil, which is substantially higher than the predicted

concentrations of ZnO in the model, suggesting limited concern for impacts resulting from

these predicted concentrations.
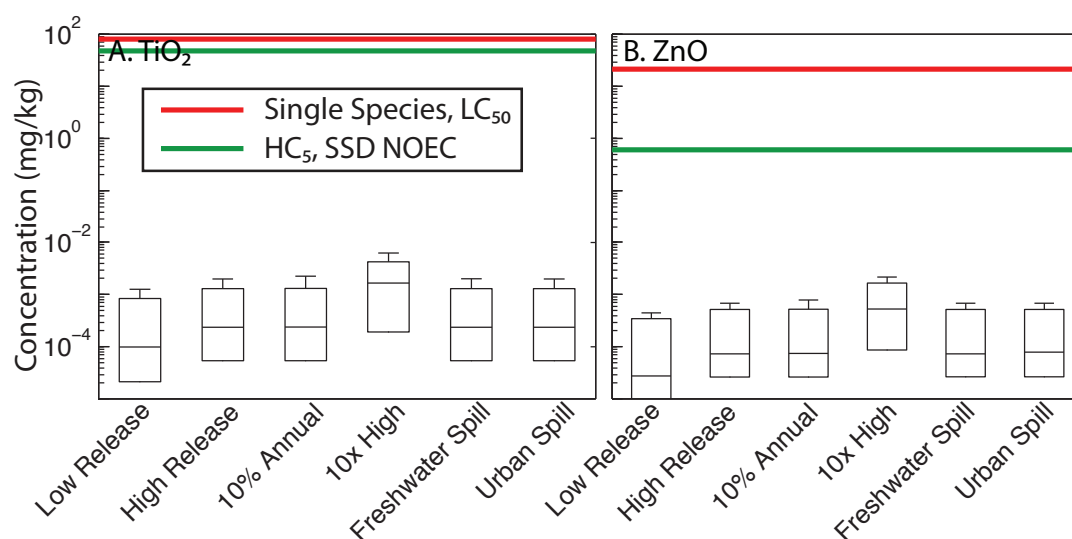
Figure 3.8 Comparison among the Range in Daily Agricultural Soil Concentrations HC$_5$ NOEC (green line) for a Soil Ecosystem Taken from Coll et al. 2015 and Single Species EC$_{50}$ for *C. elegans* (red line) (a soil dwelling nematode), for (A) TiO$_2$, and (B) ZnO

Each box and whiskers plot shows the range in daily concentrations for each release

scenario (i.e. low release, high release, increasing high release, 10x times higher than the

high release, and the accidental spill scenarios) with the mean concentration depicted as the thicker black horizontal line in the middle of each box.

3.4 Discussion

Our results point to several significant findings. (i) Soluble nanoparticles, such as ZnO and CuO can accumulate in the aquatic environment over the long term in sufficient concentrations to potentially cause toxicity (as observed for the freshwater ecosystem within the San Francisco Bay case study), even with a model that accounts for dissolution in aquatic media. Solubility, often assumed to be a primary driver of ENM toxicity, is not the only determining factor for toxicity. (ii) The highest concentrations and mass fractions of ENMs will be found in agricultural soils, freshwater, and marine sediments, which continue to increase slowly over time; aerosol concentrations are also high but their mass fraction is always quite small because the quantity of aerosols in low and the extent of attachment is thus also low (iii) If production and release of TiO_2 into the environment are substantial, the corresponding environmental concentrations likely may exceed the observed toxicity thresholds. (iv) However, even at very low release volumes, such as with CuO, the nanoparticle itself may still reach toxic concentrations regardless of solubility. (v) Environmental fluctuations (e.g. rainfall) and release fluctuations (e.g. accidental spills) have the potential to cause short-term toxic effects. Steady state fate or MFA models are unable to predict these spikes in daily concentrations. In addition, previous models have not considered the effects of accidental releases on the environment, which is something that we chose to explore and found that while the release can cause temporary spikes in environmental concentrations that may cause localized short term toxicity, an accidental spill does not appear to cause significant long term concentration increases at the regional

level. However, if current release increases and a substantial spill occurs, the effects would be of concern, primarily for ZnO and secondarily for TiO_2 and CuO.[342] In addition, while our air concentrations are generally predicted to be quite low under these specific scenarios, localized releases that result in ambient concentration spikes could cause chronic toxic effects in humans and animals.[402] Finally, we found that the environment may have some capacity to assimilate large releases of ENMs since increasing by 10x the high release scenario does not result in a corresponding increase in compartmental concentrations.

Models are always simplifications developed for specific objectives. In this case, the objective was to development a model that could evaluate the large-scale regional fate of specific ENMs, simplifying the individual particle-to-particle interactions. While we explored large scale release scenarios, no model validation is currently feasible because of a lack of experimental data designed to cover the range of environmental conditions in a large scale fate model and a lack of field observations against which one could compare the results.[357] In fact, there is a lack of field data even at small scales to validate these models.[357]

Instead, we compared the NanoFate model to existing fate models and other PECs, to determine if our range in predictions fell within the range of previous predictions (Figure 3.9). For CeO_2, for example, our range is dissimilar to two previous predictions for freshwater and sediment, but is quite similar for all the other environmental compartments (Figure 3.9A).[352,362,364] For CuO, our range in predictions overlap with all compartments, though we predict slightly higher air concentrations and slightly lower sediment concentrations than other models, which may be a result of including dissolution in sediment (Figure 3.9B).[352] TiO_2 is the most commonly modeled ENM, and the range in predicted results is quite wide (Figure 3.9C).[2,18,29,232,352,361,363,365] Our results fall well within the predicted range for other existing

110

models, though ours were on the lower end for most compartments, except in air and sediments where our results tend to be somewhat higher (Figure 3.9C). For ZnO our predictions fall within previous predicted ranges except for suspended sediment, where the NanoFate model predicts much higher concentrations (Figure 3.9D).[2,231,352,365]
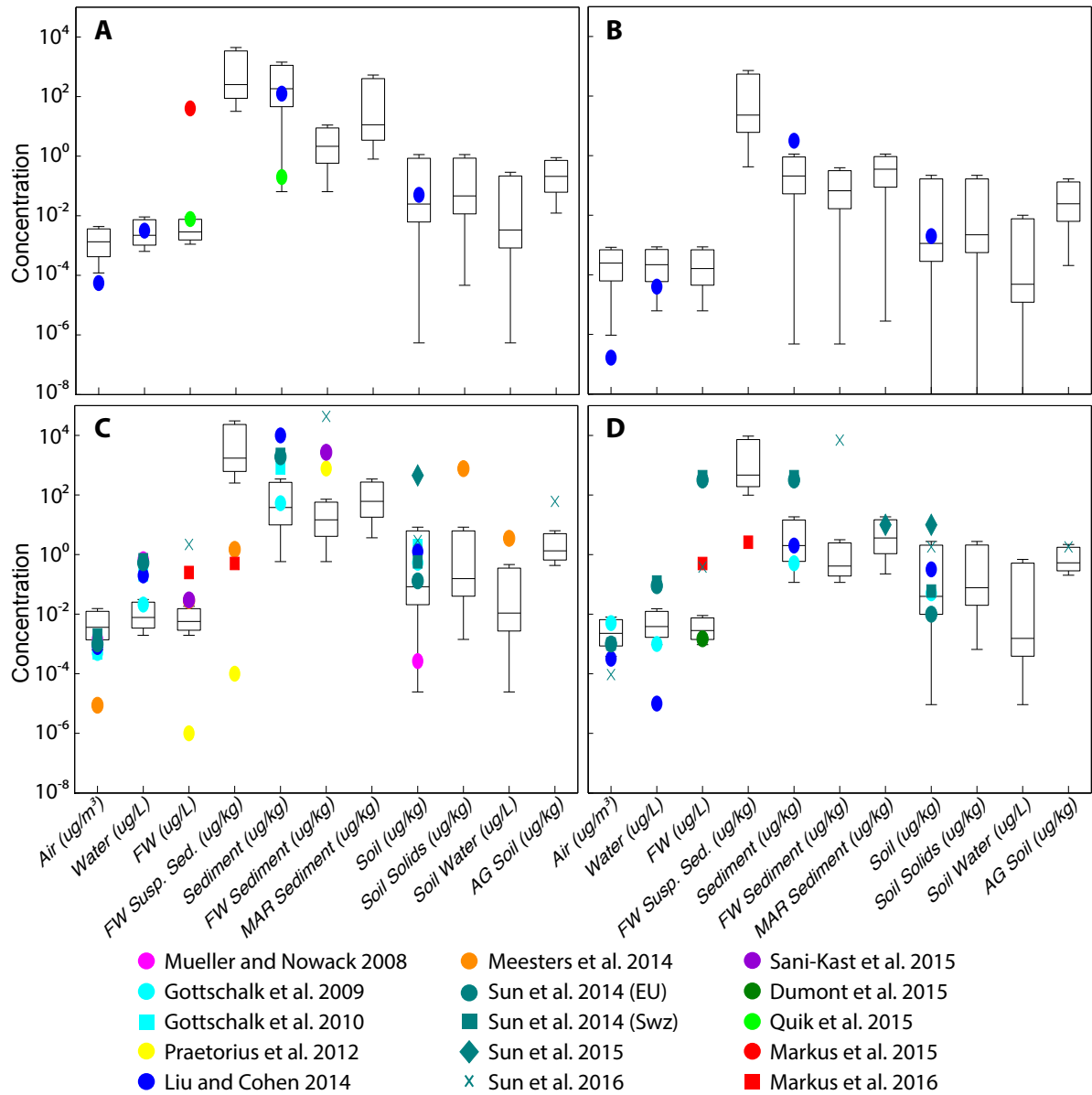
Figure 3.9 Comparison among NanoFate Model Results and Other Published Predictions

111

This comparison includes results from MFA PECs[2,348–351,361], and mechanistic fate models.[18,232,352] Comparisons are for (A) CeO_2, (B) CuO, (C) TiO_2, and (D) ZnO. The NanoFate model's results are presented as a box and whiskers plot which includes the full range of predicted concentrations from all release scenarios.

The NanoFate model sediment [ENM] predictions tend to be on the low end relative to previous models, likely resulting from the inclusion of dissolution in freshwater and marine sediment, which is quite significant for ZnO (Figure 3.5). The differences also reflect that the various models often do not consider the same ENM sources, release amounts, routes, and time periods. This figure also highlights environmental media where we are able to begin to fill in gaps regarding [ENM] predictions.

A comparison with the Gottschalk et al. (2013) review of MFA PEC also shows good agreement with the NanoFate model's results for surface water concentrations for TiO_2, ZnO, and CeO_2, though our predictions for sediment concentrations tend to be somewhat lower for both TiO2 and ZnO.[403] This may be a result of the fact that MFAs do not typically account for nano-specific processes that might limit transfer to sediment (e.g. dissolution). Differences may also reflect that these MFAs do not account for runoff and erosion, and the downward movement of particles with infiltrating soil water. For air, our predictions also fall within the same range of results indicated by the PEC study.[403] For soils and soils treated with biosolids (as with the agricultural soil compartments included in this model), the range in PECs tends to be quite wide, with our estimates being much lower than most MFA estimates for both CeO_2 and ZnO, though our TiO_2 predictions fall well within the middle range of predicted concentrations.[403]

112

Another important consideration that we did not include in our model is the extent to which the release of ENMs into the environment is actually as nanoparticles as opposed to large agglomerates or particulate matter that is not in the nano-scale. In the model, we assumed that ENM release was as pristine or small homoaggregates whereas improved end-of-use release estimates would allow us to differentiate between size fractions and chemical species. In the Supplemental Materials, we discuss the impact of assuming significant transformation of ZnO to dissolved Zn prior to release from WWTPs (Appendix Figures A3.5, A3.6).

Finally, the most important conclusion from the model development process is the need for more experimental investigations to determine medium-dependent fate processes and rates.[357] When rate constants are for specific nanomaterials, if a different type of nanomaterial is considered or the environment is very different from the one(s) used to estimate the average rate, then the short-term fate may vary considerably. We believe that the long-term accumulation will still be reasonably accurate, because long-term averages do not change substantially as a result of a moderate change in rate or ENM characteristics. Fate is also very dependent on the transfer processes that are considered within any mechanistic model. For example, while we did not run the model for nano-Ag, if we had, it would be important to include sulfidation as a transformation mechanism because without it, the nano-Ag would remain as free nanoparticles for much longer than they have been observed to in realistic environments.[94,404,405]

Humans and ecosystems are already being exposed to ENMs as they are released into the environment over their lifecycle.[4,8,226] Once released, there is sufficient understanding to know that transport will occur and that physical transformations such as aggregation, agglomeration,

and adsorption and surface transformation such as oxidation, dissolution, and sulfidation will all alter when, where, and how exposure occurs.[85,226,345,359] This study begins the process of predicting the implications of releasing ENMs into our environment and determining whether that exposure will result in hazardous concentrations. The fate and transport model estimates the environmental distribution and accumulation of ENMs under a range of release scenarios. Comparison with SSDs indicates whether we are likely to see an ecosystem-wide toxic effect resulting from exposure to a given ENM in freshwater and soil systems.

The benefit of our approach is that we do not need to wait for data-limited areas of research to be developed. We are starting to close the gap between experimental research and its incorporation into fate modeling in order to improve the predictive power of our results.[359] By using a case study of ENM release into the Greater San Francisco Bay Area region, we have begun to identify which ENMs are of concern right now, and which may become a concern if production and release rates increase for a particular ENM.
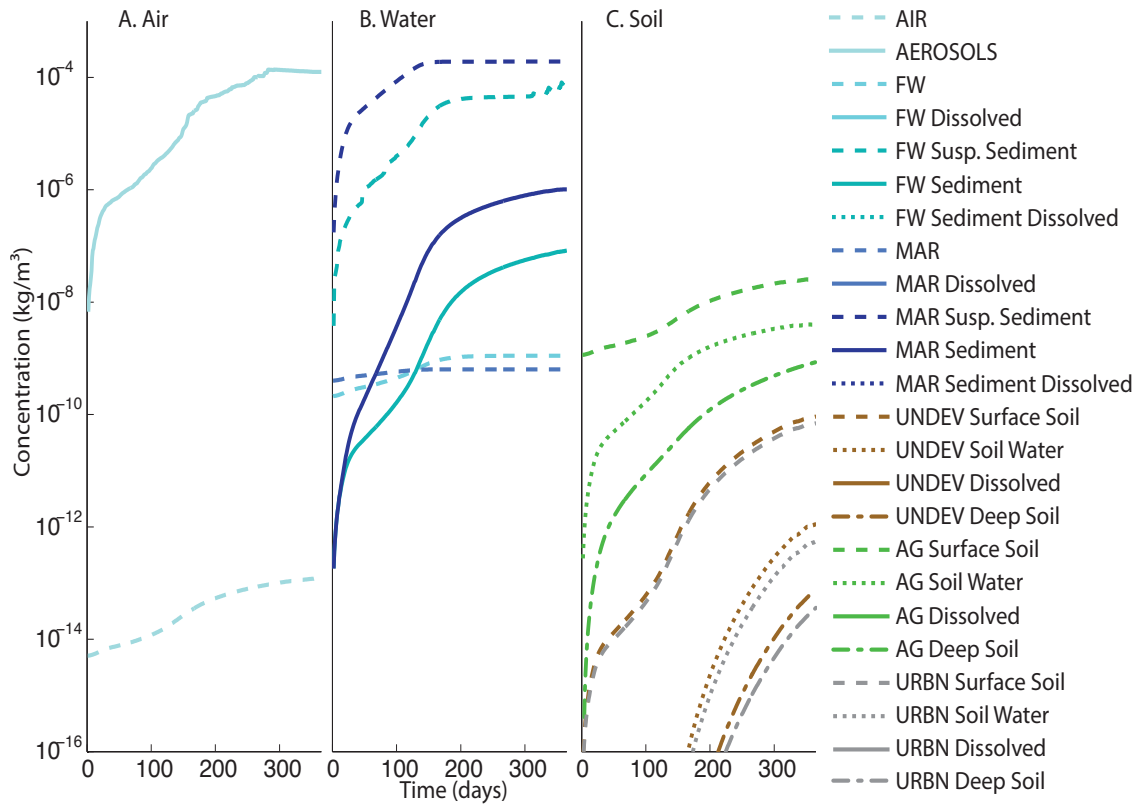
Figure A3.1 CeO₂ Concentrations under Low Release Scenario over First Year of Model Simulation in (A) Air, (B) Water, and (C) Soil
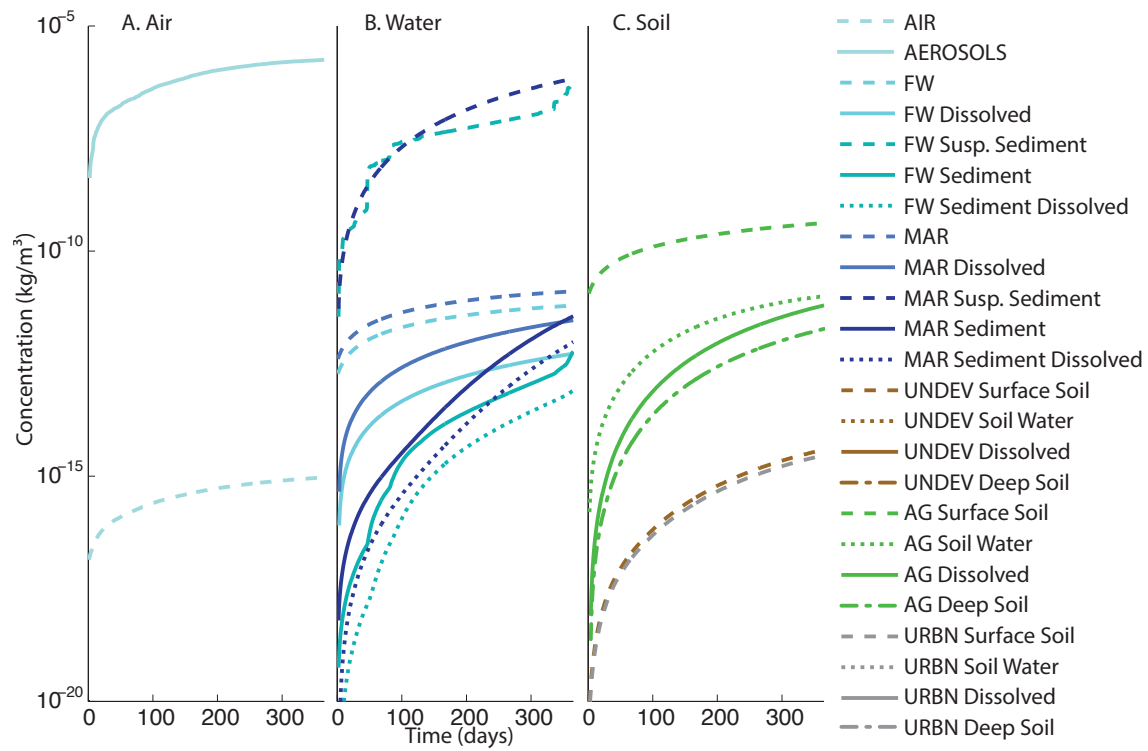
Figure A3.2 CuO Concentrations under Low Release Scenario over First Year of Model Simulation in (A) Air, (B) Water, and (C) Soil
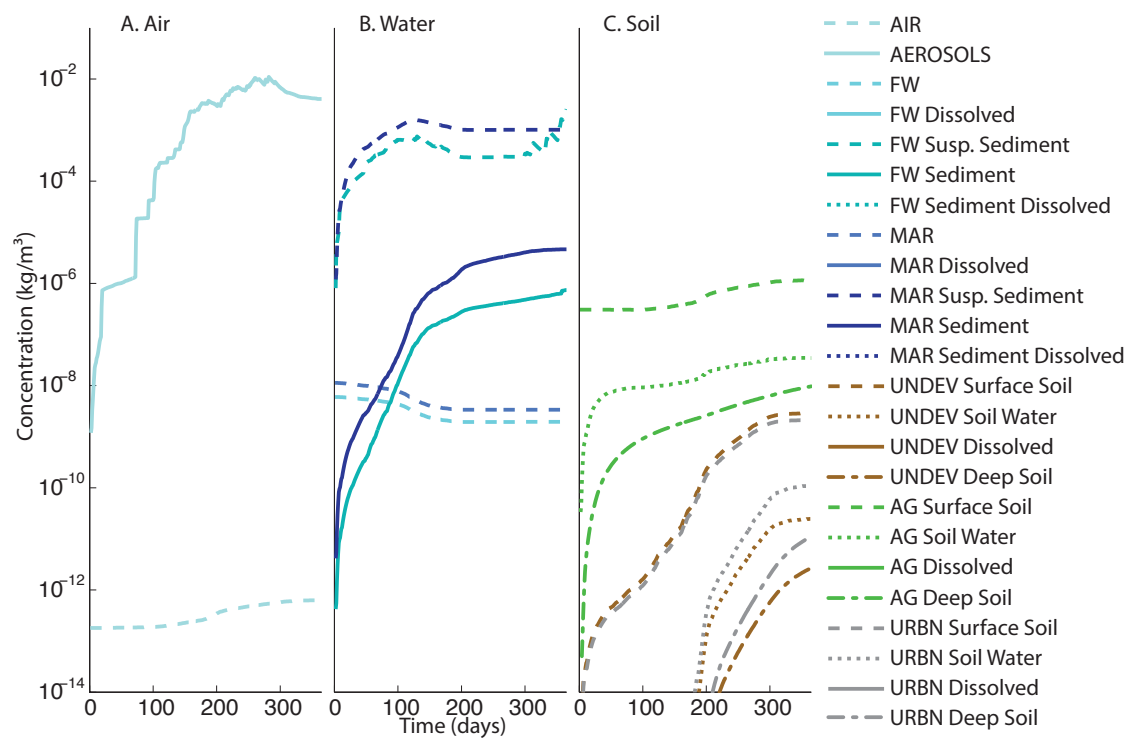
Figure A3.3 TiO$_2$ Concentrations under Low Release Scenario over First Year of Model Simulation in (A) Air, (B) Water, and (C) Soil
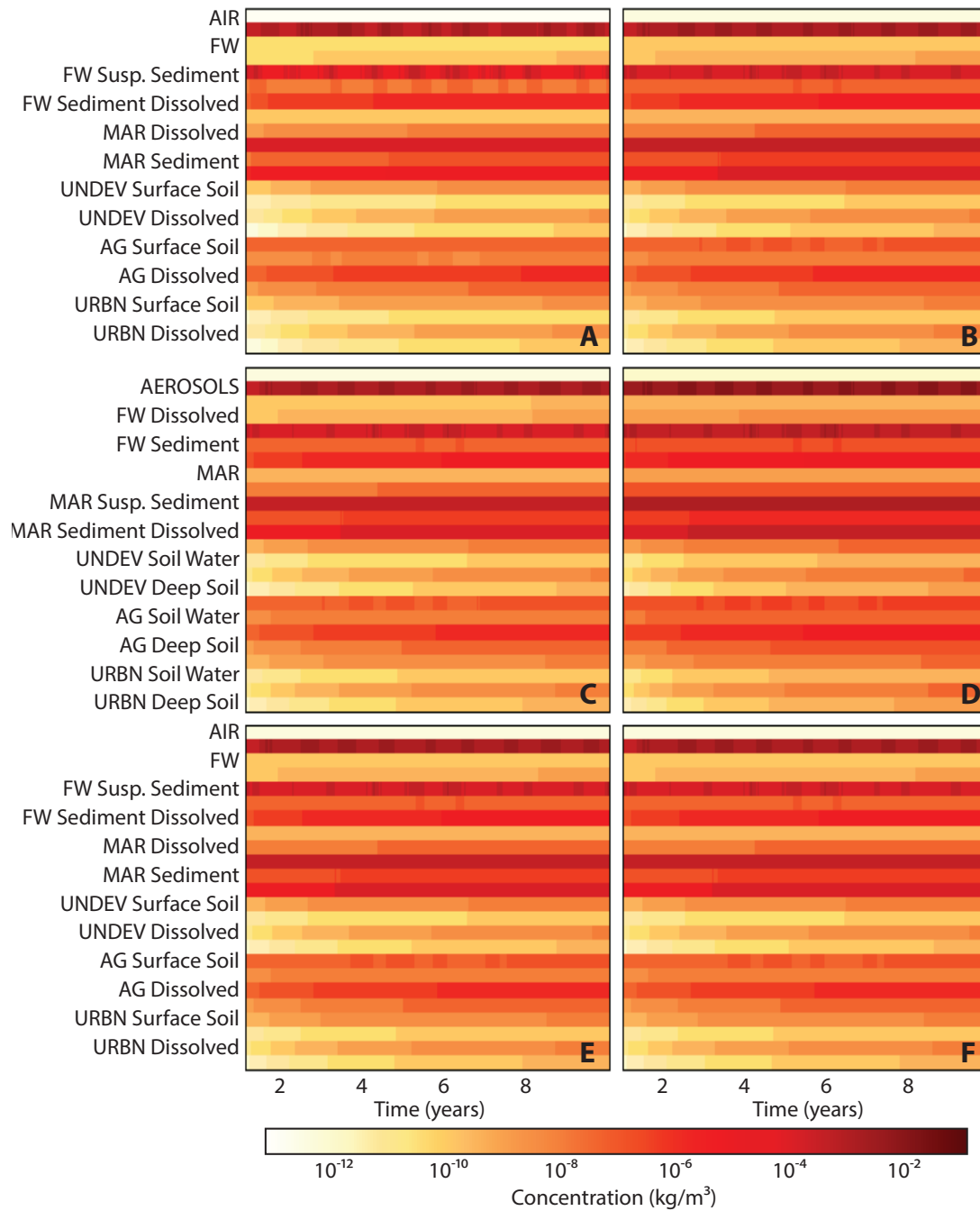
Figure A3.4 Comparison of Daily Concentrations after First Year of Model Simulation under all Six Release Scenarios for ZnO including (A) Low Release, (B) High Release, (C) High Annual Increasing Release, (D) 10x High Release, (E) High Release with Accidental Spill to Freshwater, and (F) High Release with Accidental Spill to Urban Soil Scenarios

118
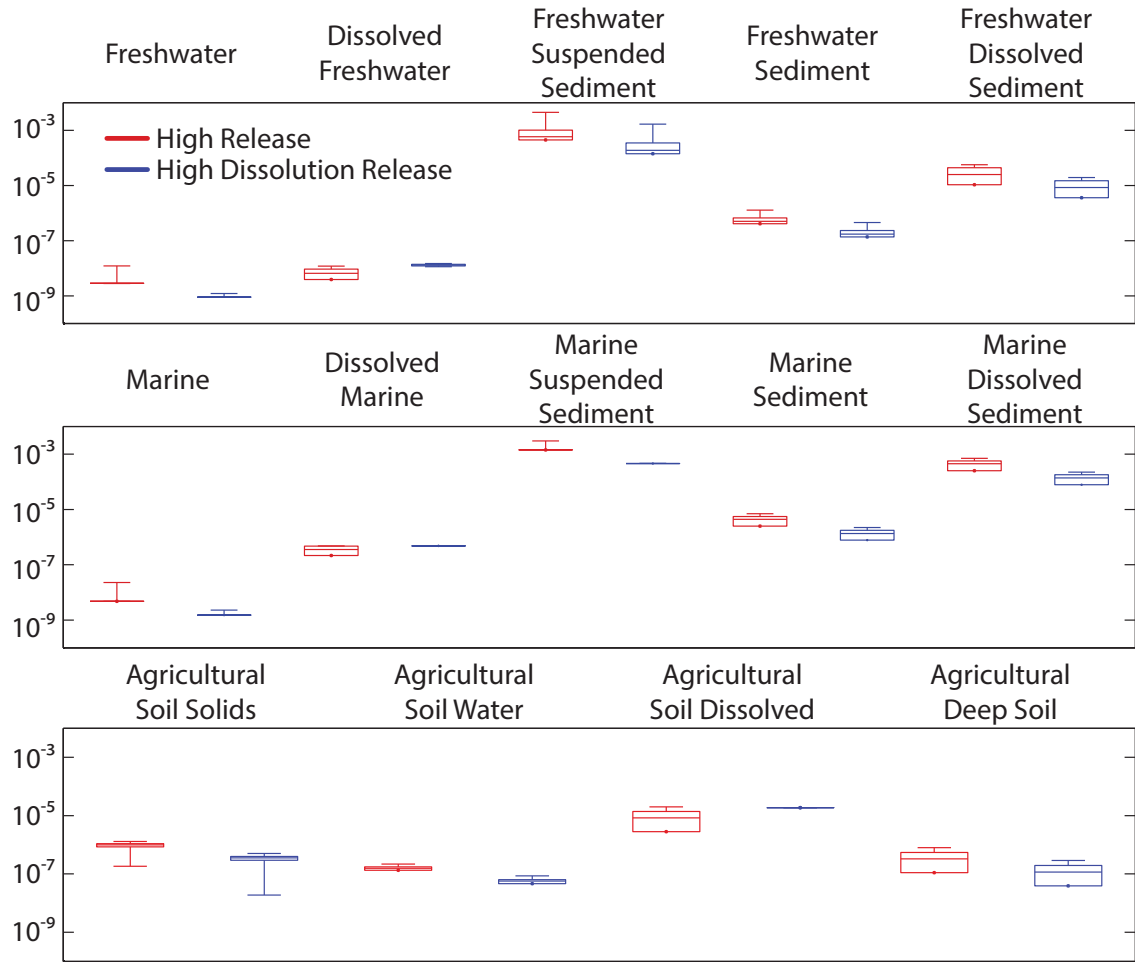
Figure A3.5 Comparison of Range in Predicted Concentrations from High Release Scenario of ZnO and High Release Scenario assuming 90% of ZnO Dissolves prior to Release from WWTP so that 10% of the High Release Scenario enters the Environment as n-ZnO and the Rest is Released as Dissolved Zn^{2+} in Freshwater, Marine, and Agricultural Soils.

The resulting range in concentrations is presented from (A) freshwater and subcompartments, (B) marine and subcompartments, and (C) agricultural soils and subcompartments.

119
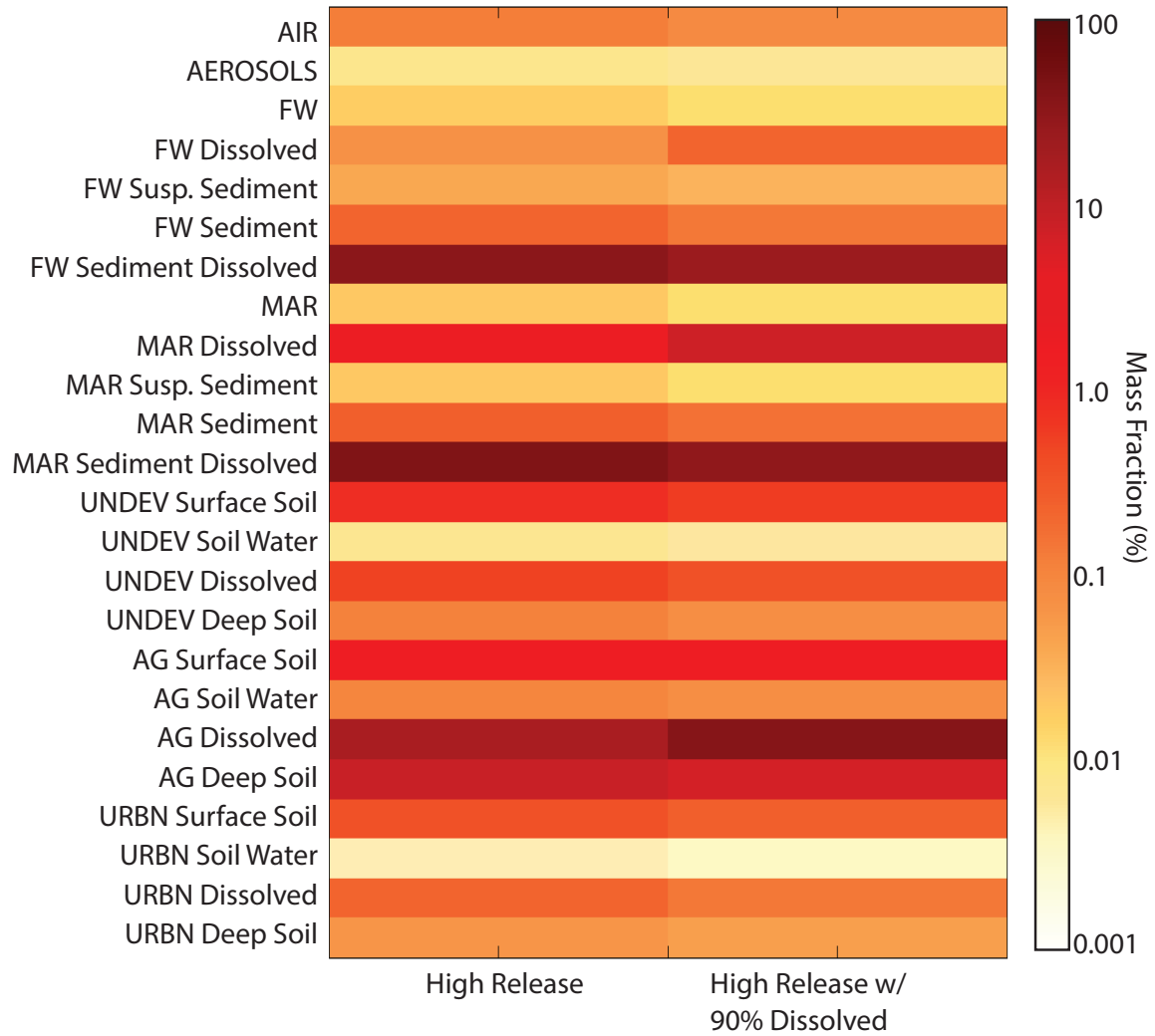
Figure A3.6 Comparison of Mass Fraction between (A) High Release Scenario of ZnO and (B) High Release Scenario assuming 90% of ZnO Dissolves prior to Release from WWTP with Average Mass Fractions Presented at the 10 Year Average
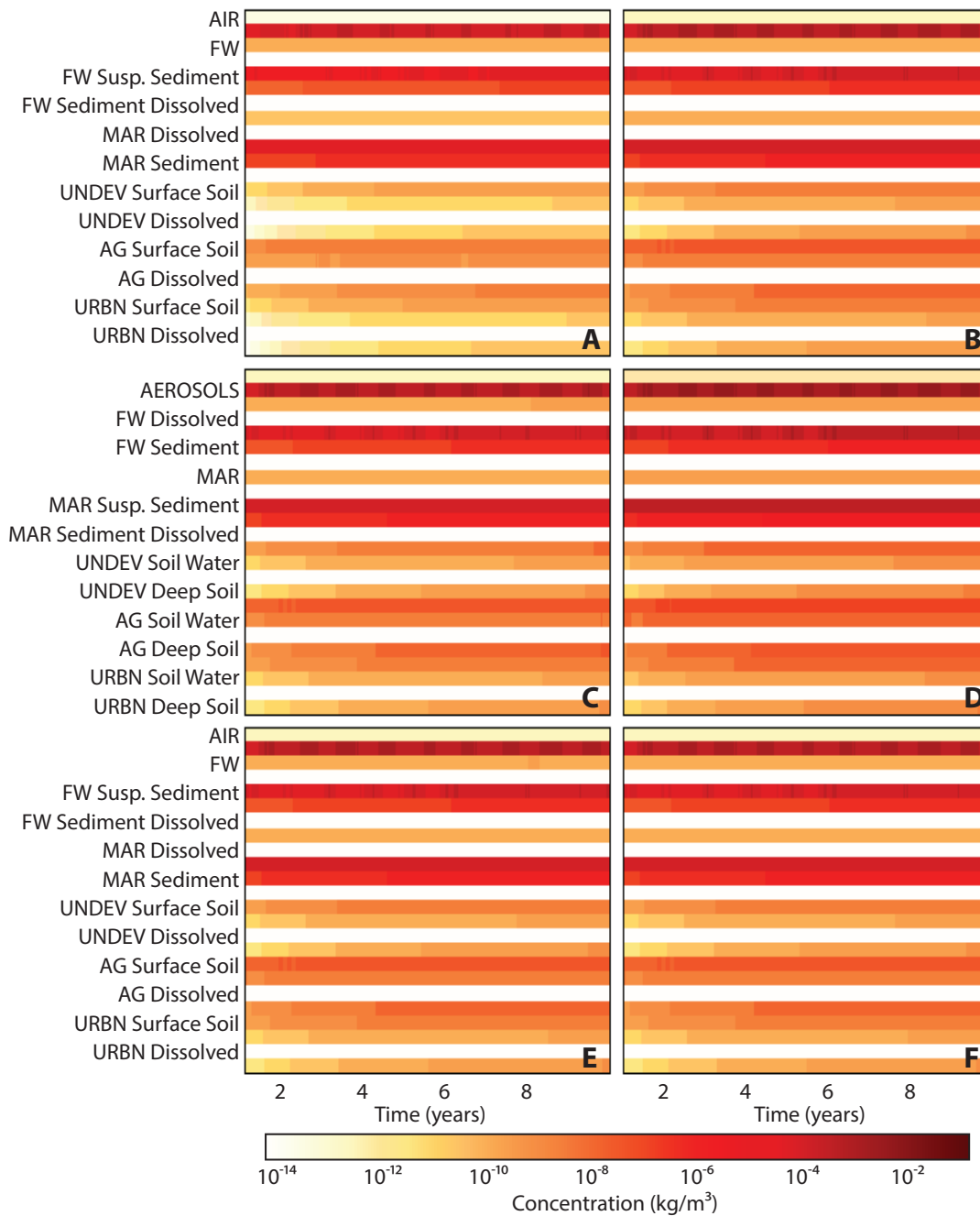
Figure A3.7 Comparison of Daily Concentrations after First Year of Model Simulation under all Six Release Scenarios for CeO₂, including (A) Low Release, (B) High Release, C) High Annual Increasing Release, (D) 10x High Release, (E) High Release with Accidental Spill to Freshwater, and (F) High Release with Accidental Spill to Urban Soil Scenarios
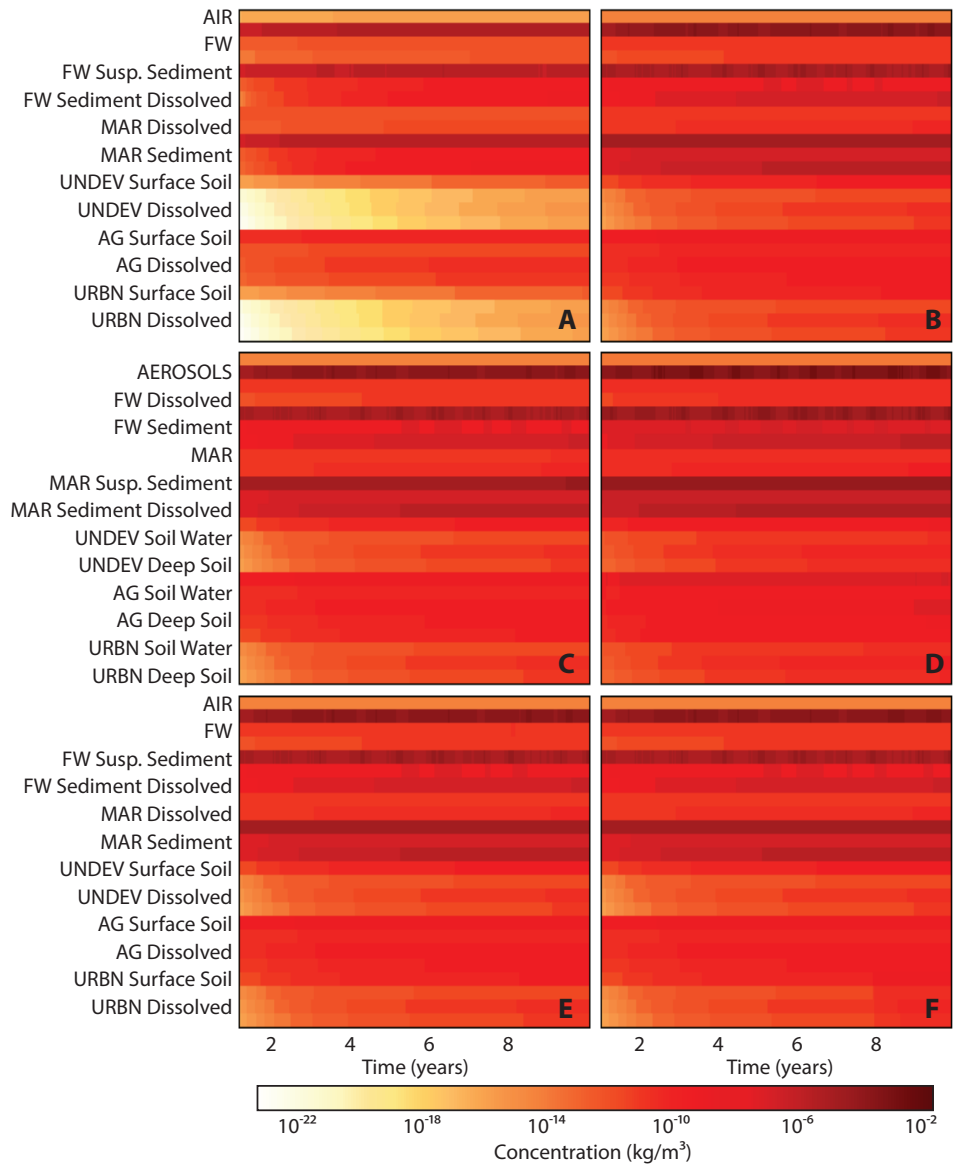
Figure A3.8 Comparison of Daily Concentrations after First Year of Model Simulation under all Six Release Scenarios for CuO, including (A) Low Release, (B) High Release, C) High Annual Increasing Release, (D) 10x High Release, (E) High Release with Accidental Spill to Freshwater, and (F) High Release with Accidental Spill to Urban Soil Scenarios

Note that the concentration scale on this figure values substantially from the other figures because the release scenarios are typically far lower for CuO.
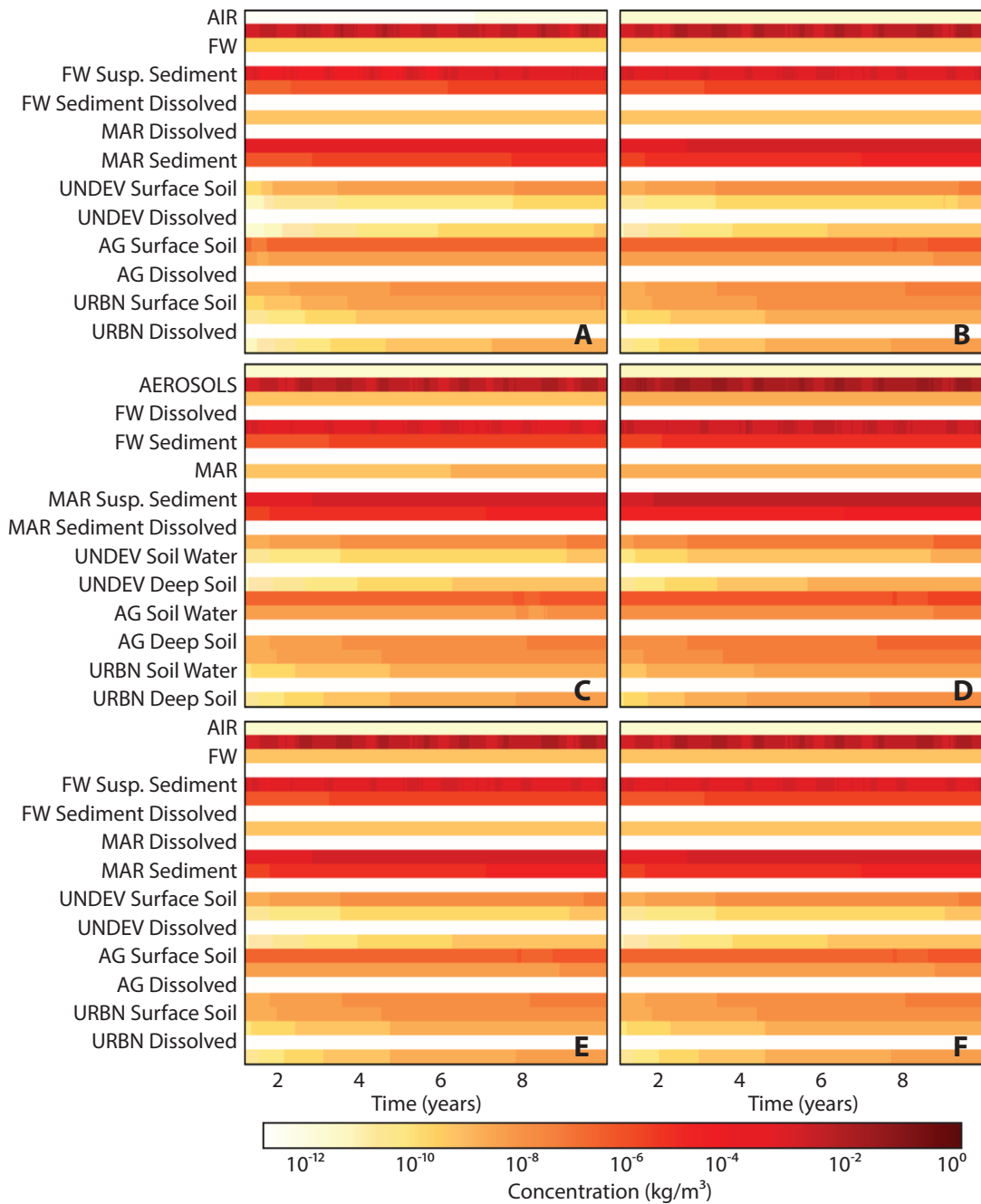
Figure A3.9 Comparison of Concentrations after First Year of Model Simulation under all Six Release Scenarios for TiO₂, including (A) Low Release, (B) High Release, C) High Annual Increasing Release, (D) 10x High Release, (E) High Release with Accidental Spill to Freshwater, and (F) High Release with Accidental Spill to Urban Soil Scenarios
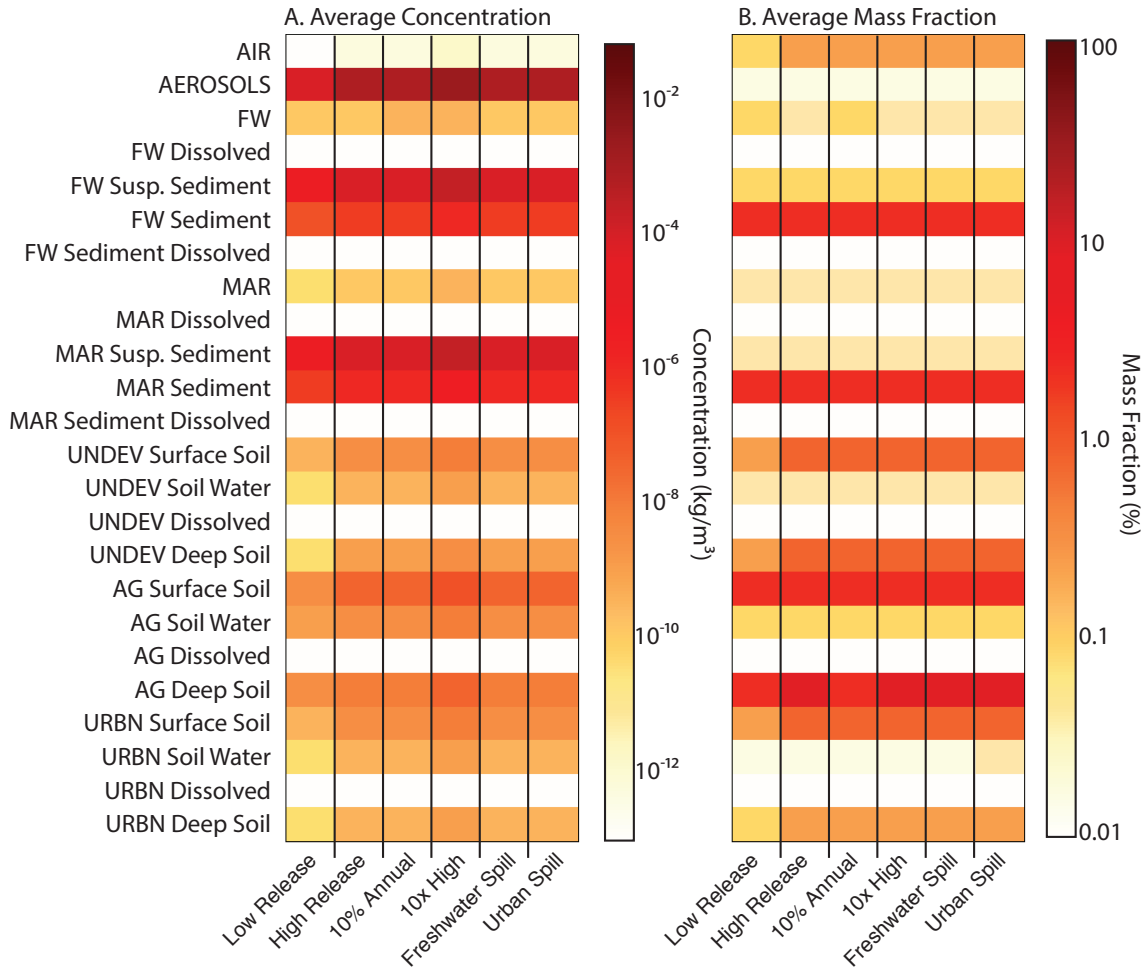
Figure A3.10 Comparison of (A) Average Concentration and (B) Mass Fraction over Final Year of Simulation across all Compartments for all Simulations for CeO₂
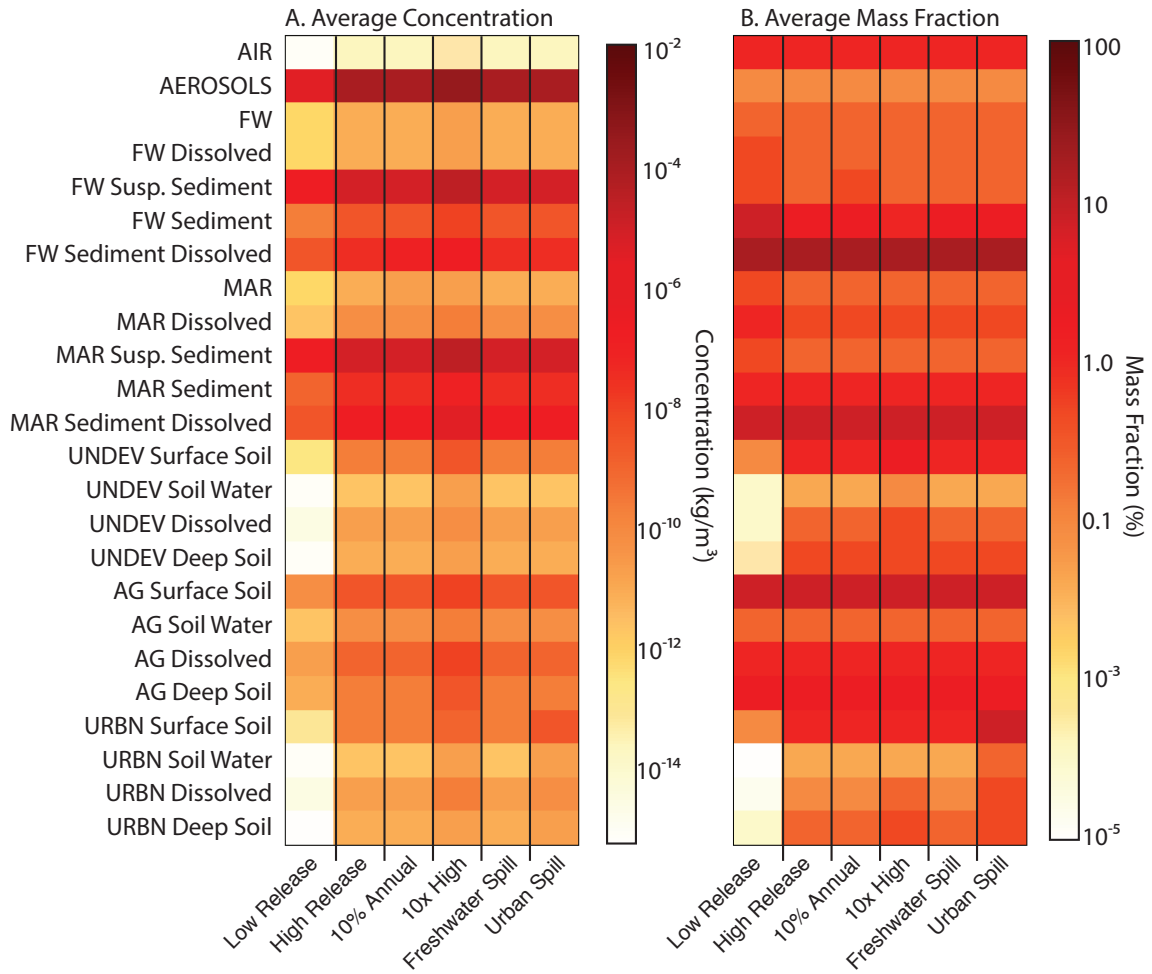
Figure A3.11 Comparison of (A) Average Concentration and (B) Mass Fraction over Final Year of Simulation across all Compartments for all Simulations for CuO.

Note that the scales vary somewhat from corresponding figures for the other ENMs as the quantity of CuO entering the environment in much lower for all scenarios than the other ENMs.
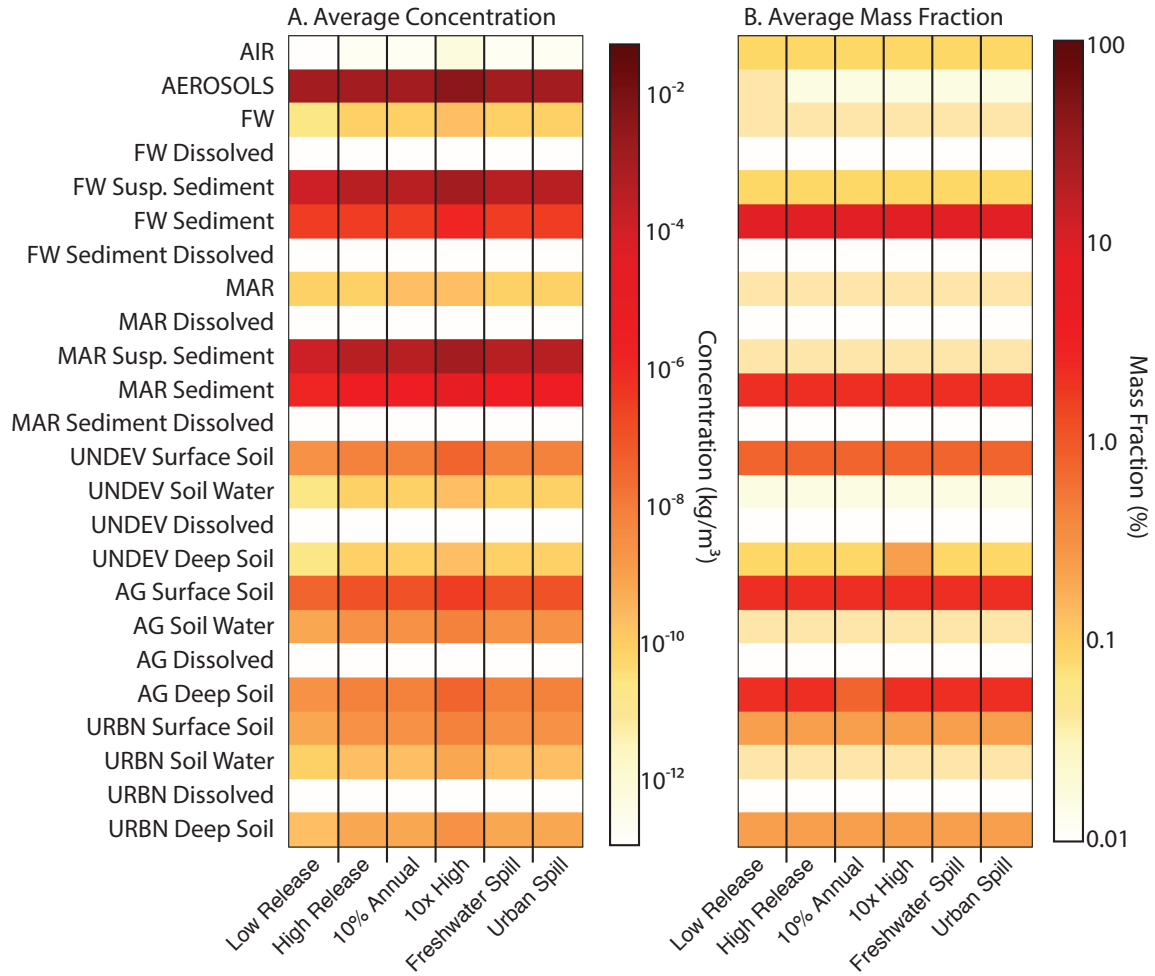
Figure A3.12 Comparison of (A) Average Concentration and (B) Mass Fraction over Final Year of Simulation across all Compartments for all Simulations for TiO₂
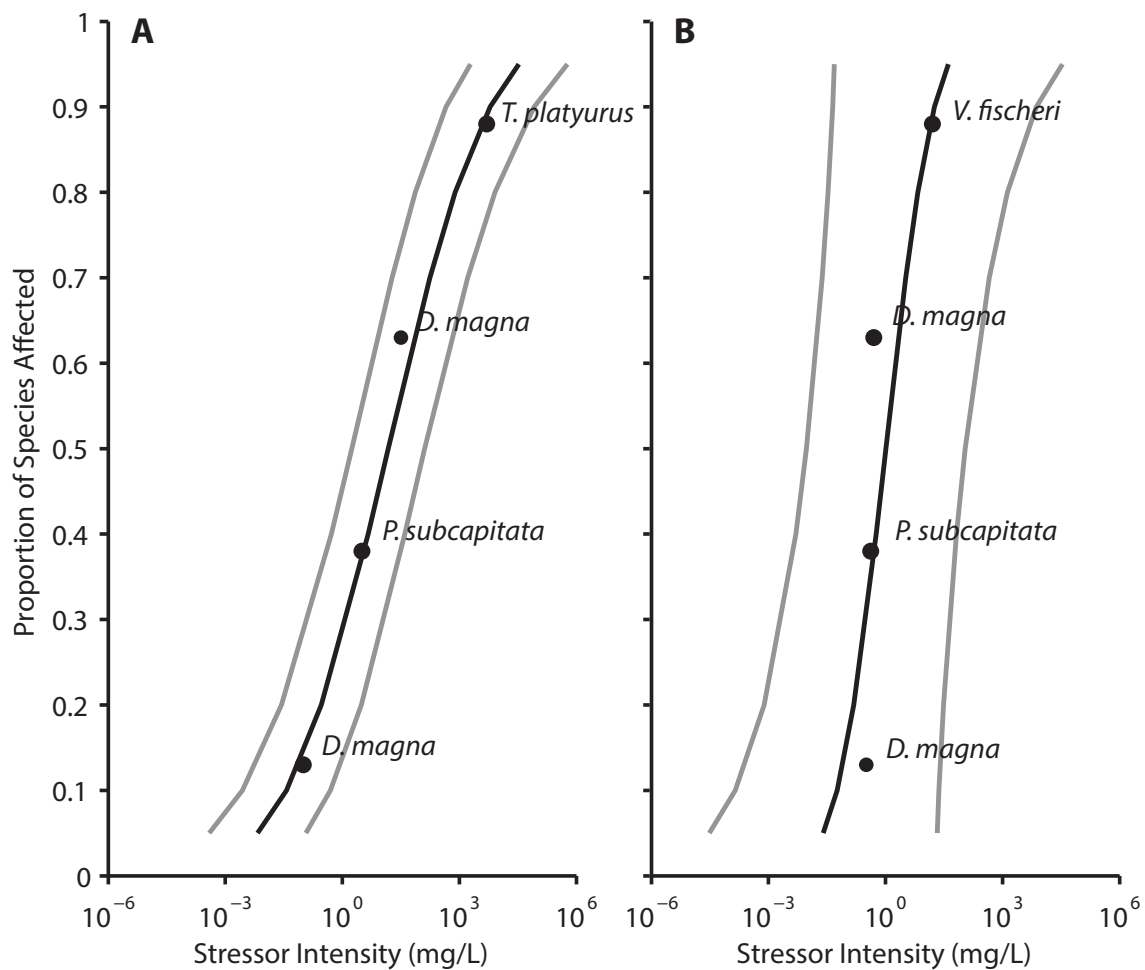
Figure A3.13 Freshwater Species Sensitivity Distributions for (A) CeO$_2$ and (B) CuO based on NOEC.[104,105,146,149,339]

3.6 User Guide for NanoFate Model

This tool is designed to allow a user to predict the long-term environmental concentration of a specific metallic engineered nanomaterial (ENM) in the environment. By most definitions, ENMs encompass nanoparticles (NPs) synthesized and modified to enhance their performance for technical or industrial purposes that have at least one dimension less than 100 nm. They are increasingly used in a variety of consumer products including electronics, textiles, cosmetics, medicine, and food.[1] ENMs are released into the environment; either during their use, by spillages, by intentional release for environmental remediation applications, or as end-of-life waste.[4] Studies estimate that more than 1,300 products that are on the market today contain NPs and production estimates of major ENMs as of 2010 range from 270,000 to 320,000 metric tons per year, of which estimates suggest that 8-28% may be released to soils, 0.4 - 7% to water, and 0.2 – 1.5% to air, with the balance entering landfills.[7,8] This model provides the ability to predict long-term fate at various environmental scales, as well as the expected concentrations in various environmental compartments. This information can be used to estimate the implications of releasing ENMs into the environment. The fact that some ENMs are known to be toxic emphasizes the need for comprehensively assessing the environmental risks of the large quantities of ENMs that increasingly enter our environment.[9]

3.6.1 Model Configuration

3.6.1.1 The Environment

The environment is composed of a series of compartments where each has dimensions, densities, and characteristics that represent specific environmental media. Examples include air, freshwater, and agricultural soil.

We have developed a selection of default environments to be used for the model, so that the user can quickly evaluate the fate of a given ENM, without spending too much effort collecting the information. As of the initial release, these environments include the San Francisco Bay (Figure B3.1), the greater Los Angeles Basin (User Guide Appendix 1-1), the 5 boroughs of New York City (User Guide Appendix 1-2), Miami and the surrounding Everglades (User Guide Appendix 1-3), Des Moines and its surrounding agricultural region (User Guide Appendix 1-4), and Salem, Oregon (User Guide Appendix 1-5). Each environment is meant to represent a distinct climate range and set of land cover types, with specific characteristics, which can have significant impacts on the rate of fate and transport processes, and the corresponding distribution and concentrations.
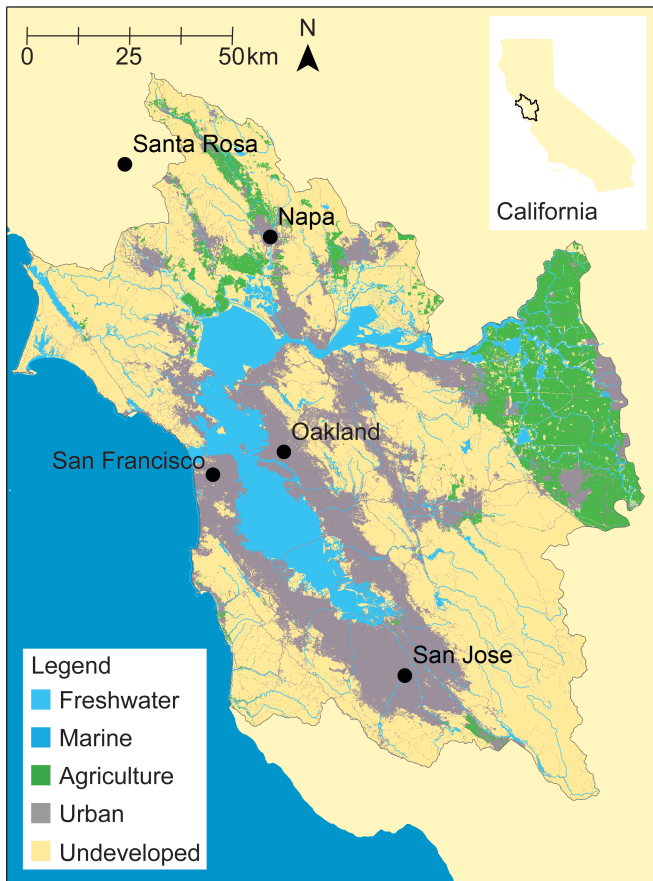
Figure B3.1 The Greater San Francisco Bay Area

The agricultural regions include both pasture and cropland, the urban regions include developed high intensity (e.g. apartment complexes, row houses, commercial and industrial regions), developed medium intensity (e.g. single family house units), developed low intensity (e.g. single family houses with large plots of land), and developed open space (e.g. parks, golf courses, etc.), and the undeveloped regions include barren land, deciduous forests, evergreen forests, mixed forests, scrub, shrub, grassland/herbaceous, and wetlands.

3.6.1.2 Environmental Parameters

The following are tables for the environmental data that are unique to the San Francisco Bay Region including air (Table B3.1), freshwater and coastal marine (Table B3.2), and undeveloped, agricultural, and urban soils (Table B3.3). Section 4 covers development of new environments for the model including the data collection process needed to populate these tables.

Table B3.1 Input Format for Air Compartment Characteristics

Characteristic	Default Value	Units
Air Height	1,000	m
Air Density	1.185	kg/m^3
Dynamic Viscosity of Air	$1.846*10^{-5}$	kg/m s
Aerosols Density	2,000	kg/m^3
Aerosols Concentration	$3.0*10^{-8}$	kg/m^3
Average Aerosols Particle Radius	$2.5*10^{-5}$	m
Wet Deposition Aerosols Scavenging Ratio	200,000	--
Wet Deposition ENMs Scavenging Ratio	2,000	--

Table B3.2 Input Format for Freshwater and Marine Compartments

Characteristic	Freshwater	Marine	Units
Area	$1.596*10^9$	$1.657*10^8$	m^2
Depth	1	6	m
Density	1,000	1,027	kg/m^3
pH	7	8.4	--
Dynamic Viscosity	$1.002*10^{-3}$	$1.004*10^{-3}$	kg/ms
Coastal Area	--	$3.24*10^7$	m^2
Suspended Sediment Density	1,500	1,500	kg/m^3
Suspended Sediment Concentration	0.01	0.01	kg/m^3

Average Suspended Sediment Particle Radius	$2.5*10^{-5}$	$2.5*10^{-5}$	m
Sediment Depth	0.05	0.25	m
Sediment Density	1,280	1,280	kg/m^3
pH	7	8.4	--
Burial Rate	4.19E-08	$4.5*10^{-8}$	m^3/m^2hr
Resuspension Rate	$3*10^{-7}$	$2*10^{-7}$	m^3/m^2hr
Sediment advective flow ratio	0.01	0.005	--

Table B3.3 Input Format for Soil Compartment

Characteristic				Units
Soil Site	undeveloped	agricultural	urban	
Soil Area	$7.575*10^9$	$1.595*10^9$	$3.487*10^9$	m^2
Depth Surface Soil	0.358	0.393	0.38	m
Density of Soil	1,500	1,500	1,500	kg/m^3
Initial Soil Water Content	0.4	0.2	0.3	%
Soil Water pH	7.5	7	8.2	--
Initial Soil Air Content	0.2	0.2	0.2	%
Organic Carbon Content Soil	0.059	0.059	0.031	%
Runoff Curve Number for Soil	82.2	91	90	--
Depth Deep Soil	1	1	1	m
Hydraulic Conductivity Soil	2.984	13.498	0.599	m/day
Saltation fitting Parameter	1	1	1	--
Threshold wind Velocity to Cause Erosion Soil	0.716	0.55	1.416	m/s
Minimum Threshold Shear Velocity	30	30	30	m/s
Height at which wind measurements are taken	1.5	1.5	1.5	m
Roughness of Soil	$2.4*10^{-3}$	0.1	0.6	m
K constant for Soil	$1.99*10^{-2}$	$3.16*10^{-3}$	$1.995*10^{-4}$	m^{-1}
Ratio of hours per day with sufficient wind for wind erosion	0.417	0.417	0.417	h/24-h
Consistency of Wind Throughout Day	0.05	0.05	0.05	%
Percent Land Uncovered and Available for Wind Erosion	0.01	0.02	0.005	%
Percent Particles that remain suspended	0.01	0.01	0.01	%

				hundreds feet-ton-in/acre-hr-year
Soil Erodibility Factor	0.286	0.306	0.289	
Slope of Soil	11.726	8.388	11.843	%
Crop management Factor for Soil	0.026	0.3	0.15	--
Support Practice Factor for Soil	0.5	0.6	0.3	--
Leaching Rate for Soil	$6.25*10^{-5}$	$6.25*10^{-5}$	$6.25*10^{-5}$	m^3/m^2hr

3.6.2 Fate and Transport Processes

Conceptually, ENMs are release into the environment either into the air, the water, or the soil. They then transfer between compartments based on environmental processes, some of which are generic to all chemicals in the environment and some, which are specific to particles and nanoparticles (Figure B3.2). Rates of all processes vary accordingly and are discussed in the following section.
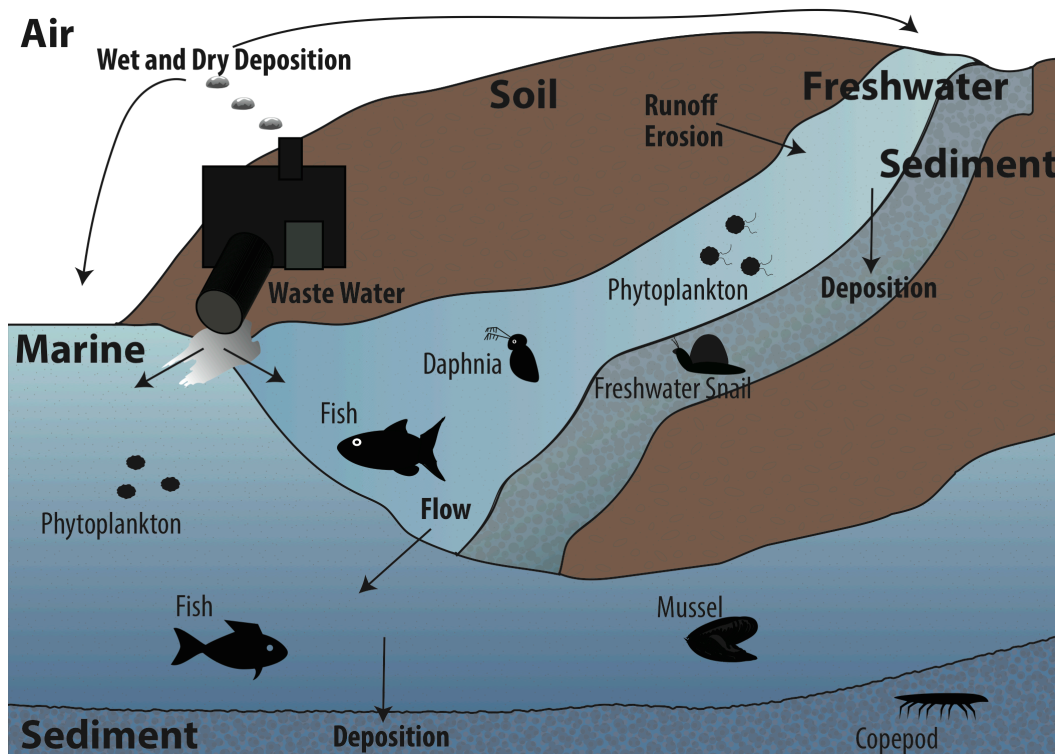
Figure B3.2 Division of Environment by Water Type

Using the environmental parameters specified in Tables B3.1-3, the model predicts the fate of ENMs in air (including air and aerosols), soil (including agricultural soil, urban soil and natural soil with surface soil solids, surface soil pore water, and deep soil for each), water (including freshwater, marine water, and suspended sediment in both), and sediment (for both freshwater and marine). The model predicts both transfers between compartments as well as transformation(s) to other forms. It tracks three states of the ENM including (i) free particles and small homoaggregates; (ii) ENM particles heteroaggregated with other particulate matter in the environment; and (iii) the resulting dissolution of ENMs in metal ions in the water phase. Note that in the natural environment, free ENM particles are unlikely but small aggregates are expected to be a common state for ENMs.[226]

3.6.2.1 Air

The atmosphere in this model contains two compartments, one representative of the air, and an aerosol compartment that is fully contained within the air compartment. An ENM (or an aggregate of ENMs) can be either freely suspended in air or it can be attached to an aerosol. Aerosols can be mostly water (e.g. fog), mineral (e.g. dust) or organic (e.g. broken leaf material). The model only considers the type of aerosol that is mostly water, since other types of aerosols either settle out quickly or are adsorbed into the water aerosols. The user can modify the properties of the aerosol compartment to best describe local conditions. Transfer processes modeled for ENM fate in air include wet and dry deposition of both free ENMs and those attached to aerosols and transfers into and out of the system via advection. Transformation processes include adsorption of the free ENMs and small aggregates to aerosols (heteroaggregation).

3.6.2.1.1 Dry Deposition

Dry deposition is the removal of vapors and particulate matter from the atmosphere as a result of gravitational settling, interception, impaction, diffusion, Brownian motion, and turbulence.[22,406] Stoke's law is used to estimate the deposition velocity of both aerosols and ENMs out of the air compartment.[353] Stokes' Law refers to the velocity at which a spherical object (e.g. a particle) with a small Reynolds number (i.e. very small particles; e.g. nanoparticles) falls through a fluid. This rate is controlled by a balance between drag force (which keeps the particle suspended) and gravitational force (which is a function of particle size).[201] Dry deposition is thus calculated as:

$$k_{dep} = \frac{2}{9}\frac{(\rho_p - \rho_a)}{\mu}g * R_p^2$$

where k_{dep} is the dry deposition velocity (m/s), ρ_p is the density of the aerosols or ENM (kg/m^3), ρ_a is the density of the air (kg/m^3), μ is the dynamic viscosity of the air (kg/m s), g is acceleration due to gravity (m/s^2), and R_p is the radius of either the aerosols or the mean aggregate radius of the ENMs. Because both the density and the radius vary substantially between aerosols and ENMs, the result is distinctly different deposition rates. [28,407,408] In addition, the rates can vary regionally if the user alters the diameter and density of aerosols and the density and viscosity of air based on local conditions. Total dry deposition is then divided based on the relative surface area of each of the receiving compartments (soils and waters).

3.6.2.1.2 Wet Deposition

Wet deposition is the removal of vapors and particulate matter associated with precipitation (rainfall or snowfall) in the atmosphere by gravitational settling, Brownian, and/or turbulent coagulation with water droplets.[406]

Wet deposition is modeled using approximately the same technique used for dry deposition. The volume fraction of aerosols is calculated accounting for adsorption of ENMs. This is then multiplied by the area (m^2), the daily regional precipitation (m/day) and a scavenging ratio of 200,000,[353] which indicates that a typical single raindrop sweeps through 200,000 times its volume of area. To convert to mass removal per day (kg/day), the result is multiplied by the normalized density of the aerosols with ENMs adsorbed to them.

Wet deposition of free ENMs in air is calculated as the precipitation (m/day) multiplied by the area (m^2), the scavenging ratio (again assuming a fraction of the scavenging rate), the volume fraction of ENMs in air, and the density of the ENMs. The scavenging ratio for ENMS was adjusted to be two orders of magnitude smaller than the scavenging ratio for aerosols because research indicates that particles in the 0.01 um range can have a scavenging ratio up to two orders of magnitude smaller than those in the 1-5 um range.[10]

3.6.2.1.3 Advection

Advection is the movement of a chemical results from the movement of media, in this case air currents.[353] The flow rate (Q_{adv}) is calculated as

$$Q_{adv} = V_w * h * \sqrt{a}$$

where V_w is the windspeed (m/s), h is the thickness of the atmosphere (m), and a is the area over which the air flows. This is used to estimate the flow of free ENMs in air (and those attached to aerosols) into and out of the system as a result of wind.

3.6.2.1.4 Heteroaggregation in Air

Heteroaggregation is the term we use for the collision and adsorption of ENMs with aerosols and other particulate matter in the atmosphere. We assume that the majority of

collisions will result in heteroaggregation rather than homoaggregation because of the higher concentration of aerosols relative to ENMs in the atmosphere.

Heteroaggregation of free ENMS to aerosols has not been well monitored for specific ENMs or even for individual larger particles beyond that of specific size classes such as $PM_{2.5}$ (particulate matter of 2.5 um or less) and PM_{10}. As such, our approach was to take the rate of aggregation used in water systems and assume a lower probability of collision, specifically three orders of magnitude lower than the rate of heteroaggregation in freshwater because fluid densities vary by approximately that much.[226]

3.6.2.2 Soil

We have incorporated the option to predict the fate of ENMs in up to three distinct soil compartments within this model. The model was designed to distinguish between agricultural soils, urban soils, and natural soils, so that release and fate to each can be better understood. However, because the model is fully customizable, there is the option of modeling three agricultural soil compartments with different soil characteristics or including only one single soil compartment. Then within each soil compartment, there are sub-compartments for surface soil, surface soil pore water, and a deep soil compartment. Note that it is particularly important to capture the fate in ENMs in the active, organism rich surface layer of the soil.

Soils are characterized by the presence of a heterogeneous mixture of gas, liquid, and soil phases, the interfaces between them, and the presence of organic matter and microbial communities.[226] The complex nature of soil systems means that our understanding of processes affecting the fate of ENMs in soil is limited, especially in unsaturated soils.[226,409] In surface soil, transfer processes include erosion by wind, erosion resulting from water

movement, and leaching to the deep soil. In the soil pore water, transfer processes include runoff resulting from precipitation. Transformation processes include sorption to and desorption from the soil particles (this is considered a transformation because the nanoparticle is no longer assumed to be nano as a result of the attachment to soil particles) and dissolution of the ENM particle in soil pore water.

A number of studies have determined that the fate of ENMs in soil is strongly dependent on primary particle size, aggregate particle size, surface charge, as well as environmental conditions such as pH, IS, the presence of NOM, clay content, and flow velocity.[108,113,114] Transport also explicitly depends on the size of the soil particles and the pore size. If the aggregate size is of similar dimensions or larger than the soil pore throats, then transport will likely be reduced by straining and/or by filtration if the particle is removed by interception, diffusion, and/or sedimentation.[109–112,116,117] As a result, it is likely that larger aggregates will be retained in the upper soil layers.[111] Sorption can be caused by electrostatic attraction, surface bridging, hydrogen bonding, or hydrophobic interactions, which in turn are influenced by soil properties such as pH, metal oxide content, IS (ionic strength), organic fraction, and cation exchange.[410]

3.6.2.2.1 Wind Erosion

Wind erosion is erosion of the top layer of soil caused by high winds when soil is relatively dry. We use the saltation equation, (given in Kelly et al., 2004) and the vertical flux conversion to estimate the total transport of soil between soil and aerosols and thus the ENMs associated with them. We chose not to use the wind erosion equation (WEQ) which estimates the average annual mass of soil transport off the downwind edge of an agricultural

field because this method does not allow spatial or temporal partitioning between wind erosion events.[411,412]

Wind erosion is assumed to occur only in natural or agricultural soils because of the frequent lack of large, open, unpaved or unvegetated spaces in urban areas. It can be estimated using Owen's saltation mass flux, which is given as:

$$Q_{Tot} = A\frac{p}{g}\sum_{u_*} u_*(u_*^2 - u_{*t}^2)\Delta T$$

The saltation mass flux (g/cm s) is representative of the mass flowing past a pane one length unit wide, perpendicular to both the wind and the ground.[385] Q_{Tot} is the total horizontal mass flux, A is a dimensionless fitting parameter, generally set to 1 but adjustable to regional variations[413,414], p is the density of air (kg/m^3), g is the acceleration of gravity (m/s^2), u_* is the wind shear velocity (m/s), and u_{*t} is the threshold shear velocity (m/s).

Threshold shear velocity is the minimum wind speed necessary to cause erosion of soil particles on the surface.[415] In order to calculate the daily flux of soil particles transported to the air by wind erosion, we first need to know if precipitation occurred recently. If precipitation did occur in the last day, the minimum threshold shear velocity (u_{*t}) is set to 30 (m/s) because wind erosion is unlikely, though not impossible, when the soil is saturated (this minimum can be altered by the user).[416] This effect is limited only to the previous day because the effect is generally small and temporary.[416] Otherwise, the threshold shear velocity is dependent on the soil texture (Table B3.4).[384,417]

Table B3.4 Threshold Shear Velocity by Soil Type (u*t)

Surface Soil Texture	Threshold Velocity According to Soil Condition (cm/s)
	Smooth, Loose Soil
Sand	25

Loamy Sand	30
Sandy Loam	35
Clay	55
Silty Clay	55
Loam	75
Silt Loam	75
Clay Loam	75
Silty Clay Loam	75
Sandy Clay Loam	75

Table recreated from Gillette and Passi (1988).[384]

Wind speed for the NOAA data is collected using anemometers situated at 1.5 m above the surface.

$$u_z = \frac{u_*}{k} \ln \left(\frac{z}{z_0} \right)$$

The wind shear velocity (u_*) is then calculated from the existing wind speed u_z (m/s) at height z (1.5 m), where k is the von Karmen constant (0.41, unitless), and z_0 is the roughness height (cm).[418] The measured wind height (z) must be greater than the roughness height (z_0) or the equation is not valid.[384,419] In simple terms, a larger z_0 would indicate a downward momentum flux, and thus no transfer from soil to air.[419] The roughness height is representative of the roughness of the soil, which has the effect of trapping soil particles and thus limiting the extent of vertical transfer. The roughness value is determined based on the predominant surface coverage of the soil as derived from the Davenport roughness classification (Table B3.5).[420] These values are representative of the roughness height characteristic of the surface of the soil.

Table B3.5 Roughness by Land Cover Type

Surface Cover Type	Roughness (m)
Open Water	0.0002
Open Smooth Terrain	0.0024
Rangeland	0.03
Big Agriculture	0.055

Medium Agriculture	0.1
Orchards	0.2
Suburbs	0.4
Urban	0.6

Taken from Wieringa et al. 1992.[420]

$$F_a = Q_{Tot}K$$

Lastly a conversion factor (K) is needed to convert from horizontal mass flux to the vertical mass flux (F_a – g/cm^2 s).[385] F_a is representative of the mass of soil leaving the surface per unit time that remains suspended in the air. The constant K reflects an observed linear relationship between F_a and Q_{Tot}, which is also based on soil type (**Error! Reference source not found.**).

Table B3.6 K Constant for Variations in F$_a$/Q$_{Tot}$

Soil Type	K constant (cm^{-1})
Clay	10^-6.4
Loam	10^-5.7
Sandy Loam	10^-3.7
Loamy Sand	10^-4.5
Sand	10^-5.7

Table taken from Gillette et al. 1997 and Kelly et al. 2004.[385,421]

In addition, we make a few limiting assumptions. Because wind tends to decrease substantially at night (~10 hrs) and is not consistent throughout the day, we assume that on average for only 5% of that time is there sufficient wind to cause erosion (though both parameters are adjustable within the model).[416] In addition, this effect is limited to occurring only over that fraction of the soil area that is uncovered due to the absence of any plant material (stubble or weeds or plant matter) that covers the surface of the soil. When vegetation is present it affords substantial protection to the whole soil surface and significantly increases the threshold velocity.[416] In addition, we assume that only 1% of the particles remain in suspension because it is only particles in the dust size range (0.1 – 0.15

mm) that remain in suspension once lifted off the ground by wind (again this value can be adjusted within the model).[416,422,423] Because the model does not make a distinction between free nanoparticles in the soil and nanoparticles associated with individual soil grains, the model does not separate the amount that remains in suspension by size class, though the smaller free nanoparticles are more likely to remain suspended in the air for longer.[424]

3.6.2.2.2 Runoff

Runoff and wet erosion were both estimated from the SCS runoff equation.[425] The equation is based on the premise that all water that enters and leaves a system is equal.

$$\text{Rainfall} = \text{Runoff} + \text{Losses} \;\therefore\; \text{Runoff} = \text{Rainfall} - \text{Losses}$$

The water balance equation is given as:

$$Q = P - (I_a + F)$$

Where Q is the direct runoff (m), P is the rainfall (m/day), I_a is the sum of all losses before the beginning of runoff (m) and F is the retention after runoff begins (m). P is provided by the daily precipitation data in the climate data set. Two assumptions go into estimating I_a and F. The first is that the ratio of the percent water that has been retained to the maximum potential retention is the same as the ratio of the percent water than ran off to the maximum rainfall available for the runoff.[387,425]

$$\frac{F}{S} = \frac{Q}{(P - I_a)}$$

Where F is the amount of rainfall retained (after runoff begins), S is the maximum potential retention (after runoff begins); and $P-I_a$ is the maximum rainfall available for runoff. At the limit where P is exceptionally large, both sides of the equation are essentially equal to 1. When no runoff occurs, both are equal to zero.

The second assumption is that I_a can be expressed as a function of S. NRCS uses the relationship[411]

$$I_a = 0.2S$$

Simplifying the equation then results in:

$$Q = \frac{(P - 0.2S)^2}{P + 0.8S}$$

The potential maximum retention after runoff begins has a range of values from 0 to infinity. A more convenient value, known as the curve number (CN) can be used.[426]

$$S = \frac{1000}{CN} - 10$$

The practical range of CN is from 40 to 98 (though strictly from 30 to 100).[426] See Table 3 on estimating appropriate curve numbers for your region. Since this equation gives S in inches, a simple conversion is used to provide S in m.

3.6.2.2.3 Wet Erosion

Soil loss resulting from erosion during precipitation events was calculated using the Revised Universal Soil Loss Equation (RUSLE).[427] This function is widely used to estimate rates of soil erosion caused by rainfall and associated overland flow.[428] The equation used is

$$A = R * K * LS * C * P$$

Where A is the annual soil erosion (tons/ha-year), R is the rainfall-runoff erosivity factor (MJ mm/ha h y), K is the soil erodibility factor (ton ha h/ha MJ mm), LS is the slope length factor (dimensionless), C is the cover management factor (dimensionless), and P is the support practice factor (dimensionless).

Rainfall-runoff erosivity (R) is a measure of the erosion force caused by rain.[429,430] The R factor is defined as the average annual sum of individual storm erosion index values

(EI$_{30}$), where E is the total storm kinetic energy per unit area, and I$_{30}$ is the maximum 30 minute rainfall intensity.[430] Given the scarce availability of data relating to rainfall intensity, mean annual precipitation is a commonly used alternative.[429,430] Since daily precipitation are available within the model, these values are used to calculate the mean annual precipitation (for each year the model is run), which can then be used in calculating the rainfall erosivity factor. The unit rainfall energy (e$_r$) (MJ/ha mm) is calculated for each time interval

$$e_r = 0.29\left[1 - 0.72 * e^{(-0.05 i_r)}\right]$$

where i$_r$ is the rainfall intensity during the time interval (mm/hr).[431] Rainfall intensity is replaced by daily precipitation due to data limitations.[429] The event erosivity (EI$_{30}$) is defined as:

$$EI = (\sum_{r=1}^{0} e_r v_r) I_{30}$$

where v$_r$ is the rainfall volume (mm) during a time period r, and I$_{30}$ is the maximum rainfall intensity during a 30-minute period of the rainfall event (mm/hr).[429] Thus the R-factor is the product of the kinetic energy of a rainfall event and its maximum 30-minute intensity.[431]

$$R = \frac{1}{n}\sum_{j=1}^{n}\sum_{k=1}^{mj}(EI_{30})_k$$

where R is the average annual rainfall erosivity, n is the number of years covered by the data records, and mj is the number of erosive events of a given year j. Since the model calculates this for each year, there is a correction that allows for partitioning the total rainfall erosivity relative to the amount of precipitation on any given day.

143

The soil erosivity factor (K) represents the susceptibility of soil to erosion based on the soil texture and composition.[432,433] These data can be collected from the STATSGO soil dataset (KFFACT) and typically range from 0 to 0.6.[434] Soils that are high in clay tend to have low K values because they are resistant to detachment. Coarse textured soils, such as sandy soils, tend to have relatively low K values because of high infiltration relative to runoff even though they are easily detached. Soils with a high silt content tend to have high K values.

The slope length factor (LS) represents the effect of slope steepness and length of field on erosion. Soil loss increases rapidly with slope steepness but is relatively insensitive to slope length.[433] Because we are dealing with substantial areas, the length is set to the maximum value (1000 ft = 304.8 m) and the average slope of each soil region can be calculated from the same STATSGO dataset.[435] The following conversion is used to determine the LS factor (Table B3.7).

Table B3.7 LS Factor by Slope

Slope	LS factor with L of 1000 ft
0.2	0.06
0.5	0.1
1	0.2
2	0.47
3	0.8
4	1.19
5	1.63
6	2.11
8	3.15
10	4.56
12	6.28
14	8.11
16	10.02
20	13.99
25	19.13

30	24.31
40	34.48
50	44.02
60	52.7

Taken from Renard et al. 1997 Table 4-2.

The crop management factor (C) is used to reflect the effect of agriculture and management practices on erosion rates.[433] The C factor is most often used to compare the relative impacts of management options, which is not really the purpose of this model. However, because it can impact the rate of erosion, it also impacts the rate of transfer of ENMs from soil to water. The C-factor is based on the concept of deviation from a standard, in this case a region under clean-tilled continuous-fallow conditions.[433] C is representative of the effects of plants, soil cover, soil biomass, and activities that may minimize erosion of the soil.[433] For simplicity, we primarily focus on the surface cover, using the NLCD 2011 land cover as a proxy, to estimate the C factor (Table B3.8).[436,437]

Table B3.8 C-Factor Estimates Based on Land Cover Type

Land Cover	C Factor
Residential and Commercial	0.15
Forest	0.01
Agriculture	0.3
Heterogeneous Crops	021
Scrubland	0.05
Barren	0.3
Pasture	0.1

Taken from USDA publication on estimating sediment loads and Panagos et al. 2015.[436,437]

The support practice factor (P) reflects the impact of support practices on the average annual erosion rate.[433] It is the ratio of soil loss that occurs with specific practices relative to straight row farming up-and-down slope.[433] The P factor differentiates between cropland,

rangeland, and permanent pasture and typically ranges from 0 to 1 (with 1 being straight row farming). The lower the value, the better the management practice is at preventing erosion.

Thus total erosion is calculated as

$$A = R * K * LC * C * P$$

We are averaging over very large areas for this calculation, which limits the accuracy. This also means that while the variability is probably quite high, we have only one value for soil erosion for each soil type. This value is then calculated over the entire area for each soil type per year. This is then calculated on a daily basis by taking the precipitation on each day relative to the total annual precipitation.

3.6.2.2.4 Sorption/Desorption

ENMs can sorb to solid matter in the soil, particularly in saturated soils; they can also desorb from the soil solids and move into the soil pore water.[226] Generally, forces such as electrostatic forces, Van Der Waals forces, hydrodynamic forces, hydration/structural forces, hydrophobic forces, and steric interactions all result in ENMs interacting with soil particles.[226] The rate of attachment to soil particles is strongly dependent on particle size, surface charge, and environmental conditions including pH, IS, the presence of natural organic matter (NOM), clay and water content, and rate of flow.[108,113,114] Because of the complex nature of soils, it is difficult to distinguish the impact of each characteristic on the rate of sorption and desorption. In addition, the effect of variability in wetting and drying cycles, (which shifts the soil from saturated to unsaturated conditions) has yet to be studied and could not be incorporated into this model.[409]

Because soil characteristics are so variable from site to site, we chose to use soil column experiments to determine the likely total attachment of ENMs to soil particles for specific

146

soil systems and specific ENMs. Most soil column experiments do not provide attachment over time, so we were limited to determining the rate of attachment from the total attachment over the experimental run period. The fraction of ENMs that remains in the column is the fraction that associates with the soil particulate matter (SOM), and the fraction that is released in the soil water at the bottom of the column is the fraction that remains in the soil water. The model then balances this fraction over time as ENMs enter the soil system or are lost through various transfer and transformation processes; an equilibrium is always the goal. To do this, the model considers the current ENM concentration in soil and soil water relative to the predicted ratio and transfers ENMs between the soil and the soil water to achieve the predicted ratio. Since research indicates that sorption and desorption in soil happens quite quickly (even faster in unsaturated soils),[108,113,226,438] it is assumed that over the course of one day, the partitioning would equilibrate based on the predicted ratio. Some caveats exist, however. This model may not be applicable to very dry soils. In this case, the rate of attachment is probably much higher, but because limited research has been conducted under these conditions to date, this will not translate well to soils that are not well described or similar to the experimental soils.[121,129,389] If the only available partitioning rates are for glass bead columns, for example, then the accuracy of the model for actual soils could be quite low. In an ideal situation, soil samples from the area(s) of concern would be used to determine the rate of partitioning between soil and soil water; however this level of data availability is unlikely. Available estimated retention ratios are provided in Table B3.9.

Table B3.9 Retention Ratio between Soil Solids and Soil Water

	CeO_2	CuO	TiO_2	ZnO
Glass Beads				
7	--	0.48[121]	0.41[121,136]	0.986[121]

Organic Soil				
5.7	--	--	0.99[132]	--
6.6	--	0.99[392]	--	0.99[392]
9	--	--	0.95[132]	--
Sandy Loam Soil				
5.5	--	--	--	0.855[203,394]
7.37	--	--	--	0.99[389]
Sandy Soil				
3	0.05[123]	--	--	--
4.5	--	--	0.999[395]	--
5.9	--	--	--	0.86[391]
6	0.95[123]	--	--	--
6.9	--	0.99[393]	--	--
7.4	--	--	--	0.99[393]
7.73	--	--	--	0.99[389]
9	0.97[123]	--	--	--

3.6.2.2.5 Leaching

Leaching, or the vertical movement of ENMs through the surface soil but associated with soil water to the deep soil, is modeled using a default leaching rate in soil of $6.25*10^{-5}$ m^3/m^2 hr accounting for the area over which the transfer occurs and the concentration of ENMs in the soil water.[353]

3.6.2.2.6 Dissolution in Soil Water

Dissolution in soil water is modeled in the same way as dissolution in freshwater and marine systems taking into account the equilibrium solubility for soil water at the specific pH of the soil and the estimated dissolution rate constant (See Section 3.6.2.3.4 for rates).

3.6.2.3 Water

The fate and transport of ENMs in water depends largely on variations in aquatic characteristics.[226] For example, the IS and concentration of NOM present in seawater versus freshwater will impact rates of aggregation, sedimentation, and dissolution for some

ENMs.[226] Variations in surface charge, surface coating, and shape can also alter the fate of ENMs in the environment.[226]

The model includes the following key processes: (i) heteroaggregation of ENMs with suspended particulate matter; (ii) sedimentation of free ENMs and smaller aggregates; (iii) dissolution of metallic ENMs to their corresponding metal ion; (iv) sedimentation of ENMs associated with suspended particulate matter; (v) resuspension of free ENMs and smaller aggregates to the air in marine coastal environments as a result of breaking waves; and (vi) advection from freshwater to marine and from marine out of the modeled system for water, suspended sediment, and sediment.

3.6.2.3.1 Heteroaggregation of ENMs with Suspended Particulate Matter

Particle aggregation refers to the formation of ENM clusters in colloidal suspension. Following release to water, most ENMs are unlikely to remain free particles.[20] We assumed homoaggregation is negligible relative to heteroaggregation at realistic environmental concentrations and as such include only heteroaggregation in our model.[36,362] The degree of aggregation and the size range of the aggregates depend on the characteristics of the particle, the concentration of the particles, and the characteristics of the environmental system.[82,109] Thus ENM aggregation behavior will dictate particle transport potential, environmental fate, bioavailability, and potential ecotoxicological impacts.[37,38,352]

In theory, aggregation rates can be calculated using the ENM collision rate and attachment efficiency.[18,36,439] The attachment efficiency represents the fraction of collisions between particles that result in attachment.[48] Attachment efficiency depends on environmental conditions such as pH, IS, ion valence, temperature, and ENM and other particle concentrations.[21] However, attachment efficiency is actually quite difficult to

predict.[346,352,359,440] As such, we follow the approach provided by Quik et al. (2014) to model heteroaggregation relative to current water and suspended sediment concentrations.[36] We also assume that heteroaggregation is a pseudo-first order rate constant (k_{het}). See Section 3.6.5.7.1 on Pseudo First Order Rate Constants, where the concentration (C) at time (t) is:

$$\frac{dC}{dt} = -k_{het}C_{ss}C_0$$

where C_{ss} is the suspended sediment concentration, and C_0 is the starting concentration of ENMs. We also assume that once heteroaggregation occurs, it is irreversible.[20,21] Estimated heteroaggregation rates are provided below (Table B3.10).

Table B3.10 Heteroaggregation Rate Constant (L/mg-hr) for Freshwater and Marine Water across pH Levels

Freshwater	CeO_2	CuO	TiO_2	ZnO
6.3	--	0.318[368]	--	--
6.56	--	--	0.0479[441]	--
6.6	--	0.372[368]	--	--
6.8	--	0.713[442]	--	--
7.8	$3.04*10^{-4}$,[443]	--	--	--
7.9	0.0108[444]	--	--	--
7.95	0.006[36]	--	--	--
7.98	--	--	0.0435[441]	--
8.16	--	--	0.0097[441]	--
8.26	--	--	0.0189[441]	--
8.38	0.0023[12]	--	0.0044[12]	0.0133[12]
Marine				
6.8	--	3.794[442]	--	--
7.3	--	0.389[368]	--	--
7.78	0.006[36]	--	--	--
7.8	0.007[444]	--	--	--
7.89	0.004[36]	--	--	--
8.05	0.372[12]	--	0.8096[12]	1.726[12]
8.17	--	--	0.0939[445]	--

3.6.2.3.2 Sedimentation of Suspended Particulate Matter

Sediment deposition is the process by which suspended particles in water settle to the bottom of a body of water.[353] This settling often occurs when flow slows down or when heavy particles are no longer supported by the innate turbulence of the water. Deposition rates tend to vary from marine to freshwater environments, with much higher rates observed in marine systems.[446] Deposition of suspended sediment is calculated using Stokes' Law. Stokes' Law refers to the velocity at which a spherical object (e.g. a particle) with a small Reynolds number (i.e. very small particles; e.g. nanoparticles) falls through a fluid. This rate is controlled by a balance between drag force (which keeps the particle suspended) and gravitational force (which is a function of particle size).[201] Settling of suspended sediment is thus calculated as:

$$k_{sed,ss} = \frac{2}{9} \frac{(\rho_p - \rho_w)}{\mu} g * R_p^2$$

where $k_{sed,ss}$ is the flow settling velocity (m/s), ρ_p is the density of the suspended sediment particles (kg/m^3), ρ_w is the density of the water (freshwater or marine for each compartment) (kg/m^3), μ is the dynamic viscosity (kg/m s), g is acceleration due to gravity (m/s^2), and R_p is the radius of the particles. For sedimentation of suspended sediment particles and the ENMs associated with them, we elected not to use the von Smoluchowski equation because that is representative of a diffusion limited aggregation scenario (DLA) which is unlikely to be the case for suspended sediment at the large scale under which the model functions.[201] Sedimentation is thus given as:

$$\frac{dC}{dt} = \frac{\frac{-k_{sed,ss}}{d} V_{ss} C_0}{V_w}$$

where d (m) is the depth of the water compartment, V_{ss} is the volume of the suspended sediment compartment (m3), and V_w is the volume of the water compartment, thus accounting for the concentration of the ENM attached to the suspended sediment.[362]

3.6.2.3.3 Sedimentation of Free ENMs and Small Aggregates

ENMs can be deposited to the sediment compartment via gravitational settling of free particles or small aggregates. Particle and aggregate particle size is a major factor affecting the rate of sedimentation along with ambient environmental characteristics, such as the presence of NOM or other stabilizing agents and the IS or presence of different electrolytes as well as the viscosity of the fluid and the initial ENM concentration.[16,447] Since we do not distinguish between free nanoparticles and small homoaggregates (largely because of the complexity in measuring their separate rates, so they are not reported separately in the literature), sedimentation is calculated separately only for ENM heteroaggregates with suspended particulate matter (See Section 3.6.2.3.2) and those that we grouped as free or small homoaggregates.

Sedimentation of free and small aggregate ENMs was modeled using literature that reported and estimated sedimentation rates, much as with aggregation. The same methodology was used to calculate the sedimentation rate constant ($k_{sed,ENM}$) (See Sections 3.6.5.7.1 and 3.6.2.3.1 on estimating rate constants).[443] However, rather than a pseudo first order rate constant, as with heteroaggregation, a standard first order rate constant was used, where the concentration (C) at time (t) can be calculated using the same sedimentation equation as in Section 3.6.2.3.2.[36,362]

$$\frac{dC}{dt} = \frac{-k_{sed,ENM}}{d} C_0$$

152

where d (m) is the depth of the water compartment.[362] Sedimentation rate estimates are provided below (Table B3.11).

Table B3.11 Sedimentation Rate Constants (m/hr) for Freshwater and Marine across pH Levels

Freshwater	CeO_2	CuO	TiO_2	ZnO
4	--	0.0035^{256}	--	--
6.3	--	$1.7*10^{-4,368}$	--	--
7	--	$0.0084^{121,256}$	$0.0056^{121,183}$	$0.0053^{62,121,335}$
7.7	0.0015^{443}	--	--	--
7.9	$7.5*10^{-4,\ 443}$	--	--	--
8	$1.9*10^{-4,\ 443}$	--	--	--
8.38	$3.4*10^{-5,12}$	--	$3.4*10^{-5,12}$	$4.2*10^{-5,12,46}$
12	--	0.0016^{256}	--	
Marine	CeO_2	CuO	TiO_2	ZnO
7	--	--	--	$0.0068^{62,97}$
7.3	--	0.0023^{368}	--	--
7.4	--	0.0035^{448}	--	--
8.05	0.0012^{12}	--	0.0012^{12}	$3.9*10^{-4,\ 12,46}$
8.2	0.0289^{95}	--	0.0245^{445}	0.0174^{95}

3.6.2.3.4 Dissolution of Metallic ENMs in Water

Dissolution is important for some ENMs, and can vary significantly by ENM and the type of aqueous media. It involves the release of dissolved ions from the ENM.[16] Dissolution is a surface-controlled process that is dependent on the surface area of the ENM and the concentration of the dissolved ions near the particle's surface.[16] Greater surface to volume ratios of NPs generally result in increased dissolution; thus decreasing the size may also result in increased dissolution.[16,88,100,147,405,449–451] The dissolution rate is also controlled by the metal ion concentration gradient between the particle surface and the bulk medium.[451] Though we were unable to include this in the model, the observed dissolution rate may actually increase if other constituents in the water (e.g. Cl^-, S^{2-}, PO_4^{3-}) can react with the released metal ions in

such a way that it alters the observed metal ion concentration and allows for further dissolution.[94,174,452]

Dissolution was modeled using predictions of the maximum dissolution for a metal and the rate at which dissolution occurs in specific waters for a given ENM. *Visual MINTeq* (version 3.1) was used to predict metal speciation in various natural waters (across a range of pH values for standard freshwater, seawater, and groundwater as reported in Keller et al. 2010) to estimate the equilibrium dissolution concentration across a range of metal conconcentrations.[12,386] This was combined with the dissolution rate (k_{dis}), calculated from the literature for first order rate constants as with sedimentation (See Sections 3.6.5.7.1 and 3.6.2.3.3), to determine the rate and extent of dissolution over time. Thus, the maximum dissolved concentration (C) at time (t) was calculated as:

$$\frac{dC}{dt} = -k_{dis}C_0$$

Dissolution is limited in the model to not exceed the equilibrium dissolved concentration for the given metal under the specific aqueous chemistry (freshwater, seawater, groundwater). So if the dissolution rate predicts a dissolved concentration that exceeds the equilibrium value, then the dissolved concentration is corrected so that the total is equal to the equilibrium concentration. We also assumed that dissolution was occurring in the freshwater and marine sediment at $1/10^{th}$ the rate of the water column dissolution rate. Estimated dissolution rates are provided below (Table B3.12). Note that some ENMs are not expected to dissolve to any significant extent (e.g. TiO_2 and CeO_2).

Table B3.12 Dissolution Rate Constants (1/hr) for Freshwater, Marine, and Soil Water across pH Levels

pH	CeO_2	CuO	TiO_2	ZnO

154

	CeO$_2$	CuO	TiO$_2$	ZnO
6	0	--	0	0.007[62,453]
6.9	0	0.005[100]	0	0.402[100]
7	0	0.006[256]	0	0.013[335,454]
7.08	0	0.112[285]	0	3.45[285]
7.2	0	0.001[52,338]	0	--
7.3	0	--	0	0.036[51]
7.5	0	--	0	0.035[88]
7.8	0	0.002[455]	0	--
8	0	0.028[101,105]	0	0.079[101,105,453]
8.1	0	--	0	0.008[292]
8.2	0	6.25*10$^{-6,55}$	0	--
8.5	0	--	0	0.080[302]
9	0	--	0	0.003[62]
Marine	CeO$_2$	CuO	TiO$_2$	ZnO
6.5	0	0.144[146]	0	0.365[306]
6.7	0	3.94*10$^{-5,456}$	0	--
7	0	0.002[227]	0	0.044[97,302]
8	0	--	0	0.001[98]
8.2	0	--	0	0.288[95]
8.3	0	--	0	0.001[457]
Soil Pore Water	CeO$_2$	CuO	TiO$_2$	ZnO
5.5	0	--	0	0.051[203]
6.1	0	--	0	0.910[394]
7	0	--	0	0.017[327]
7.2	0	--	0	0.002[391]
7.5	0	2.1*10$^{-4,368}$	0	--

3.6.2.3.5 Resuspension of ENMs to Aerosols by Coastal Wave Action

Aerosols associated with the bubble production resulting from oceanic waves breaking in response to sufficiently strong winds allows for transfer of ENMs in surface marine waters to the aerosols compartment in air.[375] Research has been conducted on the transfer of heavy metals in this way, which we assume to be similarly applicable to ENMs.[458] Aerosols from the ocean are formed through bubble formation, followed by bubble collapse and jet ejection, followed by subsequent destabilization to droplets. This process is well established.[459,460] Bursting bubbles produce two types of droplets: film drops from the

rupture of the bubble film, and jet drops by the breakup of the vertically rising jet of water from the collapsing bubble cavity.[376,461,462] We primarily focus on the formation and collapse of jet droplets as the mechanism of transfer between surface marine water and aerosols.

For simplicity, we exclude calculations regarding the various sizes of bubbles and assume they are homogeneous and contain the same quantity of ENMs; we assume all bubbles reaching the surface burst allowing for transfer from marine to air.[375] As with soil erosion caused by wind, we again assume that the wind is only sufficiently high for 14 hours out of the day, and of that time period, only 5% of the time is it maintained at sufficient speeds to cause erosion (See Section 3.6.2.2.1 on Wind Erosion).[416]

To compute a representative volume flux (the rate of bubble formation) (V_f) for aerosols with an average diameter of 20 um at a wind speed of 6 m/s, the commonly used total flux value is $1*10^{\wedge-9}$ cm/s and $9*10^{-4}$ for wind speeds greater than 12 m/s.[375,461,463] This is then used to calculate the water to aerosols transport ($k_{w,aer}$) relative to the concentration of ENMs in marine water:

$$k_{w,aer} = EF * V_F * A_c$$

where EF is the enrichment factor, V_F is the volume flux (m/day), and A_c is the coastal area (m^2) over which this process occurs. This estimate was adapted from previously completed modeling efforts on the transfer of trace metals at the air-water interface.[374,464,465] The enrichment factor is the metal-to-sodium ratios in the aerosols produced by bubble bursting compared to their ratio in bulk water.[464,466] This is included because bubbles have been shown to scavenge inorganics from the upper layers of the water.[466] Enrichment factors are specifically measured for trace metals (Table B3.13), which we assume to be comparable to the enrichment factor of the same metal in nanoparticle form.

156

Table B3.13 Enrichment Factors (EF) for Metals

Metal	Enrichment Factor (Weisel et al. 1984)	Ave. Enrichment Factor (Piotrowicz et al. 1972)	Enrichment Factor (Duce et al. 1975)	Enrichment Factor (Rahn et al. 1975)
Al	200	1.7	0	0
Cd	-	-	730	1200
Co	0.2	-	1.4	5.3
Cr	-	-	10	11
Cu	5	1.1	120	78
Fe	50	1.5	0.4	0.9
Mn	7	0	1.6	4
Pb	8	3.3	2200	800
Sb	-	-	2300	3600
Sc	0.0005	-	-	-
V	10	1.6	16	23
Zn	8	-	110	240

Composite Table from Weisel et al. 1984, Piotrowicz et al. 1972, Duce et al. 1975, and Rahn et al. 1975.[377–380]

3.6.2.3.6 Advective Flow

Advection is modeled as the transfer from freshwater to marine of both ENMs in the water column and suspended sediment and from marine out of the modeled system. Flow data were collected from the USGS database (See Section 1.3.1) that provides daily flow estimates (m^3/s) for the region. Because no marine flow data is available, we assume that the flow rate is the same for both freshwater and marine. For marine, the advective flow is treated as a loss from the system to the greater ocean. Because flow is given as a volume over time, to calculate transfer of ENMs in the water column, the rate is simply multiplied by the concentration of ENMs in the water. However, in the case of ENMs associated with suspended sediment, the concentration of suspended sediment present in the flow and the concentration of ENMs associated with the suspended sediment must be accounted for.

3.6.2.4 Sediment

In sediment only three simplified processes occur: advective transfer of surface suspended sediment, resuspension of ENMs associated with particulate matter, and burial under sediment. Resuspension is the transfer from the sediment back into the water column as a result of turbulence.[353,467] Burial is the removal from the system resulting from the accumulation of additional sediment above the initial surface of the sediment compartment.[353] It is assumed that once in the sediment compartment, all ENMs are associated with sediment and are not free primary particles or small aggregates.

3.6.2.4.1 Advective Transfer of Sediment

We assume that water column flow causes flow of sediment at $1/10^{th}$ the rate of water flow. This applies to both freshwater, as a transfer from freshwater sediment to marine sediment, and from coastal marine sediment out of the system.

3.6.2.4.2 Sediment Resuspension

Given our previously stated assumption, resuspension is simply the resuspension of sediment and thus the ENMs become associated with that sediment. It is based on the assumption that surface sediments are disturbed by water currents and biotic activity, which allow for transfer between the sediment and suspended sediment compartments. The default rates of resuspension in the model are given as $3*10^{-7}$ m^3/m^2-hr for freshwater and $2*10^{-7}$ m^3/m^2-hr for marine and can be altered to be more regionally specific. The area over which the resuspension occurs and the concentration of ENMs associated with that sediment are also accounted for in the calculation.

3.6.2.4.3 Sediment Burial

Burial is the addition of sediment above existing sediment that "removes" the ENMs from the system. The default rate of burial for sediments is $4.19*10^{-8}$ m^3/m^2-hr for

freshwater and $4.5*10^{-8}$ m^3/m^2-hr for marine, though these values can be altered by the user to account for regional variations.[353] Since this is the rate of burial of sediments, it is multiplied by the concentration of ENM in the sediment to derive the burial of the ENMs over the total area of sediment.

3.6.3 Mass Balance Equations

The nanoFTmodel is designed around a series of mass balance equations that consider transport between compartments and transformations of the ENMs to non-nano forms (e.g. dissolved, sorbed, heteroaggregated). These mass balance equations feed into a differential equation solver that solves the mass balance for each time-step over the specific time range selected for the model.

Compartmental mass balances are given by the following equations. Note: while some of the individual computations provided above use units different from SI, all are converted into SI units (e.g. kg/m^3) prior to this process.

Equation 1 is the mass balance calculation for air.

$$\frac{d[V_A C_A]}{dt} = -\left(\sum K_{F,M,S}^{dry,A} + \sum K_{F,M,SW}^{wet,A} + K_{A,Aer} + K_A^{adv}\right) + Q_A(t) + K_{A,In}^{adv} \qquad \text{Eq. 1}$$

$\sum K_{F,M,S}^{dry,A}$ is the sum of dry deposition terms to freshwater, marine, and surface soil as calculated using Stoke's Law; $\sum K_{F,M,SW}^{wet,A}$ is the sum of wet deposition terms to freshwater, marine, and surface soil water; $K_{A,Aer}$ is the adsorption with aerosols; K_A^{adv} is the advection of ENMs present in air out of the system boundaries caused by wind; $Q_A(t)$ is the release to air and $K_{A,In}^{adv}$ is the advective transfer into the system from the air outside of the system.

Equation 2 is the mass balance calculation for aerosols.

$$\frac{d[V_{Aer}C_{Aer}]}{dt} = -\left(\sum K_{FS,MS,S}^{dry,Aer} + \sum K_{FS,MS,SW}^{wet,Aer} + K_{Aer}^{adv}\right) + \left(K_{A,Aer} + K_{M,Aer} + K_{S,Aer}^{resus}\right) +$$

$$Q_{Aer+}K_{Aer,In}^{adv} \qquad\qquad \text{Eq. 2}$$

$\sum K_{FS,MS,S}^{dry,Aer}$ is the sum of dry deposition to freshwater suspended sediment, marine suspended sediment, and soil as calculated using Stoke's Law; $\sum K_{FS,MS,SW}^{wet,Aer}$ is the sum of wet deposition to freshwater suspended sediment, marine suspended sediment, and soil water; K_{Aer}^{adv} is the advection of ENMs bound to aerosols out of the system boundaries caused by wind; $K_{M,Aer}$ is the resuspension of particles in the coastal zone by waves breaking; $K_{S,Aer}^{resus}$ is the resuspension of particles by wind erosion; $Q_{Aer}(t)$ is the additional release of ENMs to the aerosols compartment and $K_{Aer,In}^{adv}$ is the advective transfer of aerosols into the system from the air outside of the system.

Equation 3 is the mass balance calculation for freshwater.

$$\frac{d[V_F C_F]}{dt} = -\left(K_F^{dep} + K_{F,FS}^{het} + K_{F,M}^{flow} + K_{disF}\right) + \left(K_F^{dry,A} + K_F^{wet,A} + K_F^{runoff}\right) + Q_F(t)$$

Eq. 3

K_F^{dep} is the deposition of ENMs in freshwater; $K_{F,FS}^{het}$ is the heteroaggregation and adsorption of nanoparticles to suspended sediment in freshwater; $K_{F,M}^{flow}$ is the flow of water from freshwater to marine; and K_{disF} is the dissolution rate in freshwater. K_F^{runoff} is the runoff of water from soil during storm events and $Q_F(t)$ is the release to freshwater.

Equation 4 is the mass balance calculation for freshwater suspended sediment.

$$\frac{d[V_{FS}C_{FS}]}{dt} = -\left(K_{FS}^{dep} + K_{FS,MS}^{flow}\right) + \left(K_{FS}^{dry,Aer} + K_{FS}^{wet,Aer} + K_{F,FS}^{het} + K_{FS}^{erosion} + K_{FSed}^{resus}\right) +$$

$$Q_{FS}(t) \qquad\qquad \text{Eq. 4}$$

K_{FS}^{dep} is the deposition of suspended sediment in freshwater using Stoke's Law and $K_{FS,MS}^{flow}$ is the flow of suspended sediment associated with the flow of water from freshwater to marine. K_{FS}^{runoff} is the erosion of soil particles caused by water movement during a storm event; K_{FSed}^{resus} is the resuspension of freshwater sediment; and $Q_{FS}(t)$ is the release to the freshwater suspended sediment compartment.

Equation 5 is the mass balance calculation for freshwater sediment.

$$\frac{d[V_{FSed}C_{FSed}]}{dt} = -\left(K_{Fsed,MSed}^{flow} + K_{FSed}^{resus} + K_F^{burial} + K_{FSed}^{dis}\right) + \left(K_F^{dep} + K_{FS}^{dep}\right) + Q_{FSed}(t)$$

Eq. 5

$K_{Fsed,MSed}^{flow}$ is the advective transfer of sediment from freshwater to marine; K_F^{burial} is the burial of freshwater sediment (treated as a loss term); K_{FSed}^{dis} is the dissolution in freshwater sediment; and $Q_{FSed}(t)$ is a term that allows for the somewhat unlikely direct release to freshwater sediment.

Equation 6 is the mass balance calculation for marine water.

$$\frac{d[V_M C_M]}{dt} = -\left(K_M^{dep} + K_{M,MS}^{het} + K_{M,Aer} + K_{disM} + K_M^{flow}\right) + \left(K_M^{dry,A} + K_M^{wet,A} + K_{F,M}^{flow}\right) +$$

$$Q_M(t) \hspace{6cm} \text{Eq. 6}$$

K_M^{dep} is the aggregation and deposition of ENMs in freshwater; $K_{M,MS}^{het}$ is the heteroaggregation and adsorption of nanoparticles to marine suspended sediment; K_{disM} is the dissolution rate in marine waters; K_M^{flow} is the advective flow of ENMs present in the marine water out of the system boundaries; and $Q_M(t)$ is the release to marine water.

Equation 7 is the mass balance calculation for marine suspended sediment.

$$\frac{d[V_{MS}C_{MS}]}{dt} = -\left(K_{MS}^{dep} + K_{MS}^{flow}\right) + \left(K_{MS}^{dry,Aer} + K_{MS}^{wet,Aer} + K_{M,MS}^{het} + K_{FS,MS}^{flow} + K_{MSed}^{resus}\right) +$$

$$Q_{MS}(t) \hspace{6cm} \text{Eq. 7}$$

K_{MS}^{dep} is the deposition of suspended sediment in marine water using Stoke's Law; K_{MS}^{flow} is the advective flow of ENMs associated with the suspended in sediment in marine systems out of the system boundaries; K_{MSed}^{resus} is the resuspension of marine sediment; and $Q_{MS}(t)$ is the release to the marine suspended sediment compartment.

Equation 8 is the mass balance calculation for marine sediment.

$$\frac{d[V_{MSed}C_{MSed}]}{dt} = -\left(K_{MSed}^{resus} + K_M^{burial} + K_{Msed}^{dis}\right) + \left(K_M^{dep} + K_{MS}^{dep} + K_{Fsed,MSed}^{flow}\right) +$$

$$Q_{MSed}(t) \hspace{4cm} \text{Eq. 8}$$

K_M^{burial} is the burial of marine sediment; K_{Msed}^{dis} is the dissolution in marine sediment; and $Q_{MSed}(t)$ that allows for direct release to the marine sediment compartment.

Equation 9 is the mass balance calculation for surface soil.

$$\frac{d[V_S C_S]}{dt} = -\left(K_{S,Aer}^{resus} + K_{FS}^{erosion} + K_S^{dep} + K_{SW}\right) + \left(K_S^{dry,A} + K_S^{dry,Aer} + K_{WS}\right) + Q_S(t)$$

Eq. 9

K_S^{dep} is the settling of soil particles from surface soil to deep soil; K_{SW} is the transfer from soil to soil water; K_{WS} is the transfer from soil water to soil particles; and $Q_S(t)$ is the release to soil (either directly or from biosolids).

Equation 10 is the mass balance calculation for surface soil water.

$$\frac{d[V_{SW}C_{SW}]}{dt} = -\left(K_{WS} + K_F^{runoff} + K_{disS}\right) + \left(K_{SW}^{wet,A} + K_{SW}^{wet,Aer} + K_{SW}\right) + Q_{SW}(t)$$

Eq. 10

K_{disS} is the dissolution rate in soil water and $Q_{SW}(t)$ is the release to soil water.

Equation 11 is the mass balance calculation for deep soil.

$$\frac{d[V_{DS}C_{DS}]}{dt} = K_S^{dep} \hspace{4cm} \text{Eq. 11}$$

The deep soil compartment is treated as a sink to which ENMs can only accumulate and only as attached to soil particles.

3.6.3.1 Solving the Differential Equation

Generally, differential equations are solved over a specific time range, with all other parameters except time remaining constant. In this model, because input parameters like rainfall, wind speed, and release of ENMs can change from day to day, we iterate through the solver for each time step (in this case, a single day) with the appropriate set of input parameters associated with that specific day. Within MATLAB, the differential equation solver selected is ode15s, which was selected for efficiency, because multiple sets of equations must be solved at each time step.

All of the input parameters to the solver are either scalars or vectors. If they are vectors, then the value that is used depends on the time step within the iteration. For example, any parameter that is affected by precipitation will be a vector and if we are simulating day 5, then the model considers the parameter value on day 5 (e.g. wet deposition), which is affected by the precipitation on day 5.

The number of iterations is dependent on the length of time for which you want to run the model (e.g. 1 year, 5 years, etc.) The time step used in the solver, however, is always 0 to 1. This is because we want the ordinary differential equation (ODE) solver to solve the equation based on the specific parameters for that single day. It then takes the value at the end of the day (since the ode integrates and solves for multiple points throughout that day) as the solution. On the next iteration, the parameters are then updated, and the initial conditions are the solution taken from the previous iteration.

3.6.4 Custom Environment Development

3.6.4.1 Environmental Compartments

To create a custom environment, you must first identify your region of interest. You will need a single polygon shapefile for this region that can be opened in ArcMap. This will help you to estimate the spatial extent of the different environmental compartments within the region.

3.6.4.1.1 Air – Air and Aerosols

The area of the compartment that we call 'air' is the same as the total area of your selected region. The height of the air column typically is set to between 500 and 1000 m since long range ENM transport is not expected.[11,468] Air density is around 1.225 kg/m^3 at sea level and decreases with increasing altitude. If the region of interest is at a higher elevation, this should be adjusted accordingly.

Aerosol density, initially assumed to be 1000 kg/m^3,[469] also does not need to be altered unless the aerosols in your region of interest have a high mineral content. The concentration of aerosols, however, can be altered if your region is particularly urban or has a naturally higher concentration of aerosols, or if your region happens to have a low aerosols concentration (the default concentration is set to $3*10^{-8}$ kg/m3).[470] Table 1 covers the default air parameters for the San Francisco Bay.

3.6.4.1.2 Land Cover Types

Land cover types are used to identify up to three distinct soil compartments and the total freshwater area within the selected region.

You can download any land cover data set for your region. The most recent National Land Cover Database (NLCD) would be ideal if your site is located in the USA.[471] The

following instructions assume you are working with a raster-based land cover data set.

1. Add both the **landuse raster** and your **polygon boundary shapefile** to ArcMap
2. Clip the raster to the area of interest
    a. Data management tools : Raster : Raster Processing : **Raster Clip**
        i. Input is the raster
        ii. Output is the cat
        iii. Save as nlcd_#AREA (replace #AREA with the name of your region. This is particularly important if you are developing multiple regions)
3. Convert the raster to polygon
    a. Conversion Tools : **From Raster** : **To Polygon**
        i. Input is the nlcd_#AREA
        ii. Save as nlcd_#AREA_poly
4. Clip the polygon to the immediate extent of your region
    a. Analysis Tools: Extract: **Clip**
        i. Input is the nlcd_#AREA_poly

<blockquote>

    ii.   Clip feature is the cat

    iii.   Save as nlcd_#AREA_poly_clip

5. Dissolve the individual points so that each land use type is grouped together
   a. Data Management Tools: Generalization: **Dissolve**
      i. Input is the nlcd_#AREA_poly_clip
      ii. Dissolve Field(s) is by GRIDCODE
      iii. Save as nlcd_#AREA_dis
6. Add an area field so that you can calculate the total area of each land use type.
   a. Data Management Tools: Fields: **Add Field**
   b. Input is nlcd_#AREA_dis
   c. Field name is **Area**
   d. Field Type is **double**
7. Calculate the area of each land use type
   a. Right click the Area title and select **calculate geometry** (choose yes)
   b. Property is area, units are **sq m** (choose yes, again)
8. Export as a .dbf file (which can be opened in excel)
   a. Right click on the nlcd_#AREA_dis layer and select Data: **Export Data**
      i. File type is **dBASE**
   b. Save as #AREA_landuse
   c. Sum the total areas of each land use type so you have the total area of water, urban, natural, and agricultural land covers.
9. Data processing in excel: Open an empty excel file
   a. Select Open
   b. Switch the file format from All Excel Files to All Files
   c. Find #AREA_landuse.dbf and open in excel
   d. The following table indicates which Gridcode values are for which land cover types if you choose to include 3 separate soil compartments in your model run (Table B3.14).

Table B3.14 NLCD Gridcode to Land Cover Type

Gridcode	Land Cover Type
11	Water
21-24	Urban
12, 31, 41, 42, 43, 52, 71, 90, 95	Natural
61, 71, 81, 82	Agricultural

    e. Sum the total areas of each set of cover types so you have the total area of water, urban, natural, and agricultural land covers.

</blockquote>

3.6.4.1.3 Water - Freshwater and Marine

Two water compartments are included in the model: a freshwater compartment and a marine compartment

Your total freshwater area is calculated from the previous step (See Section 4.2 -- 9.d). Depth can either be an estimate, or you can take the average of the depths given in Reach File, V1 as provided by BASINs for your area of interest.[472] To calculate the depth using RF1, use the below process.

1. Add the **Reach File (RF1)** to ArcMap.
2. Right click on the layer and open the attribute table. Scroll to the far right until you find the column labeled **PDEPTH**.
3. **Right click** on the label and go to **statistics**. This will give you the mean of the mean depths for each river segment in feet. This value can be entered directly into the environment file.

Total marine area requires some judgment. Generally, it is useful to measure the total coastline, and then consider the likely region influenced by human activities (e.g. 3 to 10 km) to obtain the area. Depth can be collected from actual data or set to between 5 and 10 m, depending on how far into the greater ocean you chose to take your marine region. Figure 3 shows the distinction between the marine zone and the coastal zone. A simple methodology is   listed   below.

1. Add your **polygon boundary shapefile** and a **land shapefile** (e.g. county, state, continent polygon) to ArcMap.
2. Using the **Buffer** tool, select the polygon boundary as your input
    a. Set the **linear distance** for however far out into the ocean you want and include this in your marine region (e.g. 500-1000 m)
    b. Set **Side Type** to **Outside Only**
3. This will create a new polygon layer that extends beyond your region of interest into the marine zone. Next **erase** the region of interest itself with the erase tool
    a. Input is your **buffered polygon**
    b. Erase by your **original polygon** for your region of interest
4. This eliminates your land and freshwater regions within your area in interest, but to exclude all land, also **erase** by your land shapefile (e.g. county, state, continent polygon)
    a. Input in your **erased buffered polygon** file
    b. Erase by your **land shapefile**
5. **Add a field** and calculate the total area of your marine region using calculate geometry.

167

This same procedure can be used to estimate the coastal zone within your marine region. The coastal zone is specifically used to estimate the transfer of ENMs from marine to air as a result of breaking waves (Figure B3.3). The only change would be to select a smaller buffer zone (e.g. 50-200 m). Since the environment input sheet requires coastal area percent, divide the total coastal area by the total marine region.
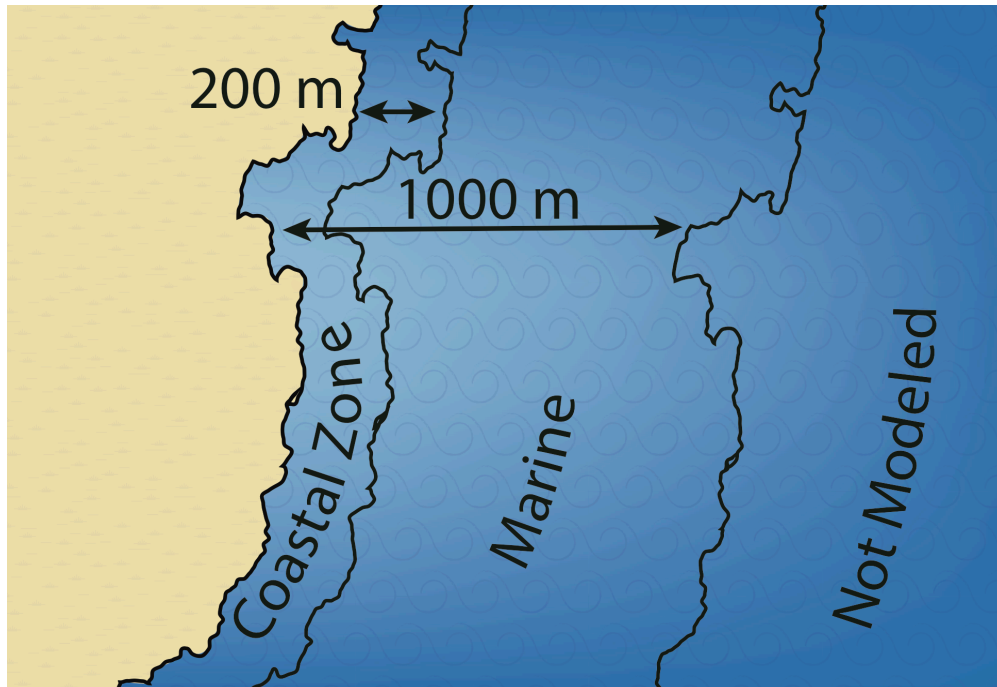
Figure B3.3 Distinguishing between Marine and Coastal Zones

The default density (1000 kg/m^3 freshwater, 1027 kg/m^3 for marine) and pH (7 for freshwater, 8.4 for marine) of both waters can be altered if more specific local data are available.

Suspended sediment density is assumed to be 1500 kg/m^3 for both freshwater and marine, to be modified as needed with local information. Estimates of suspended sediment concentration can be collected from the EPA STORET database if your region of interest is in the US.[473] A procedure for determining the local water quality (if available in STORET)

is presented below. Table 3 indicates the parameters needed to define the freshwater and marine compartments.

<div style="border:1px solid black;">

1. Select the link **Download Water Quality Data**
2. Choose the yellow button for **Modernized STORET database** which is post 01/01/1999. Then select **Download Data**
3. Search for stations within your region of interest using counties, watersheds, or your latitude-longitude bounding box.
4. Set station type to **River/Stream** and **Lake** if you want the concentration for freshwater or **Ocean** if you want the ocean concentration.
5. Set Activity Medium to **Water**.
6. Set the Characteristic Search to **Suspended Sediment Concentration**.
7. Click **Results Download**. This will open a new page where you can provide your email address so results can be emailed to you. **Select Immediate**.
8. You should receive two emails, the first saying that they are processing your request and the second with a zip file of the data.
9. The **COMPLETED** email will contain your zip file to download. Extract the files from the zip folder.
10. Open the ***_RegResults.txt** in excel as a tab delimited file.
     a. Take the average of the suspended sediment concentration values as your freshwater and marine suspended sediment concentrations.

</div>

3.6.4.1.4 Soil Characteristics

The model considers up to three different soil compartments. These are meant to consider important differences between urban, agricultural and natural soils (Figure B3.4). The model is designed to be flexible. The user has the option to include one, two or all three soil compartments, and the method for dividing them is not limited to urban, agricultural, and natural. For example, they could be separated based on a specific soil characteristic, or spatially. Section 3.6.4.2 provided guidance on estimating the total area of each soil type within your region based on land cover variations. Additional characteristics also need to be collected for each of the specific soils types.
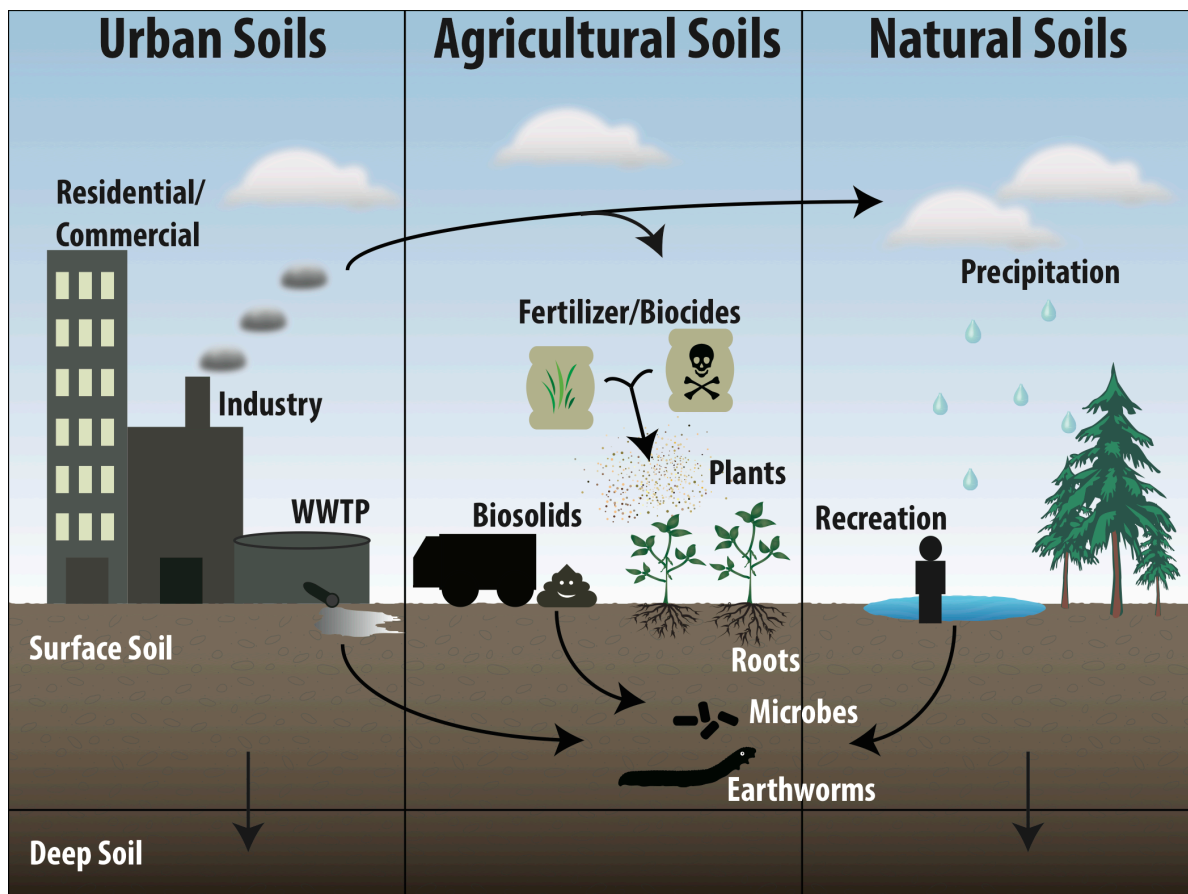
Figure B3.4 Conceptual Division between Soil Regions

Surface soil depth (typically less than 1 m), organic carbon content, and hydrologic group, soil erodibility, and soil texture can all be estimated from the SURRGO soil dataset. The SURRGO dataset can be downloaded through BASINs for your region in a set of three files including statsgo.shp, statsgoc.dbf, and statsgol.dbf or from the USDA NRCS website.[435]

1. Add the **statsgo**, **statsgoc**, and **statsgol** to ArcMap
2. **Join** the statsgoc and statsgol to statsgo using the **MUID**.
   a. Right click on statsgo, select **joins and relates**, select **join**
   b. Join by **MUID**
   c. To statsgoc.dbf
   d. Join by **MUID**
   e. Do the same for statsgo also

170

3. Join the **statsgo** data to the **land use data**.
   a. Analysis Tools : Overlay : **Spatial Join**
   b. **Target feature** is the nlcd_#AREA_poly_clip (from Section 1.1.2.2 step 5)
   c. **Join features** is the statsgo
   d. Save the output as #AREA_landuse_soiltypes
   e. Join operation is **JOIN_ONE_TO_ONE**
   f. Deselect **keep all target features**
   g. Remove all of the field map of join features using the little x next to the list of features except for:
      i. ID, GRIDCODE, LAYDEPH, TEXTURE1, OML, OMH, HYDGRP, SLOPEL, SLOPEH, and KFFACT
   h. **Match** option is **intersect**
4. Summarize the data by land use type
   a. Data Management Tools : Generalization : **Dissolve**
      i. **Input feature** is #AREA_landuse_soiltypes
      ii. Save output as #AREA_soil_summary
      iii. **Dissolve Field** is **GRIDCODE**
      iv. **Statistics fields** are the numeric attributes (LAYDEPH, OML, OMH, SLOPEL, SLOPEH, KFFACT)
      v. **Statistics type** is **MEAN** for each
5. Summarize each parameter
   a. Open excel, go to open, set the options to all files to find the #AREA_soil_summary.dbf file
   b. Summarize the **depth data** for urban, agricultural, and natural soil types using the average function. Convert the depth from inches (given units) to meters
      i. Example function =average(B3:B6) to calculate urban soil depth
   c. Summarize the **organic carbon content** as the average of the **OML and OMH** data for soil type.
      i. Example function =average(C7:D10,C15:D16) to calculate natural organic carbon percent
   d. The same method should be used to calculate the **average slope** (SLOPEL and SLOPEH) for each soil type and the **soil erodibility factor** (KFFACT)
6. Summarize the **soil type data** (**soil texture** and **hydrologic group** – qualitative data)
   a. Open excel, go to open, set the options to all files to find the #AREA_landuse_soiltype.dbf
   b. Select both columns and go to **Insert: PivotTable** (table range should be your preselected columns). Click Ok.
   c. In the pivot table field list
      i. Click and drag the **GRIDCODE** item down to the **row labels** space

> i. Click and drag the **soil texture** attribute down to the **column labels** space and **again** down to the **values space**.
> ii. Check to make sure that your **values space** is set to **COUNT** by clicking on the values space and select **Value Field Setting**. If count is not already selected, choose it
> e. In the space below, **sum up the total count for each soil texture** by soil type.
>> i. Sum each column for urban, natural, and agricultural soil.
>> ii. Use the following equation to identify the specific soil texture that is most common for each land use type
>> =INDEX(C4:Y4,1,MATCH(MAX(C25:Y25),C25:Y25,0))
>>> 1. C4:Y4 is the label row that contains the acronyms for each texture
>>> 2. C25:Y25 is the sum total count for each texture for your first land cover type
>>> 3. The equation for the next land cover row would look like
>>> =INDEX(C4:Y4,1,MATCH(MAX(C26:Y26),C26:Y26,0))
> f. This same method can be used to summarize the data for **hydrologic groups**.

The hydrologic group provides an estimate of the runoff potential, which we can use to estimate the curve number. The soils in the United States are assigned to four groups (A, B, C, and D) and three dual classes (A/D, B/D, and C/D) (Table B3.15).[474]

Table B3.15 Hydrologic Soil Groups

Group	Description
Group A	Soils having high infiltration rate (low runoff potential when thoroughly wet. These consist mainly of deep, well drained to excessively drained sands or gravelly sands.
Group B	Soils having moderate infiltration rate when thoroughly wet. These consist chiefly of moderately deep or deep, moderately well drained or well-drained soils that have moderately fine texture to moderately coarse texture.
Group C	Soils having slow infiltration when thoroughly wet. These consist chiefly of soils having a layer that impedes the downward movement of water or soils of moderately fine or fine texture.
Group D	Soils having a very slow infiltration rate (high runoff potential) when thoroughly wet. These consist chiefly of clays that have a high shrink-swell potential, soils that have a high water table, soils that have a claypan or clay layer at or near the surface, and soils that are shallow over nearly impervious material.
Dual Group	If soils are assigned to a dual hydrologic group, the first letter is for drained areas and the second is for undrained areas

A runoff Curve Number (CN) should be selected for each soil type using the primary land cover type and the soil hydrologic group and then this should be averaged across total land use types (Table B3.16).[475]

Table B3.16 Land Use and Hydrologic Groups used to Estimate Runoff Curve Number

Land Use Types	A	B	C	D
Open Space	49	69	79	84
Impervious Areas	98	98	98	98
Western Desert Urban Areas	63	77	85	88
Commercial	89	92	94	95
Residential	61	75	83	87
Row Crops	70	80	86	90
Heterogeneous Agriculture	64	75	82	86
Pasture	49	69	79	84
Meadow	30	58	71	78
Brush	35	56	70	77
Woods	36	60	73	79
Herbaceous	--	71	81	89

Summarized from USDA publication on Runoff Curve Number Computations for fair hydrologic conditions (30-70% ground cover conditions).[426]

Both surface soil and deep soil contain soil air and soil water, the ratios of which are set to a default of between 0.2 and 0.4 for soil water and 0.2 for soil air. The depth of deep soil for each of the three soil compartments is initially set to a default of 1 m, and can be modified by the user if deeper transport is expected. Table B3.6 indicates the parameters need to define one soil compartment.

3.6.4.2 Selecting the Time Range

You will need to set the length of time (in days) for which you want to run the model. A limitation here is that in addition to setting the number of days, you also need a corresponding dataset (real or otherwise) for climate and hydrology over that total length of

days. The model will report results for each day as well as the long-term average results excluding an initial "warm-up" period at the start of the model run to achieve relative constant concentrations (Figure B3.5). This default period is set to 1 year and can be altered. If you are working with a default environment, you will need to select a starting date and a length of time that corresponds with the available data for that environment. The available data range for default environments is Jan 1, 2005 – December 31, 2015.
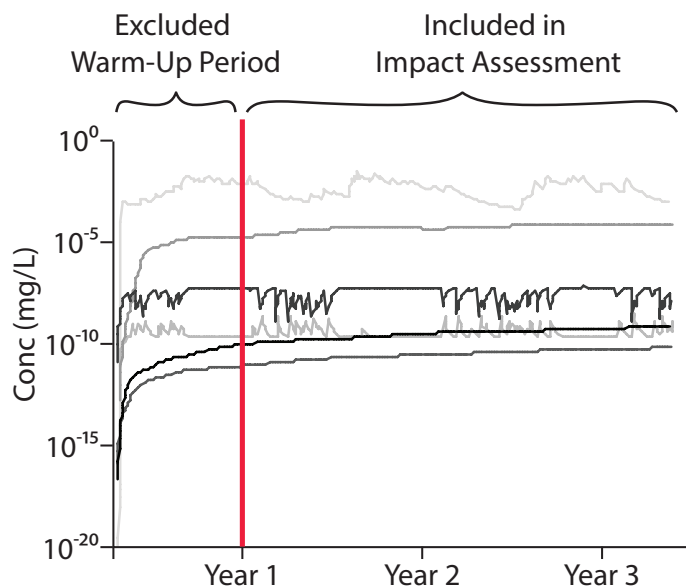
Figure B3.5 Model Warm-Up Period

3.6.4.3 Climate Data

The climate data required to run the model includes average daily temperature, precipitation, wind speed, and freshwater flow. Within the US, climate data is available from NOAA's National Climate Data Center.[476] The following procedure can be used to obtain the necessary dataset for a new region of interest or to extend the dataset for an existing region.

174

1. Select **15. Global Summary of the Day**.

2. Agree to the terms.

3. Retrieve data for: **Country: United States**, select by **Selected Station** in your State(s).

4. Select a city or area within your environment that has the time range of data that you are looking to model.

5. Select the date range for which you want to download data, and set the **Output Format** to **Comma Delimited**.

6. Right Click and select Save Link As to save the output file.

7. The climate data available from this data set includes **precipitation**, **wind speed**, and **temperature**. Precipitation is reported in tenths of mm/day and should be converted to mm/day. Wind speed is presented in tenths of m/s and should be converted to m/s. Temperature is reported in tenths of degrees Celsius and should be converted to degrees Celsius.

   a. If you open this in excel as a **comma delimited file**, you may see some formatting issues that need reformatting (units, data gaps, and extraneous alphanumeric codes). (We have provided code to translate and format this data set.)

8. Dates should be reported in three separate columns, one for month, one for day, and one for year.

If you are working with a default environment, you need only to select the start date from within the range of available data. Table B3.17 depicts the input format needed for the climate data.

Table B3.17 Input Format for Climate Data

Month	Day	Year	Precipitation (mm/d)	Wind speed (m/s)	Flow (m^3/s)	Temperature (°C)
1	1	2015	6.795	3.14	85.828	8.383
1	2	2015	18.633	2.62	59.737	7.193
1	3	2015	7.0714	2.1	64.177	6.958

3.6.4.3.1 Hydrologic Flow of Freshwater

Freshwater flow should also be included in the climate sheet with flow reported in m^3/s (Figure B3.4). Because we model both the freshwater and the marine fate of ENMs, we need to include an estimated rate of flow between the freshwater and marine environments. In a scenario with no marine environment, this is still included as a loss process from the total environment (i.e. we assume the freshwater at some point leaves the region of interest). If you are working with a default environment, you only need to select the start date from within the range of available data. In the US, the freshwater flow data can be collected from the USGS database on Surface Water.[477] Marine flow out of the coastal region is assumed to occur at the same rate as freshwater flow. In addition, we assume that some fraction of the sediment bed is transferred along with these fluid flows at a rate selected by the user.

1. Select Daily Data
2. The next menu provides options for narrowing the search area to those stations relevant to your project. Set the **Site Location** to **Lat-Long box** and click Submit.
3. In the next set of menu options, narrow your search criteria.
   a. Set the **Site Type** to **Stream**.
   b. Set the **Lat-Long box** to create a bounding box within the region where your environment is located.
   c. Set the **Available Parameters** selection to **Streamflow, ft^3/s**.
   d. Under **Choose Output Format**, select **Table of sites grouped by County** and retrieve data from the date range that you have pre-selected.
4. In the resulting list of data, identify the counties of interest to you
   a. Starting with the first county, open each site in a new tab to see if they provide the data for the time period you pre-selected.
      i. If they have the data, leave the tab open; if they don't, close the tab.
   b. For those that have data, change the dropdown menu to the **Location Map**.
   c. If the site is close to the coastal zone (provided your environment has a coastal region) or close to the outflow point (if your environment is land-bound) leave the tab open; if not (or if it appears to be upstream from another site) close the tab.

<div style="border: 1px solid black; padding: 10px;">

    d. For the sites where you have left the tab open, go back to the **Time Series: Daily Data** page and download the data.

        i. Set **start date** to your pre-selected start date.

        ii. Set **end date** to your pre-selected end date.

        iii. Output format should be **Tab-Separated**.

        iv. Right click on the resulting page and select **Save Page As** using the SiteID to track the name. Add a ***.txt** to the end of the filename so that the file can be opened in excel.

    e. Do this for each county until you have a representative dataset for your freshwater flow.

5. In excel, open each SiteID.txt file as a **Tab Delimited** file.

    a. Delete all rows and columns except those that contain the **dates** and the **flow data**.

    b. Convert the flow data from ft^3/s to m^3/s.

6. Once you have done this, aggregate all of those values into one single daily flow value for input into the model.

</div>

If your region is landlocked, you will still need a flow value, but it will be only from the single most downstream site within your region and representative of the total flow out of the region rather than the total flow of freshwater to marine.

3.6.4.4 Release of ENMs into the Environment

Release quantities are the amount (kg/day) of the nanomaterial expected to enter each environmental compartment and the rate or timing of that release. For example, releases can occur all at once, every day, or at different points in time. The release can be constant or varied over time (e.g. increasing as the use of an ENM in various applications grows). The data input is arranged so that one must enter release data for every day of the selected time period to every compartment for which a direct release is possible. Similar to the climate data sheet, you will need to include the range of dates associated with the releases for the length of time selected for the model. See Table B3.18 for the input format for the release data.

Table B3.18 Input Format for Release Data (units are kg/day)

Month	Day	Year	Air	Aer	FW	MAR	UNDEDV Soil	UNDEVL Water
1	1	2015	0.066[a]	0[b]	0.0628[c]	0.074	0.216	0 [d]
1	2	2015	0.066	0	0	0.074	0.216	0
1	3	2015	0.066	0	0.0628	0.074	0	0
1	4	2015	0.066	0	0	0.074	0	0

For constant release, populate that column with the same value for each date.

b. For no release to the compartment, populate that entire column with zeros.

c. For random release points, either populate randomly, or select your specific release dates and environments and populate only those cells in an excel dataset; the others should be set to 0.

d. Note: Additional Columns not shown include Surface Soil 2, Soil Water 2, Surface Soil 3, and Soil Water 3

3.6.4.5 Background Concentrations

Background concentrations of an ENM can be considered, should the user be interested in starting the predictions with environmental concentrations other than 0. To include existing background concentrations, identify the concentration in each compartment or if there is no background concentration, then leave the concentration set to 0. Table B3.19 shows a scenario where there is no existing ENM present in the system, but there is a dissolved component present in the aquatic, agricultural, and urban soils (Table B3.19). In addition, because the model includes advective air flows into the system, ambient concentrations for the ENM and the ENM associated with aerosols "outside" of the system need to be specified.

Table B3.19 Input Format for Background Concentrations in Compartments

Compartment	kg/m^3
Air	0
Aerosols	0
Freshwater	0
Freshwater Suspended Sediment	0
Freshwater Sediment	0

Seawater	0
Seawater Suspended Sediment	0
Seawater Sediment	0
Undeveloped Soil	0
Undeveloped Soil Water	0
Agricultural Soil	0
Agricultural Soil Water	0
Urban Soil	0
Urban Soil Water	0
Freshwater dissolved metal	$1.47*10^{-10}$
Freshwater sediment dissolved metal	$3.46*10^{-8}$
Marine dissolved metal	$2.57*10^{-8}$
Marine sediment dissolved metal	$6.37*10^{-8}$
Undeveloped soil dissolved metal	0
Agricultural soil dissolved metal	$5.23*10^{-8}$
Urban soil dissolved metal	$1.46*^{-10}$
Global air concentration	$1.79*10^{-14}$
Global aerosols concentration	$8.18*10^{-7}$

3.6.4.6 Presence or Absence of Compartments

Under some environmental scenarios, not all compartments should be included in the model. Thus, it is important to identify which compartments are excluded from the model in a given scenario. The most common example would be a scenario that does not include a marine environment if the scenario is representing a land-locked region. All that is needed for the model is a binary identification of presence (1) or absence (0) of each possible compartment (Table B3.20).

Table B3.20 Sample Presence Absence Input Format for Land-Locked Region

Compartment	Presence (1)
Air	1
Aerosols	1
Freshwater	1
Freshwater Suspended Sediment	1
Freshwater Sediment	1
Marine	0
Marine Suspended Sediment	0
Marine Sediment	0

Natural Surface Soil	1
Natural Soil Water	1
Natural Deep Soil	1
Agricultural Surface Soil	1
Agricultural Soil Water	1
Urban Surface Soil	1
Urban Soil Water	1
Urban Deep Soil	1

3.6.4.7 Selecting the Nanomaterial

In selecting the ENM and its associated chemical characteristics, you have two options. The first is to select one of the four nanomaterials for which we have detailed information (CeO_2, CuO, TiO_2, ZnO: values provided are aggregates from information collected through literature review and are specific to the environment and the pH of that environment – though characteristics do vary substantially across media). Alternately, you can import your own data for a specific nanomaterial including its size and density. This requires you to have information about the rates of aggregation, sedimentation, dissolution rate in freshwater, marine, and soil environments. Table B3.21 provides the list of characteristics that must be input into the model. Methodology for estimating these rate constants is given in Section 5 below.

Table B3.21 Input Format for Nanomaterial Characteristics (sample data)

Parameter	Value	Unit
ENM type	CuO	--
ENM diameter	30	nm
Average Aggregate Diameter	400	nm
Density	6400	kg/m^3
Dissolution Rate Freshwater	$3.84*10^{-2}$	day^{-1}
Dissolution Rate Freshwater Sediment	$3.84*10^{-3}$	day^{-1}
Dissolution Rate Marine	$5.28*10^{-2}$	day^{-1}
Dissolution Rate Marine Sediment	$5.28*10^{-3}$	day^{-1}

Dissolution Rate Soil	$5*10^{-3}$	day^{-1}
Sedimentation Rate Freshwater	$4.09*10^{-2}$	m/day
Sedimentation Rate Marine	$8.40**10^{-2}$	m/day
Heteroaggregation in air	8.92	m^3/kg day
Heteroaggregation in freshwater	8917.5	m^3/kg day
Heteroaggregation in marine	9339.9	m^3/kg day
Soil Partition Rate for Soil Type 1	0.99	%
Soil Partition Rate for Soil Type 2	0.99	%
Soil Partition Rate for Soil Type 3	0.99	%
Enrichment Factor	5	--

Modeling the fate of non-metal or metal oxide nanoparticles, such as carbon nanotubes (CNTs) or fullerenes would require distinctions between single walled carbon nanotubes (SWCNTs), multiwalled carbon nanotubes (MWCNTs), alternate shapes such as sheets of graphene or fullerenes, and the presence of impurities such as heavy metals.[226,478] In addition, further transformations are possible that are not accounted for in this model including photo-oxidation, covalent reactions, and biodegradation.[478,479] While not directly impacting the fate of the ENM, from a toxicological perspective, carbonaceous ENMs can also accumulate large quantities of other environmental pollutants (e.g. through adsorption) that could have significant long term impacts.[480,481] Other nanomaterials may also experience significant physical alternations resulting from processes not included in this model (e.g., sulfidation for n-Ag, photolysis for TiO2, phosphorylation of magnetite).[13,226,482,483] Desorption is also common with some ENMs in specific environments which is not included in the current version of this model.[479]

3.6.5 Deriving Integrated Rate Equations for ENM-Specific Fate Processes

As with many physicochemical principles, the rules governing the rate of a reaction are initially established empirically, and then subjected to extensive theoretical analysis, which eventually develops into a clear understanding of the controlling factors in a process. The

empirical observations center on establishing conditions where a rate can be measured as a function of the concentration of the material(s) of interest. In the case of ENMs, it is clearly understood that rates of transfer and transformation are highly dependent on the characteristics of the environmental media and the ENM itself.[226] In general, rates are related to concentrations in a predictable way, which allows us to develop rate constants and equation(s) for simple reactions that can fall into one of several classes:

Zero order: these are processes that occur at a rate independent of the chemical's concentration

$$rate = k[A]^0$$

First order: reactions in which the rate varies with the concentration of a single chemical and the change in concentration is exponential

$$rate = k[A]^1$$

Second order: reactions where the rate varies with the concentration of a single chemical, but the rate varies with the reciprocal of the concentration. (There can also be situations where the rate varies with the concentration of two chemicals, though each individual chemical is first order.)

$$rate = k[A]^2$$

or

$$rate = k[A]^1[B]^1$$

Higher order reactions: reactions in which more than two chemicals are involved or one chemical reacts at a greater stoichiometric coefficient.

$$rate = k[A]^n$$

or

$$rate = k[A]^n[B]^n[C]^n$$

In the case of heteroaggregation, the concentrations of both the free ENMs and the natural organic matter to which the ENMs attach both determine the rate of reaction, making it a second order reaction. However, 2nd order reactions can be challenging to follow mostly because the two reactants involved must be measured simultaneously. A pseudo-first order reaction involves treating a second order reaction like a first order reaction. If we assume that one reactant in available in excess (in this example the natural organic matter), then:

$$rate = k[A][B]$$

becomes

$$rate = k'[A]$$

because the concentration of B is essentially constant and

$$k' = k[B]$$

We used the initial rate method to calculate the rate constant (k) for heteroaggregation, sedimentation of free ENMs, and dissolution. For this, the initial rate of a reaction is the reaction rate at t=0. Measuring the rate as soon after mixing as possible gives us the initial rate. (Sample data are provided below in **Error! Reference source not found.**B3.22). In most published studies, the specific rate of reaction is not reported, so data were calculated from the published literature (e.g. plotted change in concentration over time) in order to calculate the initial rate of reaction of each of the key nano-specific processes modeled.

Table B3.22 Sample Rate Data for Estimating Rate Constants

Experiment No.	ENM Concentration (mg/L)	Natural Organic Matter (NOM) Concentration (mg/L)	Initial Rate of Reaction (mg/time)
1	0.100	10	0.09
2	0.033	10	0.01

| 3 | 0.071 | 10 | 0.03 |

We can then calculate the order by comparing two sets of values

$$\frac{\text{Rate}_1}{\text{Rate}_3} = \frac{k[\text{ENM}]^x[\text{NOM}]^y}{k[\text{ENM}]^x[\text{NOM}]^y}$$

where the rate constant k and the $[\text{NOM}]^y$ both cancel.

$$\frac{0.09}{0.01} = \frac{0.1^x}{0.033^x}$$

Then round x to the nearest integer.

$$9 = 3^x \therefore x \sim 2$$

If an additional experiment is available, this value can be confirmed.

$$\frac{0.09}{0.03} = \frac{0.1^x}{0.071^x}$$

Thus:

$$3 = 1.4^x \therefore x \sim 2$$

To confirm these estimates, one can plot the concentration versus time, the natural log of the concentration versus time, and 1/the concentration versus time (Table B3.23). Depending on which plot appears linear, this will indicate which order the reaction falls into. If the ENM concentration relative to time is linear, then it is a zero order reaction. If the natural log of the ENM concentration relative to time is linear, then it is a first order reaction. If 1 divided by the ENM concentration relative to time is linear, then it is a second order reaction (or a pseudo-first order reaction as discussed above).

Table B3.23 Sample Data for Transformation over Time

Time (s)	ENM (mg/L)	ln(ENM)	1/(ENM)
0	$1*10^{-2}$	-4.605	100

60	$6.83*10^{-3}$	-4.986	146
120	$5.18*10^{-3}$	-5.263	193
180	$4.18*10^{-3}$	-5.477	239
240	$3.5*10^{-3}$	-5.655	286
300	$3.01*10^{-3}$	-5.806	332
360	$2.64*10^{\wedge}-3$	-5.937	379

In the example given above, it is clear that the reaction is a second order reaction (Figure

B3.6).
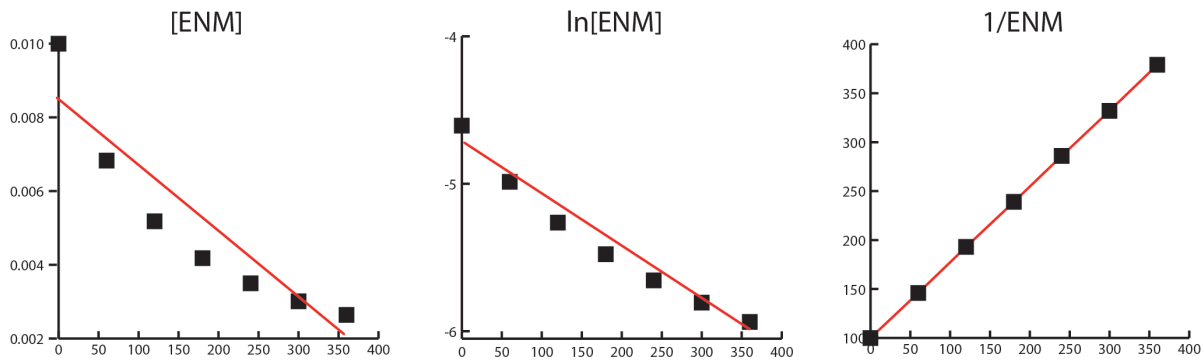
Figure B3.6 Determining Rate Order from Raw Data

From here, we place the values back into the equation.

$$0.09 = k'[0.1]^2$$

Thus:

$$0.9 = k * [10]$$

The resulting function would be as follows (although k' can be adjusted based on the

actual NOM concentration)

$$-\frac{d[\text{ENM}]}{dt} = -0.9[\text{ENM}]^2$$

And to calculate the change in concentration over time within the model, we use:

$$\frac{1}{[\text{ENM}_t]} = \frac{1}{[\text{ENM}_0]} + 0.9t$$

This process is used to simplify all ENM specific fate and transport processes into functions that can be included in a mathematical model. We have estimated these values for each key nano-specific process, for each key environmental compartment at standard temperatures. Ideally, separate rates would be predicted across a complex range of characteristics for both the environment and the ENM (e.g. a separate rate for a 10 nm CuO ENM at pH 7 relative to a 20 nm CuO ENM at pH 8). However, because our goal was to predict the generic fate of specific types of ENMs across more general environmental media, we developed rates specific only to an ENM and the general characteristics of the environmental media in which an ENM may reside. With sufficient time and resources, one could develop a matrix of rate constants for each combination of environmental and ENM characteristics, which would help our understanding of what characteristics truly control the fate of ENMs in the environment. In a scenario where one is trying to predict the fate of a very specific type of ENM, the predictive power of the model will be substantially improved if the user provides his/her own data since the current rate constants do not generally account for variations in size, shape, or charge of the ENM that could be significantly different from a more generalized ENM.

3.6.6 Sources of Uncertainty in the Model

There are a several sources of uncertainty within the model that are primarily associated with the selection of data inputs.

1. Scenario uncertainty is present in the selection of geographic boundaries. Because each compartment is a very simplified version of reality, this uncertainty largely depends upon choices made by the user rather than intrinsic uncertainty within the model. As such, there is no real quantitative method to measure this. However, the

geographic boundaries can be treated as parameters for which uncertainty can be tested by minor modifications to each value (e.g. ±10%).

2. Measurement uncertainty is present in the climate data and depends on the methods and technologies used to measure each parameter. This is hard to quantify primarily because it would be difficult to know the uncertainty in each piece of equipment used to measure these various parameters, because this typically isn't included in the datasets. We also recommend using a long period of time for the climate data in order to simulate stochastic modeling so there is a daily range in outcomes provided in the results without requiring the computing capacity and time to run a formal stochastic model.

3. Parameter uncertainty is present in nano-specific rate estimates. The exact values are estimated based on a combination of study results that provide a range in parameter estimates that in turn can be run through the model in order to provide a range in results.

Considering the above three sources of uncertainty and developing test scenarios that allow us to test the range of parameters within these sources can provide an approximation of the uncertainty and the total viable range of ENM environmental concentrations for any given scenario.

Chapter 4. Predictive Model for the Bioaccumulation of Engineered Nanomaterials in a Simplified Freshwater Ecosystem

Bioaccumulation is a fundamental process in environmental toxicology because it controls the internal dose of potential toxicants. The goal of this study was to improve our understanding of the potential scale of long-term accumulation of engineered nanomaterials (ENMs) across trophic levels given current understanding on environmental and biological fate. Specifically, we focus on n-CuO, n-TiO$_2$, and n-ZnO and their accumulation in a simple freshwater ecosystem. A toxicokinetics model was used to explore the potential range of accumulation across species. Accumulations ranged from 0.69 pg CuO g^{-1} for *Selenastrum capricornutum* (a phytoplankton) to 0.26 mg TiO$_2$ g^{-1} for *Villosa constricta* (a bivalve) and 1.8 mg TiO$_2$ g^{-1} for *Daphnia magna* (a zooplankton). Though bioconcentration is likely occurring for most species, biomagnification was not predicted to be significant with increasing trophic levels. Uncertainty analysis indicates that these results may vary by as much as two orders of magnitude. A parameter sensitivity analysis indicated that the most significant parameters include uptake rates from multiple exposure routes, assimilation efficiency (which could make the difference between biomagnification occurring or not), and elimination rates. Suspended sediment and sediment concentrations are also quite important for benthic species and have some impacts up the food chain. Further research and refinement of the biological parameters that impact bioaccumulation and biomagnification rates can target these parameters to further refine the model.

4.1 Introduction

Engineered nanomaterials (ENMs) represent a new and emerging class of environmental pollutants and we still understand relatively little about their impacts on our environment. Since the emergence of nanotechnology in the 1980s, ENMs are being used with increasing frequency in industrial applications and in consumer and medical products. Their increasing use means increasing environmental exposure, which in turn creates a compelling need to understand and predict their accumulation in organisms.[228]

ENMs are particles for which at least one dimension falls between 1 and 100 nm in length.[225] In this study we focus specifically on the potential bioaccumulation of three metal oxide nanoparticles CuO, TiO$_2$, and ZnO. These three ENMs can exist as single, aggregated, or agglomerated particles and can be manufactured with various shapes, coatings, and surface functionalities making predicting their impact on the environment a complex undertaking.

Only part of a chemical present in the environment reaches an organism, and of that percent which does, only a fraction is retained by the organism.[484] This is also the case for ENMs, for which only a portion is likely bioavailable. This portion is determined by the transformations that ENMs undergo in the environment such as aggregation, dissolution, oxidation, sulfidation, binding to larger particulate matter, and surface alterations that depend very specifically on both the type of ENM and the environment.[85,226,229,342–345,357,359] Dissolution particularly complicates our understanding of toxicity, because if an ENM dissolves, the toxic effect can come from the nanoparticle itself or from the dissolved ion, whereas if an ENM does not dissolve, then the toxic effect could be a result of their size, reactivity, or coating.[226,227] There are also biotransformations that may result from exposure

to biological byproducts or uptake into organisms.[102,256,258] These various transformations make it difficult for us to understand what happens to ENMs when they enter an organism, how significant each of the processes are and how much exposure we can expect within a given ecosystem. Currently, little is known regarding the bioaccumulation of specific ENMs through food chains, though many preliminary studies indicate that it likely.[50,221,455,485–493]

Understanding bioaccumulation is key to both ecotoxicity and risk assessment, because it controls the internal dose of potential toxicants. Typical measures for assessing bioaccumulation include the octanol-water partition coefficient (K_{ow}), bioconcentration factor (BCF), bioaccumulation factor (BAF), and biota-sediment accumulation factor (BSAF). The octanol-water partitioning coefficient (K_{ow}) is typically used as a parameter indicating the tendency of an organic chemical to partition into the lipid compartment of an organism.[494] However, most of the available partitioning coefficients are adequate predictors of hydrophobic chemical partitioning, and may not be applicable to metals or ENMs.[495,496] As such, we need an alternate model for predicting the bioaccumulation of ENMs in organisms.

Field measurements of the concentrations of ENMs would be valuable for assessing potential ecosystem exposure. However as the technologies for *in situ* measurements are not sufficiently advanced, and, more importantly, as the pace at which *in situ* experiments are conducted cannot keep up with that of new ENM development, there is an increasingly important role for model driven estimates in understanding the behavior and impact of EMNs.[18,347] While some estimates predict the bioaccumulation of specific ENMs in individual organisms,[221,252,455,485,486,497–505] a simple method for estimating the possible range of accumulation in ecosystems and across food chains would improve our understanding of

the environmental and biological fate. Identifying key biological parameters that predict bioaccumulation for targeted research purposes is also beneficial, particularly given the high cost of complex toxicity assessments.

Studies have shown that some nanoparticles can be absorbed as a whole and distributed throughout the body[488] and others remain bioavailable even with agglomeration to particulate matter.[506] While the literature is limited regarding the bioavailability of metallic nanoparticles and their subsequent accumulation in organisms,[53,507,508] exposure can occur via individual particles, aggregated particles, particles sorbed to particulate organic or biological matter, and as dissolved metal ions.[357] The form of exposure can have an impact on the rate of accumulation and on the resulting toxic effects. Metallic nanoparticles that dissolve release metal ions from the surface of the particle, which can cause latent free-ion toxicity,[507] which in turn can have different toxic impacts from exposure to the original nanoparticle.

Toxicokinetics can be used to model the uptake and accumulation of an ENM in an organism over time under non-steady state exposures and complex uptake pathways.[509–511] Toxicokinetic models are composed of a series of differential equations that represent uptake and elimination processes to estimate the internal concentration in an individual organism over time.[300,512–515] Thus, they require a basic understanding of the organism including resource acquisition, growth, reproduction, maturation, maintenance, and elimination rates.[515] These rates of uptake, translation, and accumulation depend on the biological traits and conditions of the organism (e.g., age, size, maturity), the environment (e.g., food density, temperature), and the size, type, chemical composition, functionalization, and stability of the ENM. [491,516–518]

In addition, single species toxicokinetics models have also been developed for specific ENMs including the accumulation and effects of ZnO on *Mytillus galloprovincialis*,[515] CdSe quantum dot on *P. aeruginosa*,[513] TiO_2 and Al_2O_3 on *Ceriodaphnia dubia*,[300] indicating that it is a functional approach for modeling ecosystem accumulation of ENMs. A similar biodynamic accumulation model was completed for accumulation and effects of Ag on *Peringia ulvae* and *Lymnaea. stagnalis*.[497] These models indicate that there is accumulation of nanoparticles as well as dissolved ions for some ENMs and that the toxic effects vary.[300,497,513,515] A recent study proposed using a biokinetic model that includes similar uptake and elimination kinetics to model the accumulation of Ag ENMs and dissolved silver in earthworms using parameters that were selected or deduced indirectly from the literature as a way of identifying key processes and parameters.[357]

Biomagnification is a process where the pollutant concentration in an organism of a higher trophic level exceeds that in an organism in lower levels within a food chain. Trophic transfer up the food chain has also been investigated in limited studies for ENMs.[50,184,487–490,492,519] Current evidence suggests that ENM accumulation does occur and that uptake from primary producers up through the trophic levels is also probable.[520] Dietary exposure can be a significant mode of transfer between primary producers and consumers.[50] For example, ZnO was found to assimilate efficiently into *L. stagnalis* as a result of dietary exposure. TiO_2 was found to transfer but not to biomagnify.[490] Gold and silver were found both to transfer up the food chain and to biomagnify.[50,184,519] In the terrestrial food chain, gold was found to transfer, but tissue concentration decreased with each trophic-step.[488] Cerium oxide was found to accumulate in the terrestrial food chain though it was not clear whether it was the nano-scale CeO_2 particles that accumulated with increase in trophic steps.[489] Cerium

oxide was not found to accumulate or magnify significantly in a simple aquatic food chain involving filter feeders.[492] Carboxylated and biotinylated quantum dots were found to transfer to higher trophic levels though no significant bioconcentration or biomagnification was observed.[493] CdSe quantum dots on the other hand were found to biomagnify in a simple aquatic system.[487] One study explored the uptake of nano-Ag and dissolved silver on the estuarine snail *P. ulvae.*[497] Uptake rates demonstrated that dissolved Ag is twice as bioavailable as Ag in nanoparticle form.[497] Prediction accuracy, when compared with lab experiments, indicates that this approach to modeling is effective for predicting the fate of metal and metal oxide nanoparticles in organisms. Beyond this, limited studies have investigated the addition of bioaccumulation resulting from food chain dynamics.

This present study explores the accumulation of three metallic ENMs (CuO, TiO$_2$, and ZnO) in organisms through a simple freshwater food chain. The degree to which accumulation and possible magnification occurs is investigated. Accumulation inside an organism depends on: (i) the external concentration of the ENM; (ii) absorption into the body through water, particulate matter, and sediment; (iii) dietary ingestion; (iv) metabolic transformation of the nanoparticle to the dissolved metal; and (v) excretion. The actual accumulation is the net result of these processes over time[357,509] and is dependent on ENM characteristics,[521–523] species-specific traits,[524,525] and species-species interactions[526]. In this study, we gathered an up-to-date understanding of the environmental and biological fate of ENMs (as well as observed or predicted concentrations and process rates) and constructed a bioaccumulation model that we applied to a freshwater ecosystem. A sensitivity and uncertainty analysis was then used to identify priority areas for further research and refinement within the model.

4.2 Methodology

The toxicokinetic model was developed to understand the rate of uptake and accumulation of ENMs in organisms in freshwater, based on a set of toxicokinetic calculations with differential equations to solve the internal body ENM and dissolved ion concentrations for each species over time. The model treats both the environments and the organisms as individual compartments into which ENMs and dissolved/complexed ions accumulate. Given data limitations, we treat organisms as single compartments through which uptake and removal via excretion occur.[515] The model assumes a constant population and quantity of biomass within the system and that all biological parameters remain constant in spite of exposure, because the ecosystem is assumed to be stable, even with exposure. For this specific study, ENM concentration in the environment is held constant and uses predicted environmental concentrations from a fate and transport model.[527] The model assumes that the ENMs are homogenously distributed both within the environments and the organisms, with constant exposure taken from the average long-term freshwater environment concentrations.
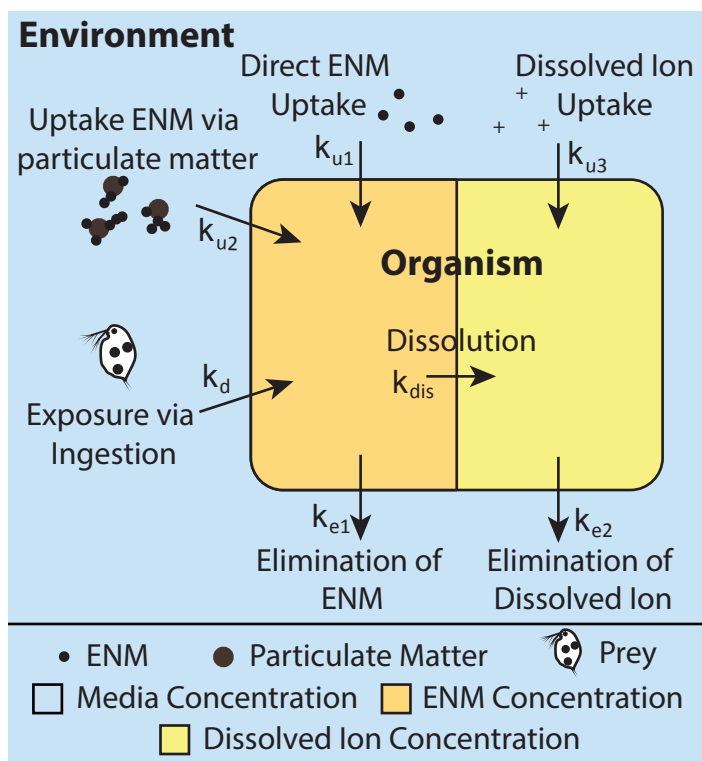
Figure 4.1 Conceptual Diagram of Organism Level Accumulation for a Generic Organism

The model is based on the assumption that the exchange of ENMs and ions between an organism and the environment can be described using a single identical equation for each organism. Uptake, elimination, and dissolution of the ENM are the only processes modeled, due to a limited understanding of the internal transformations and interactions between ENMs and biological processes (Figure 4.1). Each species is connected in a food chain where each trophic level feeds the subsequent trophic level in the food chain, where the nth level of the food chain (n=2, 3, 4, etc.) represents that specific trophic level organism and species (Equation 1). The model assumes that rate constants do not change over time and that transfers are all first order processes; thus the body burden at given trophic level ($C_{b,n}$) is

$$\frac{dC_{b,n}}{dt} = k_{u,n}C_w + \alpha_n k_{d,n}C_{b,n-1} - k_{e,n}C_{b,n} - k_{dis}C_{b,n} - D_n C_{b,n}$$

<div align="right">Eq. 1</div>

where $k_{u,n}$ is the uptake rate from the surrounding media (e.g. water) for the nth level species in the food chain, C_w is the concentration in media (in this case, water), α_n is the assimilation efficiency of the ENM from the diet (ratio of chemical absorbed over chemical ingested), $k_{d,n}$ is the dietary uptake from ingestion of food for the nth level species in the food chain, $C_{d,n-1}$ is the internal body concentration of prey (lower trophic level, n-1), $k_{e,n}$ is the elimination rate of ENMs from the nth level species in the food chain, $C_{b,n}$ is the body concentration of the nth level species in the food chain, k_{dis} is the dissolution rate of the ENM (assumed to be comparable to the dissolution rate of the ENM in the media that the organisms inhabits) (Detailed dissolution rates are provided in Appendix Table A4.1).[527] D_n is the daily mortality rate of the organism, calculated as

$$D_n = \frac{1}{L_n}$$

<div align="right">Eq. 2</div>

Where L_n is the average lifespan (in days) of an individual organism. This is included because the model is run for a longer time period than the average lifespan of any individual organism and we assume that the population remains constant over time, thus the effect of birth and death limits the total accumulation in the whole population and thus the trophic transfer.

For species with multiple routes of non-dietary exposure, such as filter feeders, uptake and exposure can occur from sources other than the water column that may vary in rate based on the exposure route. For example, for filter feeders, the exposure routes include water, suspended particulates and dietary ingestion of phytoplankton.[528] In this case, the first pair of variables in Equation 1 are expanded to include multiple $k_{u,n}$ and C_w pairs that change depending on the uptake exposure route and the concentration of the ENM in media (See

Appendix for species specific equations). This is important to include in the model because ENMs are prone to heteroaggregation with suspended particulate matter resulting in potentially higher exposures than if one were to include only direct water column exposure because heteroaggregation does not preclude bioavailability.[506]

In addition, because we include loss of the ENM through dissolution, we also modeled the body concentration of the dissolved metal ion over time resulting from uptake of the dissolved metal ion, internal dissolution of the ENM to the dissolved ion (we assume this occurs at the same rate as dissolution in the corresponding environmental media because internal species-specific dissolution rates are not available), and subsequent elimination of the dissolved ion (Figure 4.1, Equation 3).

$$\frac{dC_{dis,n}}{dt} = k_{u3,n}C_{w,dis} + k_{dis}C_{b,n} - k_{e_{dis},n}C_{dis,n} - D_nC_{dis,n} \qquad \text{Eq. 3}$$

where $k_{u3,n}$ is the uptake of the dissolved metal ion from the water for the nth level of the food chain, $C_{w,dis}$ is the dissolved ion concentration in the water, $k_{e_{dis},n}$ is the elimination rate of the dissolved ion from the nth level species in the food chain, and $C_{dis,n}$ is the concentration of the dissolved metal ion in the body.

Growth dilution was excluded because we assume that the while individuals are born, grow, and expire, we assume the total biomass in the waterbody does not change and therefore total accumulation does not change. In addition, no transfer between individuals as a result of reproduction is assumed since we do not model growth and aging.

A list of environmental parameters is provided in Table 4.1. As a case study, environmental concentrations for freshwater, freshwater suspended sediment, and freshwater sediment bed, and the dissolved metal ion in freshwater were calculated from the average long term estimates of environmental accumulation in the Greater San Francisco Bay Area

Region against the high-end release and production estimate.[4,8] In selecting ENMs, we chose both soluble and insoluble types for comparison because, while both the particulate and the dissolved form can accumulate, intracellular dissolution has the potential to cause accumulation at cumulatively higher concentrations.[357,529]

Table 4.1 List of Environmental Parameters

Definition	Parameter	Units	CuO	TiO$_2$	ZnO
ENM concentration in water	C_W	mg/L	$2.92*10^{-7}$	$5.92*10^{-6}$	$2.84*10^{-6}$
ENM concentration in suspended sediment	C_{ss}	mg/kg	$3.72*10^{-2}$	2.07	0.88
ENM concentration in sediment	C_{sed}	mg/kg	$2.32*10^{-4}$	$1.51*10^{-2}$	$6.55*10^{-3}$
Dissolved ion concentration in water	C_{wdis}	mg/L	$1.99*10^{-5}$	0	$2.77*10^{-4}$
Dissolution rate of ENM	k_{dis}	1/day	$3.84*10^{-2}$	0	0.302
Volume of water compartment	V_W	m^3	10,000	10,000	10,000
Volume of suspended sediment compartment	V_{ss}	Mg	100	100	100
Volume of sediment compartment	V_{sed}	Mg	500	500	500

To simulate the potential for biomagnification, several organisms were modeled to understand exposure pathways and accumulation rates across trophic levels. The same equation was applied to all organisms where the exposure media and environmental concentrations were specific to the biology of the organism (See Appendix). To describe possible ENM transfers through food chains, significant trophic levels were represented by one to two species. Two phytoplankton species were included at the primary producer level: a zooplankton and a benthic invertebrate represent the herbivore level, while a bivalve and a planktivorous fish represent the primary consumers; and an upper trophic level fish represents the secondary consumer in the simulated freshwater ecosystem (Figure 4.2). When actual diet compositions (from measurements or literature surveys) are translated into model input parameters, prey are represented by the organism used to represent the same

trophic guild as the general prey.[495] Thus the representative zooplankton species consumes the representative phytoplankton species as its complete diet.
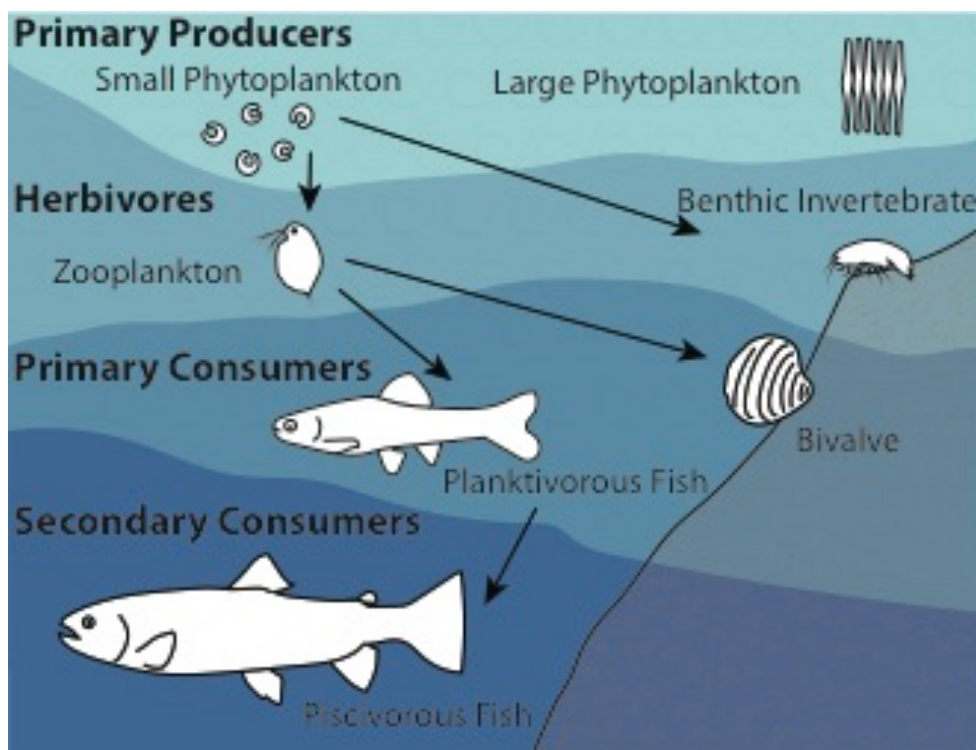
Figure 4.2 Conceptual Diagram of Food Web in Freshwater System

Food web includes two types of phytoplankton in the primary producer trophic level: a smaller consumable species (*S. capricornutum*) and a larger less edible species (*Fragilaria crotonensis*). The herbivorous trophic level includes a zooplankton (*D. magna*) and the benthic invertebrate (*Hyalella azteca*). The primary consumer level includes a planktivorous fish (*Pimephales promelas*) and a bivalve (*V. constricta*). Finally, the secondary consumer level is represented by a piscivorous fish (*Oncorhynchus mykiss*).

Species-specific rates of uptake and elimination were identified from the literature in a tiered approach. Table 4.2 shows data for the first four species in a food chain for CuO; additional data are provided in Appendix Information Table A4.2. First, if ENM-specific rates were available for the specific ENM and species, these were preferred as they were

considered more accurate. [497,513,515] When such data were not available, then ENM-specific

rates, either from similar ENMs or from similar organisms using the same ENM, were

selected (Data selection process tiers are specified in Appendix). If these were also

unavailable, then species-specific metal (not ENM or particle) rates were implemented. The

same selection process applied to uptake and elimination rates for the dissolved metal. For

example, dietary assimilation rates for ENMs and metals are quite rare, so the best available

data was the assimilation efficiency of food, with the implicit assumption that assimilation

of food and the metal present in the food occur at the same rate.[530] The implicit assumptions

in this data selection process are that: (i) rates are similar across metallic ENMs and metals

and (ii) species with similar life history traits also have similar uptake and elimination rates.

Table 4.2 Species Specific Parameters across ENMs for CuO for First Four Species in

Food Chain

Definition	Parameter	Units	*S. capricornutum*	*F. crotonensis*	*D. magna*	*H. azteca*
Wet body mass of individual organism	M_i	mg	$3.58*10^{-8,}$	$6.8*10^{-7}$	3	8
Uptake from water	$k_{u1,n}$	L/mg-day	$2.4*10^{-2, *}$	$2.4*10^{-1,*}$	$1.6*10^{-2}$	$5.79*10^{-4}$
Uptake of solids	$k_{u2,n}$	L/mg-day	NA	NA	$1.6*10^{-1}$	$4.8*10^{-5}$
Uptake of dissolved ion from water	$k_{u3,n}$	L/mg-day	$1.41*10^{\wedge -7}$	$1.41*10^{-7}$	$1.6*10^{-2}$	8.66
Ingestion rate	$k_{d,n}$	g/mg-day	NA	NA	$1.6*10^{-8}$	$4.8*10^{-5}$
Wet body concentration of ENM in prey	$C_{b,n-1}$	g/mg	Internal model prediction	Internal model prediction	Internal model prediction	Internal model prediction
Assimilation Efficiency	α_n	--	NA	NA	0.2	0.5
Fecal elimination rate	$k_{e,n}$	g/mg-day	$1.73*10^{-4}$	$3*10^{-3}$	0.29	$6.38*10^{-5}$

Fecal elimination rate of dissolved ion	$k_{edis,n}$	g/mg-day	0	0	0.29	$2.52*10^{-3}$
Lifespan	L_n	days	2	3	60	365
Biomass density	B_n	mg/m^3	1	1	12.39	52.17

Note: references provided in Appendix Table A4.2.

* Adsorption rate of CuO to particulate matter.

For some species, such as phytoplankton, adsorption to the surface of the phytoplankton may be a more significant process than actual internal accumulation.[357,531] Thus, in the model, even though it is treated the same as uptake via respiration in fish, it is really an adsorption process where uptake is the association of the nanoparticles relative to the volume of the phytoplankton,[513] which sorbs at a rate determined by the characteristics of the surrounding environment and the ENM. In this case, the rate is represented as the heteroaggregation rate constant for the ENM in freshwater based on lab studies of heteroaggregation with natural organic matter in freshwater, accounting for the relative concentration of ENMs and the phytoplankton in the sample freshwater system.[36,369,440,532]

Bioaccumulation for each ENM was determined by comparing the BCFs for primary producers, BAFs for consumers, and BSAFs for benthic organisms. Each factor was calculated as the average wet-weight body concentration over the concentration in the primary exposure media.[495] Biomagnification was estimated for consumer species as the average wet-weight body concentration of the organism over the average wet-weight body concentration in the prey organism.

Model performance was evaluated through comparison with empirical data on organism and food chain accumulation results where this was available.[50,221,252,300,455,485,486,489,490,492,497–505,513,515] A Monte Carlo-based sensitivity analysis

based on the Kolmogorov-Smirnov distances between cumulative distribution functions was applied to evaluate the importance of the input parameters that significantly impact accumulation results and the variance of the output.[533,534] This method was selected because it provides transformation invariant global sensitivity measures.[533,534] This was conducted by varying all parameters (environmental and biological, except the dimensions of the environmental media) by ±50% with a uniform distribution over 10,000 simulations because we assume relatively high uncertainty is implicit in the collected parameters. The resulting Monte Carlo gives us both a ranking of parameter significance on results and a range in the distribution of probable accumulation concentrations for both the ENM and the dissolved metal ion for each species.

4.3 Results

A comparison of accumulation over time in the sample freshwater ecosystem for the three ENMs and their dissolved component shows that the accumulation patterns vary across both ENMs and species (Figure 4.3). Also, steady-state concentrations are reached at different points for the three ENMs and the dissolved fractions. For example for both n-CuO and dissolved Cu, steady-state is reached within the first year except for fish and the bivalve (Figure 4.3A and 4.3B) while for Zn most species reach steady-state for n-ZnO (Figure 4.3D) but only phytoplankton have reached steady-state with dissolved Zn (Figure 4.3E). n-TiO$_2$ (Figure 4.3C) appears to follow a similar pattern to n-CuO regarding accumulation rates, although unlike the other two ENMs, there is no dissolution of TiO$_2$. The phytoplankton and daphnia are depicted in various green tones, the benthic copepod and bivalve are depicted in brown tones, and the fish are depicted in blue tones.
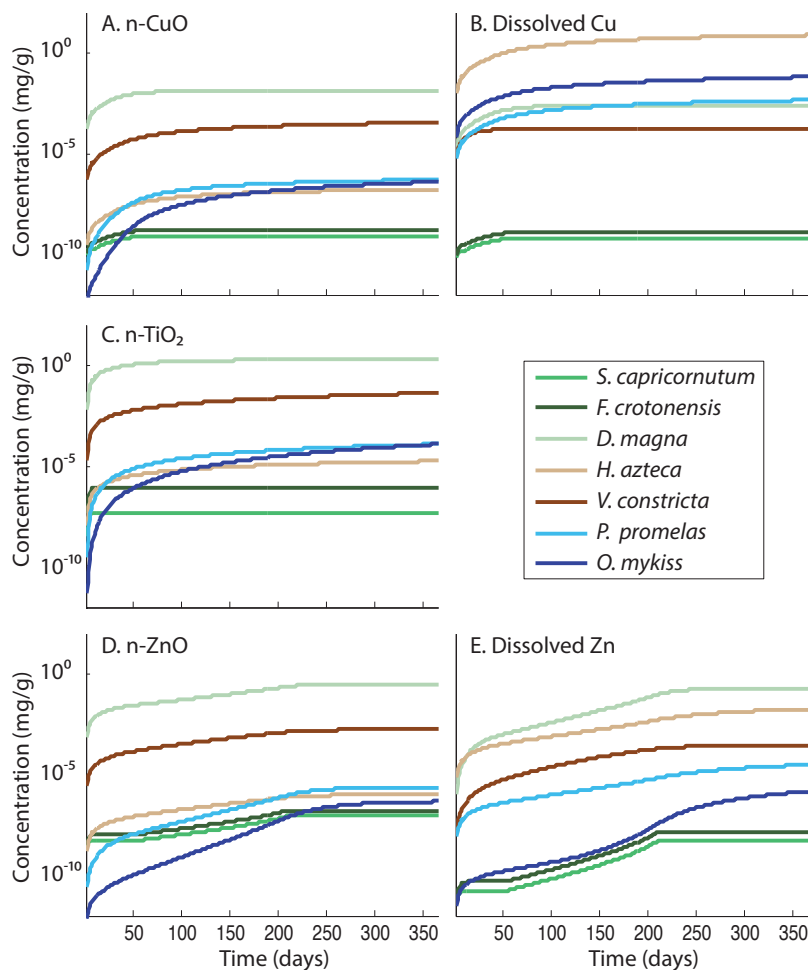
Figure 4.3 Predicted Freshwater Accumulation of (A) n-CuO, (B) Dissolved Cu, (C) n-TiO2, (D) n-ZnO, and (E) Dissolved Zn in a Simple Food Chain over the First Year of Exposure

Comparing the long-term accumulation concentrations shows that for phytoplankton (*S. capricornutum and F. crotonensis*), daphnia (*D. magna*), and the bivalve (*V. constricta*) ENM accumulation may be more significant than accumulation of the dissolved ion (Figure 4.4). For benthic copepods (*H. azteca*) and fish (*P. promelas and O. mykiss*) the opposite is true, where the dissolved ion accumulation is higher than the ENM accumulation. Total accumulation in phytoplankton, daphnia, and the bivalve are highest for TiO$_2$, then ZnO, and lowest for CuO, reflecting the predicted concentrations of these ENMs in the San Francisco

203

Bay.[527] Conversely, for the benthic copepod, accumulation is highest for dissolved Cu and dissolved ZnO over the ENMs. The fish species show the most unusual patterns with highest accumulation of dissolved Cu, followed by n-TiO$_2$, then dissolved Zn, and the lowest accumulation for n-ZnO and n-CuO.
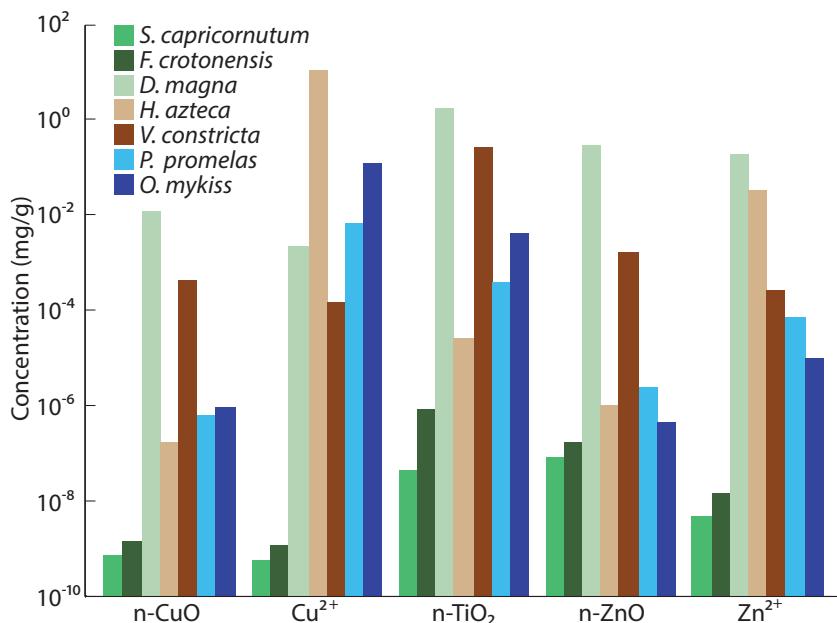
Figure 4.4 Comparison of Steady-State Concentration for ENMs and Dissolved Ions across Food Chain Species

BCFs for phytoplankton, BAFs for daphnia and fish, and BSAF for benthic organisms were calculated for each ENM relative to the exposure concentrations from either the water column or the sediment (Figure 4.5A). Results indicate that the highest bioaccumulation factors occur for daphnia and fish with the highest factors occurring for TiO$_2$. Biomagnification factors were also calculated for all consumer species and results indicate that biomagnification does not increase consistently up the trophic chain (Figure 4.5B).
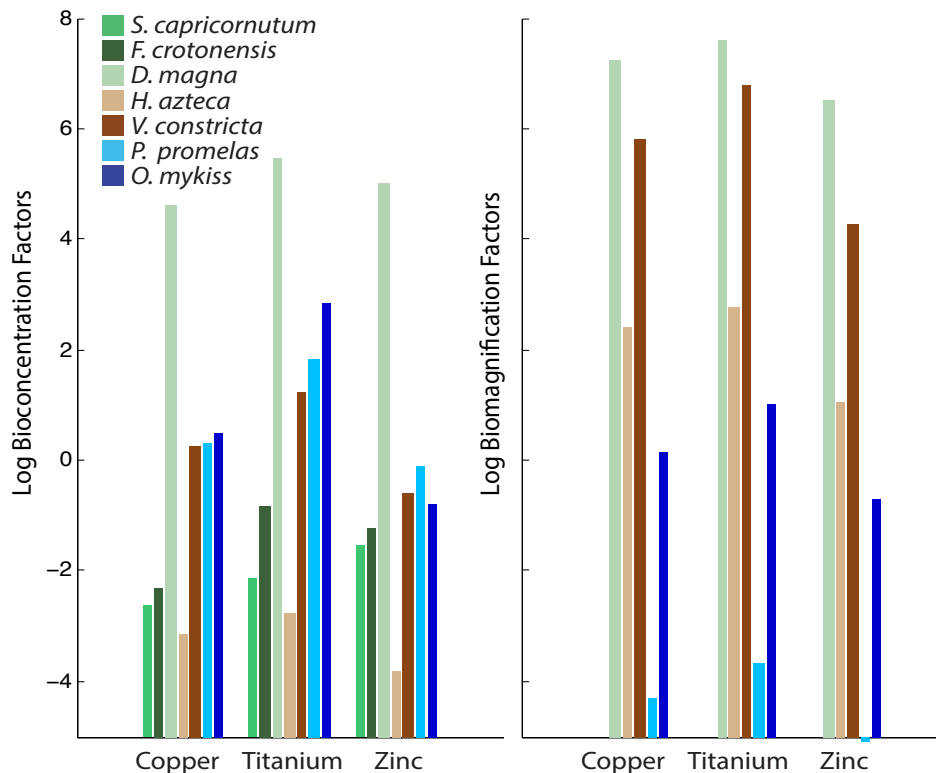
Figure 4.5 Bioaccumulation of ENMs and Dissolved Ions: (A) BCF, BAF, and BSAF for all ENMs and Species (units are L g^{-1} or kg g^{-1}); and (B) Biomagnification for all ENMs and Consumer Species Relative to the Concentration of the ENM in the Prey Species

The distribution of results provided by the Monte Carlo simulations provides a range in bioaccumulation concentrations when all input parameters are varied by ±50% for each species and each ENM (Figure 4.6). The range in predicted concentrations typically is one to two orders of magnitude with the most variable results for *O. mykiss* across all ENMs and dissolved Zn, *P. promelas* for all ENMs but not the dissolved fraction of Cu^{2+} or Zn^{2+}. The benthic species and *D. magna*, on the other hand tended to have a fairly narrow range in predicted concentrations. In general, the range resulting from varying parameters by 50% was narrower for CuO and TiO$_2$ and notably wider for ZnO.
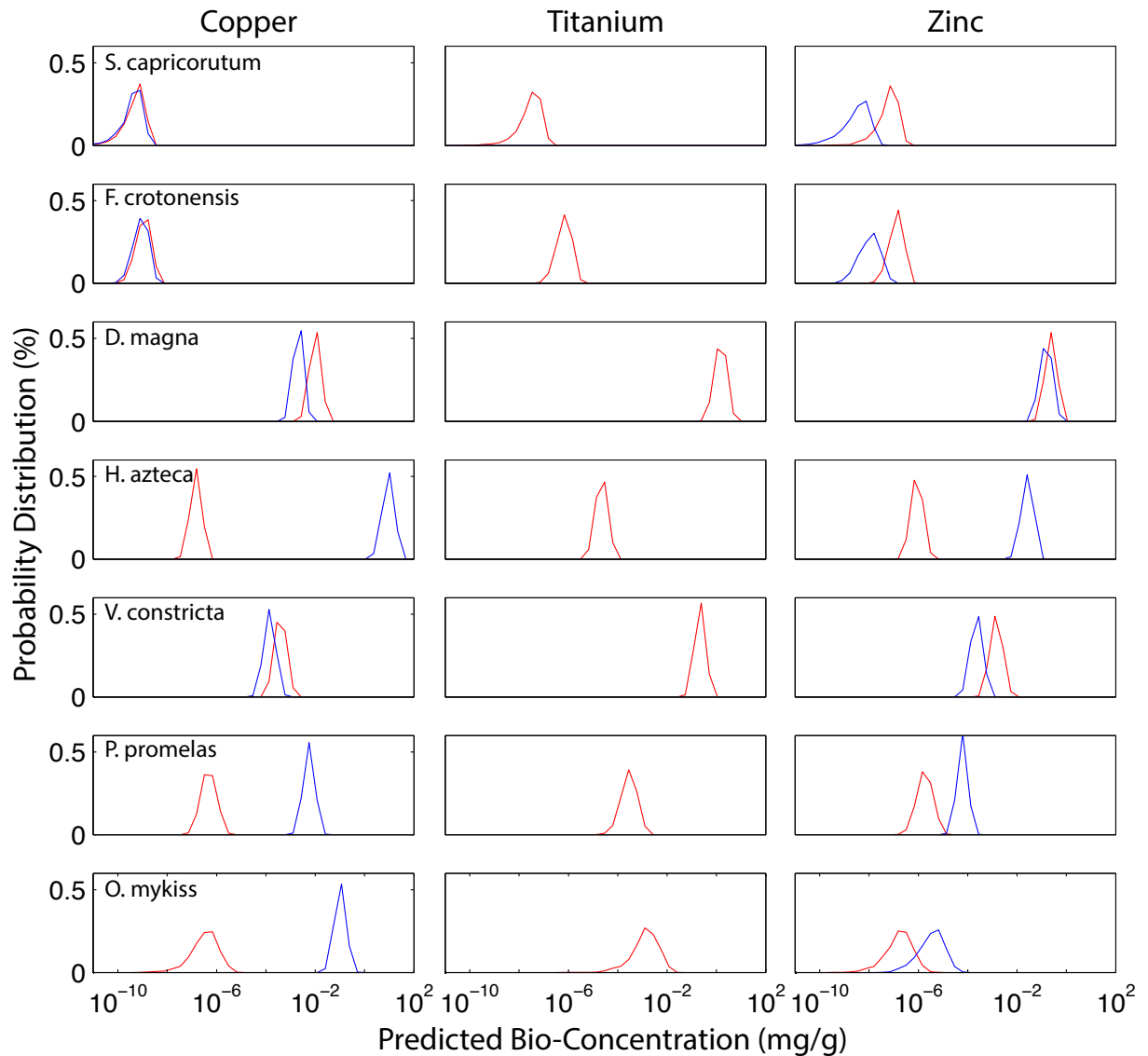
Figure 4.6 Probability Distribution of Predicted Organism ENM (red) and Dissolved Ion (blue) Concentrations

Each row is for a single species. The x-axis of each graph shows the predicted body-burden (mg/g) and the y-axis shows the frequency predicted over 10,000 Monte Carlo simulations.

Sensitivity rankings were calculated from the Monte Carlo simulation using the Kolmogorov-Smirnov test and used to identify key parameters. The parameters that most

206

impact bioaccumulation vary across ENMs and species, although there are some clear trends (Figure 4.7). Key parameters for ENM accumulation in ranked order include lifespan (L), uptake from water ($k_{u2,w}$), assimilation efficiency (α), uptake from suspended sediment/sediment ($k_{u2,s}$), dissolution rate (k_{dis}), and elimination rate (k_e). Assimilation efficiency increases in significance as trophic level increases. Conversely, lifespan decreases with importance as trophic level increases. The ENM dissolution rate, dissolved ion elimination rate, and uptake from suspended sediment and sediment are most significant for benthic species and filter feeders. Uptake of dissolved ion was a significant parameter for all species exposed to Cu^{2+} (Figure 4.7B), but surprisingly only significant to the benthic and filter feeders exposed to Zn^{2+} (Figure 4.7E). The environmental concentrations of both ENMs and dissolved ions are all important depending on the primary routes of uptake for each species. It is worth noting that because the prey concentration was a dependent variable and thus not included in this analysis, the fact that *S. capricornutum* is the base of the food chain indicates that there is some increasing impact up the food chain from the starting environmental exposure concentrations, however this analysis cannot differentiate between those impacts.
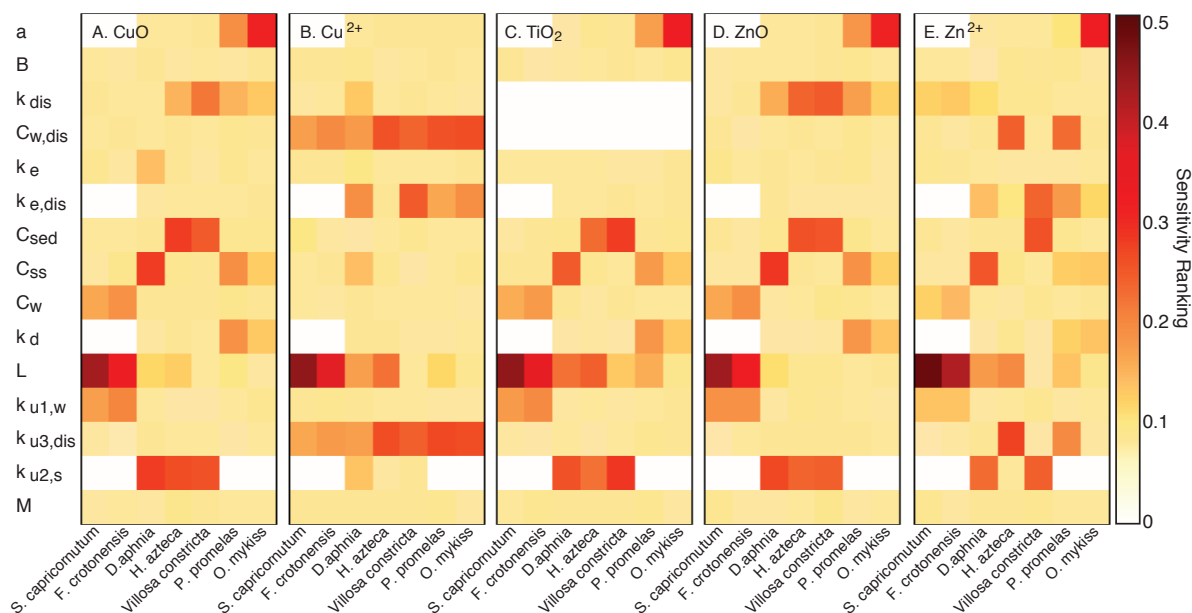
Figure 4.7 Sensitivity Ranking of Parameters for Bioaccumulation of (A) n-CuO, (B) Dissolved Cu, (C) n-TiO2, (D) n-ZnO, and (E) Dissolved Zn

Species are on the x-axis from phytoplankton on the left to fish on the right in each plot and the varied biological and environmental parameters are on the y-axis. A higher sensitivity ranking indicates ENM bioaccumulation in a given organism is more sensitive to a particular parameter. A value of zero means that the parameter does not apply to that ENM or organism.

4.4 Discussion

The toxicokinetics model suggests that bioaccumulation does occur for ENMs and their dissolution products in most organisms to varying rates and some limited biomagnification also occurs for ENMs, although it doesn't seem to increase consistently up the food chain. Biomagnification factors are also highest for $nTiO_2$ and lowest for nZnO across all species, which relates in part to the extent of dissolution considered for each ENM.

Model results suggest that filter feeders, specifically the daphnia and the bivalve, and higher trophic level fish will accumulate ENMs in the greatest quantities, probably due to the higher rates of exposure and accumulation from both the environment and their diet relative to transformation and elimination rates. Interestingly, the benthic copepod accumulates the most dissolved Cu^{2+} and Zn^{2+} according to model predictions, which is an effect of the high observed uptake rates in *H. azteca* for both ions[535] compared to that observed for other species.[536–542] It is hard to predict what the potential impacts of these estimated accumulations may be because transformations that we do not account for may be quite significant, and the model does not predict where in each organism the ENMs and dissolved metal ions are accumulating, which can alter the observed toxic impact.[543]

Establishing the relationship between exposure and toxic effect(s) requires an understanding of the internal, and sometimes site specific, concentration in the organism. Environmental concentration is often used as a surrogate for the site-specific concentration. Such values can vary substantially, but can and do affect policy and thus accuracy is key. What we have provided is a range in possible internal concentrations that can be connected with specific observed toxic effects beyond simply exposure and mortality.

The different organisms took varying lengths of time to reach steady-state accumulation concentrations within the model. Generally, the larger and longer lived the species, the longer it takes to reach steady-state body burdens. For smaller organisms, steady-state concentrations were predicted within one year, but did vary substantially between ENMs. For example, for phytoplankton steady-state was reached after 1-2 months for nCuO and $nTiO_2$, whereas it took over 7 months to reach steady-state for nZnO. Conversely, all the consumer species reached their steady-state concentrations for nZnO within 2 years, but

took 5 to 10 years to reach steady-state concentration for nCuO and nTiO$_2$ (the exception being *D. magna* where steady-state was reached in 9 and 19 months respectively). What these model results indicate is that, at the ecosystem level, short term lab experiments may not effectively reflect the maximum bioaccumulation possible; though it should be kept in mind that we used predicted environmental exposure concentrations that are much lower than actual lab exposure concentrations.[313,455,506,544,545] Food chain and mesocosm studies that are longer term and may be conducted at lower exposure concentrations, will be key to improving the predictive power of this model.

While limited studies exist, few have measured the internal, mostly short term, accumulation of various ENMs for species included in this study. We are limited in our comparison because most studies are short-term at highest exposure concentrations. Thus, either our predictions are comparable in spite of the time difference, or our predictions are lower because the studies used higher exposure concentrations than our NanoFate predicted exposure concentrations, or our predictions are higher because we modeled exposure over the long-term, allowing for more accumulation. The difficulty with comparing our results to those from studies on CuO and ZnO is that most studies measure the total accumulated metal, regardless of how much is dissolved or particulate, so we compare our results of ENM and dissolved metal accumulation to total metal accumulation.

A study of a freshwater clam, *Macoma balthica,* found accumulation of 0.464 ug g^{-1} in soft tissue over 35 days after exposure to 147.7 ug Cu g^{-1} sediment. In comparison, the modeled freshwater bivalve *(V. constricta),* over 3000+ days of exposure to 2.3*10^{-4} mg Cu kg^{-1} sediment resulted in accumulation of 0.43 ug g^{-1}.[546] These, of course, result in differing BSAF values (3.14*10^{-3} and 1.87, respectively), yet the long-term bioconcentration is

surprisingly similar.[546] A benthic snail (*Potamopyrgus antipodarum*) accumulated around 60 ug Cu g^{-1} dry weight over 2 weeks exposure at 240 ug Cu g^{-1} sediment, for a nominal BSAF of approximately 0.25, which is closer to our predicted steady-state BSAF of 1.87 for the bivalve (*V. constricta*) but considerably higher than $7.4*10^{-4}$ for the benthic copepod (*H. azteca*).[547] CuO uptake in another benthic freshwater snail, *Lytechinus variegatus,* resulted in an accumulation of around 3 ug g^{-1}, with a BSAF of 0.094.[548] It is also worth noting from this study that bioaccumulation of Cu ions was found to be substantially higher than that of bioaccumulation of n-CuO in lab studies, which we also found for some of our freshwater species.[548]

Our model predicted an accumulation of 1.78 mg g^{-1} TiO_2 for *D. magna*; an experimental study exposed *D. magna* to 0.1 mg L^{-1} TiO_2 over 14 days and found accumulation of 4.52 mg g^{-1} dry weight .[490] A study on TiO_2 accumulation of *D. magna* found a BCF of 56,600 at 0.1 mg L^{-1} exposure over 24 hours; while our predictions are higher (BCF of 301,000), resulting largely from much longer exposure periods, which are roughly of the same order of magnitude.[252] Studies on TiO_2 accumulation in *Cyprinus carpio* found a BCF ranging from 325 to 617 over 20 days and 495 over 25 days at 10 mg L^{-1} exposure, whereas for the similar trophic level species in our study (*O. mykiss*), the predicted BCF was 687 over 3650 days.[549–551]

Multiple studies have been conducted on TiO_2 accumulation in *O. mykiss* via both ambient and dietary exposure that found very low bioconcentration and biomagnification rates.[552–554] For example, a 14-day ambient exposure test found that 0.44 umol Ti g-1 after exposure to 0.1 mg TiO2 L-1 (BCF ~0.2).[552] One study on dietary exposure found nominal accumulation in the gut and across epithelial membrane over 21 days with a BMF of

approximately 0.005; the study observed that this was likely due to high aggregation rates in the presence of fish and absence of NOM, define which would act as a stabilizing agent.[554] Another study on dietary exposure over 8 weeks found that accumulation occurred in multiple organs and did not return to control concentrations during 2 week recovery period (BMF ~ 0.024).[553] While these studies found much lower BMF values, indicating some over prediction in our model, the lack of excretion during the recovery period indicates potential for further bioaccumulation under a prolonged exposure period.

In a study on trophic transfer and biomagnification, trophic transfer from *D. magna* to *Danio rerio* was observed for TiO_2, with a BCF of 25, though no biomagnification occurred (BMF of <0.024), which agrees with our model predictions of a BCF of 66 for *P. promelas* and a much smaller BMF ($2.22*10^{-4}$), indicating that magnification does not increase up the trophic chain.[490]

Very few studies have measured accumulation of ZnO in freshwater species, and those that have tried tend to find that no significant uptake occurs.[554] This is likely because exposure concentrations tend to be around $0.5 - 5$ mg ZnO L^{-1}, which will result in substantial aggregation and sedimentation. At more stable long term exposure concentrations, it seems likely that the uptake of both dietary transfer and accumulation do occur with 86% retention for *L. stagnalis*; and though not stated, this seems to imply that biomagnification was not observed.[506] Our study predicts accumulation of 1.65 ug g^{-1} in the bivalve *V. constricta* which is similar to another study that found that at an exposure of 0.1 mg L^{-1} ZnO for the bivalve *M. galloprovincialis* accumulation ranged from 100-200 ug g^{-1} (dry weight), especially given that one is a freshwater species and the other is a marine species, which corresponds to differing BAF values 581 and 1-2 respectively. [543] Worth

noting is that our predicted BSAF for *V. constricta* was 0.25 kg g^{-1} and our BAF is probably substantially higher than the other study probably because while the other study appears to have only exposed *M. galloprovincialis* to ENMs in water, we have >2x the exposure since the exposure is via water and sediment.

Modeling is still very limited by the availability of accurate parameters. Although ENM specific rates were available for some species, they were largely of marine species, such as *M. galloprovincialis* uptake of ZnO.[515,543] In some instances, we were able to identify uptake rates that are specific to the metals (such as ionic copper uptake from freshwater for *H. azteca*[535] and *V. constricta*[539]), which we used in preference to generic uptake rates. In the situations where specific uptake rates were substituted with either similar chemical uptake rates (e.g. mercury rather than copper) or when we had to assume 100% assimilation efficiency given known respiration rates, the accuracy of the model is clearly limited. The rates used in the model may also vary substantially depending on the ENM aggregation state, which also relates to variations in the environment. For example, if the pH of the freshwater system were to increase, agglomeration of many ENM would also likely increase[62,69,162,555] and this might decrease the uptake rates from water or the assimilation of the ENM into the organism during respiration, which would decrease the accumulation in water column species. It is also possible that there is a maximum accumulation beyond which the ENM simply passes through the organism (as with *M. galloprovincialis* [102,543]). This is again very system and organism specific and thus rather complicated to model without additional data and understanding.

We assumed that adsorption (heteroaggregation) to the phytoplankton would be the same as the rate of heteroaggregation with suspended particulate matter for each system. There is

evidence that this is reasonable, though there likely would be some variability based on the size and characteristics of the individual phytoplankton.[531]

In addition, we also assumed that the environmental dissolution rate of ENMs would be comparable to the internal organism dissolution rate of ENMs as there is no available research on the rate of specific ENM transformations, including dissolution. This is an important variable to differentiate because ENMs that don't dissolve internally may be more likely to cause nano-specific toxicity whereas ENMs that dissolve may cause heavy metal toxicity purely as a result of the form accumulation takes and the ratio between ENM and dissolved ion accumulation. In addition, understanding speciation of the ENM is important because while we generally assume excretion occurs for both the ENM and the dissolved ion, for most species in the model, we do not actually know what is being eliminated (nano v. ion) and how the rates actually vary from form to form, which could substantially impact the steady-state accumulation of the ENM and the dissolved ion. Only one study on *M. galloprovincialis* showed that excreted pseudofeces contained substantial quantities of CeO_2 nanoparticles but not ZnO nanoparticles, which was mostly excreted as dissolved Zn.[102]

It is generally difficult to predict if a nanoparticle passes through the lung/gill or gut wall into the body or simply remains attached to either the surface (e.g. phytoplankton) or the gut lining (*D. magna*[556]) but for the purposes of the model all routes contribute to accumulation, even though the various fates can greatly alter toxicity and not all would contribute to internal bioaccumulation.

We should stress the conditional nature of the rate constants, because the environment, the biology, and the toxicity itself can all alter such constants over time. One key variable is the transformation of the ENM, both in the environment and inside the individual through

214

biotransformation. These transformations can alter the uptake and elimination rates and our level of understanding of these processes is still quite limited for ENMs. Because it is only a bioaccumulation model, this research does not predict what the toxic impacts will be as a result of ENM accumulation. This is largely because those impacts will vary substantially from ENM to ENM across sites, media, and species. In addition, because it treats the organism as a single compartment (excluding plants) it does not account for variable impacts or transfer rates within an organism.

Quantification of rate constants for uptake of ENMs, excretion rates, and transfer through simple food chains should be a primary focus. It would be ideal if toxicity studies could also begin to measure body burden and the forms that the ENM take after entering the organism rather than just measuring external exposure and toxic effect. This would greatly improve the ability to model bioaccumulation dynamics. Additionally, there is a need to differentiate between uptake and accumulation of ionic and particulate ENMs as the toxic impacts may vary. One option, proposed by Baalousha et al. (2016) and used by Ramskov et al. (2015) is the use of isotopically labeled ENMs to track uptake, accumulation and form.[357,548]

Modeling feedback of changes to biological rates as a result of exposure to ENMs (e.g. ingestion and respiration may decrease as a result of increasing exposure and accumulation) is currently a major gap in our understanding of bioaccumulation and potential biomagnification of ENMs. This limitation could be addressed if researchers incorporated this into accumulation and toxicity assessments, as they have begun to with *M. galloprovincialis* and *O. mykiss*.[102,492,543] One study, for example, looked at the possible feedback effects on growth and food consumption resulting from exposure to TiO_2.[553] In

addition to this feedback, it would be useful to incorporate mortality as a result of accumulation, but no studies currently are available that measured this relative to accumulation. Instead studies only measure the external exposure concentration.

We found that uptake, assimilation, dissolution, and elimination are all relatively important parameters for predicting bioaccumulation. Assimilation efficiency will prove to be important specifically for predicting biomagnification, whereas uptake from the various environmental media depends largely on the primary routes of exposure for each species.[534,557] The results of the sensitivity analysis can be used to guide future research, specifically on primary modes of uptake and how rates vary with time. In addition, the assimilation efficiency and elimination will have a substantial impact on the actual accumulation of nanoparticles within organisms. For example, some organs will retain more of the accumulated ENM than others, which would have impacts on the total accumulation and the associated toxic impacts.[552,553] While we identified which parameters are most sensitive, vis-à-vis their impact on accumulation, this does not tell us which may be more sensitive to accumulation feedbacks or environmental changes. For example, uptake can vary greatly by temperature and prey density.[558] Though the estimates of bioaccumulation are very preliminary and our uncertainty analysis indicates a wide range in possible bioaccumulation, the framework is now available and can help guide future research to better predict these factors. Further work might include investigating accumulation and retention of ENMs in specific organs. Collectively, this research serves as a means to screen the potential for bioaccumulation characteristics of ENMs relative to biological parameters and identifies which parameters are targets for further research and refinement vis-à-vis accumulation mechanisms and rates. Though uncertainty in the predictions is high, this still

allows for improved cost-effectiveness in research by targeting research towards specific

sensitive biological and environmental parameters.

Data selection tiers

Parameter selection for each species and each ENM was conducted in a tiered process where the preference ranking was as follows:

1. parameter measured for specific ENM and specific species
2. parameter measured for specific ENM for similar species
3. parameter measured for any ENM for specific species
4. parameter measured for any ENM for similar species
5. parameter measured for metal ion of ENM for specific species
6. parameter measured for metal ion of ENM for similar species
7. parameter measured for similar metal ion for specific species
8. parameter measured for similar metal ion for similar species
9. parameter measured for any metal ion for specific species
10. parameter measured for any metal ion for similar species

The search process started by looking for the specific parameter for each individual organism for each ENM. If no ENM specific parameters could be identified, the metal ion equivalent was explored. If parameters for the specific metal ion could not be found, then other commonly studied metal ions (e.g. mercury, cadium, etc.) were investigated. This was done separately species by species for each parameter and ENM. When a parameter for the specific species could not be identified, the parameter for a similar species (e.g. *D. pulex* instead of *D. magna*) was substituted. The uncertainty increases moving down the ranking table.

Bioaccumulation Equations by Species

1. *S. capricornutum*

$$\frac{dC_{b,1}}{dt} = k_{u1,1}C_w - k_{e,1}C_{b,1} - k_{dis}C_{b,1} - D_1C_{b,1}$$

$$\frac{dC_{dis,1}}{dt} = k_{u3,1}C_{w,dis} + k_{dis}C_{b,1} - k_{e_{dis},1}C_{dis,1} - D_1C_{b,1}$$

2. *F. crotonensis*

$$\frac{dC_{b,2}}{dt} = k_{u1,2}C_w - k_{e,2}C_{b,2} - k_{dis}C_{b,2} - D_2C_{b,2}$$

$$\frac{dC_{dis,2}}{dt} = k_{u3,2}C_{w,dis} + k_{dis}C_{b,2} - k_{e_{dis},2}C_{dis,2} - D_2C_{b,2}$$

3. *D. magna*

$$\frac{dC_{b,3}}{dt} = k_{u1,3}C_w + k_{u2,3}C_{ss} + \alpha_3 k_{d,3}C_{b,1} - k_{e,3}C_{b,3} - k_{dis}C_{b,3} - D_3C_{b,3}$$

$$\frac{dC_{dis,3}}{dt} = k_{u3,3}C_{w,dis} + k_{dis}C_{b,3} - k_{e_{dis},3}C_{dis,3} - D_3C_{b,3}$$

4. *H. azteca*

$$\frac{dC_{b,4}}{dt} = k_{u1,4}C_w + k_{u2,4}C_{sed} + \alpha_4 k_{d,4}C_{b,1} - k_{e,4}C_{b,4} - k_{dis}C_{b,4} - D_4C_{b,4}$$

$$\frac{dC_{dis,4}}{dt} = k_{u3,4}C_{w,dis} + k_{dis}C_{b,4} - k_{e_{dis},4}C_{dis,4} - D_4C_{b,4}$$

5. *V. constricta*

$$\frac{dC_{b,5}}{dt} = k_{u1,5}C_w + k_{u2,5}C_{sed} + \alpha_5 k_{d,5}C_{b,3} - k_{e,5}C_{b,5} - k_{dis}C_{b,5} - D_5C_{b,5}$$

$$\frac{dC_{dis,5}}{dt} = k_{u3,5}C_{w,dis} + k_{dis}C_{b,5} - k_{e_{dis},n}C_{dis,5} - D_5C_{b,5}$$

6. *P. promelas*

$$\frac{dC_{b,6}}{dt} = k_{u1,6}C_w + \alpha_6 k_{d,6}C_{b,3} - k_{e,6}C_{b,6} - k_{dis}C_{b,6} - D_6C_{b,6}$$

$$\frac{dC_{dis,6}}{dt} = k_{u3,6}C_{w,dis} + k_{dis}C_{b,6} - k_{e_{dis},6}C_{dis,6} - D_6C_{b,6}$$

7. *O. mykiss*

$$\frac{dC_{b,7}}{dt} = k_{u1,7}C_w + \alpha_7 k_{d,7}C_{b,6} - k_{e,7}C_{b,7} - k_{dis}C_{b,7} - D_7C_{b,7}$$

$$\frac{dC_{dis,7}}{dt} = k_{u3,7}C_{w,dis} + k_{dis}C_{b,7} - k_{e_{dis},7}C_{dis,7} - D_7C_{b,7}$$

Supplemental Table References

Table A4.1 Dissolution rates for CuO and ZnO across a range of environments

References: [51,52,55,62,88,95,97,98,100,101,105,146,203,227,256,285,292,302,306,327,335,338,368,391,394,453–457]

Table A4.2 Table of model parameter values for each organism and ENM indicating rates of uptake and elimination, biomass and biomass density, and average lifespan provided with references

CuO: [535,536,538–541,559–589]

TiO$_2$: [535,536,538,539,541,542,559–591]

ZnO: [266,535–539,541,542,559–590,592–594]

Table A4.3 Sensitivity Ranking of all model parameters for each ENM

Conclusions

This doctoral research has improved our understanding on which processes significantly impact fate and bioaccumulation of ENMs in complex environmental systems. The role of heteroaggregation, adsorption, and dissolution in environmental fate and the significance of uptake, metabolic dissolution, and elimination of ENMs from organisms were identified as particularly important for both fate and bioaccumulation.

In Chapter 1, we found while there is still a need to better understand the implications of ENMs, emerging patterns with regards to ENM fate, transport, and exposure combined with emerging information on toxicity suggested that risk would be low for most ENMs. In the atmosphere, high concentrations are not expected because of high removal rates resulting from heteroaggregation and wet and dry deposition. While these processes are all strongly dependent on particle size, removal is expected to be quite rapid and concentrations are expected to be low despite the small size of ENMs. The fate and transport of ENMs in natural waters is dependent on the characteristics of the ENM and the chemical properties of the water, specifically the ionic strength and the presence of NOM. Given that the rate of ENM-specific processes varies significantly between different water types, it is reasonable to assume that fate will vary substantially also. The fate of ENMs in soil is expected to be similar to those of traditional chemicals and colloids. The fate is strongly dependent on both primary particle size and aggregate particle size, as well as soil pore size, soil particle size, and soil characteristics. Under neutral pH, high ionic strength (e.g. high salinity or hardness), low NOM, and low flow conditions, ENMs are unlikely to be transported great distances.

A few processes were identified as key for predicting ENM fate including aggregation, sedimentation, and dissolution; the former two of which will occur in most environmental media whereas dissolution will only occur in systems with water. Aggregation and sedimentation were found to occur at fairly similar rates for most ENMs across the different water-types. Faster aggregation indicates that ENMs will not remain in the water column for long, and thus exposure to true nano-scale particles will be limited, whereas slower aggregation may result in greater likelihood of exposure. Faster sedimentation generally indicates lowered exposure to species living in the water column, but increased and prolonged exposure for benthic species. Slower sedimentation indicates that ENMs will be transported over greater distances, but it may also mean greater dilution over time. In most cases, dissolution is highly dependent on ENM composition and those that dissolve over relevant time scales cause the release of the metal ions and disappearance of the ENM. Those that do dissolve require further consideration because of the potential for both nano-toxicological impacts and heavy metal impacts from the dissolved ion.

In Chapter 2, we found that the toxicity thresholds for different ENMs in freshwater vary by many orders of magnitude for the low-end HC_5 from 100 ng L^{-1} for n-Ag up to 3 mg L^{-1} for CNTs. Exposure models that estimate the exposure of individuals or populations can be compared with the HC_5 values estimated here to predict the ecotoxicological effects of ENMs and give an idea of how significant the risk associated with their use could be. Because the HC_5 values are derived from acute LC_{50} observations, these predicted concentrations highlight the worst case scenario where, should these concentrations be exceeded in the actual environment, devastating ecological impacts would arise. When working with ENMs, the various possible configurations (e.g., size, shape, charge, and

presence of a coating or functional group) must be considered, because these can all alter chemical behavior in the environment and impact toxicity.[226] Thus, it is important to consider ENM characteristics as well as possible environmental transformations that increase the uncertainty in toxic outcomes that underlie the SSDs.

It is also important to recognize the uncertainty associated with our results, as the range of sensitivities of the species we included is quite variable from ENM to ENM, and no SSD was constructed with enough species to represent a comprehensive ecosystem. Despite these limitations, our results are useful in gauging and comparing the ecotoxicological impact of different ENMs. However, as more data become available to separate ENMs into clearly defined physico-chemically distinct groups (e.g. those based on size, shape, or coating) when developing SSDs, and specifically as more chronic data become available, the toxicological threshold predictions resulting from differing physico-chemical characteristics of the ENMs will improve. For example, Coll et al. (2015) was recently able to develop freshwater and soil chronic SSDs for TiO_2 and ZnO based on NOEC levels rather than LC_{50} levels. These can be used to estimate the concentrations in the environment above which toxic effects will begin to be observed.

The objective in Chapter 3 was to develop a model that can evaluate the large-scale regional fate of specific ENMs. Humans and ecosystems are already being exposed to ENMs as these are released into the environment over their lifecycle.[4,8,226] Once released, there is already sufficient understanding to know that transport will occur and that physical transformation such as aggregation, agglomeration, adsorption and surface transformation such as oxidation, dissolution, and sulfidation will all alter when, where, and how exposure occurs.[85,226,345,359] This study begins to predict the implications of releasing ENMs into our

223

environment and determining whether that exposure will result in hazardous concentrations. The fate and transport model estimates the environmental distribution and accumulation of ENMs under a range of release scenarios. Comparison with SSDs indicates whether we are likely to see an ecosystem-wide toxic effects resulting from exposure to ENMs in freshwater and soil systems.

Perhaps the most important conclusion from the model development process is the need for more experimental investigations designed to determine medium-dependent fate processes, rates, and both short and long term fate.[357] When transfer and transformation rate constants are for specific nanomaterials, if a different type of nanomaterial is considered or the environment is very different from the one(s) used to estimate the average rate, then the short-term fate may vary considerably. In addition, the lack of observed data meant that only limited approaches were available to validate the results of the NanoFate model. While the benefit of our approach is that we do not need to wait for data-limited areas of research to be developed, we were still limited in that we could only compare our predictions of fate to other models that typically used a wide range of approaches and test scenarios. Never the less, our results still fell well within the predicted range from other existing models, though on the lower end for most compartments, except in air and sediments where our results tend to be somewhat higher. The differences also reflect that the various models often do not consider the same ENM sources, release amounts, routes, and time periods.

By using a case study of ENM release into the Greater San Francisco Bay Area region, we have begun to identify which ENMs are of concern right now, and which may become a concern if production and release rates increase for a particular ENM. The case study results suggest that if current releases continue to increase and/or a substantial spill occurs, the

primary concern would be for ZnO and secondarily for TiO_2 and CuO, particularly for agricultural soils and freshwater and marine sediments. Even accounting for the rapid rate of dissolution of ZnO in aquatic systems and the high levels of uncertainty implicit within the model, we predict that concentrations are likely to exceed the NOEC. As production and release increase, the volume of ENMs entering the environment (even for less toxic ENMs such as TiO_2), could become sufficient to cause toxicity. In addition, the likelihood of accidental spills will increase and these are of concern, because of the potential for short-term and highly localized concentration spikes that could cause acute toxicity in a substantial part of an ecosystem. Additionally, even at low release volumes, the more toxic ENMs, such as CuO may still reach toxic concentrations.

In Chapter 4, we found that bioaccumulation is likely to occur for metallic ENMs and some limited biomagnification may be observed, although there isn't a consistent pattern of biomagnification up the food chain. Predicted biomagnification was highest for TiO_2, likely due to a lack of dissolution of TiO_2 within the model, and lowest for ZnO, likely due to substantial predicted dissolution. Model results suggest that filter feeders and higher trophic level fish may accumulate ENMs in the greatest quantities, probably due to the high rates of exposure and accumulation from both the environment and their diet. The different organisms took varying lengths of time to reach steady-state accumulation concentrations within the model. Generally, the larger and longer lived the species, the longer it takes to reach steady-state body burdens. For smaller organisms, steady-state concentrations were predicted within one year, but these did vary substantially between ENMs. What these model results indicate is that, at the ecosystem level, short term lab experiments may not effectively describe the maximum bioaccumulation possible; (although it should be kept in

mind that we used predicted environmental exposure concentrations that are much lower than actual lab exposure concentrations[313,455,506,544,545]). Food chain and mesocosm studies that are longer-term and that could be conducted at lower exposure concentrations will be key to improving the predictive power of this model.

We found that uptake, assimilation, dissolution, and elimination are all relatively important parameters for predicting bioaccumulation. Assimilation efficiency will prove to be important specifically for predicting biomagnification whereas uptake from the various environmental media depends largely on the primary routes of exposure for each species.[534,557] The results of the sensitivity analysis can be used to guide future research, specifically on primary modes of uptake and how rates vary with time. We also need to stress the conditional nature of the rate constants, because the environment, the biology, and the toxicity itself can all alter such constants over time. Quantification of rate constants for uptake of ENMs, excretion rates, and transfer through simple food chains should be a primary focus for future research. At the same time, these predictions of bioaccumulation are very preliminary and our uncertainty analysis indicates a wide range in possible bioaccumulation. Collectively, the research in this chapter serves as a means to screen the potential for bioaccumulation characteristics of ENMs relative to biological parameters and to identify which parameters are targets for further research and refinement vis-à-vis accumulation mechanisms and rates.

The primary goal of this research was to investigate how environmental fate and bioaccumulation vary between different ENMs as environmental media also varies. This work identified key questions that need to be considered moving forward in order to

improve the quality of environmental risk assessment models for ENMs. These include the following three key questions.

(i) How will fate vary in different regional environments? There are strong indications that climatic variables (such as precipitation) and regional characteristics (such as population) have implications for use and release, and may greatly alter the fate of ENMs.

(ii) How will fate and bioaccumulation vary for ENMs not included in this research? For example, SiO_2 is assumed to be relatively non-toxic much as with TiO_2,[151,210,211] but given the probability of very high production and release rates, it is still possible that toxic thresholds could be exceeded.[4,8,367] In addition, ENMs such as n-Ag or CNTs may require further model development to include fate processes such as sulfidation, photo-oxidation, covalent reactions, and biodegradation which would change both the long-term environmental distribution as well as the forms that the ENM transforms into and thus the forms of exposure to biota.[13,226,478–480,482,483]

(iii) How accurate are the preliminary estimated bioaccumulation factors in this research? As more accurate parameters for uptake, biotransformation, and elimination of specific ENMs become available the direct toxicological impacts of these predicted bioaccumulation rates will be greatly improved.

"For the first time in the history of the world, every human being is now subjected to contact with dangerous chemicals, from the moment of conception until death."

"We are accustomed to look for the gross and immediate effects and to ignore all else. Unless this appears promptly and in such obvious form that it cannot be ignored, we deny the existence of hazard."

"If we are going to live so intimately with these chemicals eating and drinking them, taking them into the very marrow of our bones - we had better know something about their nature and their power."

--Rachel Carson

References

(1)   Peralta-Videa, J. R.; Zhao, L.; Lopez-Moreno, M. L.; de la Rosa, G.; Hong, J.;
        Gardea-Torresdey, J. L. Nanomaterials and the environment: A review for the
        biennium 2008–2010. *J. Hazard. Mater.* **2011**, *186* (1), 1–15.
(2)   Gottschalk, F.; Sonderer, T.; Scholz, R. W.; Nowack, B. Modeled Environmental
        Concentrations of Engineered Nanomaterials (TiO2, ZnO, Ag, CNT, Fullerenes) for
        Different Regions. *Environ. Sci. Technol.* **2009**, *43* (24), 9216–9222.
(3)   Hendren, C. O.; Lowry, M.; Grieger, K. D.; Money, E. S.; Johnston, J. M.; Wiesner,
        M. R.; Beaulieu, S. M. Modeling Approaches for Characterizing and Evaluating
        Environmental Exposure to Engineered Nanomaterials in Support of Risk-Based
        Decision Making. *Environ. Sci. Technol.* **2013**, *47* (3), 1190–1205.
(4)   Keller, A. A.; McFerran, S.; Lazareva, A.; Suh, S. Global life cycle releases of
        engineered nanomaterials. *J. Nanoparticle Res.* **2013**, *15* (6), 1–17.
(5)   Tovar-Sánchez, A.; Sánchez-Quiles, D.; Basterretxea, G.; Benedé, J. L.; Chisvert,
        A.; Salvador, A.; Moreno-Garrido, I.; Blasco, J. Sunscreen Products as Emerging
        Pollutants to Coastal Waters. *PLoS ONE* **2013**, *8* (6), e65451.
(6)   Hennebert, P.; Avellan, A.; Yan, J.; Aguerre-Chariol, O. Experimental evidence of
        colloids and nanoparticles presence from 25 waste leachates. *Waste Manag.* **2013**,
        33 (9), 1870–1881.
(7)   Bondarenko, O.; Juganson, K.; Ivask, A.; Kasemets, K.; Mortimer, M.; Kahru, A.
        Toxicity of Ag, CuO and ZnO nanoparticles to selected environmentally relevant
        test organisms and mammalian cells in vitro: a critical review. *Arch. Toxicol.* **2013**,
        87 (7), 1181–1200.
(8)   Keller, A. A.; Lazareva, A. Predicted releases of engineered nanomaterials: From
        global to regional to local. *Environ. Sci. Technol. Lett.* **2013**, *1* (1), 65–70.
(9)   French, R. A.; Jacobson, A. R.; Kim, B.; Isley, S. L.; Penn, R. L.; Baveye, P. C.
        Influence of Ionic Strength, pH, and Cation Valence on Aggregation Kinetics of
        Titanium Dioxide Nanoparticles. *Environ. Sci. Technol.* **2009**, *43* (5), 1354–1359.
(10)   Keller, A. A.; Garner, K.; Miller, R. J.; Lenihan, H. S. Toxicity of Nano-Zero Valent
        Iron to Freshwater and Marine Organisms. *PLoS ONE* **2012**, *7* (8), e43983.
(11)   Mackay, D.; Paterson, S.; Shiu, W. Y. Generic models for evaluating the regional
        fate of chemicals. *Chemosphere* **1992**, *24* (6), 695–717.
(12)   Keller, A. A.; Wang, H.; Zhou, D.; Lenihan, H. S.; Cherr, G.; Cardinale, B. J.;
        Miller, R.; Ji, Z. Stability and Aggregation of Metal Oxide Nanoparticles in Natural
        Aqueous Matrices. *Environ. Sci. Technol.* **2010**, *44* (6), 1962–1967.
(13)   Lowry, G. V.; Gregory, K. B.; Apte, S. C.; Lead, J. R. Transformations of
        nanomaterials in the environment. *Environ. Sci. Technol.* **2012**, *46* (13), 6893–6899.
(14)   Zhou, D.; Bennett, S. W.; Keller, A. A. Increased Mobility of Metal Oxide
        Nanoparticles Due to Photo and Thermal Induced Disagglomeration. *PLoS ONE*
        2012, *7* (5), e37363.
(15)   Johnston, J.; Lowry, M.; Beaulieu, S.; Bowles, E. State-of-the-Science Report on
        Predictive Models and Modeling Approaches for Characterizing and Evaluating
        Exposure to Nanomaterials. National Exposure Research Laboratory 2010.

(16)   Quik, J. T. K.; Vonk, J. A.; Hansen, S. F.; Baun, A.; Van De Meent, D. How to assess exposure of aquatic organisms to manufactured nanoparticles? *Environ. Int.* **2011**, *37* (6), 1068–1077.

(17)   Stebounova, L.; Guio, E.; Grassian, V. Silver nanoparticles in simulated biological media: a study of aggregation, sedimentation, and dissolution. *J. Nanoparticle Res.* **2011**, *13* (1), 233–244.

(18)   Praetorius, A.; Scheringer, M.; Hungerbühler, K. Development of Environmental Fate Models for Engineered Nanoparticles—A Case Study of TiO2 Nanoparticles in the Rhine River. *Environ. Sci. Technol.* **2012**, *46* (12), 6705–6713.

(19)   Boxall, A.; Chaudhry, Q.; Sinclair, C.; Jones, A.; Aitken, R.; Jefferson, B.; Watts, C. Current and future predicted environmental exposure to engineered nanoparticles http://hero.epa.gov/index.cfm?action=reference.details&reference_id=196111 (accessed Jul 26, 2012).

(20)   Zhang, Y.; Chen, Y.; Westerhoff, P.; Hristovski, K.; Crittenden, J. C. Stability of commercial metal oxide nanoparticles in water. *Water Res.* **2008**, *42* (8–9), 2204–2212.

(21)   Arvidsson, R.; Molander, S.; Sandén, B. A.; Hassellöv, M. Challenges in Exposure Modeling of Nanoparticles in Aquatic Environments. *Hum. Ecol. Risk Assess. Int. J.* **2011**, *17* (1), 245–262.

(22)   Friedlander, S. K.; Pui, D. Y. H. Emerging Issues in Nanoparticle Aerosol Science and Technology. *J. Nanoparticle Res.* **2004**, *6* (2), 313–320.

(23)   Kumar, P.; Ketzel, M.; Vardoulakis, S.; Pirjola, L.; Britter, R. Dynamics and dispersion modelling of nanoparticles from road traffic in the urban atmospheric environment—A review. *J. Aerosol Sci.* **2011**, *42* (9), 580–603.

(24)   Jacobson, M. *Fundamentals of Atmospheric Modeling*, 2nd ed.; Cambridge University Press, 2005.

(25)   Fushimi, A.; Hasegawa, S.; Takahashi, K.; Fujitani, Y.; Tanabe, K.; Kobayashi, S. Atmospheric fate of nuclei-mode particles estimated from the number concentrations and chemical composition of particles measured at roadside and background sites. *Atmos. Environ.* **2008**, *42* (5), 949–959.

(26)   Kittelson, D. B.; Watts, W. F.; Johnson, J. P. Nanoparticle emissions on Minnesota highways. *Atmos. Environ.* **2004**, *38* (1), 9–19.

(27)   Laakso, L.; Grönholm, T.; Rannik, Ü.; Kosmale, M.; Fiedler, V.; Vehkamäki, H.; Kulmala, M. Ultrafine particle scavenging coefficients calculated from 6 years field measurements. *Atmos. Environ.* **2003**, *37* (25), 3605–3613.

(28)   Jacobson, M. Z. Development of mixed-phase clouds from multiple aerosol size distributions and the effect of the clouds on aerosol removal. *J. Geophys. Res. Atmospheres* **2003**, *108* (D8), n/a–n/a.

(29)   Gottschalk, F.; Scholz, R. W.; Nowack, B. Probabilistic material flow modeling for assessing the environmental exposure to compounds: Methodology and an application to engineered nano-TiO2 particles. *Environ. Model. Softw.* **2010**, *25* (3), 320–332.

(30)   Zhang, K. M.; Wexler, A. S. Evolution of particle number distribution near roadways—Part I: analysis of aerosol dynamics and its implications for engine emission measurement. *Atmos. Environ.* **2004**, *38* (38), 6643–6653.

(31)   Navarro, E.; Baun, A.; Behra, R.; Hartmann, N. B.; Filser, J.; Miao, A.-J.; Quigg, A.; Santschi, P. H.; Sigg, L. Environmental behavior and ecotoxicity of engineered nanoparticles to algae, plants, and fungi. *Ecotoxicology* **2008**, *17* (5), 372–386.

(32)   Chang, M.-C. O.; Chow, J. C.; Watson, J. G.; Hopke, P. K.; Yi, S.-M.; England, G. C. Measurement of Ultrafine Particle Size Distributions from Coal-, Oil-, and Gas-Fired Stationary Combustion Sources. *J. Air Waste Manag. Assoc.* **2004**, *54* (12), 1494–1505.

(33)   Jeong, C.-H.; Hopke, P. K.; Chalupa, D.; Utell, M. Characteristics of Nucleation and Growth Events of Ultrafine Particles Measured in Rochester, NY. *Environ. Sci. Technol.* **2004**, *38* (7), 1933–1940.

(34)   Stanier, C. O.; Khlystov, A. Y.; Pandis, S. N. Nucleation Events During the Pittsburgh Air Quality Study: Description and Relation to Key Meteorological, Gas Phase, and Aerosol Parameters Special Issue of Aerosol Science and Technology on Findings from the Fine Particulate Matter Supersites Program. *Aerosol Sci. Technol.* **2004**, *38* (sup1), 253–264.

(35)   Maynard, A. D.; Baron, P. A.; Foley, M.; Shvedova, A. A.; Kisin, E. R.; Castranova, V. Exposure to Carbon Nanotube Material: Aerosol Release During the Handling of Unrefined Single-Walled Carbon Nanotube Material. *J. Toxicol. Environ. Health A* **2004**, *67* (1), 87–107.

(36)   Quik, J. T. K.; Velzeboer, I.; Wouterse, M.; Koelmans, A. A.; van de Meent, D. Heteroaggregation and sedimentation rates for nanomaterials in natural waters. *Water Res.* **2014**, *48*, 269–279.

(37)   Blaser, S. A.; Scheringer, M.; MacLeod, M.; Hungerbühler, K. Estimation of cumulative aquatic exposure and risk due to silver: Contribution of nano-functionalized plastics and textiles. *Sci. Total Environ.* **2008**, *390* (2–3), 396–409.

(38)   Petosa, A. R.; Jaisi, D. P.; Quevedo, I. R.; Elimelech, M.; Tufenkji, N. Aggregation and Deposition of Engineered Nanomaterials in Aquatic Environments: Role of Physicochemical Interactions. *Environ. Sci. Technol.* **2010**, *44* (17), 6532–6549.

(39)   Elimelech, M.; Jia, X.; Gregory, J.; Williams, R. *Particle Deposition and Aggregation: Measurement, Modeling, and Simulation*; Butterworth-Heinmann, 1998.

(40)   Isrealachvili, J. N. *Intermolecular and Surface Forces*, 2nd ed.; Academic Press: London, 1992.

(41)   Wang, P.; Keller, A. A. Natural and Engineered Nano and Colloidal Transport: Role of Zeta Potential in Prediction of Particle Deposition. *Langmuir* **2009**, *25* (12), 6856–6862.

(42)   Elzey, S.; Grassian, V. Agglomeration, isolation and dissolution of commercially manufactured silver nanoparticles in aqueous environments. *J. Nanoparticle Res.* **2010**, *12* (5), 1945–1958.

(43)   Hyung, H.; Kim, J.-H. Natural Organic Matter (NOM) Adsorption to Multi-Walled Carbon Nanotubes: Effect of NOM Characteristics and Water Quality Parameters. *Environ. Sci. Technol.* **2008**, *42* (12), 4416–4421.

(44)   Zhu, X.; Cai, Z. Behavior and effect of manufactured nanomaterials in the marine environment. *Integr. Environ. Assess. Manag.* **2012**, *8* (3), 566–567.

(45)   Zhou, D.; Keller, A. A. Influence of Material Properties of TiO2 Nanoparticle Agglomeration. *PLOS ONE* **2013**, *In Press*.

(46)   Zhou, D.; Keller, A. A. Role of morphology in the aggregation kinetics of ZnO nanoparticles. *Water Res.* **2010**, *44* (9), 2948–2956.

(47)   Zhou, D.; Ji, Z.; Jiang, X.; Dunphy, D.; Brinker, J.; Keller, A. A. Influence of Material Properties on TiO2 Nanoparticle Agglomeration. *PLOS ONE* **In Press**.

(48)   Andrew J. Pelley; Tufenkji, N. Effect of particle size and natural organic matter on the migration of nano- and microscale latex particles in saturated porous media. *J. Colloid Interface Sci.* **2008**, *321* (1), 74–83.

(49)   Adeleye, A. S.; Keller, A. A.; Miller, R. J.; Lenihan, H. S. Persistence of commercial nanoscaled zero-valent iron (nZVI) and by-products. *J. Nanoparticle Res.* **2013**, *15* (1), 1–18.

(50)   Judy, J. D.; Unrine, J. M.; Bertsch, P. M. Evidence for Biomagnification of Gold Nanoparticles within a Terrestrial Food Chain. *Environ. Sci. Technol.* **2011**, *45* (2), 776–781.

(51)   Reed, R. B.; Ladner, D. A.; Higgins, C. P.; Westerhoff, P.; Ranville, J. F. Solubility of nano-zinc oxide in environmentally and biologically important matrices. *Environ. Toxicol. Chem.* **2012**, *31* (1), 93–99.

(52)   Wang, Z.; Li, J.; Zhao, J.; Xing, B. Toxicity and Internalization of CuO Nanoparticles to Prokaryotic Alga Microcystis aeruginosa as Affected by Dissolved Organic Matter. *Environ. Sci. Technol.* **2011**, *45* (14), 6032–6040.

(53)   Handy, R.; von der Kammer, F.; Lead, J.; Hassellöv, M.; Owen, R.; Crane, M. The ecotoxicology and chemistry of manufactured nanoparticles. *Ecotoxicology* **2008**, *17* (4), 287–314.

(54)   Delay, M.; Dolt, T.; Woellhaf, A.; Sembritzki, R.; Frimmel, F. H. Interactions and stability of silver nanoparticles in the aqueous phase: Influence of natural organic matter (NOM) and ionic strength. *J. Chromatogr. A* **2011**, *1218* (27), 4206–4212.

(55)   Griffitt, R. J.; Luo, J.; Gao, J.; Bonzongo, J.-C.; Barber, D. S. Effects of particle composition and species on toxicity of metallic nanomaterials in aquatic organisms. *Environ. Toxicol. Chem.* **2008**, *27* (9), 1972–1978.

(56)   Limbach, L. K.; Bereiter, R.; Müller, E.; Krebs, R.; Gälli, R.; Stark, W. J. Removal of Oxide Nanoparticles in a Model Wastewater Treatment Plant: Influence of Agglomeration and Surfactants on Clearing Efficiency. *Environ. Sci. Technol.* **2008**, *42* (15), 5828–5833.

(57)   Quik, J. T. K.; Lynch, I.; Hoecke, K. V.; Miermans, C. J. H.; Schamphelaere, K. A. C. D.; Janssen, C. R.; Dawson, K. A.; Stuart, M. A. C.; Meent, D. V. D. Effect of natural organic matter on cerium dioxide nanoparticles settling in model fresh water. *Chemosphere* **2010**, *81* (6), 711–715.

(58)   Sunkara, B.; Zhan, J.; He, J.; McPherson, G. L.; Piringer, G.; John, V. T. Nanoscale Zerovalent Iron Supported on Uniform Carbon Microspheres for the In situ Remediation of Chlorinated Hydrocarbons. *ACS Appl. Mater. Interfaces* **2010**, *2* (10), 2854–2862.

(59)   Yin, K.; Lo, I. M. C.; Dong, H.; Rao, P.; Mak, M. S. H. Lab-scale simulation of the fate and transport of nano zero-valent iron in subsurface environments: Aggregation, sedimentation, and contaminant desorption. *J. Hazard. Mater.* **2012**, *227–228*, 118–125.

(60)   Ghosh, S.; Mashayekhi, H.; Bhowmik, P.; Xing, B. Colloidal Stability of Al2O3 Nanoparticles as Affected by Coating of Structurally Different Humic Acids. *Langmuir* **2010**, *26* (2), 873–879.

(61)   Petosa, A. R.; Brennan, S. J.; Rajput, F.; Tufenkji, N. Transport of two metal oxide nanoparticles in saturated granular porous media: Role of water chemistry and particle coating. *Water Res.* **2012**, *46* (4), 1273–1285.

(62)   Bian, S.-W.; Mudunkotuwa, I. A.; Rupasinghe, T.; Grassian, V. H. Aggregation and Dissolution of 4 nm ZnO Nanoparticles in Aqueous Environments: Influence of pH, Ionic Strength, Size, and Adsorption of Humic Acid. *Langmuir* **2011**, *27* (10), 6059–6068.

(63)   Jiang, W.; Mashayekhi, H.; Xing, B. Bacterial toxicity comparison between nano- and micro-scaled oxide particles. *Environ. Pollut.* **2009**, *157* (5), 1619–1625.

(64)   Hitchman, A.; Sambrook Smith, G. H.; Ju-Nam, Y.; Sterling, M.; Lead, J. R. The effect of environmentally relevant conditions on PVP stabilised gold nanoparticles. *Chemosphere* **2013**, *90* (2), 410–416.

(65)   Christian, P.; Kammer, F. V. der; Baalousha, M.; Hofmann, T. Nanoparticles: structure, properties, preparation and behaviour in environmental media. *Ecotoxicology* **2008**, *17* (5), 326–343.

(66)   Chen, K. L.; Mylon, S. E.; Elimelech, M. Enhanced Aggregation of Alginate-Coated Iron Oxide (Hematite) Nanoparticles in the Presence of Calcium, Strontium, and Barium Cations. *Langmuir* **2007**, *23* (11), 5920–5928.

(67)   Fabrega, J.; Fawcett, S. R.; Renshaw, J. C.; Lead, J. R. Silver Nanoparticle Impact on Bacterial Growth: Effect of pH, Concentration, and Organic Matter. *Environ. Sci. Technol.* **2009**, *43* (19), 7285–7290.

(68)   Gilbert, B.; Lu, G.; Kim, C. S. Stable cluster formation in aqueous suspensions of iron oxyhydroxide nanoparticles. *J. Colloid Interface Sci.* **2007**, *313* (1), 152–159.

(69)   Baalousha, M.; Manciulea, A.; Cumberland, S.; Kendall, K.; Lead, J. R. Aggregation and surface properties of iron oxide nanoparticles: Influence of ph and natural organic matter. *Environ. Toxicol. Chem.* **2008**, *27* (9), 1875–1882.

(70)   Pakrashi, S.; Dalai, S.; Ritika; Sneha, B.; Chandrasekaran, N.; Mukherjee, A. A temporal study on fate of Al2O3 nanoparticles in a fresh water microcosm at environmentally relevant low concentrations. *Ecotoxicol. Environ. Saf.* **2012**, *84*, 70–77.

(71)   Gong, N.; Shao, K.; Feng, W.; Lin, Z.; Liang, C.; Sun, Y. Biotoxicity of nickel oxide nanoparticles and bio-remediation by microalgae Chlorella vulgaris. *Chemosphere* **2011**, *83* (4), 510–516.

(72)   Saleh, N.; Kim, H.-J.; Phenrat, T.; Matyjaszewski, K.; Tilton, R. D.; Lowry, G. V. Ionic Strength and Composition Affect the Mobility of Surface-Modified Fe0 Nanoparticles in Water-Saturated Sand Columns. *Environ. Sci. Technol.* **2008**, *42* (9), 3349–3355.

(73)   Bennett, S. W.; Adeleye, A.; Ji, Z.; Keller, A. A. Stability, metal leaching, photoactivity and toxicity in freshwater systems of commercial single wall carbon nanotubes. *Water Res.* **2014**.

(74)   Wang, P.; Shi, Q.; Liang, H.; Steuerman, D. W.; Stucky, G. D.; Keller, A. A. Enhanced Environmental Mobility of Carbon Nanotubes in the Presence of Humic Acid and Their Removal from Aqueous Solution. *Small* **2008**, *4* (12), 2166–2170.

(75)   Zhang, Y.; Chen, Y.; Westerhoff, P.; Crittenden, J. Impact of natural organic matter and divalent cations on the stability of aqueous nanoparticles. *Water Res.* **2009**, *43* (17), 4249–4257.

(76)   Stankus, D. P.; Lohse, S. E.; Hutchison, J. E.; Nason, J. A. Interactions between Natural Organic Matter and Gold Nanoparticles Stabilized with Different Organic Capping Agents. *Environ. Sci. Technol.* **2010**, *45* (8), 3238–3244.

(77)   Unrine, J. M.; Hunyadi, S. E.; Tsyusko, O. V.; Rao, W.; Shoults-Wilson, W. A.; Bertsch, P. M. Evidence for Bioavailability of Au Nanoparticles from Soil and Biodistribution within Earthworms (Eisenia fetida). *Environ. Sci. Technol.* **2010**, *44* (21), 8308–8313.

(78)   Chen, K. L.; Elimelech, M. Influence of humic acid on the aggregation kinetics of fullerene (C60) nanoparticles in monovalent and divalent electrolyte solutions. *J. Colloid Interface Sci.* **2007**, *309* (1), 126–134.

(79)   Fortner, J. D.; Lyon, D. Y.; Sayes, C. M.; Boyd, A. M.; Falkner, J. C.; Hotze, E. M.; Alemany, L. B.; Tao, Y. J.; Guo, W.; Ausman, K. D.; et al. C60 in Water: Nanocrystal Formation and Microbial Response. *Environ. Sci. Technol.* **2005**, *39* (11), 4307–4316.

(80)   Lin, D.; Liu, N.; Yang, K.; Xing, B.; Wu, F. Different stabilities of multiwalled carbon nanotubes in fresh surface water samples. *Environ. Pollut.* **2010**, *158* (5), 1270–1274.

(81)   Chen, K. L.; Mylon, S. E.; Elimelech, M. Aggregation Kinetics of Alginate-Coated Hematite Nanoparticles in Monovalent and Divalent Electrolytes. *Environ. Sci. Technol.* **2006**, *40* (5), 1516–1523.

(82)   Phenrat, T.; Saleh, N.; Sirk, K.; Tilton, R. D.; Lowry, G. V. Aggregation and Sedimentation of Aqueous Nanoscale Zerovalent Iron Dispersions. *Environ. Sci. Technol.* **2007**, *41* (1), 284–290.

(83)   Westerhoff, P.; Kiser, A.; Hristovski, K. Nanomaterial Removal and Transformation During Biological Wastewater Treatment. *Environ. Eng. Sci.* **2013**, *30* (3).

(84)   Zhou, D.; Abdel-Fattah, A. I.; Keller, A. A. Clay Particles Destabilize Engineered Nanoparticles in Aqueous Environments. *Environ. Sci. Technol.* **2012**, *46* (14), 7520–7526.

(85)   Klaine, S. J.; Alvarez, P. J. J.; Batley, G. E.; Fernandes, T. F.; Handy, R. D.; Lyon, D. Y.; Mahendra, S.; McLaughlin, M. J.; Lead, J. R. Nanomaterials in the environment: Behavior, fate, bioavailability, and effects. *Environ. Toxicol. Chem.* **2008**, *27* (9), 1825–1851.

(86)   Li, Z.; Greden, K.; Alvarez, P. J. J.; Gregory, K. B.; Lowry, G. V. Adsorbed Polymer and NOM Limits Adhesion and Toxicity of Nano Scale Zerovalent Iron to E. coli. *Environ. Sci. Technol.* **2010**, *44* (9), 3462–3467.

(87)   Schrick, B.; Hydutsky, B. W.; Blough, J. L.; Mallouk, T. E. Delivery Vehicles for Zerovalent Metal Nanoparticles in Soil and Groundwater. *Chem. Mater.* **2004**, *16* (11), 2187–2193.

(88)   Franklin, N. M.; Rogers, N. J.; Apte, S. C.; Batley, G. E.; Gadd, G. E.; Casey, P. S. Comparative Toxicity of Nanoparticulate ZnO, Bulk ZnO, and ZnCl2 to a Freshwater Microalga (Pseudokirchneriella subcapitata): The Importance of Particle Solubility. *Environ. Sci. Technol.* **2007**, *41* (24), 8484–8490.

(89)   Chinnapongse, S. L.; MacCuspie, R. I.; Hackley, V. A. Persistence of singly dispersed silver nanoparticles in natural freshwaters, synthetic seawater, and simulated estuarine waters. *Sci. Total Environ.* **2011**, *409* (12), 2443–2450.

(90)   Lowry, G. V.; Espinasse, B. P.; Badireddy, A. R.; Richardson, C. J.; Reinsch, B. C.; Bryant, L. D.; Bone, A. J.; Deonarine, A.; Chae, S.; Therezien, M.; et al. Long-Term Transformation and Fate of Manufactured Ag Nanoparticles in a Simulated Large Scale Freshwater Emergent Wetland. *Environ. Sci. Technol.* **2012**, *46* (13), 7027–7036.

(91)   Zhu, X.; Tian, S.; Cai, Z. Toxicity Assessment of Iron Oxide Nanoparticles in Zebrafish (Danio rerio) Early Life Stages. *PLoS ONE* **2012**, *7* (9), e46286.

(92)   Allen, H. E.; Hansen, D. J. The importance of trace metal speciation to water quality criteria. *Water Environ. Res.* **1996**, *68* (1), 42–54.

(93)   Li, X.; Lenhart, J. J.; Walker, H. W. Dissolution-Accompanied Aggregation Kinetics of Silver Nanoparticles. *Langmuir* **2010**, *26* (22), 16690–16698.

(94)   Levard, C.; Reinsch, B. C.; Michel, F. M.; Oumahi, C.; Lowry, G. V.; Brown, G. E. Sulfidation Processes of PVP-Coated Silver Nanoparticles in Aqueous Solution: Impact on Dissolution Rate. *Environ. Sci. Technol.* **2011**, *45* (12), 5260–5266.

(95)   Fairbairn, E. A.; Keller, A. A.; Mädler, L.; Zhou, D.; Pokhrel, S.; Cherr, G. N. Metal oxide nanomaterials in seawater: Linking physicochemical characteristics with biological response in sea urchin development. *J. Hazard. Mater.* **2011**, *192* (3), 1565–1571.

(96)   Li, M.; Lin, D.; Zhu, L. Effects of water chemistry on the dissolution of ZnO nanoparticles and their toxicity to Escherichia coli. *Environ. Pollut.* **2013**, *173*, 97–102.

(97)   Miller, R. J.; Lenihan, H. S.; Muller, E. B.; Tseng, N.; Hanna, S. K.; Keller, A. A. Impacts of Metal Oxide Nanoparticles on Marine Phytoplankton. *Environ. Sci. Technol.* **2010**, *44* (19), 7329–7334.

(98)   Wong, S. W. Y.; Leung, P. T. Y.; Djurišić, A. B.; Leung, K. M. Y. Toxicities of nano zinc oxide to five marine organisms: influences of aggregate size and ion solubility. *Anal. Bioanal. Chem.* **2010**, *396* (2), 609–618.

(99)   Xia, T.; Kovochich, M.; Liong, M.; Mädler, L.; Gilbert, B.; Shi, H.; Yeh, J. I.; Zink, J. I.; Nel, A. E. Comparison of the Mechanism of Toxicity of Zinc Oxide and Cerium Oxide Nanoparticles Based on Dissolution and Oxidative Stress Properties. *ACS Nano* **2008**, *2* (10), 2121–2134.

(100) Mortimer, M.; Kasemets, K.; Kahru, A. Toxicity of ZnO and CuO nanoparticles to ciliated protozoa Tetrahymena thermophila. *Toxicology* **2010**, *269* (2–3), 182–189.

(101) Blinova, I.; Ivask, A.; Heinlaan, M.; Mortimer, M.; Kahru, A. Ecotoxicity of nanoparticles of CuO and ZnO in natural water. *Environ. Pollut.* **2010**, *158* (1), 41–47.

(102) Montes, M. O.; Hanna, S. K.; Lenihan, H. S.; Keller, A. A. Uptake, accumulation, and biotransformation of metal oxide nanoparticles by a marine suspension-feeder. *J. Hazard. Mater.* **2012**, *225–226*, 139–145.

(103) Cornelis, G.; Ryan, B.; McLaughlin, M. J.; Kirby, J. K.; Beak, D.; Chittleborough, D. Solubility and Batch Retention of CeO2 Nanoparticles in Soils. *Environ. Sci. Technol.* **2011**, *45* (7), 2777–2782.

(104) Gaiser, B. K.; Biswas, A.; Rosenkranz, P.; Jepson, M. A.; Lead, J. R.; Stone, V.; Tyler, C. R.; Fernandes, T. F. Effects of silver and cerium dioxide micro- and nano-sized particles on Daphnia magna. *J. Environ. Monit.* **2011**, *13* (5), 1227.

(105) Aruoja, V.; Dubourguier, H.-C.; Kasemets, K.; Kahru, A. Toxicity of nanoparticles of CuO, ZnO and TiO2 to microalgae Pseudokirchneriella subcapitata. *Sci. Total Environ.* **2009**, *407* (4), 1461–1468.

(106) Kandah, M. I. Zinc and cadmium adsorption on low-grade phosphate. *Sep. Purif. Technol.* **2004**, *35* (1), 61–70.

(107) Tiede, K.; Hassellöv, M.; Breitbarth, E.; Chaudhry, Q.; Boxall, A. B. A. Considerations for environmental fate and ecotoxicity testing to support environmental risk assessments for engineered nanoparticles. *J. Chromatogr. A* **2009**, *1216* (3), 503–509.

(108) Tourinho, P. S.; van Gestel, C. A. M.; Lofts, S.; Svendsen, C.; Soares, A. M. V. M.; Loureiro, S. Metal-based nanoparticles in soil: Fate, behavior, and effects on soil invertebrates. *Environ. Toxicol. Chem.* **2012**, *31* (8), 1679–1692.

(109) Dunphy Guzman, K. A.; Finnegan, M. P.; Banfield, J. F. Influence of Surface Potential on Aggregation and Transport of Titania Nanoparticles. *Environ. Sci. Technol.* **2006**, *40* (24), 7688–7693.

(110) Sirivithayapakorn, S.; Keller, A. Transport of colloids in unsaturated porous media: A pore-scale observation of processes during the dissolution of air-water interface. *Water Resour. Res.* **2003**, *39* (12), n/a–n/a.

(111) Fang, J.; Shan, X.; Wen, B.; Lin, J.; Owens, G. Stability of titania nanoparticles in soil suspensions and transport in saturated homogeneous soil columns. *Environ. Pollut.* **2009**, *157* (4), 1101–1109.

(112) Bradford, S. A.; Yates, S. R.; Bettahar, M.; Simunek, J. Physical factors affecting the transport and fate of colloids in saturated porous media. *Water Resour. Res.* **2002**, *38* (12), 1327.

(113) Darlington, T. K.; Neigh, A. M.; Spencer, M. T.; Guyen, O. T. N.; Oldenburg, S. J. Nanoparticle characteristics affecting environmental fate and transport through soil. *Environ. Toxicol. Chem.* **2009**, *28* (6), 1191–1199.

(114) Tufenkji, N.; Elimelech, M. Correlation Equation for Predicting Single-Collector Efficiency in Physicochemical Filtration in Saturated Porous Media. *Environ. Sci. Technol.* **2004**, *38* (2), 529–536.

(115) Wang, C.; Bobba, A. D.; Attinti, R.; Shen, C.; Lazouskaya, V.; Wang, L.-P.; Jin, Y. Retention and Transport of Silica Nanoparticles in Saturated Porous Media: Effect of Concentration and Particle Size. *Environ. Sci. Technol.* **2012**, *46* (13), 7151–7158.

(116) Sirivithayapakorn, S.; Keller, A. Transport of colloids in saturated porous media: A pore-scale observation of the size exclusion effect and colloid acceleration. *Water Resour. Res.* **2003**, *39* (4), n/a–n/a.

(117) Nowack, B.; Bucheli, T. D. Occurrence, behavior and effects of nanoparticles in the environment. *Environ. Pollut.* **2007**, *150* (1), 5–22.

(118) Godinez, I. G.; Darnault, C. J. G. Aggregation and transport of nano-TiO2 in saturated porous media: Effects of pH, surfactants and flow velocity. *Water Res.* **2011**, *45* (2), 839–851.

(119) Kanel, S. R.; Goswami, R. R.; Clement, T. P.; Barnett, M. O.; Zhao, D. Two Dimensional Transport Characteristics of Surface Stabilized Zero-valent Iron Nanoparticles in Porous Media. *Environ. Sci. Technol.* **2008**, *42* (3), 896–900.

(120) Jones, E. H.; Su, C. Fate and transport of elemental copper (Cu0) nanoparticles through saturated porous media in the presence of organic materials. *Water Res.* **2012**, *46* (7), 2445–2456.

(121) Ben-Moshe, T.; Dror, I.; Berkowitz, B. Transport of metal oxide nanoparticles in saturated porous media. *Chemosphere* **2010**, *81* (3), 387–393.

(122) Brant, J.; Lecoanet, H.; Wiesner, M. R. Aggregation and Deposition Characteristics of Fullerene Nanoparticles in Aqueous Systems. *J. Nanoparticle Res.* **2005**, *7* (4–5), 545–553.

(123) Li, Z.; Sahle-Demessie, E.; Hassan, A. A.; Sorial, G. A. Transport and deposition of CeO2 nanoparticles in water-saturated porous media. *Water Res.* **2011**, *45* (15), 4409–4418.

(124) Tian, Y.; Gao, B.; Wu, L.; Muñoz-Carpena, R.; Huang, Q. Effect of solution chemistry on multi-walled carbon nanotube deposition and mobilization in clean porous media. *J. Hazard. Mater.* **2012**, *231–232*, 79–87.

(125) Wang, Y.; Li, Y.; Pennell, K. D. Influence of electrolyte species and concentration on the aggregation and transport of fullerene nanoparticles in quartz sands. *Environ. Toxicol. Chem.* **2008**, *27* (9), 1860–1867.

(126) Tosco, T.; Bosch, J.; Meckenstock, R. U.; Sethi, R. Transport of Ferrihydrite Nanoparticles in Saturated Porous Media: Role of Ionic Strength and Flow Rate. *Environ. Sci. Technol.* **2012**, *46* (7), 4008–4015.

(127) Espinasse, B.; Hotze, E. M.; Wiesner, M. R. Transport and Retention of Colloidal Aggregates of C60 in Porous Media: Effects of Organic Macromolecules, Ionic Composition, and Preparation Method. *Environ. Sci. Technol.* **2007**, *41* (21), 7396–7402.

(128) Jaisi, D. P.; Elimelech, M. Single-Walled Carbon Nanotubes Exhibit Limited Transport in Soil Columns. *Environ. Sci. Technol.* **2009**, *43* (24), 9161–9166.

(129) Jaisi, D. P.; Saleh, N. B.; Blake, R. E.; Elimelech, M. Transport of Single-Walled Carbon Nanotubes in Porous Media: Filtration Mechanisms and Reversibility. *Environ. Sci. Technol.* **2008**, *42* (22), 8317–8323.

(130) Johnson, R. L.; Johnson, G. O.; Nurmi, J. T.; Tratnyek, P. G. Natural Organic Matter Enhanced Mobility of Nano Zerovalent Iron. *Environ. Sci. Technol.* **2009**, *43* (14), 5455–5460.

(131) Ghosh, S.; Mashayekhi, H.; Pan, B.; Bhowmik, P.; Xing, B. Colloidal Behavior of Aluminum Oxide Nanoparticles As Affected by pH and Natural Organic Matter. *Langmuir* **2008**, *24* (21), 12385–12391.

(132) Chen, G.; Liu, X.; Su, C. Distinct Effects of Humic Acid on Transport and Retention of TiO2 Rutile Nanoparticles in Saturated Sand Columns. *Environ. Sci. Technol.* **2012**, *46* (13), 7142–7150.

(133) Chowdhury, I.; Cwiertny, D. M.; Walker, S. L. Combined Factors Influencing the Aggregation and Deposition of nano-TiO2 in the Presence of Humic Acid and Bacteria. *Environ. Sci. Technol.* **2012**, *46* (13), 6968–6976.

(134) Jeong, S.-W.; Kim, S.-D. Aggregation and transport of copper oxide nanoparticles in porous media. *J. Environ. Monit.* **2009**, *11* (9), 1595.

(135) Cheng, X.; Kan, A. T.; Tomson, M. B. Study of C60 transport in porous media and the effect of sorbed C60 on naphthalene transport. *J. Mater. Res.* **2005**, *20* (12), 3244–3254.

(136) Lecoanet, H. F.; Bottero, J.-Y.; Wiesner, M. R. Laboratory Assessment of the Mobility of Nanomaterials in Porous Media. *Environ. Sci. Technol.* **2004**, *38* (19), 5164–5169.

(137) Lecoanet, H. F.; Wiesner, M. R. Velocity Effects on Fullerene and Oxide Nanoparticle Deposition in Porous Media. *Environ. Sci. Technol.* **2004**, *38* (16), 4377–4382.

(138) Mattison, N. T.; O'Carroll, D. M.; Kerry Rowe, R.; Petersen, E. J. Impact of Porous Media Grain Size on the Transport of Multi-walled Carbon Nanotubes. *Environ. Sci. Technol.* **2011**, *45* (22), 9765–9775.

(139) Tian, Y.; Silvera-Batista, C.; Ziegler, K. Transport of engineered nanoparticles in saturated porous media. *J. Nanoparticle Res.* **2010**.

(140) Grieger, K. D.; Fjordbøge, A.; Hartmann, N. B.; Eriksson, E.; Bjerg, P. L.; Baun, A. Environmental benefits and risks of zero-valent iron nanoparticles (nZVI) for in situ remediation: Risk mitigation or trade-off? *J. Contam. Hydrol.* **2010**, *118* (3–4), 165–183.

(141) Velzeboer, I.; Hendriks, A. J.; Ragas, A. M. J.; van de Meent, D. Aquatic ecotoxicity tests of some nanomaterials. *Environ. Toxicol. Chem.* **2008**, *27* (9), 1942–1947.

(142) Zhu, X.; Zhu, L.; Chen, Y.; Tian, S. Acute toxicities of six manufactured nanomaterial suspensions to Daphnia magna. *J. Nanoparticle Res.* **2009**, *11* (1), 67–75.

(143) Zhu, X.; Zhu, L.; Li, Y.; Duan, Z.; Chen, W.; Alvarez, P. J. J. Developmental toxicity in zebrafish (Danio rerio) embryos after exposure to manufactured nanomaterials: Buckminsterfullerene aggregates (nC60) and fullerol. *Environ. Toxicol. Chem.* **2007**, *26* (5), 976–979.

(144) García, A.; Espinosa, R.; Delgado, L.; Casals, E.; González, E.; Puntes, V.; Barata, C.; Font, X.; Sánchez, A. Acute toxicity of cerium oxide, titanium oxide and iron oxide nanoparticles using standardized tests. *Desalination* **2011**, *269* (1–3), 136–141.

(145) Griffitt, R. J.; Weil, R.; Hyndman, K. A.; Denslow, N. D.; Powers, K.; Taylor, D.; Barber, D. S. Exposure to Copper Nanoparticles Causes Gill Injury and Acute Lethality in Zebrafish (Danio rerio). *Environ. Sci. Technol.* **2007**, *41* (23), 8178–8186.

(146) Heinlaan, M.; Ivask, A.; Blinova, I.; Dubourguier, H.-C.; Kahru, A. Toxicity of nanosized and bulk ZnO, CuO and TiO2 to bacteria Vibrio fischeri and crustaceans Daphnia magna and Thamnocephalus platyurus. *Chemosphere* **2008**, *71* (7), 1308–1316.

(147) Baek, Y.-W.; An, Y.-J. Microbial toxicity of metal oxide nanoparticles (CuO, NiO, ZnO, and Sb2O3) to Escherichia coli, Bacillus subtilis, and Streptococcus aureus. *Sci. Total Environ.* **2011**, *409* (8), 1603–1608.

(148) Horie, M.; Nishio, K.; Fujita, K.; Kato, H.; Nakamura, A.; Kinugasa, S.; Endoh, S.; Miyauchi, A.; Yamamoto, K.; Murayama, H.; et al. Ultrafine NiO Particles Induce Cytotoxicity in Vitro by Cellular Uptake and Subsequent Ni(II) Release. *Chem. Res. Toxicol.* **2009**, *22* (8), 1415–1426.

(149) Hoecke, K. V.; Quik, J. T. K.; Mankiewicz-Boczek, J.; Schamphelaere, K. A. C. D.; Elsaesser, A.; Meeren, P. V. der; Barnes, C.; McKerr, G.; Howard, C. V.; Meent, D. V. D.; et al. Fate and Effects of CeO2 Nanoparticles in Aquatic Ecotoxicity Tests. *Environ. Sci. Technol.* **2009**, *43* (12), 4537–4546.

(150) Rogers, N. J.; Franklin, N. M.; Apte, S. C.; Batley, G. E.; Angel, B. M.; Lead, J. R.; Baalousha, M. Physico-chemical behaviour and algal toxicity of nanoparticulate CeO2 in freshwater. *Environ. Chem.* **2010**, *7* (1), 50–60.

(151) Adams, L. K.; Lyon, D. Y.; Alvarez, P. J. J. Comparative eco-toxicity of nanoscale TiO2, SiO2, and ZnO water suspensions. *Water Res.* **2006**, *40* (19), 3527–3532.

(152) Simon-Deckers, A.; Loo, S.; Mayne-L'hermite, M.; Herlin-Boime, N.; Menguy, N.; Reynaud, C.; Gouget, B.; Carrière, M. Size-, Composition- and Shape-Dependent Toxicological Impact of Metal Oxide Nanoparticles and Carbon Nanotubes toward Bacteria. *Environ. Sci. Technol.* **2009**, *43* (21), 8423–8429.

(153) Li, T.; Albee, B.; Alemayehu, M.; Diaz, R.; Ingham, L.; Kamal, S.; Rodriguez, M.; Bishnoi, S. W. Comparative toxicity study of Ag, Au, and Ag–Au bimetallic nanoparticles on Daphnia magna. *Anal. Bioanal. Chem.* **2010**, *398* (2), 689–700.

(154) Horie, M.; Nishio, K.; Endoh, S.; Kato, H.; Fujita, K.; Miyauchi, A.; Nakamura, A.; Kinugasa, S.; Yamamoto, K.; Niki, E.; et al. Chromium(III) oxide nanoparticles induced remarkable oxidative stress and apoptosis on culture cells. *Environ. Toxicol.* **2013**, *28* (2), 61–75.

(155) Singh, G.; Vajpayee, P.; Khatoon, I.; Jyoti, A.; Dhawan, A.; Gupta, K. C.; Shanker, R. Chromium Oxide Nano-Particles Induce Stress in Bacteria: Probing Cell Viability. *J. Biomed. Nanotechnol.* **2011**, *7* (1), 166–167.

(156) Benn, T. M.; Westerhoff, P. Nanoparticle Silver Released into Water from Commercially Available Sock Fabrics. *Environ. Sci. Technol.* **2008**, *42* (11), 4133–4139.

(157) Coleman, J. G.; Johnson, D. R.; Stanley, J. K.; Bednar, A. J.; Weiss, C. A.; Boyd, R. E.; Steevens, J. A. Assessing the fate and effects of nano aluminum oxide in the terrestrial earthworm, Eisenia fetida. *Environ. Toxicol. Chem.* **2010**, *29* (7), 1575–1580.

(158) Shoults-Wilson, W. A.; Reinsch, B. C.; Tsyusko, O. V.; Bertsch, P. M.; Lowry, G. V.; Unrine, J. M. Role of Particle Size and Soil Type in Toxicity of Silver Nanoparticles to Earthworms. *Soil Sci. Soc. Am. J.* **2011**, *75* (2), 365.

(159) Ben-Moshe, T.; Frenk, S.; Dror, I.; Minz, D.; Berkowitz, B. Effects of metal oxide nanoparticles on soil properties. *Chemosphere* **2013**, *90* (2), 640–646.

(160) Tong, Z.; Bischoff, M.; Nies, L.; Applegate, B.; Turco, R. F. Impact of Fullerene (C60) on a Soil Microbial Community. *Environ. Sci. Technol.* **2007**, *41* (8), 2985–2991.

(161) Afrooz, A. R. M. N.; Sivalapalan, S. T.; Murphy, C. J.; Hussain, S. M.; Schlager, J. J.; Saleh, N. B. Spheres vs. rods: The shape of gold nanoparticles influences aggregation and deposition behavior. *Chemosphere* **2013**, *91* (1), 93–98.

(162) Baalousha, M. Aggregation and disaggregation of iron oxide nanoparticles: Influence of particle concentration, pH and natural organic matter. *Sci. Total Environ.* **2009**, *407* (6), 2093–2101.

(163) Chen, K. L.; Elimelech, M. Aggregation and Deposition Kinetics of Fullerene (C60) Nanoparticles. *Langmuir* **2006**, *22* (26), 10994–11001.

(164) Chowdhury, I.; Hong, Y.; Honda, R. J.; Walker, S. L. Mechanisms of TiO2 nanoparticle transport in porous media: Role of solution chemistry, nanoparticle concentration, and flowrate. *J. Colloid Interface Sci.* **2011**, *360* (2), 548–555.

(165) Diedrich, T.; Dybowska, A.; Schott, J.; Valsami-Jones, E.; Oelkers, E. H. The Dissolution Rates of SiO2 Nanoparticles As a Function of Particle Size. *Environ. Sci. Technol.* **2012**, *46* (9), 4909–4915.

(166) Domingos, R. F.; Tufenkji, N.; Wilkinson, K. J. Aggregation of Titanium Dioxide Nanoparticles: Role of a Fulvic Acid. *Environ. Sci. Technol.* **2009**, *43* (5), 1282–1286.

(167) Furman, O.; Usenko, S.; Lau, B. L. T. Relative Importance of the Humic and Fulvic Fractions of Natural Organic Matter in the Aggregation and Deposition of Silver Nanoparticles. *Environ. Sci. Technol.* **2013**, *47* (3), 1349–1356.

(168) He, F.; Zhao, D. Preparation and Characterization of a New Class of Starch-Stabilized Bimetallic Nanoparticles for Degradation of Chlorinated Hydrocarbons in Water. *Environ. Sci. Technol.* **2005**, *39* (9), 3314–3320.

(169) Hotze, E. M.; Phenrat, T.; Lowry, G. V. Nanoparticle Aggregation: Challenges to Understanding Transport and Reactivity in the Environment. *J. Environ. Qual.* **2010**, *39* (6), 1909.

(170) Huynh, K. A.; Chen, K. L. Aggregation Kinetics of Citrate and Polyvinylpyrrolidone Coated Silver Nanoparticles in Monovalent and Divalent Electrolyte Solutions. *Environ. Sci. Technol.* **2011**, *45* (13), 5564–5571.

(171) Hyung, H.; Fortner, J. D.; Hughes, J. B.; Kim, J.-H. Natural Organic Matter Stabilizes Carbon Nanotubes in the Aqueous Phase. *Environ. Sci. Technol.* **2006**, *41* (1), 179–184.

(172) Li, X.; Lenhart, J. J.; Walker, H. W. Aggregation Kinetics and Dissolution of Coated Silver Nanoparticles. *Langmuir* **2011**, *28* (2), 1095–1104.

(173) Liu, J.; Aruguete, D. M.; Murayama, M.; Hochella, M. F. Influence of Size and Aggregation on the Reactivity of an Environmentally and Industrially Relevant Nanomaterial (PbS). *Environ. Sci. Technol.* **2009**, *43* (21), 8178–8183.

(174) Ma, R.; Levard, C.; Michel, F. M.; Brown, G. E.; Lowry, G. V. Sulfidation Mechanism for Zinc Oxide Nanoparticles and the Effect of Sulfidation on Their Solubility. *Environ. Sci. Technol.* **2013**, *47* (6), 2527–2534.

(175) Pettibone, J. M.; Cwiertny, D. M.; Scherer, M.; Grassian, V. H. Adsorption of Organic Acids on TiO2 Nanoparticles: Effects of pH, Nanoparticle Size, and Nanoparticle Aggregation. *Langmuir* **2008**, *24* (13), 6659–6667.

(176) Reinsch, B. C.; Levard, C.; Li, Z.; Ma, R.; Wise, A.; Gregory, K. B.; Brown, G. E.; Lowry, G. V. Sulfidation of Silver Nanoparticles Decreases Escherichia coli Growth Inhibition. *Environ. Sci. Technol.* **2012**, *46* (13), 6992–7000.

(177) Saleh, N. B.; Pfefferle, L. D.; Elimelech, M. Aggregation Kinetics of Multiwalled Carbon Nanotubes in Aquatic Systems: Measurements and Environmental Implications. *Environ. Sci. Technol.* **2008**, *42* (21), 7963–7969.

(178) Shih, Y.; Zhuang, C.; Peng, Y.-H.; Lin, C.; Tseng, Y. The effect of inorganic ions on the aggregation kinetics of lab-made TiO2 nanoparticles in water. *Sci. Total Environ.* **2012**, *435–436*, 446–452.

(179) Thio, B. J. R.; Zhou, D.; Keller, A. A. Influence of natural organic matter on the aggregation and deposition of titanium dioxide nanoparticles. *J. Hazard. Mater.* **2011**, *189* (1–2), 556–563.

(180) von der Kammer, F.; Ottofuelling, S.; Hofmann, T. Assessment of the physico-chemical behavior of titanium dioxide nanoparticles in aquatic environments using multi-dimensional parameter testing. *Environ. Pollut.* **2010**, *158* (12), 3472–3481.

(181) Wang, Y.; Gao, B.; Morales, V. L.; Tian, Y.; Wu, L.; Gao, J.; Bai, W.; Yang, L. Transport of titanium dioxide nanoparticles in saturated porous media under various solution chemistry conditions. *J. Nanoparticle Res.* **2012**, *14* (9), 1–9.

(182) Zook, J. M.; Halter, M. D.; Cleveland, D.; Long, S. E. Disentangling the effects of polymer coatings on silver nanoparticle agglomeration, dissolution, and toxicity to determine mechanisms of nanotoxicity. *J. Nanoparticle Res.* **2012**, *14* (10), 1–9.

(183) Battin, T. J.; Kammer, F. v.d.; Weilhartner, A.; Ottofuelling, S.; Hofmann, T. Nanostructured TiO2: Transport Behavior and Effects on Aquatic Microbial Communities under Environmental Conditions. *Environ. Sci. Technol.* **2009**, *43* (21), 8098–8104.

(184) Ferry, J. L.; Craig, P.; Hexel, C.; Sisco, P.; Frey, R.; Pennington, P. L.; Fulton, M. H.; Scott, I. G.; Decho, A. W.; Kashiwada, S.; et al. Transfer of gold nanoparticles from the water column to the estuarine food web. *Nat. Nanotechnol.* **2009**, *4* (7), 441–444.

(185) Kennedy, A. J.; Hull, M. S.; Steevens, J. A.; Dontsova, K. M.; Chappell, M. A.; Gunter, J. C.; Weiss, C. A. Factors influencing the partitioning and toxicity of nanotubes in the aquatic environment. *Environ. Toxicol. Chem.* **2008**, *27* (9), 1932–1941.

(186) Mackenzie, K.; Bleyl, S.; Georgi, A.; Kopinke, F.-D. Carbo-Iron – An Fe/AC composite – As alternative to nano-iron for groundwater treatment. *Water Res.* **2012**, *46* (12), 3817–3826.

(187) David, C. A.; Galceran, J.; Rey-Castro, C.; Puy, J.; Companys, E.; Salvador, J.; Monné, J.; Wallace, R.; Vakourov, A. Dissolution Kinetics and Solubility of ZnO Nanoparticles Followed by AGNES. *J. Phys. Chem. C* **2012**, *116* (21), 11758–11767.

(188) Dobias, J.; Bernier-Latmani, R. Silver Release from Silver Nanoparticles in Natural Waters. *Environ. Sci. Technol.* **2013**.

(189) Ho, C.; Yau, S.; Lok, C.; So, M.; Che, C. Oxidative Dissolution of Silver Nanoparticles by Biologically Relevant Oxidants: A Kinetic and Mechanistic Study. *Chem. - Asian J.* **2010**, *5* (2), 285–293.

(190) Kasemets, K.; Ivask, A.; Dubourguier, H.-C.; Kahru, A. Toxicity of nanoparticles of ZnO, CuO and TiO2 to yeast Saccharomyces cerevisiae. *Toxicol. In Vitro* **2009**, *23* (6), 1116–1122.

(191) Liu, J.; Hurt, R. H. Ion Release Kinetics and Particle Persistence in Aqueous Nano-Silver Colloids. *Environ. Sci. Technol.* **2010**, *44* (6), 2169–2175.

(192) Liu, J.; Sonshine, D. A.; Shervani, S.; Hurt, R. H. Controlled Release of Biologically Active Silver from Nanosilver Surfaces. *ACS Nano* **2010**, *4* (11), 6903–6913.

(193) Mahmood, T.; Saddique, M. T.; Naeem, A.; Westerhoff, P.; Mustafa, S.; Alum, A. Comparison of Different Methods for the Point of Zero Charge Determination of NiO. *Ind. Eng. Chem. Res.* **2011**, *50* (17), 10017–10023.

(194)   Rimer, J. D.; Trofymluk, O.; Navrotsky, A.; Lobo, R. F.; Vlachos, D. G. Kinetic and Thermodynamic Studies of Silica Nanoparticle Dissolution. *Chem. Mater.* **2007**, *19* (17), 4189–4197.

(195)   Roelofs, F.; Vogelsberger, W. Dissolution kinetics of nanodispersed γ-alumina in aqueous solution at different pH: Unusual kinetic size effect and formation of a new phase. *J. Colloid Interface Sci.* **2006**, *303* (2), 450–459.

(196)   Roelofs, F.; Vogelsberger, W. Dissolution Kinetics of Synthetic Amorphous Silica in Biological-Like Media and Its Theoretical Description. *J. Phys. Chem. B* **2004**, *108* (31), 11308–11316.

(197)   Vogelsberger, W.; Schmidt, J.; Roelofs, F. Dissolution kinetics of oxidic nanoparticles: The observation of an unusual behaviour. *Colloids Surf. Physicochem. Eng. Asp.* **2008**, *324* (1–3), 51–57.

(198)   Xie, B.; Xu, Z.; Guo, W.; Li, Q. Impact of Natural Organic Matter on the Physicochemical Properties of Aqueous C60 Nanoparticles. *Environ. Sci. Technol.* **2008**, *42* (8), 2853–2859.

(199)   Griffitt, R. J.; Hyndman, K.; Denslow, N. D.; Barber, D. S. Comparison of Molecular and Histological Changes in Zebrafish Gills Exposed to Metallic Nanoparticles. *Toxicol. Sci.* **2009**, *107* (2), 404–415.

(200)   Cornelis, G.; Kirby, J. K.; Beak, D.; Chittleborough, D.; McLaughlin, M. J. A method for determination of retention of silver and cerium oxide manufactured nanoparticles in soils. *Environ. Chem.* **2010**, *7* (3), 298–308.

(201)   Grant, S. B.; Kim, J. H.; Poor, C. Kinetic Theories for the Coagulation and Sedimentation of Particles. *J. Colloid Interface Sci.* **2001**, *238* (2), 238–250.

(202)   Grolimund, D.; Elimelech, M.; Borkovec, M. Aggregation and deposition kinetics of mobile colloidal particles in   natural porous media. *Colloids Surf. -Physicochem. Eng. Asp.* **2001**, *191* (1–2), 179–188.

(203)   Kool, P. L.; Ortiz, M. D.; van Gestel, C. A. M. Chronic toxicity of ZnO nanoparticles, non-nano ZnO and ZnCl2 to Folsomia candida (Collembola) in relation to bioavailability in soil. *Environ. Pollut.* **2011**, *159* (10), 2713–2719.

(204)   Li, Y.; Wang, Y.; Pennell, K. D.; Abriola, L. M. Investigation of the Transport and Deposition of Fullerene (C60) Nanoparticles in Quartz Sands under Varying Flow Conditions. *Environ. Sci. Technol.* **2008**, *42* (19), 7174–7180.

(205)   Milani, N.; McLaughlin, M.; Hettiaratchchi, G.; Beak, D.; Kirby, J.; Stacey, S.; Gilkes, R. Fate of nanoparticulate zinc oxide fertilisers in soil: solubility, diffusion and solid phase speciation. *Soil Solut. Chang. World 19th World Congr. Soil Sci. Brisb. QLD Aust.* No. August 2010.

(206)   Phenrat, T.; Cihan, A.; Kim, H.-J.; Mital, M.; Illangasekare, T.; Lowry, G. V. Transport and Deposition of Polymer-Modified Fe0 Nanoparticles in 2-D Heterogeneous Porous Media: Effects of Particle Concentration, Fe0 Content, and Coatings. *Environ. Sci. Technol.* **2010**, *44* (23), 9086–9093.

(207)   Vecchia, E. D.; Luna, M.; Sethi, R. Transport in Porous Media of Highly Concentrated Iron Micro- and Nanoparticles in the Presence of Xanthan Gum. *Environ. Sci. Technol.* **2009**, *43* (23), 8942–8947.

(208)   Xiao, Y.; Wiesner, M. R. Transport and Retention of Selected Engineered Nanoparticles by Porous Media in the Presence of a Biofilm. *Environ. Sci. Technol.* **2013**, *47* (5), 2246–2253.

(209) Baun, A.; Sørensen, S. N.; Rasmussen, R. F.; Hartmann, N. B.; Koch, C. B. Toxicity and bioaccumulation of xenobiotic organic compounds in the presence of aqueous suspensions of aggregates of nano-C60. *Aquat. Toxicol.* **2008**, *86* (3), 379–387.

(210) Canesi, L.; Fabbri, R.; Gallo, G.; Vallotto, D.; Marcomini, A.; Pojana, G. Biomarkers in Mytilus galloprovincialis exposed to suspensions of selected nanoparticles (Nano carbon black, C60 fullerene, Nano-TiO2, Nano-SiO2). *Aquat. Toxicol.* **2010**, *100* (2), 168–177.

(211) Canesi, L.; Ciacci, C.; Vallotto, D.; Gallo, G.; Marcomini, A.; Pojana, G. In vitro effects of suspensions of selected nanoparticles (C60 fullerene, TiO2, SiO2) on Mytilus hemocytes. *Aquat. Toxicol.* **2010**, *96* (2), 151–158.

(212) Crane, M.; Handy, R.; Garrod, J.; Owen, R. Ecotoxicity test methods and environmental hazard assessment for engineered nanoparticles - Springer. *Ecotoxicology* **2008**, *17*, 421–437.

(213) Gomes, T.; Pinheiro, J. P.; Cancio, I.; Pereira, C. G.; Cardoso, C.; Bebianno, M. J. Effects of Copper Nanoparticles Exposure in the Mussel Mytilus galloprovincialis. *Environ. Sci. Technol.* **2011**, *45* (21), 9356–9362.

(214) Ji, J.; Long, Z.; Lin, D. Toxicity of oxide nanoparticles to the green algae Chlorella sp. *Chem. Eng. J.* **2011**, *170* (2–3), 525–530.

(215) Kadar, E.; Simmance, F.; Martin, O.; Voulvoulis, N.; Widdicombe, S.; Mitov, S.; Lead, J. R.; Readman, J. W. The influence of engineered Fe2O3 nanoparticles and soluble (FeCl3) iron on the developmental toxicity caused by CO2-induced seawater acidification. *Environ. Pollut.* **2010**, *158* (12), 3490–3497.

(216) Li, H.; Zhou, Q.; Wu, Y.; Fu, J.; Wang, T.; Jiang, G. Effects of waterborne nano-iron on medaka (Oryzias latipes): Antioxidant enzymatic activity, lipid peroxidation and histopathology. *Ecotoxicol. Environ. Saf.* **2009**, *72* (3), 684–692.

(217) Li, M.; Zhu, L.; Lin, D. Toxicity of ZnO Nanoparticles to Escherichia coli: Mechanism and the Influence of Medium Components. *Environ. Sci. Technol.* **2011**, *45* (5), 1977–1983.

(218) Manabe, M.; Tatarazako, N.; Kinoshita, M. Uptake, excretion and toxicity of nano-sized latex particles on medaka (Oryzias latipes) embryos and larvae. *Aquat. Toxicol.* **2011**, *105* (3–4), 576–581.

(219) Manzo, S.; Rocco, A.; Carotenuto, R.; Picione, F. D. L.; Miglietta, M. L.; Rametta, G.; Francia, G. D. Investigation of ZnO nanoparticles' ecotoxicological effects towards different soil organisms. *Environ. Sci. Pollut. Res.* **2011**, *18* (5), 756–763.

(220) Miao, A.-J.; Schwehr, K. A.; Xu, C.; Zhang, S.-J.; Luo, Z.; Quigg, A.; Santschi, P. H. The algal toxicity of silver engineered nanoparticles and detoxification by exopolymeric substances. *Environ. Pollut.* **2009**, *157* (11), 3034–3041.

(221) Parks, A. N.; Portis, L. M.; Schierz, P. A.; Washburn, K. M.; Perron, M. M.; Burgess, R. M.; Ho, K. T.; Chandler, G. T.; Ferguson, P. L. Bioaccumulation and toxicity of single-walled carbon nanotubes to benthic organisms at the base of the marine food chain. *Environ. Toxicol. Chem.* **2013**, *32* (6), 1270–1277.

(222) Ringwood, A. H.; Levi-Polyachenko, N.; Carroll, D. L. Fullerene Exposures with Oysters: Embryonic, Adult, and Cellular Responses. *Environ. Sci. Technol.* **2009**, *43* (18), 7136–7141.

(223) Tedesco, S.; Doyle, H.; Blasco, J.; Redmond, G.; Sheehan, D. Oxidative stress and toxicity of gold nanoparticles in Mytilus edulis. *Aquat. Toxicol.* **2010**, *100* (2), 178–186.

(224) Adeleye, A. S.; Keller, A. A. Long-term colloidal stability and metal leaching of single wall carbon nanotubes: Effect of temperature and extracellular polymeric substances. *Water Res.* **2014**, *49*, 236–250.

(225) Hatto, P. Nano safety for success dialogue 2011, slide 1 ISO consensus definitions relevant to nanomaterials and nanotechnologies. 4th Annual Nano Safety for Success Dialogue 2011.

(226) Garner, K.; Keller, A. Emerging Patterns for Engineered Nanomaterials in the Environment: A Review of Fate and Toxicity Studies. *J. Nanoparticle Res.* **2014**, *2503* (16), 1–28.

(227) Bielmyer-Fraser, G. K.; Jarvis, T. A.; Lenihan, H. S.; Miller, R. J. Cellular Partitioning of Nanoparticulate versus Dissolved Metals in Marine Phytoplankton. *Environ. Sci. Technol.* **2014**, *48* (22), 13443–13450.

(228) Gottschalk, F.; Nowack, B. The release of engineered nanomaterials to the environment. *J. Environ. Monit.* **2011**, *13* (5), 1145.

(229) Cohen, Y.; Rallo, R.; Liu, R.; Liu, H. H. In Silico Analysis of Nanomaterials Hazard and Risk. *Acc. Chem. Res.* **2013**, *46* (3), 802–812.

(230) Hendren, C. O.; Mesnard, X.; Dröge, J.; Wiesner, M. R. Estimating Production Data for Five Engineered Nanomaterials As a Basis for Exposure Assessment. *Environ. Sci. Technol.* **2011**, *45* (7), 2562–2569.

(231) Dumont, E.; Johnson, A. C.; Keller, V. D. J.; Williams, R. J. Nano silver and nano zinc-oxide in surface waters – Exposure estimation for Europe at high spatial and temporal resolution. *Environ. Pollut.* **2015**, *196*, 341–349.

(232) Meesters, J. A. J.; Koelmans, A. A.; Quik, J. T. K.; Hendriks, A. J.; van de Meent, D. Multimedia Modeling of Engineered Nanoparticles with SimpleBox4nano: Model Definition and Evaluation. *Environ. Sci. Technol.* **2014**, *48* (10), 5726–5736.

(233) Posthuma, L.; Suter, G.; Traas, T. *Species Sensitivity Distributions in Ecotoxicology*; Lew Publishers, 2002.

(234) Wheeler, J. R.; Leung, K. M. Y.; Morritt, D.; Sorokin, N.; Rogers, H.; Toy, R.; Holt, M.; Whitehouse, P.; Crane, M. Freshwater to saltwater toxicity extrapolation using species sensitivity distributions. *Environ. Toxicol. Chem.* **2002**, *21* (11), 2459–2467.

(235) von der Ohe, P. C.; Liess, M. Relative sensitivity distribution of aquatic invertebrates to organic and metal compounds. *Environ. Toxicol. Chem.* **2004**, *23* (1), 150–156.

(236) Frampton, G. K.; Jänsch, S.; Scott-Fordsmand, J. J.; Römbke, J.; van den Brink, P. J. Effects of pesticides on soil invertebrates in laboratory studies: A review and analysis using species sensitivity distributions. *Environ. Toxicol. Chem.* **2006**, *25* (9), 2480–2489.

(237) Hose, G. C.; Brink, P. J. V. den. Confirming the Species-Sensitivity Distribution Concept for Endosulfan Using Laboratory, Mesocosm, and Field Data. *Arch. Environ. Contam. Toxicol.* **2004**, *47* (4), 511–520.

(238) Maltby, L.; Blake, N.; Brock, T. C. M.; Van den Brink, P. J. Insecticide species sensitivity distributions: Importance of test species selection and relevance to aquatic ecosystems. *Environ. Toxicol. Chem.* **2005**, *24* (2), 379–388.

244

(239) Wang, B.; Yu, G.; Huang, J.; Hu, H. Development of species sensitivity distributions and estimation of HC5 of organochlorine pesticides with five statistical approaches. *Ecotoxicology* **2008**, *17* (8), 716–724.

(240) Van den Brink, P. J.; Blake, N.; Brock, T. C. M.; Maltby, L. Predictive Value of Species Sensitivity Distributions for Effects of Herbicides in Freshwater Ecosystems. *Hum. Ecol. Risk Assess. Int. J.* **2006**, *12* (4), 645–674.

(241) Solomon, K. R.; Baker, D. B.; Richards, R. P.; Dixon, K. R.; Klaine, S. J.; La Point, T. W.; Kendall, R. J.; Weisskopf, C. P.; Giddings, J. M.; Giesy, J. P.; et al. Ecological risk assessment of atrazine in North American surface waters. *Environ. Toxicol. Chem.* **1996**, *15* (1), 31–76.

(242) van Straalen, N. M. Threshold models for species sensitivity distributions applied to aquatic risk assessment for zinc. *Environ. Toxicol. Pharmacol.* **2002**, *11* (3–4), 167–172.

(243) Brix, K. V.; DeForest, D. K.; Adams, W. J. Assessing acute and chronic copper risks to freshwater aquatic life using species sensitivity distributions for different taxonomic groups. *Environ. Toxicol. Chem.* **2001**, *20* (8), 1846–1856.

(244) Rodrigues, A. C. M.; Jesus, F. T.; Fernandes, M. A. F.; Morgado, F.; Soares, A. M. V. M.; Abreu, S. N. Mercury Toxicity to Freshwater Organisms: Extrapolation Using Species Sensitivity Distribution. *Bull. Environ. Contam. Toxicol.* **2013**, *91* (2), 191–196.

(245) Haye, S.; Slaveykova, V. I.; Payet, J. Terrestrial ecotoxicity and effect factors of metals in life cycle assessment (LCA). *Chemosphere* **2007**, *68* (8), 1489–1496.

(246) Verones, F.; Hanafiah, M. M.; Pfister, S.; Huijbregts, M. A. J.; Pelletier, G. J.; Koehler, A. Characterization Factors for Thermal Pollution in Freshwater Aquatic Environments. *Environ. Sci. Technol.* **2010**, *44* (24), 9364–9369.

(247) ISO. ISO 14044:2006E. Environmental management - Life Cycle Assessment - Requirements and Guidelines. International Organization for Standardization (IS), Geneva, Switzerland 2006.

(248) Henderson, A. D.; Hauschild, M. Z.; Meent, D. van de; Huijbregts, M. A. J.; Larsen, H. F.; Margni, M.; McKone, T. E.; Payet, J.; Rosenbaum, R. K.; Jolliet, O. USEtox fate and ecotoxicity factors for comparative assessment of toxic emissions in life cycle analysis: sensitivity to key chemical properties. *Int. J. Life Cycle Assess.* **2011**, *16* (8), 701–709.

(249) Larsen, H. F.; Hauschild, M. Z.; Larsen, H. F.; Hauschild, M. Z. GM-troph – a low data demand ecotoxicity effect indicator for use in LCIA. *Int. J. LCA* **2007**, *12* (2), 79–91.

(250) Grist, E. P. M.; O'Hagan, A.; Crane, M.; Sorokin, N.; Sims, I.; Whitehouse, P. Bayesian and Time-Independent Species Sensitivity Distributions for Risk Assessment of Chemicals. *Environ. Sci. Technol.* **2006**, *40* (1), 395–401.

(251) Aldenberg, T.; Jaworska, J. S. Uncertainty of the Hazardous Concentration and Fraction Affected for Normal Species Sensitivity Distributions. *Ecotoxicol. Environ. Saf.* **2000**, *46* (1), 1–18.

(252) Zhu, X.; Chang, Y.; Chen, Y. Toxicity and bioaccumulation of TiO2 nanoparticle aggregates in Daphnia magna. *Chemosphere* **2010**, *78* (3), 209–215.

(253) He, L.; Liu, Y.; Mustapha, A.; Lin, M. Antifungal activity of zinc oxide nanoparticles against Botrytis cinerea and Penicillium expansum. *Microbiol. Res.* **2011**, *166* (3), 207–215.

(254) Duboudin, C.; Ciffroy, P.; Magaud, H. Acute-to-chronic species sensitivity distribution extrapolation. *Environ. Toxicol. Chem.* **2004**, *23* (7), 1774–1785.

(255) Posthuma, L.; de Zwart, D. Predicted effects of toxicant mixtures are confirmed by changes in fish species assemblages in Ohio, USA, rivers. *Environ. Toxicol. Chem.* **2006**, *25* (4), 1094–1105.

(256) Adeleye, A.; Conway, J.; Perez, J; Rutten, P; Keller, AA. Influence of extracellular polymeric substances on the long-term fate, dissolution, and speciation of copper-based nanoparticles. *Environ. Sci. Technol.* **2014**, *48* (21), 12561–12568.

(257) Hagen, T. G.; Douglas, R. W. Comparative chemical sensitivity between marine Australian and Northern Hemisphere ecosystems: Is an uncertainty factor warranted for water-quality–guideline setting? *Environ. Toxicol. Chem.* **2014**, *33* (5), 1187–1192.

(258) Zhang, L. Environmental behaviors of nanoparticles: distribution, biotransformation and ecotoxicity https://getd.libs.uga.edu/pdfs/zhang_liwen_201308_phd.pdf.

(259) Newman, M. C.; Ownby, D. R.; Mézin, L. C. A.; Powell, D. C.; Christensen, T. R. L.; Lerberg, S. B.; Anderson, B.-A. Applying species-sensitivity distributions in ecological risk assessment: Assumptions of distribution type and sufficient numbers of species. *Environ. Toxicol. Chem.* **2000**, *19* (2), 508–515.

(260) Fedorenkova, A.; Vonk, J. A.; Lenders, H. J. R.; Ouborg, N. J.; Breure, A. M.; Hendriks, A. J. Ecotoxicogenomics: Bridging the Gap between Genes and Populations. *Environ. Sci. Technol.* **2010**, *44* (11), 4328–4333.

(261) Raimondo, S.; Montague, B. J.; Barron, M. G. Determinants of variability in acute to chronic toxicity ratios for aquatic invertebrates and fish. *Environ. Toxicol. Chem.* **2007**, *26* (9), 2019–2023.

(262) Angel, B. M.; Batley, G. E.; Jarolimek, C. V.; Rogers, N. J. The impact of size on the fate and toxicity of nanoparticulate silver in aquatic systems. *Chemosphere* **2013**, *93* (2), 359–365.

(263) Artells, E.; Issartel, J.; Auffan, M.; Borschneck, D.; Thill, A.; Tella, M.; Brousset, L.; Rose, J.; Bottero, J.-Y.; Thiéry, A. Exposure to Cerium Dioxide Nanoparticles Differently Affect Swimming Performance and Survival in Two Daphnid Species. *PLoS ONE* **2013**, *8* (8), e71260.

(264) Asghari, S.; Johari, S.; Lee, J.; Kim, Y.; Jeon, Y.; Choi, H.; Moon, M.; Yu, I. Toxicity of various silver nanoparticles compared to silver ions in Daphnia magna. *J. Nanobiotechnology* **2012**, *10* (14).

(265) Binaeian, E.; Safekordi, A.; Saber, R.; Chaichi, M. Study on Toxicity of Seven Manufactured Nano Particles and Two Phenolic Compounds to Bacteria Vibrio fischeri Using Homemade Luminometer. *Asian J. Chem.* **2012**.

(266) Blaise, C.; Gagné, F.; Férard, J. f.; Eullaffroy, P. Ecotoxicity of selected nano-materials to aquatic organisms. *Environ. Toxicol.* **2008**, *23* (5), 591–598.

(267) Brandt, O.; Mildner, M.; Egger, A. E.; Groessl, M.; Rix, U.; Posch, M.; Keppler, B. K.; Strupp, C.; Mueller, B.; Stingl, G. Nanoscalic silver possesses broad-spectrum antimicrobial activities and exhibits fewer toxicological side effects than silver sulfadiazine. *Nanomedicine Nanotechnol. Biol. Med.* **2012**, *8* (4), 478–488.

(268) Chae, Y. J.; Pham, C. H.; Lee, J.; Bae, E.; Yi, J.; Gu, M. B. Evaluation of the toxic impact of silver nanoparticles on Japanese medaka (Oryzias latipes). *Aquat. Toxicol.* **2009**, *94* (4), 320–327.

(269) Cho, K.-H.; Park, J.-E.; Osaka, T.; Park, S.-G. The study of antimicrobial activity and preservative effects of nanosilver ingredient. *Electrochimica Acta* **2005**, *51* (5), 956–960.

(270) Collin, B.; Auffan, M.; Johnson, A. C.; Kaur, I.; Keller, A. A.; Lazareva, A.; Lead, J. R.; Ma, X.; Merrifield, R. C.; Svendsen, C.; et al. Environmental release, fate and ecotoxicological effects of manufactured ceria nanomaterials. *Environ. Sci. Nano* **2014**, *1*, 533–548.

(271) Cunningham, S.; Brennan-Fournet, M. E.; Ledwith, D.; Byrnes, L.; Joshi, L. Effect of Nanoparticle Stabilization and Physicochemical Properties on Exposure Outcome: Acute Toxicity of Silver Nanoparticle Preparations in Zebrafish (Danio rerio). *Environ. Sci. Technol.* **2013**, *47* (8), 3883–3892.

(272) Ellegaard-Jensen, L.; Jensen, K. A.; Johansen, A. Nano-silver induces dose-response effects on the nematode Caenorhabditis elegans. *Ecotoxicol. Environ. Saf.* **2012**, *80*, 216–223.

(273) Gaiser, B. K.; Fernandes, T. F.; Jepson, M. A.; Lead, J. R.; Tyler, C. R.; Baalousha, M.; Biswas, A.; Britton, G. J.; Cole, P. A.; Johnston, B. D.; et al. Interspecies comparisons on the uptake and toxicity of silver and cerium dioxide nanoparticles. *Environ. Toxicol. Chem.* **2012**, *31* (1), 144–154.

(274) Gallego, A.; Martín-González, A.; Ortega, R.; Gutiérrez, J. C. Flow cytometry assessment of cytotoxicity and reactive oxygen species generation by single and binary mixtures of cadmium, zinc and copper on populations of the ciliated protozoan Tetrahymena thermophila. *Chemosphere* **2007**, *68* (4), 647–661.

(275) Gao, J.; Youn, S.; Hovsepyan, A.; Llaneza, V. L.; Wang, Y.; Bitton, G.; Bonzongo, J.-C. J. Dispersion and Toxicity of Selected Manufactured Nanomaterials in Natural River Water Samples: Effects of Water Chemical Composition. *Environ. Sci. Technol.* **2009**, *43* (9), 3322–3328.

(276) Govindasamy, R.; Rahuman, A. A. Histopathological studies and oxidative stress of synthesized silver nanoparticles in Mozambique tilapia (Oreochromis mossambicus). *J. Environ. Sci.* **2012**, *24* (6), 1091–1098.

(277) Greenlee, L. F.; Lawler, D. F.; Freeman, B. D.; Marrot, B.; Moulin, P. Reverse osmosis desalination: Water sources, technology, and today's challenges. *Water Res.* **2009**, *43* (9), 2317–2348.

(278) Hall, S.; Bradley, T.; Moore, J. T.; Kuykindall, T.; Minella, L. Acute and chronic toxicity of nano-scale TiO2 particles to freshwater fish, cladocerans, and green algae, and effects of organic and inorganic substrate on TiO2 toxicity. *Nanotoxicology* **2009**, *3* (2), 91–97.

(279) Hanna, S. K.; Miller, R. J.; Zhou, D.; Keller, A. A.; Lenihan, H. S. Accumulation and toxicity of metal oxide nanoparticles in a soft-sediment estuarine amphipod. *Aquat. Toxicol.* **2013**, *142–143*, 441–446.

(280) He, D.; Dorantes-Aranda, J. J.; Waite, T. D. Silver nanoparticle-algae interactions: oxidative dissolution, reactive oxygen species generation and synergistic toxic effects. *Environ. Sci. Technol.* **2012**, *46* (16), 8731–8738.

(281) Hernández-Sierra, J. F.; Ruiz, F.; Cruz Pena, D. C.; Martínez-Gutiérrez, F.; Martínez, A. E.; de Jesús Pozos Guillén, A.; Tapia-Pérez, H.; Martínez Castañón, G. The antimicrobial sensitivity of Streptococcus mutans to nanoparticles of silver, zinc oxide, and gold. *Nanomedicine Nanotechnol. Biol. Med.* **2008**, *4* (3), 237–240.

(282) Hoheisel, S. M.; Diamond, S.; Mount, D. Comparison of nanosilver and ionic silver toxicity in Daphnia magna and Pimephales promelas. *Environ. Toxicol. Chem.* **2012**, *31* (11), 2557–2563.

(283) Hund-Rinke, K.; Simon, M. Ecotoxic Effect of Photocatalytic Active Nanoparticles (TiO2) on Algae and Daphnids (8 pp). *Environ. Sci. Pollut. Res.* **2006**, *13* (4), 225–232.

(284) Hu, X.; Cook, S.; Wang, P.; Hwang, H. In vitro evaluation of cytotoxicity of engineered metal oxide nanoparticles. *Sci. Total Environ.* **2009**, *407* (8), 3070–3072.

(285) Ivask, A.; Bondarenko, O.; Jepihhina, N.; Kahru, A. Profiling of the reactive oxygen species-related ecotoxicity of CuO, ZnO, TiO2, silver and fullerene nanoparticles using a set of recombinant luminescent Escherichia coli strains: differentiating the impact of particles and solubilised metals - Springer. *Anal Bioanal Chem* **2010**, *398*, 701–716.

(286) Jin, Y. H.; Dunlap, P. E.; McBride, S. J.; Al-Refai, H.; Bushel, P. R.; Freedman, J. H. Global Transcriptome and Deletome Profiles of Yeast Exposed to Transition Metals. *PLoS Genet* **2008**, *4* (4), e1000053.

(287) Jo, H. J.; Choi, J. W.; Lee, S. H.; Hong, S. W. Acute toxicity of Ag and CuO nanoparticle suspensions against Daphnia magna: The importance of their dissolved fraction varying with preparation methods. *J. Hazard. Mater.* **2012**, *227–228*, 301–308.

(288) Kasemets, K.; Suppi, S.; Künnis-Beres, K.; Kahru, A. Toxicity of CuO Nanoparticles to Yeast Saccharomyces cerevisiae BY4741 Wild-Type and Its Nine Isogenic Single-Gene Deletion Mutants. *Chem. Res. Toxicol.* **2013**, *26* (3), 356–367.

(289) Kennedy, A. J.; Chappell, M. A.; Bednar, A. J.; Ryan, A. C.; Laird, J. G.; Stanley, J. K.; Steevens, J. A. Impact of Organic Carbon on the Stability and Toxicity of Fresh and Stored Silver Nanoparticles. *Environ. Sci. Technol.* **2012**, *46* (19), 10772–10780.

(290) Kennedy, A. J.; Hull, M. S.; Bednar, A. J.; Goss, J. D.; Gunter, J. C.; Bouldin, J. L.; Vikesland, P. J.; Steevens, J. A. Fractionating Nanosilver: Importance for Determining Toxicity to Aquatic Test Organisms. *Environ. Sci. Technol.* **2010**, *44* (24), 9571–9577.

(291) Kim, J.; Kim, S.; Lee, S. Differentiation of the toxicities of silver nanoparticles and silver ions to the Japanese medaka (Oryzias latipes) and the cladoceran Daphnia magna. *Nanotoxicology* **2010**, *5* (2), 208–214.

(292) Poynton, H. C.; Lazorchak, J. M.; Impellitteri, C. A.; Smith, M. E.; Rogers, K.; Patra, M.; Hammer, K. A.; Allen, H. J.; Vulpe, C. D. Differential Gene Expression in Daphnia magna Suggests Distinct Modes of Action and Bioavailability for ZnO Nanoparticles and Zn Ions. *Environ. Sci. Technol.* **2011**, *45* (2), 762–768.

(293) Kim, K.-J.; Sung, W. S.; Suh, B. K.; Moon, S.-K.; Choi, J.-S.; Kim, J. G.; Lee, D. G. Antifungal activity and mode of action of silver nano-particles on Candida albicans. *BioMetals* **2009**, *22* (2), 235–242.

(294) Kim, K. T.; Klaine, S. J.; Cho, J.; Kim, S.-H.; Kim, S. D. Oxidative stress responses of Daphnia magna exposed to TiO2 nanoparticles according to size fraction. *Sci. Total Environ.* **2010**, *408* (10), 2268–2272.

(295) Kim, S. W.; Nam, S.-H.; An, Y.-J. Interaction of Silver Nanoparticles with Biological Surfaces of Caenorhabditis elegans. *Ecotoxicol. Environ. Saf.* **2012**, *77*, 64–70.

(296) Kwok, K. W. H.; Auffan, M.; Badireddy, A. R.; Nelson, C. M.; Wiesner, M. R.; Chilkoti, A.; Liu, J.; Marinakos, S. M.; Hinton, D. E. Uptake of silver nanoparticles and toxicity to early life stages of Japanese medaka (Oryzias latipes): Effect of coating materials. *Aquat. Toxicol.* **2012**, *120–121*, 59–66.

(297) Laban, G.; Nies, L. F.; Turco, R. F.; Bickham, J. W.; Sepúlveda, M. S. The effects of silver nanoparticles on fathead minnow (Pimephales promelas) embryos. *Ecotoxicology* **2010**, *19* (1), 185–195.

(298) Li, J.; Liu, X.; Zhang, Y.; Tian, F.; Zhao, G.; Yu, Q.; Jiang, F.; Liu, Y. Toxicity of nano zinc oxide to mitochondria. *Toxicol. Res.* **2012**, *1* (2), 137.

(299) Li, K.; Chen, Y.; Zhang, W.; Pu, Z.; Jiang, L.; Chen, Y. Surface Interactions Affect the Toxicity of Engineered Metal Oxide Nanoparticles toward Paramecium. *Chem. Res. Toxicol.* **2012**, *25* (8), 1675–1681.

(300) Li, M.; Czymmek, K. J.; Huang, C. P. Responses of Ceriodaphnia dubia to TiO2 and Al2O3 nanoparticles: A dynamic nano-toxicity assessment of energy budget distribution. *J. Hazard. Mater.* **2011**, *187* (1–3), 502–508.

(301) Lim, D.; Roh, J.; Eom, H.; Choi, J.-Y.; Hyun, J.; Choi, J. Oxidative stress-related PMK-1 P38 MAPK activation as a mechanism for toxicity of silver nanoparticles to reproduction in the nematode Caenorhabditis elegans. *Environ. Toxicol. Chem.* **2012**, *31* (3), 585–592.

(302) Li, M.; Pokhrel, S.; Jin, X.; Mädler, L.; Damoiseaux, R.; Hoek, E. M. V. Stability, Bioavailability, and Bacterial Toxicity of ZnO and Iron-Doped ZnO Nanoparticles in Aquatic Media. *Environ. Sci. Technol.* **2011**, *45* (2), 755–761.

(303) Lovern, S. B.; Klaper, R. Daphnia magna mortality when exposed to titanium dioxide and fullerene (C60) nanoparticles. *Environ. Toxicol. Chem.* **2006**, *25* (4), 1132–1137.

(304) Lovern, S. B.; Strickler, J. R.; Klaper, R. Behavioral and Physiological Changes in Daphnia magna when Exposed to Nanoparticle Suspensions (Titanium Dioxide, Nano-C60, and C60HxC70Hx). *Environ. Sci. Technol.* **2007**, *41* (12), 4465–4470.

(305) Ma, H.; Bertsch, P. M.; Glenn, T. C.; Kabengi, N. J.; Williams, P. L. Toxicity of manufactured zinc oxide nanoparticles in the nematode Caenorhabditis elegans. *Environ. Toxicol. Chem.* **2009**, *28* (6), 1324–1330.

(306) Ma, H.; Kabengi, N. J.; Bertsch, P. M.; Unrine, J. M.; Glenn, T. C.; Williams, P. L. Comparative phototoxicity of nanoparticulate and bulk ZnO to a free-living nematode Caenorhabditis elegans: The importance of illumination mode and primary particle size. *Environ. Pollut.* **2011**, *159* (6), 1473–1480.

(307) Manusadžianas, L.; Caillet, C.; Fachetti, L.; Gylytė, B.; Grigutytė, R.; Jurkonienė, S.; Karitonas, R.; Sadauskas, K.; Thomas, F.; Vitkus, R.; et al. Toxicity of copper oxide nanoparticle suspensions to aquatic biota. *Environ. Toxicol. Chem.* **2012**, *31* (1), 108–114.

(308) Martínez-Castañón, G. A.; Niño-Martínez, N.; Martínez-Gutierrez, F.; Martínez-Mendoza, J. R.; Ruiz, F. Synthesis and antibacterial activity of silver nanoparticles with different sizes. *J. Nanoparticle Res.* **2008**, *10* (8), 1343–1348.

(309) McLaughlin, J.; Bonzongo, J.-C. J. Effects of natural water chemistry on nanosilver behavior and toxicity to Ceriodaphnia dubia and Pseudokirchneriella subcapitata. *Environ. Toxicol. Chem.* **2012**, *31* (1), 168–175.

(310) McShane, H.; Sarrazin, M.; Whalen, J. K.; Hendershot, W. H.; Sunahara, G. I. Reproductive and behavioral responses of earthworms exposed to nano-sized titanium dioxide in soil. *Environ. Toxicol. Chem.* **2012**, *31* (1), 184–193.

(311) Meyer, J. N.; Lord, C. A.; Yang, X. Y.; Turner, E. A.; Badireddy, A. R.; Marinakos, S. M.; Chilkoti, A.; Wiesner, M. R.; Auffan, M. Intracellular uptake and associated toxicity of silver nanoparticles in Caenorhabditis elegans. *Aquat. Toxicol.* **2010**, *100* (2), 140–150.

(312) Mortimer, M.; Kasemets, K.; Heinlaan, M.; Kurvet, I.; Kahru, A. High throughput kinetic Vibrio fischeri bioluminescence inhibition assay for study of toxic effects of nanoparticles. *Toxicol. In Vitro* **2008**, *22* (5), 1412–1417.

(313) Mortimer, M.; Kasemets, K.; Vodovnik, M.; Marinšek-Logar, R.; Kahru, A. Exposure to CuO Nanoparticles Changes the Fatty Acid Composition of Protozoa Tetrahymena thermophila. *Environ. Sci. Technol.* **2011**, *45* (15), 6617–6624.

(314) Navarro, E.; Piccapietra, F.; Wagner, B.; Marconi, F.; Kaegi, R.; Odzak, N.; Sigg, L.; Behra, R. Toxicity of Silver Nanoparticles to Chlamydomonas reinhardtii. *Environ. Sci. Technol.* **2008**, *42* (23), 8959–8964.

(315) Oberdörster, E.; Zhu, S.; Blickley, T. M.; McClellan-Green, P.; Haasch, M. L. Ecotoxicology of carbon-based engineered nanoparticles: Effects of fullerene (C60) on aquatic organisms. *Carbon* **2006**, *44* (6), 1112–1120.

(316) Oukarroum, A.; Bras, S.; Perreault, F.; Popovic, R. Inhibitory effects of silver nanoparticles in two green algae, Chlorella vulgaris and Dunaliella tertiolecta. *Ecotoxicol. Environ. Saf.* **2012**, *78*, 80–85.

(317) Panacek, A.; Prucek, R.; Safarova, D.; Dittrich, M.; Richtrova, J.; Benickova, K.; Zboril, R.; Kvitek, L. Acute and Chronic Toxicity Effects of Silver Nanoparticles (NPs) on Drosophila melanogaster. *Environ. Sci. Technol.* **2011**, *45* (11), 4974–4979.

(318) Patra, P.; Mitra, S.; Debnath, N.; Goswami, A. Biochemical-, Biophysical-, and Microarray-Based Antifungal Evaluation of the Buffer-Mediated Synthesized Nano Zinc Oxide: An in Vivo and in Vitro Toxicity Study. *Langmuir* **2012**, *28* (49), 16966–16978.

(319) Poynton, H. C.; Lazorchak, J. M.; Impellitteri, C. A.; Blalock, B. J.; Rogers, K.; Allen, H. J.; Loguinov, A.; Heckman, J. L.; Govindasmawy, S. Toxicogenomic Responses of Nanotoxicity in Daphnia magna Exposed to Silver Nitrate and Coated Silver Nanoparticles. *Environ. Sci. Technol.* **2012**, *46* (11), 6288–6296.

(320) Pradhan, A.; Seena, S.; Pascoal, C.; Cássio, F. Copper oxide nanoparticles can induce toxicity to the freshwater shredder Allogamus ligonifer. *Chemosphere* **2012**, *89* (9), 1142–1150.

(321) Rodea-Palomares, I.; Boltes, K.; Fernández-Piñas, F.; Leganés, F.; García-Calvo, E.; Santiago, J.; Rosal, R. Physicochemical Characterization and Ecotoxicological

Assessment of CeO2 Nanoparticles Using Two Aquatic Microorganisms. *Toxicol. Sci.* **2011**, *119* (1), 135–145.

(322) Sadiq, I.; Pakrashi, S.; Chandrasekaran, N.; Mukherjee, A. Studies on toxicity of aluminum oxide (Al2O3) nanoparticles to microalgae species: Scenedesmus sp. and Chlorella sp. - Springer. *J. Nanoparticle Res.* **2011**, *13*, 3287–3299.

(323) Sovova, T.; Koci, V.; Kochankova, L. Ecotoxicity of nano and bulk forms of metal oxides. *Proc. NANOCON Conf. Roznoc Pod Radhostem Czech Repub.* **2009**, 62–71.

(324) Takatsuki, M.; Seki, M.; Fujishima, S.; Gondo, Y.; Inoue, Y.; Nozaka, T.; Suemura, K. Acute toxicity of fullerene C60 in aquatic organisms. *Environ. Sci. Jpn.* **2008**.

(325) Usenko, C. Y.; Harper, S. L.; Tanguay, R. L. In vivo evaluation of carbon fullerene toxicity using embryonic zebrafish. *Carbon* **2007**, *45* (9), 1891–1898.

(326) Vargas-Reus, M. A.; Memarzadeh, K.; Huang, J.; Ren, G. G.; Allaker, R. P. Antimicrobial activity of nanoparticulate metal oxides against peri-implantitis pathogens. *Int. J. Antimicrob. Agents* **2012**, *40* (2), 135–139.

(327) Wang, H.; Wick, R. L.; Xing, B. Toxicity of nanoparticulate and bulk ZnO, Al2O3 and TiO2 to the nematode Caenorhabditis elegans. *Environ. Pollut.* **2009**, *157* (4), 1171–1177.

(328) Wang, Z.; Chen, J.; Li, X.; Shao, J.; Peijnenburg, W. Aquatic toxicity of nanosilver colloids to different trophic organisms: Contributions of particles and free silver ion. *Environ. Toxicol. Chem.* **2012**, *31*, 2408–2413.

(329) Warheit, D. B.; Hoke, R. A.; Finlay, C.; Donner, E. M.; Reed, K. L.; Sayes, C. M. Development of a base set of toxicity tests using ultrafine TiO2 particles as a component of nanoparticle risk management. *Toxicol. Lett.* **2007**, *171* (3), 99–110.

(330) Wiench, K.; Wohlleben, W.; Hisgen, V.; Radke, K.; Salinas, E.; Zok, S.; Landsiedel, R. Acute and chronic effects of nano- and non-nano-scale TiO2 and ZnO particles on mobility and reproduction of the freshwater invertebrate Daphnia magna. *Chemosphere* **2009**, *76* (10), 1356–1365.

(331) Wu, Y.; Zhou, Q. Silver nanoparticles cause oxidative damage and histological changes in medaka (Oryzias latipes) after 14 days of exposure. *Environ. Toxicol. Chem.* **2013**, *32* (1), 165–173.

(332) Xie, Y.; He, Y.; Irwin, P. L.; Jin, T.; Shi, X. Antibacterial Activity and Mechanism of Action of Zinc Oxide Nanoparticles against Campylobacter jejuni. *Appl. Environ. Microbiol.* **2011**, *77* (7), 2325–2331.

(333) Xiong, D.; Fang, T.; Yu, L.; Sima, X.; Zhu, W. Effects of nano-scale TiO2, ZnO and their bulk counterparts on zebrafish: Acute toxicity, oxidative stress and oxidative damage. *Sci. Total Environ.* **2011**, *409* (8), 1444–1452.

(334) Yang, X.; Gondikas, A. P.; Marinakos, S. M.; Auffan, M.; Liu, J.; Hsu-Kim, H.; Meyer, J. N. Mechanism of Silver Nanoparticle Toxicity Is Dependent on Dissolved Silver and Surface Coating in Caenorhabditis elegans. *Environ. Sci. Technol.* **2012**, *46* (2), 1119–1127.

(335) Yu, L.; Fang, T.; Xiong, D.; Zhu, W.; Sima, X. Comparative toxicity of nano-ZnO and bulk ZnO suspensions to zebrafish and the effects of sedimentation, ˙OH production and particle dissolution in distilled water. *J. Environ. Monit.* **2011**, *13* (7), 1975–1982.

(336) Zarrindokht Emami-Karvani. Antibacterial activity of ZnO nanoparticle on Gram-positive and Gram-negative bacteria. *Afr. J. Microbiol. Res.* **2012**, *5* (18).

(337) Zhao, C.-M.; Wang, W.-X. Importance of surface coatings and soluble silver in silver nanoparticles toxicity to Daphnia magna. *Nanotoxicology* **2011**, *6* (4), 361–370.

(338) Zhao, J.; Wang, Z.; Liu, X.; Xie, X.; Zhang, K.; Xing, B. Distribution of CuO nanoparticles in juvenile carp (Cyprinus carpio) and their potential toxicity. *J. Hazard. Mater.* **2011**, *197*, 304–310.

(339) Zhao, Z.; Lu, G.; Xia, J.; Jin, S. Toxicity of nanoscale CuO and ZnO to Daphnia magna. *Chem Res Chin U* **2012**, *28* (2), 209–213.

(340) Zhu, S.; Oberdörster, E.; Haasch, M. L. Toxicity of an engineered nanoparticle (fullerene, C60) in two aquatic species, Daphnia and fathead minnow. *Mar. Environ. Res.* **2006**, *62*, *Supplement 1*, S5–S9.

(341) Zhu, X.; Zhu, L.; Duan, Z.; Qi, R.; Li, Y.; Lang, Y. Comparative toxicity of several metal oxide nanoparticle aqueous suspensions to Zebrafish (Danio rerio) early developmental stage. *J. Environ. Sci. Health Part A* **2008**, *43* (3), 278–284.

(342) O'Brien, N.; Cummins, E. Nano-Scale Pollutants: Fate in Irish Surface and Drinking Water Regulatory Systems. *Hum. Ecol. Risk Assess. Int. J.* **2010**, *16* (4), 847–872.

(343) Koelmans, A. A.; Nowack, B.; Wiesner, M. R. Comparison of manufactured and black carbon nanoparticle concentrations in aquatic sediments. *Environ. Pollut.* **2009**, *157* (4), 1110–1116.

(344) Gottschalk, F.; Ort, C.; Scholz, R. W.; Nowack, B. Engineered nanomaterials in rivers – Exposure scenarios for Switzerland at high spatial and temporal resolution. *Environ. Pollut.* **2011**, *159* (12), 3439–3445.

(345) Cornelis, G.; Hund-Rinke, K.; Kuhlbusch, T.; van den Brink, N.; Nickel, C. Fate and Bioavailability of Engineered Nanoparticles in Soils: A Review. *Crit. Rev. Environ. Sci. Technol.* **2014**, *44* (24), 2720–2764.

(346) Dale, A. L.; Lowry, G. V.; Casman, E. A. Much ado about α: reframing the debate over appropriate fate descriptors in nanoparticle environmental risk modeling. *Env. Sci Nano* **2015**.

(347) von der Kammer, F.; Ferguson, P. L.; Holden, P. A.; Masion, A.; Rogers, K. R.; Klaine, S. J.; Koelmans, A. A.; Horne, N.; Unrine, J. M. Analysis of engineered nanomaterials in complex matrices (environment and biota): General considerations and conceptual case studies. *Environ. Toxicol. Chem.* **2012**, *31* (1), 32–49.

(348) Gottschalk, F.; Sonderer, T.; Scholz, R. W.; Nowack, B. Possibilities and limitations of modeling environmental exposure to engineered nanomaterials by probabilistic material flow analysis. *Environ. Toxicol. Chem.* **2010**, *29* (5), 1036–1048.

(349) Sun, T. Y.; Gottschalk, F.; Hungerbühler, K.; Nowack, B. Comprehensive probabilistic modelling of environmental emissions of engineered nanomaterials. *Environ. Pollut.* **2014**, *185*, 69–76.

(350) Sun, T.; Conroy, G.; Donner, E.; Hungerbuhler, K.; Lombi, E.; Nowack, B. Probabilistic modelling of engineered nanomaterial emissions to the environment: a spatio-temporal approach. *Environ. Sci. Nanotechnol.* **2015**, *2*, 340–351.

(351) Sun, T.; Bornhöft, N. A.; Hungerbuehler, K.; Nowack, B. Dynamic Probabilistic Modelling of Environmental Emissions of Engineered Nanomaterials. *Environ. Sci. Technol.* **2016**.

(352) Liu, H. H.; Cohen, Y. Multimedia Environmental Distribution of Engineered Nanomaterials. *Environ. Sci. Technol.* **2014**.

(353) Mackay, D. *Multimedia Environmental Models: The Fugacity Approach, Second Edition*; CRC Press, 2001.

(354) Mackay, D.; Arnot, J. A. The Application of Fugacity and Activity to Simulating the Environmental Fate of Organic Contaminants. *J. Chem. Eng. Data* **2011**, *56*, 1348–1355.

(355) Thibodeaux, L. J.; Mackay, D. *Handbook of Chemical Mass Transport in the Environment*; CRC Press, 2010.

(356) Warren, C.; Mackay, D.; Whelan, M.; Fox, K. Mass balance modelling of contaminants in river basins: Application of the flexible matrix approach. *Chemosphere* **2007**, *68* (7), 1232–1244.

(357) Baalousha, M.; Cornelis, G.; Kuhlbusch, T.; Lynch, I.; Nickel, C.; Peijnenburg, W.; van den Brink, N. Modeling Nanomaterials Fate and Uptake in the Environment: Current Knowledge and Future Trends. *R. Soc. Chem.* **2016**.

(358) Brunner, P. H.; Rechberger, H. Practical handbook of material flow analysis. *Int. J. Life Cycle Assess.* **2004**, *9* (5), 337–338.

(359) Dale, A.; Casman, E. A.; Lowry, G. V.; Lead, J. R.; Viparelli, E.; Baalousha, M. A. Modeling nanomaterial environmental fate in aquatic systems. *Environ. Sci. Technol.* **2015**.

(360) Westerhoff, P.; Nowack, B. Searching for Global Descriptors of Engineered Nanomaterial Fate and Transport in the Environment. *Acc. Chem. Res.* **2013**, *46* (3), 844–853.

(361) Mueller, N. C.; Nowack, B. Exposure Modeling of Engineered Nanoparticles in the Environment. *Environ. Sci. Technol.* **2008**, *42* (12), 4447–4453.

(362) Markus, A. A.; Parsons, J. R.; Roex, E. W. M.; de Voogt, P.; Laane, R. W. P. M. Modeling aggregation and sedimentation of nanoparticles in the aquatic environment. *Sci. Total Environ.* **2015**, *506–507*, 323–329.

(363) Sani-Kast, N.; Scheringer, M.; Slomberg, D.; Labille, J.; Praetorius, A.; Ollivier, P.; Hungerbühler, K. Addressing the complexity of water chemistry in environmental fate modeling for engineered nanoparticles. *Sci. Total Environ.* **2015**, *535*, 150–159.

(364) Quik, J. T. K.; de Klein, J. J. M.; Koelmans, A. A. Spatially explicit fate modelling of nanomaterials in natural waters. *Water Res.* **2015**, *80*, 200–208.

(365) Markus, A. A.; Parsons, J. R.; Roex, E. W. M.; de Voogt, P.; Laane, R. W. P. M. Modelling the transport of engineered metallic nanoparticles in the river Rhine. *Water Res.* **2016**, *91*, 214–224.

(366) *PCS-ICIS Customized Search: Facility Information*.

(367) Lazareva, A.; Keller, A. A. Estimating Potential Life Cycle Releases of Engineered Nanomaterials from Wastewater Treatment Plants. *ACS Sustain. Chem. Eng.* **2014**, *2* (7), 1656–1665.

(368) Conway, J. R.; Adeleye, A. S.; Gardea-Torresdey, J.; Keller, A. A. Aggregation, Dissolution, and Transformation of Copper Nanoparticles in Natural Waters. *Environ. Sci. Technol.* **2015**, *49* (5), 2749–2756.

(369) Wang, H.; Adeleye, A. S.; Huang, Y.; Li, F.; Keller, A. A. Heteroaggregation of nanoparticles with biocolloids and geocolloids. *Adv. Colloid Interface Sci.* **2015**, *226, Part A*, 24–36.

(370) Baalousha, M.; Kammer, F.; Motelica-Heino, M.; Le Coustumer, P. 3D characterization of natural colloids by FlFFF-MALLS-TEM. *Anal. Bioanal. Chem.* **2005**, *383* (4), 549–556.

(371) Wigginton, N.; Haus, K.; Hochella, M. Aquatic environmental nanoparticles. *J. Environ. Monit.* **2007**, *9*, 1306–1316.

(372) Nho-Kim, E.-Y.; Michou, M.; Peuch, V.-H. Parameterization of size-dependent particle dry deposition velocities for global modeling. *Atmos. Environ.* **2004**, *38* (13), 1933–1942.

(373) Zhang, L.; Wang, X.; Moran, M.; Feng, J. Review and uncertainty assessment of size-resolved scavenging coefficient formulations for below-cloud snow scavenging of atmospheric aerosols. *Atmospheric Chem. Phys.* **2013**, *13*.

(374) Eisenreich, S. J. Atmospheric Role in Trace Metal Exchange at the Air-Water Interface. *J. Gt. Lakes Res.* **1982**, *8* (2), 243–256.

(375) Kerman, B. R. On aerosol production and enrichment by breaking wind waves. *Atmosphere-Ocean* **1986**, *24* (4), 329–345.

(376) Cipriano, R. J.; Blanchard, D. C. Bubble and aerosol spectra produced by a laboratory "breaking wave." *J. Geophys. Res. Oceans* **1981**, *86* (C9), 8085–8092.

(377) Weisel, C.; Duce, R.; Fasching, J.; Heaton, R. Estimates of the Transport of Trace Metals from the Ocean to the Atmosphere. *J. Geophys. Res.* **1984**, *89* (D7), 11607–11618.

(378) Piotrowicz, S. R.; Ray, B. J.; Hoffman, G. L.; Duce, R. A. Trace metal enrichment in the sea-surface microlayer. *J. Geophys. Res.* **1972**, *77* (27), 5243–5254.

(379) Duce, R.; Hoffman, G.; Zoller, W. Atmospheric trace metals at remove northern and southern hemisphere sites: pollution or natural. *Science* **1975**, *187*, 59–61.

(380) Rahn, K. *The Chemical Composition of the Atmospheric Aerosol*; University of Rhode Island, School of Oceanography: Kingston, Rhode Island, 1975.

(381) Langevin, S. A. The role of metals in air-water interactions in Lake Superior. MS Thesis, University of Minnesota: Minneapolis, 1978.

(382) Gillette, D. A. Threshold friction velocities for dust production for agricultural soils. *J. Geophys. Res. Atmospheres* **1988**, *93* (D10), 12645–12662.

(383) Gillette, D. A.; Adams, J.; Endo, A.; Smith, D.; Kihl, R. Threshold velocities for input of soil particles into the air by desert soils. *J. Geophys. Res. Oceans* **1980**, *85* (C10), 5621–5630.

(384) Gillette, D. A.; Passi, R. Modeling dust emission caused by wind erosion. *J. Geophys. Res. Atmospheres* **1988**, *93* (D11), 14233–14242.

(385) Kelly, R.; Drake, N.; Barr, S. *Spatial Modelling of the terrestrial environment*; Wiley, 2004.

(386) Visual MINTEQ | Visual MINTEQ – a free equilibrium speciation model.

(387) Steenhuis, T.; Winchell, M.; Rossing, J.; Zollweg, J.; Walter, M. SCS Runoff Equation Revisited for Variable-Source Runoff Areas. *J. Irrig. Drain. Eng.* **1995**, *121* (3), 234–238.

(388) Han, P.; Wang, X.; Cai, L.; Tong, M.; Kim, H. Transport and retention behaviors of titanium dioxide nanoparticles in iron oxide-coated quartz sand: Effects of pH, ionic strength, and humic acid. *Colloids Surf. Physicochem. Eng. Asp.*

(389) Zhao, L. J.; Peralta-Videa, J. R.; Hernandez-Viezcas, J. A.; Hong, J.; Gardea-Torresdey, J. L. Transport and Retention Behavior of ZnO Nanoparticles in Two

Natural Soils: Effect of Surface Coating and Soil Composition. *J. Nano Res.* **2012**, *17*, 229–242.

(390) Jiang, X.; Wang, X.; Tong, M.; Kim, H. Initial transport and retention behaviors of ZnO nanoparticles in quartz sand porous media coated with Escherichia coli biofilm. *Environ. Pollut.* **2013**, *174*, 38–49.

(391) Heggelund, L. R.; Diez-Ortiz, M.; Lofts, S.; Lahive, E.; Jurkschat, K.; Wojnarowicz, J.; Cedergreen, N.; Spurgeon, D.; Svendsen, C. Soil pH effects on the comparative toxicity of dissolved zinc, non-nano and nano ZnO to the earthworm Eisenia fetida. *Nanotoxicology* **2013**, *8* (5), 559–572.

(392) Rousk, J.; Ackermann, K.; Curling, S. F.; Jones, D. L. Comparative Toxicity of Nanoparticulate CuO and ZnO to Soil Bacterial Communities. *PLoS ONE* **2012**, *7* (3), e34197.

(393) Dimkpa, C. O.; Latta, D. E.; McLean, J. E.; Britt, D. W.; Boyanov, M. I.; Anderson, A. J. Fate of CuO and ZnO Nano- and Microparticles in the Plant Environment. *Environ. Sci. Technol.* **2013**, *47* (9), 4734–4742.

(394) Waalewijn-Kool, P. L.; Diez Ortiz, M.; van Straalen, N. M.; van Gestel, C. A. M. Sorption, dissolution and pH determine the long-term equilibration and toxicity of coated and uncoated ZnO nanoparticles in soil. *Environ. Pollut.* **2013**, *178*, 59–64.

(395) Choy, C. C.; Wazne, M.; Meng, X. Application of an empirical transport model to simulate retention of nanocrystalline titanium dioxide in sand columns. *Chemosphere* **2008**, *71* (9), 1794–1801.

(396) Park, C. M.; Chu, K. H.; Heo, J.; Her, N.; Jang, M.; Son, A.; Yoon, Y. Environmental behavior of engineered nanomaterials in porous media: a review. *J. Hazard. Mater.* **2016**.

(397) Phenrat, T.; Song, J. E.; Cisneros, C. M.; Schoenfelder, D. P.; Tilton, R. D.; Lowry, G. V. Estimating Attachment of Nano- and Submicrometer-particles Coated with Organic Macromolecules in Porous Media: Development of an Empirical Model. *Environ. Sci. Technol.* **2010**, *44* (12), 4531–4538.

(398) Garner, K. L.; Suh, S.; Lenihan, H. S.; Keller, A. A. Species Sensitivity Distributions for Engineered Nanomaterials. *Environ. Sci. Technol.* **2015**, *49* (9), 5753–5759.

(399) Coll, C.; Notter, D.; Gottschalk, F.; Sun, T.; Som, C.; Nowack, B. Probabilistic environmental risk assessment of five nanomaterials (nano-TiO2, nano-Ag, nano-ZnO, CNT, and fullerenes). *Nanotoxicology* **2015**, *0* (0), 1–9.

(400) Gottschalk, F.; Kost, E.; Nowack, B. Engineered nanomaterials in water and soils: a risk quantification based on probabilistic exposure and effect modeling. *Environ. Toxicol. Chem. SETAC* **2013**, *32* (6), 1278–1287.

(401) Adam, N.; Vakurov, A.; Knapen, D.; Blust, R. The chronic toxicity of CuO nanoparticles and copper salt to Daphnia magna. *J. Hazard. Mater.* **2015**, *283*, 416–422.

(402) Li, N.; Georas, S.; Alexis, N.; Fritz, P.; Xia, T.; Williams, M. A.; Horner, E.; Nel, A. Why Ambient Ultrafine and Engineered Nanoparticles Should Receive Special Attention for Possible Adverse Health Outcomes in Humans. *J. Allergy Clin. Immunol.* **2016**.

(403) Gottschalk, F.; Sun, T.; Nowack, B. Environmental concentrations of engineered nanomaterials: Review of modeling and analytical studies. *Environ. Pollut.* **2013**, *181*, 287–300.

(404) Thalmann, B.; Voegelin, A.; Sinnet, B.; Morgenroth, E.; Kaegi, R. Sulfidation Kinetics of Silver Nanoparticles Reacted with Metal Sulfides. *Environ. Sci. Technol.* **2014**, *48* (9), 4885–4892.

(405) Liu, J.; Pennell, K. G.; Hurt, R. H. Kinetics and mechanisms of nanosilver oxysulfidation. *Environ. Sci. Technol.* **2011**, *45* (17), 7345–7353.

(406) Seinfeld, J.; Pandis, S. *Atmospheric Chemistry and Physics: From Air Pollution to Climate Change, John H. Seinfeld, Spyros N. Pandis*, 2nd ed.; Wiley, 2006.

(407) Wang, X.; Zhang, L.; Moran, M. D. Uncertainty assessment of current size-resolved parameterizations for below-cloud particle scavenging by rain. *Atmos Chem Phys* **2010**, *10* (12), 5685–5705.

(408) Pranesha, T. S.; Kamra, A. K. Scavenging of aerosol particles by large water drops: 3. Washout coefficients, half-lives, and rainfall depths. *J. Geophys. Res. Atmospheres* **1997**, *102* (D20), 23947–23953.

(409) Peijnenburg, W.; Praetorius, A.; Scott-Fordsmand, J.; Cornelis, G. Fate assessment of engineered nanoparticles in solids dominated media – Current insights and the way forward. *Environ. Pollut.*

(410) ter Laak, T. L.; Gebbink, W. A.; Tolls, J. Estimation of soil sorption coefficients of veterinary pharmaceuticals from soil properties. *Environ. Toxicol. Chem. SETAC* **2006**, *25* (4), 933–941.

(411) Wind Erosion Equation | NRCS http://www.nrcs.usda.gov/wps/portal/nrcs/main/national/technical/tools/weps/equation/ (accessed Jan 22, 2016).

(412) Woodruff, N. P.; Siddoway, F. H. A Wind Erosion Equation1. *Soil Sci. Soc. Am. J.* **1965**, *29* (5), 602.

(413) Gillette, D. A.; Fryrear, D. W.; Xiao, J. B.; Stockton, P.; Ono, D.; Helm, P. J.; Gill, T. E.; Ley, T. Large-scale variability of wind erosion mass flux rates at Owens Lake: 1. Vertical profiles of horizontal mass fluxes of wind-eroded particles with diameter greater than 50 μm. *J. Geophys. Res. Atmospheres* **1997**, *102* (D22), 25977–25987.

(414) Webb, N.; Galloza, M.; Zobeck, T.; Herrick, J. Threshold wind velocity dynamics as a driver of aeolian sediment mass flux. *Aeolian Res.* **2016**, *20*, 45–58.

(415) Shao, Y.; Lu, H. A simple expression for wind erosion threshold friction velocity. *J. Geophys. Res. Atmospheres* **2000**, *105* (D17), 22437–22443.

(416) Chepil, W. S. Dynamics of Wind Erosion: II. Initiation of Soil Movement. *Soil Sci.* **1945**, *60* (5), 397–411.

(417) Belnap, J.; Gillette, D. A. Vulnerability of desert biological soil crusts to wind erosion: the influences of crust development, soil texture, and disturbance. *J. Arid Environ.* **1998**, *39* (2), 133–142.

(418) Priestley, C. H. B. *Turbulent Transfer in the lower atmosphere*; The University of Chicago Press: Chicago, USAiestieieste, 1959.

(419) Shao, Y. *Physics and Modelling of Wind Erosion*; Springer Science & Business Media, 2008.

(420) Wieringa, J. Updating the Davenport roughness classification. *J. Wind Eng. Ind. Aerodyn.* **1992**, *41* (1–3), 357–368.

(421) Gillette, D. A.; Fryrear, D. W.; Gill, T. E.; Ley, T.; Cahill, T. A.; Gearhart, E. A. Relation of vertical flux of particles smaller than 10 μm to total aeolian horizontal

mass flux at Owens Lake. *J. Geophys. Res. Atmospheres* **1997**, *102* (D22), 26009–26015.

(422) Chepil, W. S. Dynamics of Wind Erosion:1 . Nature of Movement of Soil by Wind. *Soil Sci.* **1945**, *60* (4), 305–320.

(423) Gillette, D. A.; Blifford, I. H.; Fryrear, D. W. The influence of wind velocity on the size distributions of aerosols generated by the wind erosion of soils. *J. Geophys. Res.* **1974**, *79* (27), 4068–4075.

(424) Gillette, D.; Walker, T. CHARACTERISTICS OF AIRBORNE PARTICLES PRODUCED BY WIND EROSION OF SANDY SOIL, HIGH PLAINS OF WEST TEXAS. *Soil Sci.* **1977**, *123* (2).

(425) National Employee Development Center. Engineering Hydrology Training Series - Module 205 - SCS Runoff Equation. National Employee Development Center & Natural Resources Conservation Service & United States Department of Agriculture 1999.

(426) Soil Conservation Service. Hydrology Training Series - Module 104 - Runoff Curve Number Computations. National Employee Development Staff & United States Department of Agriculture & Soil Conservation Service 1989.

(427) Jones, D.; Kowalski, D. G.; Shaw, R. S. Calculating Revised Universal Soil Loss Equation (RUSLE) Estimates on Department of Defense Lands: A Review of RUSLE Factors and U.S. Army Land Condition Trend Analysis (LCTA) Data Gaps. *Cent. Ecol. Manag. Mil. Lands Dep. For. Sci. Colo. State Univ.* **1996**.

(428) S.), S. and W. C. S. (U; Lal, R. *Soil Erosion Research Methods*; CRC Press, 1994.

(429) Panagos, P.; Ballabio, C.; Borrelli, P.; Meusburger, K.; Klik, A.; Rousseva, S.; Percec Tadic, M.; Michaelides, S.; Hrabalikova, M.; Olsen, P.; et al. Rainfall erosivity in Europe. *Sci. Total Environ.* **2015**, *511*, 801–814.

(430) Cooper, K. Evaluation of the Relationship Between the RUSLE R-Factor and Mean Annual Precipitaiton. *Colo. State* **2011**, 1:37.

(431) Brown; Foster. Storm erosivity using idealized intesntiy distributions. *Trans ASAE* **1987**, *30*, 379–386.

(432) Romkens, M.; Young, R.; Poesen, J.; McCool, D.; El-Swaify, S.; Bradford, J. Chapter 3. Soil Erodibility Factor (K). In *Predicting Soil Erosion by Water: A Guide to Conservation Planning with the Revised Universal Soil Loss Equation (RUSLE)*; USDA, 1997.

(433) Renard, K.; Foster, G.; Weesies, G.; McCool, D.; Yoder, D. *Predicting Soil Erosion by WateR: A Guide to Conservation Planning with the Revised Universal Soil Loss Equation (RUSLE)*; USDA, 1997.

(434) Home | NRCS Michigan http://www.nrcs.usda.gov/wps/portal/nrcs/site/mi/home/ (accessed Jan 25, 2016).

(435) Description of STATSGO2 Database | NRCS Soils http://www.nrcs.usda.gov/wps/portal/nrcs/detail/soils/survey/geo/?cid=nrcs142p2_0 53629 (accessed Jan 20, 2016).

(436) Using the TMDL USLE Tool to Estimate Sediment Loads. USDA-NRCS 1983.

(437) Panagos, P.; Borrelli, P.; Meusburger, K.; Alewell, C.; Lugato, E.; Montanarella, L. Estimating the soil erosion cover-management factor at the European scale. *Land Use Policy* **2015**, *48*, 38–50.

(438) Cornelis, G.; DooletteMadeleine Thomas, C.; McLaughlin, M. J.; Kirby, J. K.; Beak, D. G.; Chittleborough, D. Retention and Dissolution of Engineered Silver Nanoparticles in Natural Soils. *Soil Sci. Soc. Am. J.* **2012**, *76* (3), 891.

(439) Quik, J. T. K.; van De Meent, D.; Koelmans, A. A. Simplifying modeling of nanoparticle aggregation–sedimentation behavior in environmental systems: A theoretical analysis. *Water Res.* **2014**, *62*, 193–201.

(440) Praetorius, A.; Labille, J.; Scheringer, M.; Thill, A.; Hungerbühler, K.; Bottero, J.-Y. Heteroaggregation of Titanium Dioxide Nanoparticles with Model Natural Colloids under Environmentally Relevant Conditions. *Environ. Sci. Technol.* **2014**, *48* (18), 10690–10698.

(441) Topuz, E.; Traber, J.; Sigg, L.; Talinli, I. Agglomeration of Ag and TiO2 nanoparticles in surface and wastewater: Role of calcium ions and of organic carbon fractions. *Environ. Pollut.* **2015**, *204*, 313–323.

(442) Miao, L.; Wang, C.; Wang, P.; Ao, Y.; Li, Y.; Lv, Y.; Yang, Y.; You, G.; Xu, Y. Effect of alginate on the aggregation kinetics of copper oxide nanoparticles (CuO NPs): bridging interaction and hetero-aggregation induced by Ca2+. *Environ. Sci. Pollut. Researhc* **2016**, 1–9.

(443) Quik, J. T. K.; Stuart, M. C.; Wouterse, M.; Peijnenburg, W.; Hendriks, A. J.; van de Meent, D. Natural colloids are the dominant factor in the sedimentation of nanoparticles. *Environ. Toxicol. Chem.* **2012**, *31* (5), 1019–1022.

(444) Velzeboer, I.; Quik, J. t. k.; van de Meent, D.; Koelmans, A. a. Rapid settling of nanoparticles due to heteroaggregation with suspended sediment. *Environ. Toxicol. Chem.* **2014**, n/a-n/a.

(445) Brunelli, A.; Pojana, G.; Callegaro, S.; Marcomini, A. Agglomeration and sedimentation of titanium dioxide nanoparticles (n-TiO2) in synthetic and real waters. *J. Nanoparticle Res.* **2013**, *15* (1648).

(446) Hakanson, L. The relationship between salinity, suspended particulate matter, and water clarity in aquatic systems. *Ecol Res* **2006**, *21*, 75–90.

(447) Phenrat, T.; Saleh, N.; Sirk, K.; Kim, H.-J.; Tilton, R. D.; Lowry, G. V. Stabilization of aqueous nanoscale zerovalent iron dispersions by anionic polyelectrolytes: adsorbed anionic polyelectrolyte layer properties and their effect on aggregation and sedimentation. *J. Nanoparticle Res.* **2008**, *10* (5), 795–814.

(448) Torres-Duarte, C.; Adeleye, A. S.; Pokhrel, S.; Mädler, L.; Keller, A. A.; Cherr, G. N. Developmental effects of two different copper oxide nanomaterials in sea urchin (Lytechinus pictus) embryos. *Nanotoxicology* **2015**, *0* (0), 1–9.

(449) Levard, C.; Hotze, E. M.; Lowry, G. V.; Brown, G. E. Environmental Transformations of Silver Nanoparticles: Impact on Stability and Toxicity. *Environ. Sci. Technol.* **2012**, *46* (13), 6900–6914.

(450) Ma, R.; Levard, C.; Marinakos, S. M.; Cheng, Y.; Liu, J.; Michel, F. M.; Brown, G. E.; Lowry, G. V. Size-Controlled Dissolution of Organic-Coated Silver Nanoparticles. *Environ. Sci. Technol.* **2012**, *46* (2), 752–759.

(451) Misra, S. K.; Dybowska, A.; Berhanu, D.; Luoma, S. N.; Valsami-Jones, E. The complexity of nanoparticle dissolution and its importance in nanotoxicological studies. *Sci. Total Environ.* **2012**, *438*, 225–232.

(452) Thio, B. J. R.; Montes, M. O.; Mahmoud, M. A.; Lee, D.-W.; Zhou, D.; Keller, A. A. Mobility of Capped Silver Nanoparticles under Environmentally Relevant Conditions. *Environ. Sci. Technol.* **2012**, *46* (13), 6985–6991.

(453) Rathnayake, S.; Unrine, J. M.; Judy, J.; Miller, A.-F.; Rao, W.; Bertsch, P. M. Multitechnique Investigation of the pH Dependence of Phosphate Induced Transformations of ZnO Nanoparticles. *Environ. Sci. Technol.* **2014**, *48* (9), 4757–4764.

(454) Lv, J.; Zhang, S.; Luo, L.; Han, W.; Zhang, J.; Yang, K.; Christie, P. Dissolution and Microstructural Transformation of ZnO Nanoparticles under the Influence of Phosphate. *Environ. Sci. Technol.* **2012**, *46* (13), 7215–7221.

(455) Croteau, M.-N.; Misra, S. K.; Luoma, S. N.; Valsami-Jones, E. Bioaccumulation and Toxicity of CuO Nanoparticles by a Freshwater Invertebrate after Waterborne and Dietborne Exposures. *Environ. Sci. Technol.* **2014**, *48* (18), 10929–10937.

(456) Buffet, P.-E.; Richard, M.; Caupos, F.; Vergnoux, A.; Perrein-Ettajani, H.; Luna-Acosta, A.; Akcha, F.; Amiard, J.-C.; Amiard-Triquet, C.; Guibbolini, M.; et al. A Mesocosm Study of Fate and Effects of CuO Nanoparticles on Endobenthic Species (Scrobicularia plana, Hediste diversicolor). *Environ. Sci. Technol.* **2012**, *47* (3), 1620–1628.

(457) Peng, X.; Palma, S.; Fisher, N. S.; Wong, S. S. Effect of morphology of ZnO nanostructures on their toxicity to marine algae. *Aquat. Toxicol.* **2011**, *102* (3–4), 186–196.

(458) Duce, R. A mutli-institutional investigation of the sea/air exchange of pollutants and natural substances. *Mar. Pollut. Transf. Process.* **1981**.

(459) Macintyre, F. Geochemical fractionation during mass transfer from sea to air by breaking bubbles. *Tellus* **1970**, *22* (4), 451–462.

(460) MacIntyre, F. Bubbles. Boundary-layer "microtome" for micronthick samples of a liquid surface. *J. Phys. Chem.* **1968**, *72* (2), 589–592.

(461) Blanchard, D. C. The electrification of the atmosphere by particles from bubbles in the sea. *Prog. Oceanogr.* **1963**, *1*, 73–202.

(462) Thorpe, S. A. On the Clouds of Bubbles Formed by Breaking Wind-Waves in Deep Water, and their Role in Air -- Sea Gas Transfer. *Philos. Trans. R. Soc. Lond. Ser. Math. Phys. Sci.* **1982**, *304* (1483), 155–210.

(463) Wu, J.; Murray, J. J.; Lai, R. J. Production and distributions of sea spray. *J. Geophys. Res. Oceans* **1984**, *89* (C5), 8163–8169.

(464) Eisenreich, S. J. Atmospheric input of trace metals to Lake Michigan. *Water. Air. Soil Pollut.* **1980**, *13* (3), 287–301.

(465) Sievering, H.; Dave, M.; Dolske, D.; McCoy, P. Trace element concentrations over midlake michigan as a function of meteorology and source region. *Atmospheric Environ. 1967* **1980**, *14* (1), 39–53.

(466) Duce, R.; Hoffman, E. Chemical fractionation at the air/sea interface. *Annu. Rev. Earth Planet. Sci.* **1976**, *4*, 187–228.

(467) Lou, J.; Schwab, D. J.; Beletsky, D.; Hawley, N. A model of sediment resuspension and transport dynamics in southern Lake Michigan. *J. Geophys. Res. Oceans* **2000**, *105* (C3), 6591–6610.

(468) Mackay, D.; Di Guardo, A.; Paterson, S.; Cowan, C. E. Evaluating the environmental fate of a variety of types of chemicals using the EQC model. *Environ. Toxicol. Chem.* **1996**, *15* (9), 1627–1637.

(469) Wiley: Aerosol Technology: Properties, Behavior, and Measurement of Airborne Particles, 2nd Edition - William C. Hinds http://www.wiley.com/WileyCDA/WileyTitle/productCd-0471194107.html (accessed Jan 20, 2016).

(470) AQS Data Mart | Air Quality System | US EPA https://aqs.epa.gov/aqsweb/documents/data_mart_welcome.html (accessed Jan 24, 2016).

(471) Multi-Resolution Land Characteristics Consortium (MRLC) http://www.mrlc.gov/nlcd2011.php (accessed Jan 20, 2016).

(472) US EPA, O. BASINS User Information and Guidance http://www.epa.gov/exposure-assessment-models/basins-user-information-and-guidance (accessed Jan 20, 2016).

(473) US EPA, O. Home, STORET/WQX System for EPA, Office of Water http://www3.epa.gov/storet/ (accessed Jan 20, 2016).

(474) USDA. National Engineering Handbook - Hydrology Chapters. United States Department of Agriculture & Natural Resources Conservation Service 1997.

(475) Mockus, V.; Fox Moody, H. Hydrologic Soil-Cover Complexes. In *Hydrology National Engineering Handbook*; USDA; Natural Resources Conservation Service, 2004; Vol. 630.

(476) NOAA NCDC Measurement Data https://www.ncdc.noaa.gov/crn/measurements.html (accessed Jan 23, 2016).

(477) USGS Surface-Water Daily Data for the Nation http://waterdata.usgs.gov/nwis/dv/?referred_module=sw (accessed Jan 20, 2016).

(478) Petersen, E. J.; Zhang, L.; Mattison, N. T.; O'Carroll, D. M.; Whelton, A. J.; Uddin, N.; Nguyen, T.; Huang, Q.; Henry, T. B.; Holbrook, R. D.; et al. Potential Release Pathways, Environmental Fate, And Ecological Risks of Carbon Nanotubes. *Environ. Sci. Technol.* **2011**, *45* (23), 9837–9856.

(479) Nowack, B.; Ranville, J. F.; Diamond, S.; Gallego-Urrea, J. A.; Metcalfe, C.; Rose, J.; Horne, N.; Koelmans, A. A.; Klaine, S. J. Potential scenarios for nanomaterial release and subsequent alteration in the environment. *Environ. Toxicol. Chem.* **2012**, *31* (1), 50–59.

(480) Mauter, M. S.; Elimelech, M. Environmental Applications of Carbon-Based Nanomaterials. *Environ. Sci. Technol.* **2008**, *42* (16), 5843–5859.

(481) Adeleye, A. S.; Conway, J. R.; Garner, K. L.; Huang, Y.; Su, Y.; Keller, A. A. Engineered nanomaterials for water treatment and remediation: Costs, benefits, and applicability. *Chem. Eng. J.* **2015**.

(482) Peijnenburg, W. J. G. M.; Baalousha, M.; Chen, J.; Chaudry, Q.; kammer, F. V. der; Kuhlbusch, T. A. J.; Lead, J.; Nickel, C.; Quik, J. T. K.; Renker, M.; et al. A Review of the Properties and Processes Determining the Fate of Engineered Nanomaterials in the Aquatic Environment. *Crit. Rev. Environ. Sci. Technol.* **2015**, *45* (19), 2084–2134.

(483) Daou, T. J.; Begin-Colin, S.; Grenèche, J. M.; Thomas, F.; Derory, A.; Bernhardt, P.; Legaré, P.; Pourroy, G. Phosphate Adsorption Properties of Magnetite-Based Nanoparticles. *Chem. Mater.* **2007**, *19* (18), 4494–4505.

(484) Luoma, S. N.; Rainbow, P. S. Metal contamination in aquatic environments: science and lateral management. **2008**, xix + 573 pp.

(485) Pipan-Tkalec, Ž.; Drobne, D.; Jemec, A.; Romih, T.; Zidar, P.; Bele, M. Zinc bioaccumulation in a terrestrial invertebrate fed a diet treated with particulate ZnO or ZnCl2 solution. *Toxicology* **2010**, *269* (2–3), 198–203.

(486) Croteau, M.-N.; Misra, S. K.; Luoma, S. N.; Valsami-Jones, E. Silver Bioaccumulation Dynamics in a Freshwater Invertebrate after Aqueous and Dietary Exposures to Nanosized and Ionic Ag. *Environ. Sci. Technol.* **2011**, *45* (15), 6600–6607.

(487) Werlin, R.; Priester, J. H.; Mielke, R. E.; Kramer, S.; Jackson, S.; Stoimenov, P. K.; Stucky, G. D.; Cherr, G. N.; Holden, P. A. Biomagnification of cadmium selenide quantum dots in a simple experimental microbial food chain. *Nat. Nanotechnol.* **2011**, *6*, 65–71.

(488) Unrine, J. M.; Shoults-Wilson, W. A.; Zhurbich, O.; Bertsch, P. M.; Tsyusko, O. V. Trophic Transfer of Au Nanoparticles from Soil along a Simulated Terrestrial Food Chain. *Environ. Sci. Technol.* **2012**, *46* (17), 9753–9760.

(489) Hawthorne, J.; De la Torre Roche, R.; Xing, B.; Newman, L. A.; Ma, X.; Majumdar, S.; Gardea-Torresdey, J.; White, J. C. Particle-Size Dependent Accumulation and Trophic Transfer of Cerium Oxide through a Terrestrial Food Chain. *Environ. Sci. Technol.* **2014**, *48* (22), 13102–13109.

(490) Zhu, X.; Wang, J.; Zhang, X.; Chang, Y.; Chen, Y. Trophic transfer of TiO2 nanoparticles from daphnia to zebrafish in a simplified freshwater food chain. *Chemosphere* **2010**, *79* (9), 928–933.

(491) Gardea-Torresdey, J. L.; Rico, C. M.; White, J. C. Trophic Transfer, Transformation, and Impact of Engineered Nanomaterials in Terrestrial Environments. *Environ. Sci. Technol.* **2014**, *48* (5), 2526–2540.

(492) Conway, J. R.; Hanna, S. K.; Lenihan, H. S.; Keller, A. A. Effects and Implications of Trophic Transfer and Accumulation of CeO2 Nanoparticles in a Marine Mussel. *Environ. Sci. Technol.* **2014**, *48* (3), 1517–1524.

(493) Holbrook, R. D.; Murphy, K. E.; Morrow, J. B.; Cole, K. D. Trophic transfer of nanoparticles in a simplified invertebrate food web. *Nat. Nanotechnol.* **2008**, *3* (6), 352–355.

(494) Praetorius, A.; Tufenkji, N.; Goss, K.-U.; Scheringer, M.; Kammer, F. von der; Elimelech, M. The road to nowhere: equilibrium partition coefficients for nanoparticles. *Environ. Sci. Nano* **2014**, *1* (4), 317–323.

(495) Arnot, J. A.; Gobas, F. A. P. C. A food web bioaccumulation model for organic chemicals in aquatic ecosystems. *Environ. Toxicol. Chem.* **2004**, *23* (10), 2343–2355.

(496) Mackay, D.; Fraser, A. Bioaccumulation of persistent organic chemicals: mechansism and models. *Environ. Pollut.* **2000**, *110* (3), 375–391.

(497) Khan, F. R.; Misra, S. K.; García-Alonso, J.; Smith, B. D.; Strekopytov, S.; Rainbow, P. S.; Luoma, S. N.; Valsami-Jones, E. Bioaccumulation Dynamics and Modeling in an Estuarine Invertebrate Following Aqueous Exposure to Nanosized and Dissolved Silver. *Environ. Sci. Technol.* **2012**, *46* (14), 7621–7628.

(498)   Cong, Y.; Banta, G. T.; Selck, H.; Berhanu, D.; Valsami-Jones, E.; Forbes, V. E. Toxic effects and bioaccumulation of nano-, micron- and ionic-Ag in the polychaete, Nereis diversicolor. *Aquat. Toxicol.* **2011**, *105* (3–4), 403–411.

(499)   Collin, B.; Oostveen, E.; Tsyusko, O. V.; Unrine, J. M. Influence of Natural Organic Matter and Surface Charge on the Toxicity and Bioaccumulation of Functionalized Ceria Nanoparticles in Caenorhabditis elegans. *Environ. Sci. Technol.* **2014**, *48* (2), 1280–1289.

(500)   Hu, J.; Wang, D.; Wang, J.; Wang, J. Bioaccumulation of Fe2O3(magnetic) nanoparticles in Ceriodaphnia dubia. *Environ. Pollut.* **2012**, *162*, 216–222.

(501)   Jackson, B. P.; Bugge, D.; Ranville, J. F.; Chen, C. Y. Bioavailability, Toxicity, and Bioaccumulation of Quantum Dot Nanoparticles to the Amphipod Leptocheirus plumulosus. *Environ. Sci. Technol.* **2012**, *46* (10), 5550–5556.

(502)   Lasagna-Reeves, C.; Gonzalez-Romero, D.; Barria, M. A.; Olmedo, I.; Clos, A.; Sadagopa Ramanujam, V. M.; Urayama, A.; Vergara, L.; Kogan, M. J.; Soto, C. Bioaccumulation and toxicity of gold nanoparticles after repeated administration in mice. *Biochem. Biophys. Res. Commun.* **2010**, *393* (4), 649–655.

(503)   Luoma, S. N.; Khan, R.; Croteau, M.-N. Bioavailability and bioaccumulation of metal-based engineered nanomaterials in aquatic environments: concepts and processes. In *Nanoscience and the Environment*; Frontiers of Nanoscience, 2014; Vol. 7.

(504)   Shoults-Wilson, W. A.; Reinsch, B. C.; Tsyusko, O. V.; Bertsch, P. M.; Lowry, G. V.; Unrine, J. M. Effect of silver nanoparticle surface coating on bioaccumulation and reproductive toxicity in earthworms (Eisenia fetida). *Nanotoxicology* **2011**, *5* (3), 432–444.

(505)   Zhao, L.; Sun, Y.; Hernandez-Viezcas, J. A.; Servin, A. D.; Hong, J.; Niu, G.; Peralta-Videa, J. R.; Duarte-Gardea, M.; Gardea-Torresdey, J. L. Influence of CeO2 and ZnO Nanoparticles on Cucumber Physiological Markers and Bioaccumulation of Ce and Zn: A Life Cycle Study. *J. Agric. Food Chem.* **2013**, *61* (49), 11945–11951.

(506)   Croteau, M.-N.; Dybowska, A. D.; Luoma, S. N.; Valsami-Jones, E. A novel approach reveals that zinc oxide nanoparticles are bioavailable and toxic after dietary exposures. *Nanotoxicology* **2011**, *5* (1), 79–90.

(507)   Shaw, B. J.; Al-Bairuty, G.; Handy, R. D. Effects of waterborne copper nanoparticles and copper sulphate on rainbow trout, (Oncorhynchus mykiss): Physiology and accumulation. *Aquat. Toxicol.* **2012**, *116–117*, 90–101.

(508)   Shaw, B. J.; Handy, R. D. Physiological effects of nanoparticles on fish: A comparison of nanometals versus metal ions. *Environ. Int.* **2011**, *37* (6), 1083–1097.

(509)   Krishnan, K.; Peyret, T. Physiologically Based Toxicokinetic (PBTK) Modeling in Ecotoxicology. In *Ecotoxicology Modeling*; Devillers, J., Ed.; Emerging Topics in Ecotoxicology; Springer US, 2009; pp 145–175.

(510)   Landrum, P. F.; Lydy, M. J.; Lee, H. Toxicokinetics in aquatic systems: Model comparisons and use in hazard assessment. *Environ. Toxicol. Chem.* **1992**, *11* (12), 1709–1725.

(511)   Ashauer, R.; Agatz, A.; Albert, C.; Ducrot, V.; Galic, N.; Hendriks, J.; Jager, T.; Kretschmann, A.; O'Connor, I.; Rubach, M. N.; et al. Toxicokinetic-toxicodynamic

modeling of quantal and graded sublethal endpoints: A brief discussion of concepts. *Environ. Toxicol. Chem.* **2011**, *30* (11), 2519–2524.

(512)   Jager, T.; Zimmer, E. I. Simplified Dynamic Energy Budget model for analysing ecotoxicity data. *Ecol. Model.* **2012**, *225*, 74–81.

(513)   Klanjscek, T.; Nisbet, R. M.; Priester, J. H.; Holden, P. A. Dynamic energy budget approach to modeling mechanisms of CdSe quantum dot toxicity. *Ecotoxicology* **2012**, *22* (2), 319–330.

(514)   van der Meer, J. An introduction to Dynamic Energy Budget (DEB) models with special emphasis on parameter estimation. *J. Sea Res.* **2006**, *56* (2), 85–102.

(515)   Muller, E. B.; Hanna, S. K.; Lenihan, H. S.; Miller, R. J.; Nisbet, R. M. Impact of engineered zinc oxide nanoparticles on the energy budgets of Mytilus galloprovincialis. *J. Sea Res.* **2014**, *94*, 29–36.

(516)   Ma, X.; Geiser-Lee, J.; Deng, Y.; Kolmakov, A. Interactions between engineered nanoparticles (ENPs) and plants: Phytotoxicity, uptake and accumulation. *Sci. Total Environ.* **2010**, *408* (16), 3053–3061.

(517)   Rico, C. M.; Majumdar, S.; Duarte-Gardea, M.; Peralta-Videa, J. R.; Gardea-Torresdey, J. L. Interaction of Nanoparticles with Edible Plants and Their Possible Implications in the Food Chain. *J. Agric. Food Chem.* **2011**, *59* (8), 3485–3498.

(518)   Holden, P. A.; Nisbet, R. M.; Lenihan, H. S.; Miller, R. J.; Cherr, G. N.; Schimel, J. P.; Gardea-Torresdey, J. L. Ecological Nanotoxicology: Integrating Nanomaterial Hazard Considerations Across the Subcellular, Population, Community, and Ecosystems Levels. *Acc. Chem. Res.* **2013**, *46* (3), 813–822.

(519)   Cleveland, D.; Long, S. E.; Pennington, P. L.; Cooper, E.; Fulton, M. H.; Scott, G. I.; Brewer, T.; Davis, J.; Petersen, E. J.; Wood, L. Pilot estuarine mesocosm study on the environmental fate of Silver nanomaterials leached from consumer products. *Sci. Total Environ.* **2012**, *421–422*, 267–272.

(520)   Hou, W.-C.; Westerhoff, P.; Posner, J. D. Biological accumulation of engineered nanomaterials: a review of current knowledge. *Environ. Sci. Process. Impacts* **2013**, *15* (1), 103.

(521)   Burkhard, L. P.; Arnot, J. A.; Embry, M. R.; Farley, K. J.; Hoke, R. A.; Kitano, M.; Leslie, H. A.; Lotufo, G. R.; Parkerton, T. F.; Sappington, K. G.; et al. Comparing laboratory- and field-measured biota–sediment accumulation factors. *Integr. Environ. Assess. Manag.* **2012**, *8* (1), 32–41.

(522)   Selck, H.; Drouillard, K.; Eisenreich, K.; Koelmans, A. A.; Palmqvist, A.; Ruus, A.; Salvito, D.; Schultz, I.; Stewart, R.; Weisbrod, A.; et al. Explaining differences between bioaccumulation measurements in laboratory and field data through use of a probabilistic modeling approach. *Integr. Environ. Assess. Manag.* **2012**, *8* (1), 42–63.

(523)   Weisbrod, A. V.; Woodburn, K. B.; Koelmans, A. A.; Parkerton, T. F.; McElroy, A. E.; Borgå, K. Evaluation of Bioaccumulation Using In Vivo Laboratory and Field Studies. *Integr. Environ. Assess. Manag.* **2009**, *5* (4), 598–623.

(524)   Gaskell, P. N.; Brooks, A. C.; Maltby, L. Variation in the Bioaccumulation of a Sediment-Sorbed Hydrophobic Compound by Benthic Macroinvertebrates: Patterns and Mechanisms. *Environ. Sci. Technol.* **2007**, *41* (5), 1783–1789.

(525)   Rubach, M. N.; Ashauer, R.; Buchwalter, D. B.; De Lange, H.; Hamer, M.; Preuss, T. G.; Töpke, K.; Maund, S. J. Framework for traits-based assessment in ecotoxicology. *Integr. Environ. Assess. Manag.* **2011**, *7* (2), 172–186.

(526)   Diepens, N. J.; Van den Heuvel-Greve, M. J.; Koelmans, A. A. Modeling of bioaccumulation in marine benthic inverebrates using a multispecies experimental approach. *Environ. Sci. Technol.* **2015**, *49* (22), 13575–13585.

(527)   Garner, K. L.; Suh, S.; Nisbet, R.; Keller, A. A. Fate of Nanomaterials in the Environment: Case Study of multimedia nano-Fate model for metallic nanoparticles in the San Francisco Bay Region. *Prep.* **2016**.

(528)   Morrison, H. A.; Gobas, F. A. P. C.; Lazar, R.; Haffner, G. D. Development and verification of a bioaccumulation model for organic contamiants in benthic invertebrates. *Environ. Sci. Technol.* **1996**, *30* (11), 3377–3384.

(529)   Singh, R. P.; Ramarao, P. Cellular uptake, intracellular trafficking and cytotoxicity of silver nanoparticles. *Toxicol. Lett.* **2012**, *213* (2), 249–259.

(530)   Mathews, T.; Fisher, N. S. Evaluating the trophic transfer of cadmium, polonium, and methylmercury in an estuarine food chain. *Environ. Toxicol. Chem.* **2008**, *27* (5), 1093–1101.

(531)   Miller, R. J.; Bennett, S.; Keller, A. A.; Pease, S.; Lenihan, H. S. TiO2 Nanoparticles Are Phototoxic to Marine Phytoplankton. *PLoS ONE* **2012**, *7* (1), e30321.

(532)   Shen, C.; Wu, L.; Zhang, S.; Ye, H.; Li, B.; Huang, Y. Heteroaggregation of microparticles with nanoparticles changes the chemical reversibility of the microparticles' attachment to planar surfaces. *J. Colloid Interface Sci.* **2014**, *421*, 103–113.

(533)   Baucells, M.; Borgonovo, E. Invariant Probabilistic Sensitivity Analysis. *Manag. Sci.* **2013**, *59* (11), 2536–2549.

(534)   Borgonovo, E.; Plischke, E. Sensitivity analysis: A review of recent advances. *Eur. J. Oper. Res.* **2016**, *248* (3), 869–887.

(535)   Borgmann, U.; Norwood, W. P. Kinetics of excess (above background) copper and zinc in Hyalella azteca and their relationship to chronic toxicity. *Can. J. Fish. Aquat. Sci.* **1994**, *52* (4), 864–874.

(536)   Errecalde, O.; Campbell, P. G. C. Cadmium and zinc bioavailability to selenastrum capricornutum: accidental metal uptake and toxicity in the presence of citrate. *J. Phycol.* **2000**, *36*, 473–483.

(537)   Yu, R.-Q.; Wang, W.-X. Kinetic uptake of bioavailable cadmium, selenium, and zinc by daphnia magna. *Environ. Toxicol.* **2002**, *21* (11), 2348–2355.

(538)   Burns, C. W. Relation Between Filtering Rate, Temperature, and Body Size in Four Species of Daphnia. *Limnol. Oceanogr.* **1969**, *14*, 693–700.

(539)   Loayza-Muro, R.; Elias-Letts, R. Responses to the mussel Anodontites trapesialis (unionidae) to environmental stressors: Effect of pH, temperature, and metals on filtration rate. *Environ. Polluton* **2007**, *149* (2), 209–215.

(540)   Carbonell, G.; Tarazona, J. V. Toxicokinetics of copper in rainbow trout. *Aquat. Toxicol.* **1994**, *29*, 213–221.

(541)   Bertram, P. E.; Brooks, A. S. Kinetics of accumulation of selenium from food and water by fathead minnows. *Water Res.* **1986**, *20* (7), 877–884.

(542) Aslop, D. H.; Wod, Ch. M. Influence of waterborne cations on zinc uptake and toxicity in rainbow trout, Oncorhynchus mykiss. *Can. J. Fish. Aquat. Sci.* **1999**, *56* (11), 2112–2119.

(543) Hanna, S. K.; Miller, R. J.; Muller, E. B.; Nisbet, R. M.; Lenihan, H. S. Impact of Engineered Zinc Oxide Nanoparticles on the Individual Performance of Mytilus galloprovincialis. *PLoS ONE* **2013**, *8* (4), e61800.

(544) Al-Jubory, A.; Handy, R. D. Uptake of titanium from TIO2 nanoparticle exposure in the isolated perfused intestine of rainbow trout: nystatin, vanadate and novel CO2-sensitive components. *Nanotoxicology* **2013**, *7* (8), 1282–1301.

(545) Poynton, H. C.; Lazorchak, J. M.; Impellitteri, C. A.; Blalock, B.; Smith, M. E.; Struewing, K.; Unrine, J.; Roose, D. Toxicity and Transcriptomic Analysis in Hyalella azteca Suggests Increased Exposure and Susceptibility of Epibenthic Organisms to Zinc Oxide Nanoparticles. *Environ. Sci. Technol.* **2013**, *47* (16), 9453–9460.

(546) Dai, L.; Syberg, K.; Banta, G. T.; Selck, H.; Forbes, V. E. Effects, Uptake, and Depuration Kinetics of Silver Oxide and Copper Oxide Nanoparticles in a Marine Deposit Feeder, Macoma balthica. *ACS Sustain. Chem. Eng.* **2013**, *1* (7), 760–767.

(547) Ramskov, T.; Selck, H.; Banta, G.; Misra, S. K.; Berhanu, D.; Valsami-Jones, E.; Forbes, V. E. Bioaccumulation and effects of different-shaped copper oxide nanoparticles in the deposit-feeding snail Potamopyrgus antipodarum. *Environ. Toxicol. Chem.* **2014**, *33* (9), 1976–1987.

(548) Ramskov, T.; Thit, A.; Croteau, M.-N.; Selck, H. Biodynamics of copper oxide nanoparticles and copper ions in an oligochaete – Part I: Relative importance of water and sediment as exposure routes. *Aquat. Toxicol.* **2015**, *164*, 81–91.

(549) Zhang, X.; Sun, H.; Zhang, Z.; Niu, Q.; Chen, Y.; Crittenden, J. C. Enhanced bioaccumulation of cadmium in carp in the presence of titanium dioxide nanoparticles. *Chemosphere* **2007**, *67* (1), 160–166.

(550) Sun, H.; Zhang, X.; Niu, Q.; Chen, Y.; Crittenden, J. C. Enhanced Accumulation of Arsenate in Carp in the Presence of Titanium Dioxide Nanoparticles. *Water. Air. Soil Pollut.* **2006**, *178* (1–4), 245–254.

(551) Sun, H.; Zhang, X.; Zhang, Z.; Chen, Y.; Crittenden, J. C. Influence of titanium dioxide nanoparticles on speciation and bioavailability of arsenite. *Environ. Pollut.* **2009**, *157* (4), 1165–1170.

(552) Federici, G.; Shaw, B. J.; Handy, R. D. Toxicity of titanium dioxide nanoparticles to rainbow trout (Oncorhynchus mykiss): Gill injury, oxidative stress, and other physiological effects. *Aquat. Toxicol.* **2007**, *84* (4), 415–430.

(553) Ramsden, C. S.; Smith, T. J.; Shaw, B. J.; Handy, R. D. Dietary exposure to titanium dioxide nanoparticles in rainbow trout, (Oncorhynchus mykiss): no effect on growth, but subtle biochemical disturbances in the brain. *Ecotoxicology* **2009**, *18* (7), 939–951.

(554) Johnston, B. D.; Scown, T. M.; Moger, J.; Cumberland, S. A.; Baalousha, M.; Linge, K.; van Aerle, R.; Jarvis, K.; Lead, J. R.; Tyler, C. R. Bioavailability of Nanoscale Metal Oxides TiO2, CeO2, and ZnO to Fish. *Environ. Sci. Technol.* **2010**, *44* (3), 1144–1151.

(555) Badawy, A. M. E.; Luxton, T. P.; Silva, R. G.; Scheckel, K. G.; Suidan, M. T.; Tolaymat, T. M. Impact of Environmental Conditions (pH, Ionic Strength, and

Electrolyte Type) on the Surface Charge and Aggregation of Silver Nanoparticles Suspensions. *Environ. Sci. Technol.* **2010**, *44* (4), 1260–1266.

(556) Lovern, S. B.; Owen, H. A.; Klaper, R. Electron microscopy of gold nanoparticle intake in the gut of Daphnia magna. *Nanotoxicology* **2008**, *2* (1), 43–48.

(557) Felli, J. C.; Hazen, G. B. Javelin Diagrams: A Graphical Tool for Probabilistic Sensitivity Analysis. *Decis. Anal.* **2004**, *1* (2), 93–107.

(558) Heugens, E. H. W.; Jager, T.; Creyghton, R.; Kraak, M. H. S.; Hendriks, A. J.; Van Straalen, N. M.; Admiraal, W. Temperature-Dependent Effects of Cadmium on Daphnia magna: Accumulation versus Sensitivity. *Environ. Sci. Technol.* **2003**, *37* (10), 2145–2151.

(559) Claesson, A. Variation in cell composition and utilization of N and P for growth of Selenastrum capricornutum. *Physiol. Plant.* **1980**, *48* (1), 59–64.

(560) Reynolds, C. S. *The ecology of freshwater phytoplankton*; Cambridge University Press, 1984.

(561) Othman, M. S.; Pascoe, D. Growth, Development and Reproduction of Hyalella Azteca (Saussure, 1858) in Laboratory Culture. *Crustaceana* **2001**, *74* (2), 171–181.

(562) Henry, R.; Simao, C. A. Evaluation of density and biomass of a bivalve population (diplon delodontus expansus) in a small tropical reservoir. *Rev Hydrobiol Trop* **1984**, *17* (4), 309–318.

(563) Sommer, A. Pimephales promelas (Black-head minnow). *Animal Diversity Web*; University of Michigan.

(564) Ridolfi, K. Oncorhynchus mykiss. *Animal Diversity Web*; University of Michigan.

(565) Nichols, J. W.; McKim, J. M.; Lien, G. J.; Hoffman, A. D.; Bertelsen, S. L. Physiologically based toxicokinetic modeling of three waterborne chloroethanes in rainbow trout (Oncorhynchus mykiss). *Toxicol. Appl. Pharmacol.* **1991**, *110* (3), 374–389.

(566) Duffy, W. G. Population dynamics, production, and prey consumption of fathead minnows (Pimephales promelas) in prairie wetlands: a bioenergetics approach. *Can. J. Fish. Aquat. Sci.* **1998**, *54*, 15–27.

(567) Panov, V. E.; McQueen, D. J. Effects of temperature on individual growth rate and body size of a freshwater amphipod. *Can. J. Zool.* **1998**, *76* (6), 1107–1116.

(568) Hargrave, B. T. Distribution, Grwoth, and Seasonal Abundance of Hyalella azteca (Amphipoda) in Relation to Sediment Microflora. *J. Fish. Res. Board Can.* **1970**, *27* (4), 685–699.

(569) Hargrave, B. T. The utilization of benthic microflora by Hyalella azteca (amphipoda). *J. Anim. Ecol.* **1970**, *39* (2), 427–437.

(570) Hargrave, B. T. Prediction of egestion by the despoti-feeding amphipod hyalella azteca. *Oikos* **1972**, *23* (1), 116–124.

(571) Herwig, B. R.; Zimmer, K. D. POpulation ecology and prey consumption by fatehead minnows in prairie wetlands: importance of detritus and larval fish. *Ecol. Freshw. Fish* **2007**, *16* (3), 282–294.

(572) van Dam, A. A.; Penning De Vries, F. W. T. Parameterization and calibration of a model to simulate effects of feeding level and feed composition on growth of Oreochromis niloticus and Oncorhynchus mykiss. *Aquac. Res.* **1995**, *26*, 415–425.

(573) Taipale, S.; Brett, M.; Martin-Creuzburg, D.; Yeung, S.; Hiltenun, M.; Strandberg, U.; Kankaala, P. Differing daphnia magna assimilation efficiencies for terrestrial, bacterial, and algal carbon and fatty acids. *Ecology* **2014**, *95* (2), 563–576.

(574) Patterson, M. A. Energy Reserves in native freshwater mussels (bivalvia: unionidae) with and without attached zebra mussels: effects of food deprivation, Virginia Tech: Virginia, 1998.

(575) Lapointe, D.; Couture, P. Influence of the Route of Exposure on the Accumulation and Subcellular distribution of nickel and thallium in juvenile fathead minnows. *Arch. Environ. Contam. Toxicol.* **2009**, *57*, 571–580.

(576) Thomann, R. V.; Shkreli, F.; Harrison, S. A pharmacokinetic model of cadmium in rainbow trout. *Environ. Toxicol. Chem.* **1997**, *16* (11), 2268–2274.

(577) Nalewajko, C. Photosynthesis and excretion in various planktonic algae. *Limnol. Oceanogr.* **1966**, *11* (1), 1–10.

(578) Le Faucheur, S.; Campbell, P. G. .; Fortin, C.; Slaveykova, V. L. Interactions between mercury and phytoplankton: SPeciation, bioavailability, and internal handling. *Environ. Toxicol. Chem.* **2014**, *33* (6), 1211–1224.

(579) Guan, R.; Wang, W.-X. Dietary assimilation and elimination of Cd, Se, and Zn by Daphnia magna at different metal concentrations. *Environ. Toxicol.* **2004**, *23* (11), 2689–2698.

(580) Dietz, T. H. Uptake of sodium and chloride by freshwater mussels. *Can. J. Zool.* **1979**, *57*, 156–160.

(581) Winhold, L. Unionidae. *Animal Diversity Web*; University of Michigan.

(582) Wen, Y. H. Life History and production of Hyalella azteca (Crustacea: Amphiopoda) in a hypereutrophic prairie pond in southern Alberta. *Can. J. Zool.* **1992**, *70* (7), 1417–1424.

(583) Elenbaas, M. Daphnia Magna. *Animal Diversity Web*.

(584) Gotham, I. J.; Rhee, G.-Y. Effects of nitrate and phosphate limitations on cyclostat growth of two freshwater diatoms. *J. Gen. Microbiol.* **1982**, *128*, 199–205.

(585) Blaise, C.; Ferard, J.-F. *Small-scale freshwater toxicity investicationgs: Hazard assessment schemes*; Springer: The Netherlands, 2005; Vol. 2.

(586) Fakioglu, O. Phytoplankton biomass impact on the lake water quality. In *Biomass Now - Cultivation and Utilization*; Darko, M., Ed.; Intech Open, 2013.

(587) Stich, H. B.; Maier, G. Distribution and abundance of Daphnia pulicaria, a large Daphnia of the "pulex group", in Lake Constance (Lower Lake). *Limnol. - Ecol. Manag. Inland Waters* **2007**, *37* (4), 303–310.

(588) Ricciardi, A.; Bourget, E. Weight-to-wegith conversion factors for marine benthic macroinvertebrates. *Mar. Ecol. Prog. Sreies* **1998**, *163*, 245–251.

(589) Harvey, B. C.; White, J. L.; Nakamoto, R. J. Habitat-specific biomass, survival, and growth of rainbow trouth (Oncorhynchus mykiss) during summer in a small coastal stream. *Can. J. Fish. Aquat. Sci.* **2005**, *62*, 650–658.

(590) Borgmann, U. A mechanistic model of copper accumulation in hyalella azteca. *Sci. Total Environ.* **1998**, *219* (2–3), 137–145.

(591) Trudel, M.; Rasmussen, J. Modeling the elimination of mercury by fish. *Environ. Sci. Technol.* **1997**, *31* (6), 1716–1722.

(592) Nichols, J. W.; McKim, J. M.; Andersen, M. E.; Gargas, M. L.; Clewell, H. J.; Erickson, R. J. A physiologically based toxicokinetics model for the uptake and

disposition of waterborne organic chemicals in fish. *Toxicol. Appl. Pharmacol.* **1990**, *106* (3), 433–447.

(593)   Thomann, R. V. Bioaccumulation model of organic chemical distribution in aquatic food chains. *Environ. Sci. Technol.* **1989**, *23* (6), 699–707.

(594)   Gotham, I. J.; Rhee, G. Y. Comparative kinetic studies of phosphate-limited growth and phosphate uptake in phytoplankton in continuous culture. *J. Phycol.* **1981**, *17*, 257–265.